Catalytic ozonation for the removal of anthropogenic organic contaminants in water

Amir Ikhlaq

M.Sc (Chemistry), M.Phil (Chemistry)

Submitted for the Degree of Doctor of Philosophy (PhD)

United Kingdom

July 2012

Abstract

The ZSM-5 zeolites with varying silica to alumina ratios and with both hydrogen and sodium counter ions (Z1000H:SiO_2/Al_2O_3 = 1000, Z900Na:SiO_2/Al_2O_3 = 900, Z25H:SiO_2/Al_2O_3 = 25 and Z25Na:SiO_2/Al_2O_3 = 25) and γ-alumina have been selected as catalysts. The first investigation was initiated to study the mechanisms of catalytic ozonation on zeolites and alumina. The formation of reactive oxygen species (ROS) such as hydroxyl radicals (^{o}OH), hydrogen peroxide (H_2O_2) and superoxide ion radical ($^{o}O_2^-$) have been investigated by using coumarin (COU), amplex red and 4-chloro-7-nitrobenzo-2-oxa-1,3-dizole (NBD-Cl) as probes respectively. The effects of hydroxyl radical scavenger and phosphates have also been studied to investigate the mechanism. The results show that alumina catalyses radical pathways involving ROS, showing its highest activity at pH close to the point of zero charge. However, zeolites do not promote the formation of ROS. The presence of phosphates and t-butanol (TBA) significantly reduces the formation of ROS in the case of alumina. However, in the case of zeolites TBA and phosphates do not have a significant effect on ROS formation.

The second investigation involved the study of the efficiency of catalysts to remove organic contaminants. The ibuprofen and volatile organic chemicals (VOCs) such as cumene, 1,2-dichlorobenzene and 1,2,4-trichlorobenzene have been selected as target pollutants. The results show that within the family of zeolites, silica to alumina ratio is important for the adsorption of pollutants and for catalytic efficiency of zeolites. Therefore, Z1000H and Z900Na have been found to effectively catalyse the removal of VOCS and Z25H and Z25Na were the better catalysts for the removal of ibuprofen in its ionized form. The alumina was found to be ineffective for the removal of VOCs. However, alumina effectively removes ibuprofen. This is because of high adsorption of ibuprofen on alumina. Therefore, it is hypothesized that zeolites operate through a simple mechanism involving the direct reaction of adsorbed species on their surfaces; their activity depends upon their silica to alumina ratios and is insensitive to the nature of counter ions. The alumina operates through a radical mechanism involving the formation of ROS. Furthermore, the adsorption of pollutants plays an important role in the catalytic ozonation process.

List of publications

Parts of this PhD thesis have already been published or in process for publication in the following form:

1. A. Ikhlaq, R. Brown, B. Kasprzyk-Hordern, Mechanisms of catalytic ozonation on alumina and ZSM-5 zeolites in water: formation of hydroxyl radicals, Applied Catalysis B: Environmental, 123-124 (2012) 94-106.
2. A. Ikhlaq, R. Brown, B. Kasprzyk-Hordern, Catalytic ozonation of VOCs in water on ZSM-5 zeolites and alumina, 10th International Conference on Materials Chemistry (MC10) 4-7 July 2011 Manchester, U.K. (abstract and poster).
3. A. Ikhlaq, R. Brown, B. Kasprzyk-Hordern, Mechanisms of catalytic ozonation: An investigation into superoxide ion and hydrogen peroxide formation during catalytic ozonation on alumina and zeolites in water (Accepted (2012) to Applied Catalysis B: Environmental).
4. A. Ikhlaq, R. Brown, B. Kasprzyk-Hordern, Catalytic ozonation for the removal of pharmaceuticals in water, Postgraduate research conference 23rd March 2011 University of Huddersfield U.K. (Poster).
5. A. Ikhlaq, R. Brown, B. Kasprzyk-Hordern, Catalytic ozonation for the removal of anthropogenic organic contaminants in water, Postgraduate research conference 13th March 2010 University of Huddersfield U.K. (Poster).
6. A. Ikhlaq, R. Brown, B. Kasprzyk-Hordern, Catalytic ozonation for the removal of VOCs in water on ZSM-5 zeolites and alumina (In process).
7. A. Ikhlaq, R. Brown, B. Kasprzyk-Hordern, Catalytic ozonation for the removal of ibuprofen in water on ZSM-5 zeolites and alumina (In process).

Acknowledgements

First of all, I would like to express my deepest gratitude to my supervisors Dr. Barbara Kasprzyk-Hordern and Prof. David Rob Brown for their helpful guidance, encouragement and support throughout the journey. During the study, their advice and enormous support gave me an inspiration to finish the study.

I am also grateful to laboratory staff; Richard Hughes, Ibrahim George, Natasha Reea and Margaret Scot, for their assistance and help during the research.

I would like to acknowledge that this study has been supported by HEC (Pakistan) and Institute of Environmental Engineering and Research University of Engineering and Technology, Lahore, Pakistan (faculty development programme scholarship).

Finally grateful acknowledgement is made to all research fellows. I have enjoyed working with those people greatly.

Dedication

With

Love to

My beloved parents, daughter and wife

Whose prayers are sources of strength for me in every walk of life

List of abbreviations

AC	Activated carbon
AOPs	Advanced oxidation processes
Al_2O_3/O_3	Ozonation process catalyses by alumina
BET	Brunauer, Emmett and Teller
COD	Chemical oxygen demand
COU	Coumarin
DEPMPO	5-Diethoxyphosphoryl-5-methyl-1-pyrroline N-oxide
DMPO	5,5-Dimethyl-1-5pyrroline N-oxide
DPD	N,N-Diethyl-p-phenylenediamine
ECD	Electrical conductivity detector
EDX	Energy dispersive X-ray spectroscopy
FTIR	Fourier transform infrared spectra
GAC	Granular activated carbon
GC	Gas chromatography
HA	Humic acid
7HC	7-hydroxy coumarin
HPLC	High performance liquid chromatography
IBU	Ibuprofen
IC	Ion chromatography
LOD	Limits of detection
LOQ	Limits of quantification
MCLA	2-Methyl-6-(p-methoxyphenyl)-3,7-dihydroimidazol(1,2-)pyrazin-3-one

NBD-Cl	4-chloro-7-nitrobenz-2-oxa-1,3-diazole
NOM	Natural organic matter
$^{o}O_2^-$	Superoxide ion radical
O_3	Ozone
$^{o}O_3^-$	Ozonide ion radical
^{o}OH	Hydroxyl radical
OH^-	Hydroxide ion
PFOA	Perfluoroctyl alumina
pH_{PZC}	pH of point of zero charge
pKa	Acid dissociation constant
ROS	Reactive oxygen species
TBA	Tert-butyl alcohol ($C_4H_{10}O$)
UV	Ultraviolet light
VOCs	Volatile organic chemicals
XXT	2,3-Bis(1-methoxy-4-nitro-5-sulphophenyl)-5-[(phenylamino)carbonyl]-2H-tetrazolium hydroxide
ZSM-5	Zeolite Socony Mobil Five
ZSM-5/O_3	Ozonation process catalyses by ZSM-5 zeolites
Z1000H	Hydrogen forms ZSM-5 zeolite with silica to alumina ratio 1000
Z900Na	The sodium form ZSM-5 zeolite with silica to alumina ratio 900
Z25H	Hydrogen forms ZSM-5 zeolite with silica to alumina ratio 25
Z25Na	The sodium form ZSM-5 zeolite with silica to alumina ratio 25

Contents

List of tables

List of figures

CHAPTER 1-INTRODUCTION

“In this chapter the general introduction with a brief summary of the work has been described. In addition, the overview of the literature related to the areas of study has been provided”.

1.1 Overview

Catalytic ozonation is one of the advanced oxidation techniques in which ozone is used together with a catalyst in both homogeneous and heterogeneous forms. This process gained much attention in the past few years because of its ability to remove pollutants effectively. Unfortunately, the mechanisms of the processes are still largely unknown and there have been different mechanisms proposed. Three possible reaction mechanisms reported to highlight the role of catalysts in the process [1].

1. Chemisorption of organic molecules on the surface of the catalyst and their reaction with adsorbed aqueous ozone.

2. Chemisorption of ozone on the surface of the catalyst, which results in the formation of active oxygen species which then react with chemisorbed or non-chemisorbed organic molecules.

3. Chemisorption of ozone and organic molecules onto the catalyst and their interactions with one another resulting in the formation of active oxygen species.

Recently, catalytic ozonation has been used for effective degradation of organic pollutants from water. The catalytic ozonation can be further divided into homogeneous and heterogeneous catalytic ozonation processes. The former involves ozone decomposition catalysed by transition metal ions and in the later the ozone decomposition is catalysed by solid catalysts. Heterogeneous catalytic ozonation has been successfully used for the effective removal of organic pollutants. Among the catalysts used are: Al_2O_3, TiO_2, Fe_2O_3, Y-zeolites, activated carbons and ZSM-5 zeolites [2-11]. Unfortunately, despite several research groups having successfully used heterogeneous catalytic ozonation for pollution control, the mechanisms of these processes are still not clear [1, 12]. Furthermore, in order

to introduce this technique for water treatment on an industrial scale, it is important to understand the mechanism of the catalytic ozonation process. The following are vital points that are to be answered in order to understand the catalytic ozonation process [12]:

- It is not clear whether a direct ozone attack or radical mechanism (the catalyst causes ozone decomposition leading to the formation of hydroxyl radicals) is responsible for the degradation of organic pollutants.

- The pathways of aqueous ozone decomposition in catalytic ozonation processes are not clear and several mechanisms have been proposed. The major question is whether the formation of hydroxyl radicals is as a result of aqueous ozone decomposition on the surface of the catalyst, or indirectly as a result of secondary reactions.

- It is not clear whether the adsorption of pollutants on the surface of the catalyst is vital for high reaction rates (some reports favour it and others oppose it).

- What is the effect of natural water constituents such as phosphates, carbonates, bicarbonates, sulphates and natural organic matter on the catalytic activity?

- What are the important factors that can affect the catalytic activity?

The aim of this study was to verify the effectiveness and mechanism of catalytic ozonation on alumina and ZSM-5 zeolites with different silica to alumina ratios and counter ions (Z1000H: SiO_2/Al_2O_3 = 1000, Z900Na: SiO_2/Al_2O_3 = 900, Z25H: SiO_2/Al_2O_3 = 25 and Z25Na: SiO_2/Al_2O_3 = 25).

Alumina has been reported by several authors as an effective catalyst of organic acids, chlorinated organic compounds, chlorinated phenols [13, 14], and natural organic matter

[3] ozonation in water. There are however reports indicating the lack of catalytic activity of alumina (e.g. ozonation of ethers and hydrocarbons [4, 15]). Furthermore, the importance of the adsorption of pollutants on the surface of the catalyst is questionable. Some authors considered adsorption as a vital step in catalytic ozonation [4, 16] while others opposed it and suggested that the adsorption of organic compounds is not important for effective removal of pollutants [17]. The surface properties of alumina were also considered vital for ozone decomposition. Furthermore, it was hypothesized that surface the hydroxyl groups of alumina are responsible for ozone decomposition and the highest catalytic activity of alumina was reported at its point of zero charge [18-20]. However, it has been reported by Lin et al [21] that aqueous ozone is not decomposed by alumina. Pocostales et al [2] hypothesized that aqueous ozone adsorbed on the surface of pollutants react directly with adsorbed organic compounds. In the light of the above discussion further investigations are required to evaluate the mechanism of catalytic ozonation on alumina.

Recently high silica zeolites (HSZ) have also been tested as a catalyst and were found to be good adsorbents of ozone [22]. They have been also successfully applied as heterogeneous catalyst for pollution abatements. [11, 23, 24]. The hydrophobic nature of HSZ also attracts organic pollutants on its surface [25] and that results in enhanced reaction rates among ozone and pollutants on the zeolites surface [11]. It has been hypothesized by Valdes et al [26, 27] that Lewis and Bronsted acid sites of zeolites may decompose the aqueous ozone leading to the generation of hydroxyl radicals. Unfortunately, no extensive investigation has been undertaken in order to understand the process occurring during the ozonation in the presence of ZSM-5 zeolites.

In this study reactive oxygen species (ROS) such as hydroxyl radicals, hydrogen peroxide and the superoxide ion have been investigated in the ozonation of ZSM-5 zeolites and alumina, these investigations were undertaken in order to understand the mechanism of the ozonation process over alumina and ZSM-5 zeolites. For this purpose probe molecules such as coumarin (to investigate the formation of hydroxyl radicals), amplex red (to analyse the formation of hydrogen peroxide) and 4-chloro-7-nitrobenz-2-oxa-1,3-diazole (to investigate the formation of superoxide ion) have been used in the ozonation process in the presence of alumina and ZSM-5 zeolites.

In order to investigate the effect of the nature of the pollutants on catalytic ozonation different types of pollutants such as VOCs (hydrocarbons; nonpolar compounds), pharmaceuticals (ibuprofen, polar compound) and organic acids (acetic acid; ozone resistant compound) have been selected. This investigation would be helpful to understand the effect of adsorption of pollutants on catalysts, as it was expected that hydrophobic compounds (VOCs) may be more likely to adsorb on the hydrophobic high silica zeolites than that of alumina in contrast to ibuprofen.

Additionally, variables such as the pH of the solution, the surface properties of materials, the effect of inorganic ions, the effect of humic acids, the effect of silica to alumina ratios of ZSM-5 zeolites, the role of counter ions, the aqueous ozone decay rates, the effect of catalyst amounts and the reuse performance of the catalysts were studied in order to understand the processes occurring during the catalytic ozonation. Finally, on the bases of above studies the mechanism of ozonation on ZSM-5 zeolites and alumina has been hypothesized. In this work cumene, chlorobenzenes (1,2- dichlorobenzene and 1,2,4-trichlorobenzene), ibuprofen and acetic acid were used as target pollutants.

1.2 Main objectives

1. To investigate mechanisms of catalytic ozonation of pollutants on ZSM-5 zeolites and alumina.

2. To verify the phenomena influencing catalytic ozonation (e.g. sorption of organic pollutants on the surface of catalysts, the effect of the pH of the solution, surface properties of catalyst, inorganic ions and natural organic matter on degradation efficiency of catalytic ozonation.

3. To verify the efficiency of catalytic ozonation towards common water pollutants (VOCs and pharmaceuticals).

1.3 Organization of thesis

Chapter 1

A general introduction with a brief summary of the work and an overview of the literature related to the areas of study.

Chapter 2

This chapter has been divided into two parts. The first part (experimental) describes the materials, equipments and methods used in this research. The second part (method development and validation) describes the methods development and validation.

Chapter 3

Chapter 3 describes the characterization of ZSM-5 zeolites and alumina. The techniques used for characterization are FTIR, SEM, XRD and mass titration.

Chapter 4

In this chapter the results of an investigation of the formation of the active oxygen species such as hydroxyl radicals, hydrogen peroxide and superoxide ion radical formation in the ozonation process on ZSM-5 zeolites and alumina have been presented. Coumarin, amplex red and NBD-Cl were used as probe molecules for an investigation of hydroxyl radicals, hydrogen peroxide and superoxide ions respectively. Furthermore, the effect of pH, catalyst dose, phosphates and t-butyl alcohol has been studied. The aqueous ozone decomposition rates (with and without catalysts) have been investigated at pH 3.0, 6.2 and 13.0. On the bases of results from the above work, mechanisms of ozonation in the presence of zeolites and alumina have been proposed.

Chapter 5

The results for the catalytic ozonation of organic pollutants such as VOCs, ibuprofen and acetic acid on ZSM-5 zeolites and alumina have been presented in this chapter. The VOCs selected are cumene, 1,2- dichlorobenzene and 1,2,4-trichlorobenzene. The effect of pH, adsorption, TBA, phosphates, humic acid, reuse performance of catalyst and catalyst efficiency in tap water is described.

1.4 General overview of ozone

Ozone is a triatomic molecule and is an allotrope of oxygen that is much less stable than the diatomic allotrope. It was derived from the Greek word ozein (to smell) and was known to accompany electrical storms, since ancient times. It was first discovered in 1840 by a German chemist C. F. Schonbein and later on in 1856 Thomas Andrews showed that ozone was formed only by oxygen. In 1863 Soret found that the three volumes of oxygen produce two volumes of ozone [28].

Ozone in the lower atmosphere is an air pollutant and is harmful for humans, animals and plants. However, stratospheric ozone protects life on earth from the harmful ultraviolet radiation from the sun [29, 30]. It has been used as a reagent in the synthesis of organic compounds, as a disinfectant, for the bleaching of natural fibbers and oxidant for water purification [31]. It is an environmental friendly oxidant since it decomposes to oxygen without producing self-derived by-products in oxidation reactions. Therefore, it has been used as an effective oxidant for the removal of organic pollutants from both the aqueous [32, 33] and the gas phases [34]. Recently, ozone has been used in advanced oxidation processes such as catalytic ozonation reactions and mineralization of pollutants was found to be much higher when compared with ozonation alone [31].

1.5 Physicochemical properties of ozone

Ozone is a pale blue gas and is heavier than air. It is a very reactive and highly unstable gas and therefore cannot be stored and transported, so it has to be generated in ‘‘situ’’ [31]. The molecule of ozone is considered to have resonance structure as shown in the Fig. 1.1, characterized by end oxygen atoms with only six electrons. This indicates the electrophilic nature of ozone in most of its reactions.

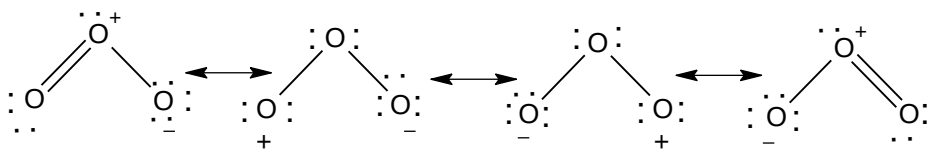

Figure 1.1: Resonance structures of ozone [35]**.**

The solubility of ozone in aqueous solutions is 14 times higher than oxygen. The solubility of ozone in aqueous solutions is influenced by the presence of impurities such as heavy metal ions, metal oxides, temperature and pressure. Generally, the solubility of ozone

increases with an increase in pressure and decrease in temperature. The solubility of ozone at different temperatures is presented in Table 1.1.

Table 1.1: Solubility of ozone in water [31]

Temperature (^{o}C)	**Solubility (kg m^{-3})**
0	1.09
10	0.78
20	0.57
30	0.40
40	0.27
50	0.19
60	0.14

Some of the important physical properties of ozone are presented in Table 1.2.

Table 1.2: Physical properties of ozone [31]

Physical properties	**Value**
Boiling point (101 kPa)	-111.9 ^{o}C
Melting point	-192.7 ^{o}C
Molecular weight	48.0 u
Critical pressure	5.53 M pa
Critical temperature	-12.1 ^{o}C
Density, liquid (-112 ^{o}C)	1358 kg m^{-3}
Density, gas (0 ^{o}C, 101 kPa)	2.144 kg m^{-3}
Viscosity, liquid (- 183 ^{o}C)	1.57 × 10^{-3} Pa·s
Heat of vaporization	15.2 KJ mol^{-1}
Heat capacity, liquid (-183 to -145 ^{o}C)	1884 J kg^{-1}K^{-1}
Heat capacity, gas (25 ^{o}C)	818 J kg^{-1}K^{-1}
Surface tension (-183 ^{o}C)	3.84 × 10^{-2} N m^{-1}

Ozone has a higher oxidation potential than that of hydrogen peroxide, perhydroxyl radical, hypochlorous acid and chlorine. It may decompose to hydroxyl radicals by advanced oxidation catalysis hence it has a great potential in water treatment. The relative oxidation potentials are presented in Table 1.3.

Table 1.3: Relative oxidation potentials [31]

Species	Oxidation Potential, V
Fluorine	3.06
Hydroxyl radical	2.80
Nascent oxygen	2.42
Ozone	2.07
Hydrogen peroxide	1.77
Perhydroxyl radical	1.70
Hypochlorous acid	1.49
Chlorine	1.36

1.6 Reactivity of ozone in water

In aqueous media ozone can react with organic molecules in two different ways (Fig. 1.2). It can either react directly with a compound or it can produce hydroxyl radicals which then react with organic compounds [36, 37]. The direct and indirect pathways depend upon the pH of water. Normally, under acidic conditions (pH < 4) the direct pathway dominates, at neutral pH values (pH 7) both the indirect and direct pathways are important. However, at pH above 10 only indirect pathways dominate [36, 38].

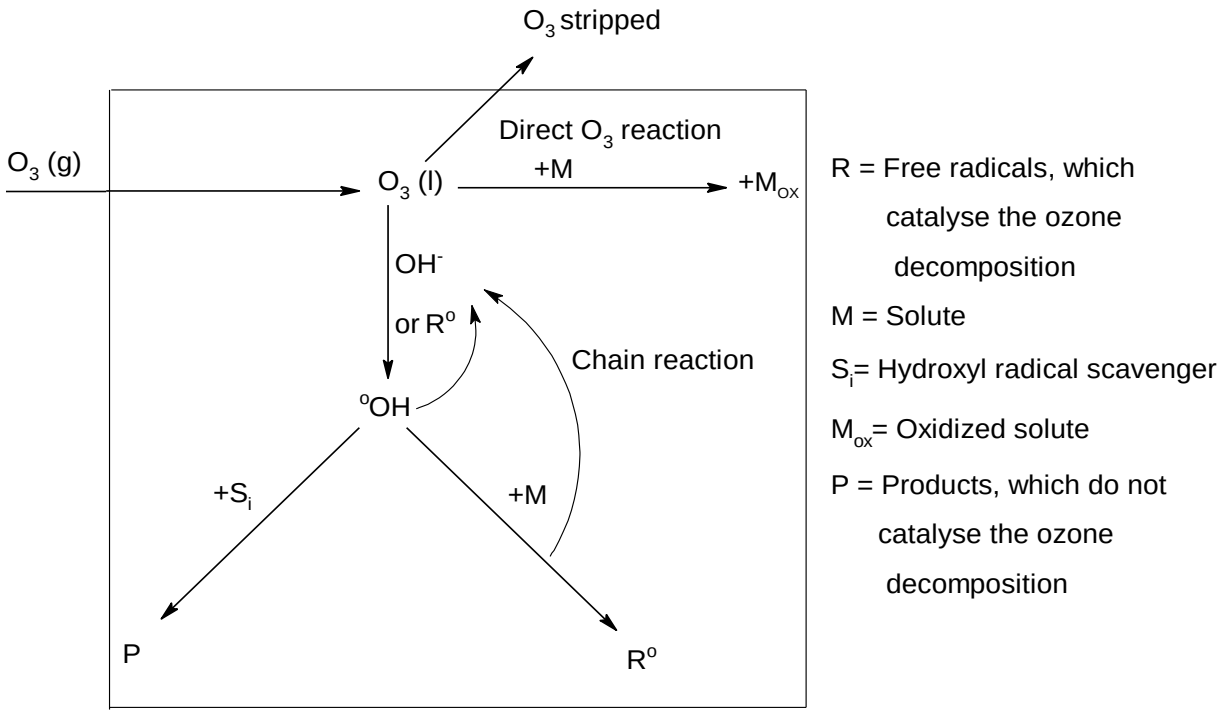

Figure 1.2: Reactions of ozone in aqueous phase [38].

1.6.1 Direct reactions of molecular ozone

The direct reactions of molecular ozone with organic compounds are highly selective reactions and are characterized by very slow rate constants. Because of the chemical nature of ozone (Fig. 1) it can act as dipole, nucleophilic agent and electrophilic agent [35]. Following are the mechanisms for the direct attack of ozone on organic molecules.

1.6.1.1 Cyclo addition (Criegee mechanism)

As a result of its dipolar structure, the molecule of O_3 may lead to 1-3 dipolar cyclo addition reaction with unsaturated organic compounds, with the formation of primary ozonide as shown in the Fig. 1.3. The Criegee's mechanism has three steps, as shown in the Fig. 1.3. In the first step, an unstable primary ozonide is formed. This breaks down in the second step to produce zwitterion (II), this zwitterions reacts in different ways depending upon the solvent system [39]. Theses are the decomposition of ozonide in inert

(Fig. 1.3a), participating (Fig. 1.3b) and so called abnormal ozonolysis that could developed in both participating and nonparticipatinf solvents (Fig. 1.3c). In such a reaction ketones, aldehydes and carboxylic acids can be formed (Fig. 1.3c) [39].

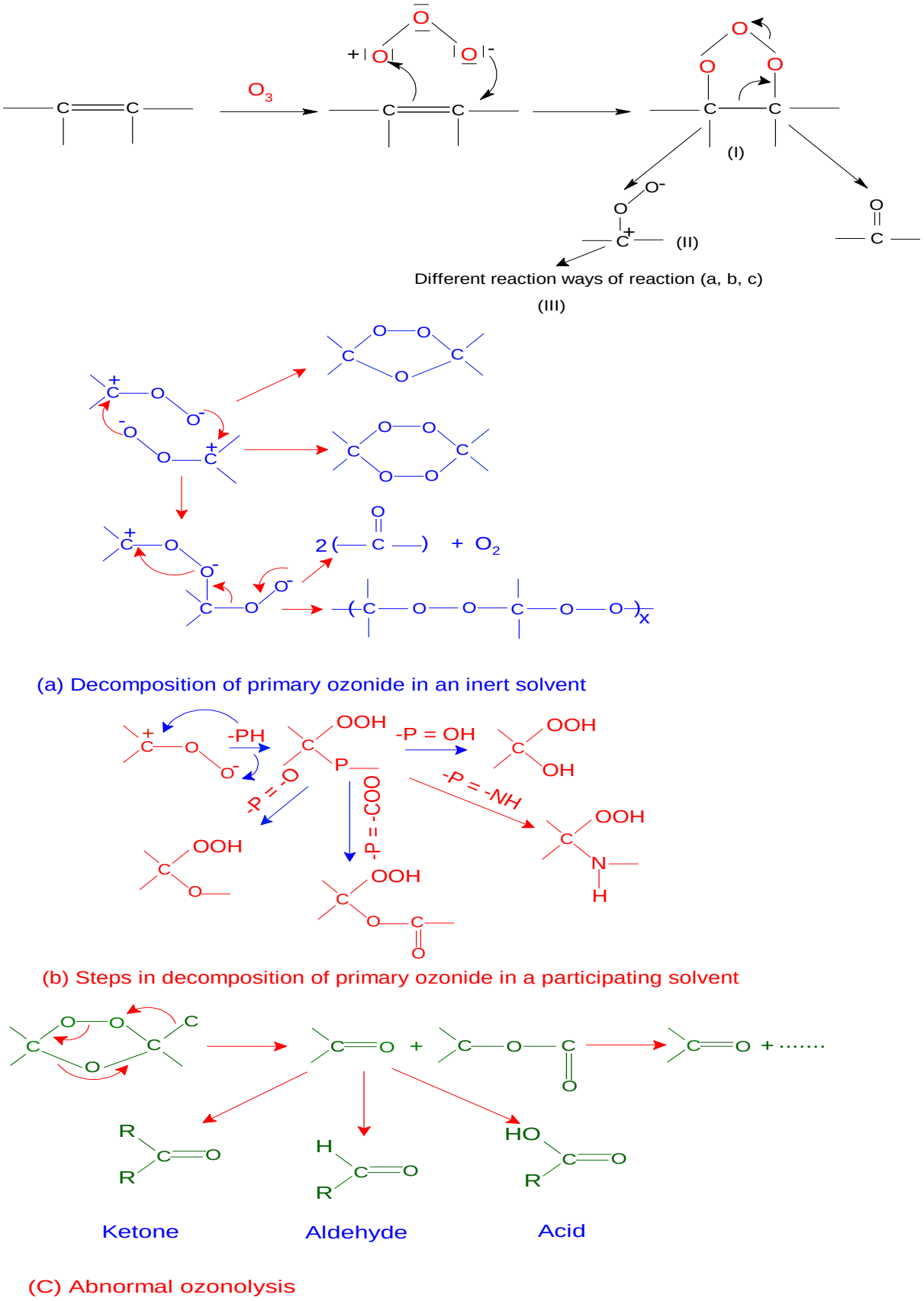

Figure 1.3: Cyclo addition of ozone in protic and aprotic solvents [39].

1.6.1.2 Nucleophilic reactions

The reactions of molecular ozone are very selective and limited to unsaturated aliphatic and aromatic compounds as well as to specific functional groups. Some of the functional groups, which undergo reactions with ozone, are shown in Fig. 1.4. In these reactions ozone acts as a nucleophile. The nuleophilic reaction is found locally on molecular sites showing an electron deficit and on carbon carrying electron withdrawing groups [40].

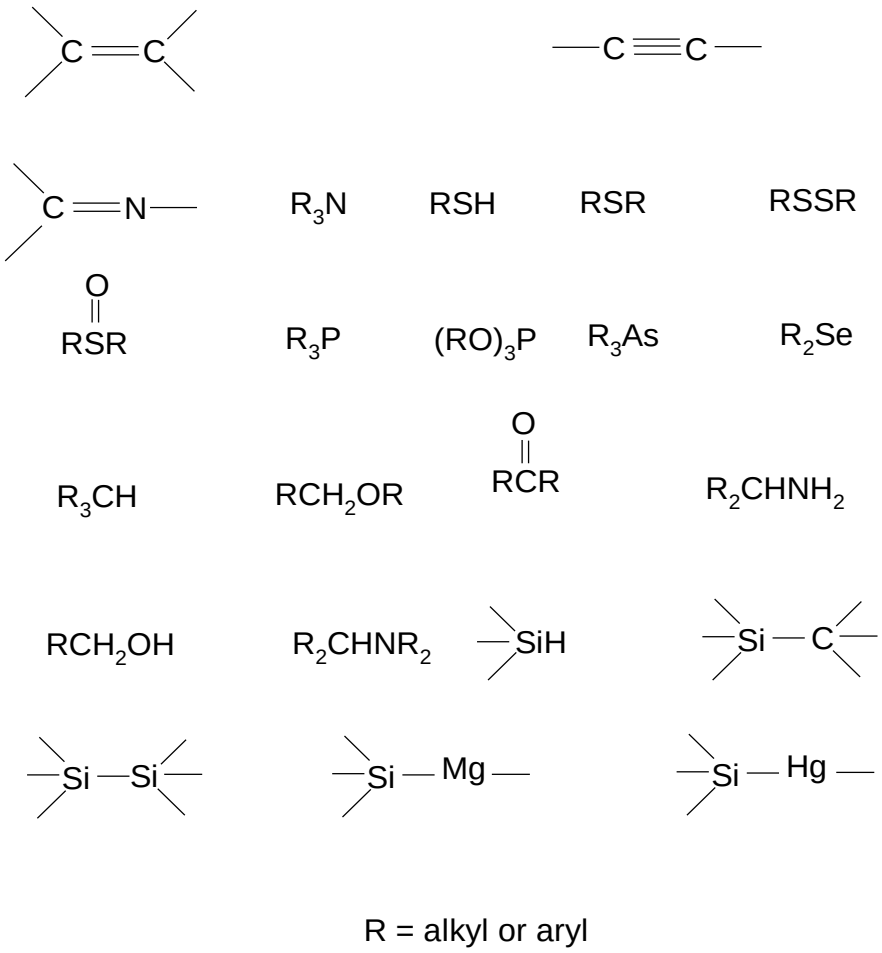

Figure 1.4: Organic groups open to attack by ozone [40].

1.6.1.3 Electrophilic reactions

The molecular ozone may act as an electrophile in reactions with certain organic groups. These reactions take place with the compounds containing strong electronic density and particularly to certain aromatic organic compounds. For example the aromatic compounds

containing electron donating groups (OH, NH_2 etc.) can have electrophilic reactions with ozone. In contrast, the aromatic compounds containing electron withdrawing groups (-COOH, -NO_2, Cl etc.) are less reactive with ozone. An example of the electrophilic reaction of ozone is presented in the Fig. 1.5.

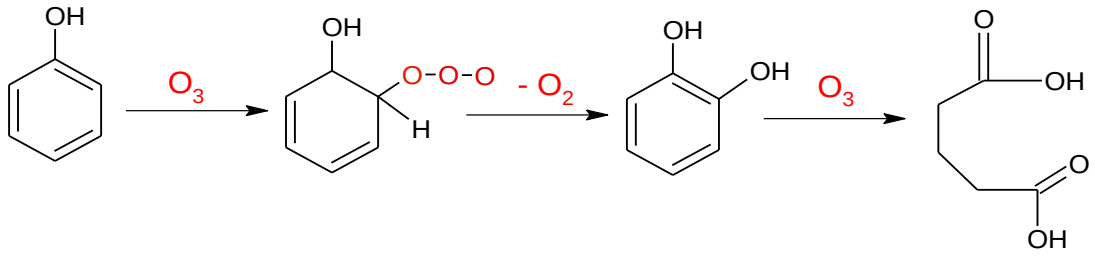

Figure 1.5: Electrophilic reaction of ozone with aromatic compounds [35].

The scheme presented in Fig. 1.5 indicate that initial attack of ozone on the organic compound containing electron donating group (OH), leads to the formation of hydroxylated by-products. Furthermore, these by-products may further react with ozone and lead to the opening of the aromatic cycle, which results in the formation of aliphatic products with carbonyl and carboxyl functional groups.

1.6.1.4 Ozone reaction to aromatic nucleus: by-products

The reaction products of ozone with aromatic compounds are usually ozonides of benzenes. The interaction of ozone with the aromatic ring results in the formation of ozonide and finally the destruction of the aromatic ring leading to the production of by-products such as aldehydes, ketones and organic acids [41]. An example of a direct ozone attack to aromatic compounds is its reaction with cumene (Fig.1.6). This reaction suggested that first ozonide formed that may result in the formation of other products. The formation of some active oxygen species has also been reported during the ozonation of cumene that may further react with organic molecules and lead to the production of by-products [42]. The reactions of ozone with a wide range of organic compounds including

aromatic compounds have been studied previously [43]. Furthermore, the organic compounds studied have additional functionalities including ketone, aldehydes, carboxylic acids and halogens etc. The conclusion drawn from that work was that an addition reaction occurs between any type of the double bond and ozone to give addition products. The further ozonation of theses products results in the production of smaller fractions. The most common by-products reported were aldehydes, ketones and carboxylic acids [43]. Therefore, it is important to identify ozonation by-products such as carboxylic acids to understand the mechanism of the process.

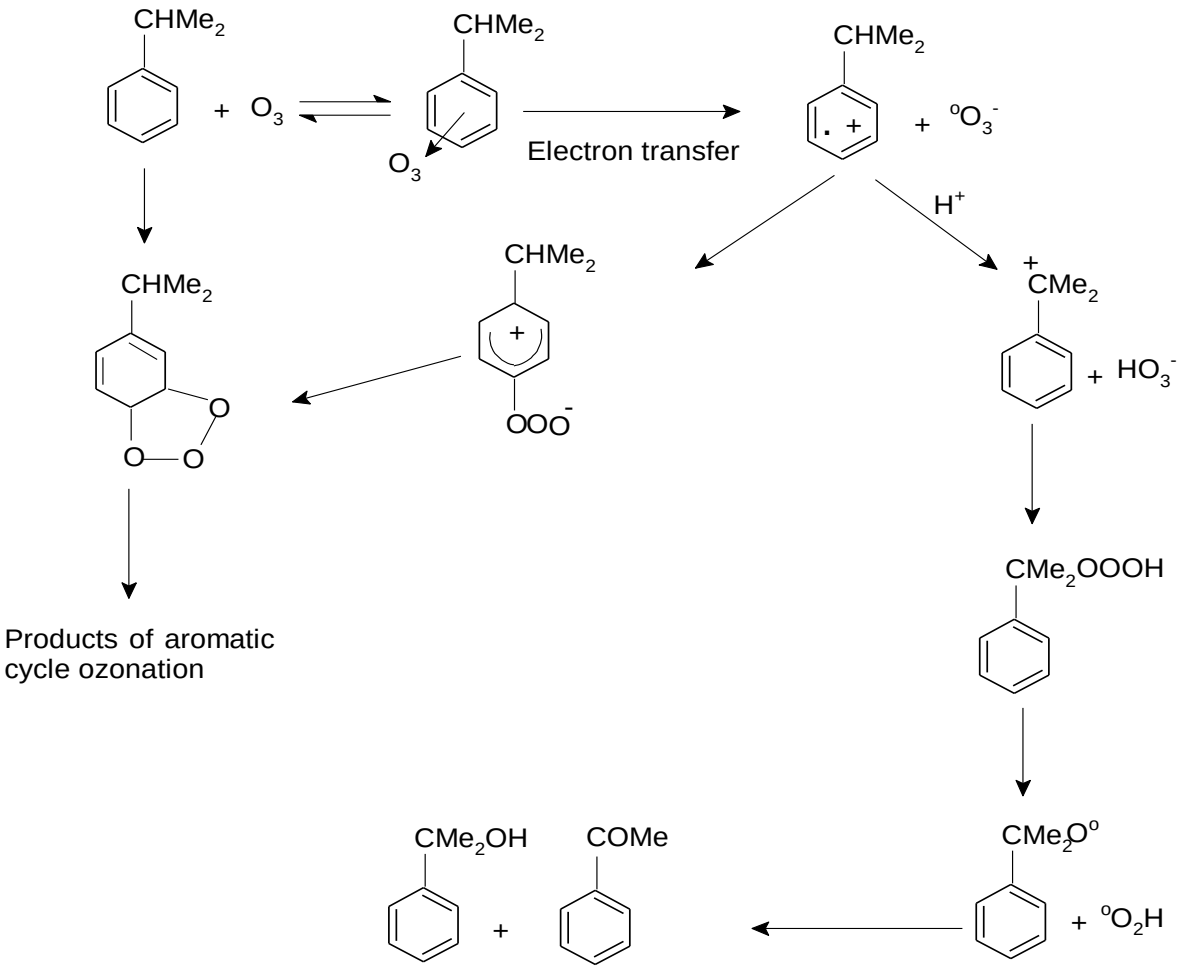

Figure 1.6: Reaction of ozone with cumene [42].

1.6.2 Indirect reactions

The indirect reaction involves the decomposition of ozone in water, resulting in the formation of reactive oxygen species such as hydroxyl radicals. These hydroxyl radicals are more reactive than molecular ozone and can quickly degrade organic compounds. The radical pathway is very complex and there are many factors that can affect the mechanism. The mechanism of ozone decomposition in water has been explained by Staehelin et al [45], and it can be divided in to three main steps (initiation, radical chain and termination). The initiation step involves the reaction of ozone with hydroxide ions (OH^-), leading to the formation of superoxide ions (O_2^{o-}) and hydroperoxyl radicals HO_2^o (Equation, 1.1). These reactions depend upon the pH of the water and occur at basic pH values, as there are more OH^- ions at these pH values (Equation 1.2).

$$O_3 + OH^- \rightarrow O_2^{o-} + HO_2^o \qquad k_1 = 70\ M^{-1}\ s^{-1} \qquad 1.1$$

The hydroperoxyl radical is in an acid-base equilibrium and is more stable at acidic pH values.

$$HO_2^o \longleftrightarrow O_2^{o-} + H^+ \qquad pK_a = 4.8 \qquad 1.2$$

The second stage a radical chain reaction starts when O_3 reacts with O_2^{o-}, leading to the formation of ozonide anion radical (O_3^{o-}) (Equation 1.3) and this radical reacts with H^+ ions and is immediately decomposed to hydroxyl radicals (Equations 1.4, 1.5).

$$O_3 + O_2^{o-} \rightarrow O_3^{o-} + O_2 \qquad k_2 = 1.6 \times 10^9\ M^{-1}\ s^{-1} \qquad 1.3$$

$$HO_3^o \rightarrow O_3^{o-} + H^+ \qquad pK_a = 6.2 \qquad 1.4$$

$$HO_3^o \rightarrow OH^o + O_2 \qquad k_3 = 1.1 \times 10^8\ M^{-1}\ s^{-1} \qquad 1.5$$

The hydroxyl radicals may further react with ozone and formed HO_4^o radicals [ref]

$^{o}OH + O_3 \rightarrow HO_4^{o}$ $k_4 = 2.0 \times 10^9\ M^{-1}\ s^{-1}$ 1.6

$HO_4^{o} \rightarrow O_2 + HO_2^{o}$ $k_5 = 2.0 \times 10^9\ M^{-1}\ s^{-1}$ 1.7

After the decay of HO_4^{o} into O_2 and HO_2^{o} a new chain reaction starts as shown in equation 1.1. Furthermore, the organic molecules (R), can also act as promoters and some of them may contain functional groups that may react with hydroxyl radicals and form organic radicals (Equation 1.8).

$H_2R + {}^{o}OH \rightarrow HR^{o} + H_2O$ 1.8

The HR^{o} radical may further react with the O_2 and these reactions lead to the OH^{o} radicals (Equations 1.9-1.11).

$HR^{o} + O_2 \rightarrow HRO_2^{o}$ 1.9

$HRO_2^{o} \rightarrow R + HO_2^{o}$ 1.10

$HRO_2^{o} \rightarrow RO + {}^{o}OH$ 1.11

The indirect chain reaction of ozone in water is explained by the following scheme.

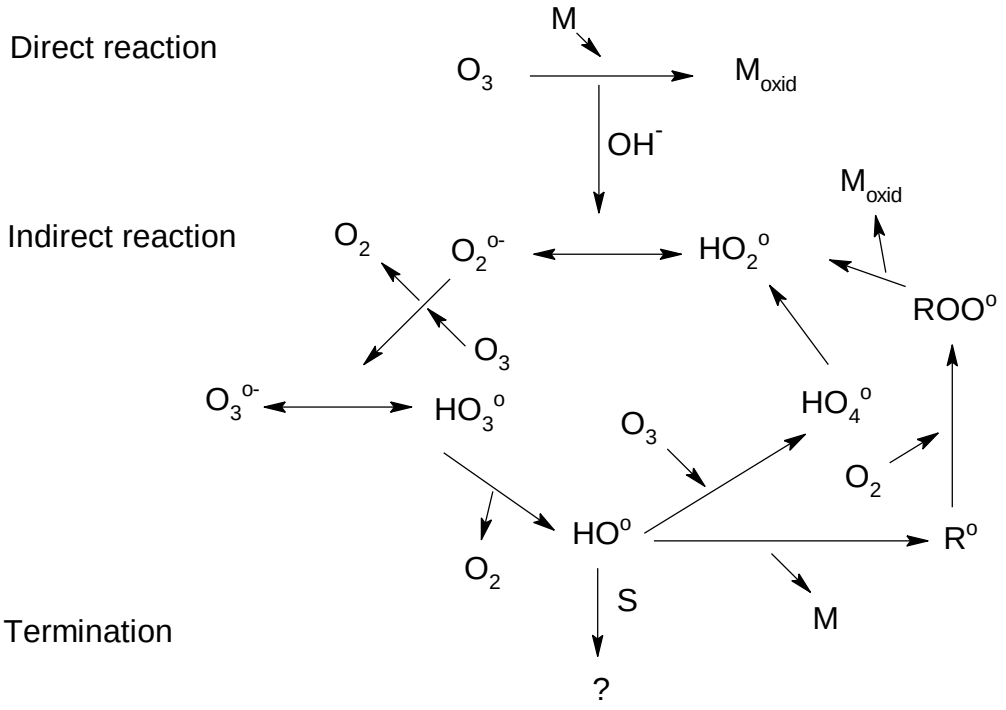

Figure 1.7: Scheme of chain reaction of ozone in aqueous phase [44].

The inorganic ions such as carbonates, bicarbonates and phosphates can inhibit radical chains and act as hydroxyl radical scavengers (Equations 1.12, 1.13); especially the role of carbonates and bicarbonates is important as they are present in significant amount in water [36, 45].

$$^{o}OH + CO_3^{2-} \rightarrow OH^- + CO_3^{o-} \qquad k_6 = 4.2 \times 10^8\ M^{-1}\ s^{-1} \qquad 1.12$$

$$^{o}OH + HCO_3^- \rightarrow OH^- + HCO_3^{o} \qquad k_7 = 1.5 \times 10^7\ M^{-1}\ s^{-1} \qquad 1.13$$

The two radicals may also react to terminate the chain reaction as follows.

$$^{o}OH + HO_2^{o} \rightarrow O_2 + H_2O \qquad k_8 = 3.7\times 10^{10}\ M^{-1}\ s^{-1} \qquad 1.14$$

1.7 Applications of ozone in drinking water treatment

Ozone is one of the strongest oxidants that can be implied for the removal of pollutants from drinking water. Due to the high oxidation and disinfection efficiency, ozone has been used in drinking water treatment for many years. Ozone has been applied for the removal of inorganic species from water. Pre-oxidation using ozone followed by the filtration or coagulation-flocculation-decantation have been used for the elimination of inorganic species from water. The metallic ions form insoluble species upon oxidation and can easily removed [46]. Another advantage of ozone is its ability to remove ammonia from water [46]. Another important application of ozone is its ability to kill microorganisms from water. It has been implied for the inactivation of bacteria, viruses and the control of algal growth. It can inactivate microorganisms such as protozoa, E. coli, Bacillus sublilis spores, Rotavirus and Giardia lamblia cysts [47]. Ozone can penetrate through the cell membrane of Escherichia coli and react with the cytoplasmic substances. In addition, the degradation of nucleic acids, is being one of the important factors responsible for cell killing [46]. The ozone can inactive the viruses by attacking their protein coat or direct damage of nucleic acids. It has been reported that ozone can attack both the protein coat and ribonucleic acids of tobacco mosaic virus [46].

Ozone can remove effectively organic pollutants from drinking waters. However, it reacts slowly with some organic compounds such as organic acids, methyl tertiary butyl ethers (MTBE) and chlorinated organic compounds. [44]. Despite the many advantages of ozone treatment as discussed above, the major disadvantage of ozone is the formation of toxic by-products (e.g. organic acids). Therefore, it is important to imply advanced oxidation processes. Many advanced oxidation processes have been developed which have high

efficienciently of mineralize organic compounds, when compared with ozonation alone, for example catalytic ozonation, O_3/UV, O_3/H_2O_2 and UV/ H_2O_2 [48-51].

1.8 Advanced oxidation processes (AOP)

The processes which involve the formation of hydroxyl radicals in sufficient quantity to affect the water purification are known as advanced oxidation processes [44]. The most common advanced oxidation processes are O_3/UV, O_3/H_2O_2, UV/ H_2O_2 and catalytic ozonation. These processes are effective for the rapid removal of organic pollutants from water, since most of the organic pollutants are resistant to biological and chemical treatment advanced oxidation processes are therefore one of the best options in the near future. The AOPs offers a variety of possible ways to produce hydroxyl radicals. The hydroxyl radicals can be produced by the direct use of ozone or of ozone and hydrogen peroxide. Various methods such as Fenton based systems, photocatalytic processes, acoustic cavitations methods, electrical, electrochemical methods and radiolysis have been used to produce hydroxyl radicals. Based on the way hydroxyl radicals are generated the AOPs may be classified into ultrasound, electrochemical, chemical and photochemical processes (Table 1.4).

Table 1.4: Classification of advanced oxidation processes on the bases of hydroxyl radical generation

Process	Production of hydroxyl radicals from ozone	Peroxone-based	Direct energy transfer	Fenton homogeneous or heterogeneous processes	Heterogeneous catalytic processes
Photochemical	O_3-UV Ozone photolysis	O_3-H_2O_2-UV Ultraviolet peroxone	Direct photolysis	H_2O_2-Fe(II)/Fe(III)-UV Photo-Fenton process	Catalysts-UV or Catalysts/O_3/UV
Chemical	O_3-OH^- Alkaline ozonation	O_3-H_2O_2 Peroxone process	-	H_2O_2-Fe(II)/Fe(III) Fenton likes and Fenton processes	Catalytic ozonation e.g. metal oxides metals
Ultrasound	O_3-US Ozone assisted cavitations	O_3-H_2O_2-US Ultrasound Peroxone	Sonolysis	H_2O_2-Fe(II)/Fe(III)-US Sono-Fenton and US Fenton like processes	Catalytic ultrasonic processes
Electrochemical	Electrolytic generation of ozone	Electrolytic generation of O_3	Anodic oxidation	Electro-Fenton methods	Wet electrocatalytic oxidation

1.9 Catalytic ozonation and its mechanisms

The process in which ozone is used together with a catalyst in both homogeneous and heterogeneous forms is known as a catalytic ozonation process. It has gained significant attention in recent years as an effective removal of organic pollutants from water. However, the mechanisms of these processes are not well under-stood and there have been different proposals for the mechanisms of the catalytic ozonation process [12]. It is therefore, very important to understand the mechanism of catalytic ozonation in order to introduce it to larger scales.

1.9.1 Homogeneous catalytic ozonation and its mechanisms

In homogeneous catalytic ozonation the ozone decomposition takes place as a result of interactions of ozone with transition metal ions such as Fe(II), Mn(II), Ni(II), Co(II), Cd(II), Cu(II), Ag(I), Cr(III) and Zn(II) [1]. There have been two major mechanisms of homogeneous catalytic ozonation [52-54]. Some authors reported that metal ions can decompose ozone leading to the generation of hydroxyl radicals [55]. However, others suggested that metal ions form complexes with organic molecules, which are subsequently oxidised [56]. Several homogeneous catalysts have been successfully used for the degradation of organic pollutants and some of them are presented in Table 1.5. The homogeneous catalysts are usually in solution and therefore access to the pollutants is easier so there is improved activity. Another advantage of the homogeneous catalysts is that heat transfer for exothermic and endothermic reactions is not a problem. Furthermore, the mechanisms of homogeneous catalytic ozonation are simple and are better understood. Despite the several advantages of homogeneous catalysts they have some disadvantages. For example, this process involves the introduction of toxic and harmful metals to water. Thus an undesirable and additional cost is required to remove these metals from water

after treatment. Furthermore, the homogeneous catalyst cannot be recycled or regenerated. Therefore, in order to avoid these problems heterogeneous catalysts have been suggested for drinking water treatment.

Table 1.5: Homogeneous catalytic ozonation

Catalyst	Organic compound	References
Mn(II), Fe(II), Fe(III), Cr(III), Ag(I), Cu(II), Zn(II), Cd(II), Co(II)	Humic substances	[54, 57]
Mn(II), Fe(II), Fe(III)	Chlorobenzenes	[58]
Mn(IV)	Propionic acid	[59]
M(II), Fe(II)	Simazine	[60]
Mn(II), Co(II), Fe(III), Fe(II)	Lignin sulfonate	[61]
Co(II)	Oxalic acid	[56]
Cu(II)	Oxalic acid, pyruvic acid	[59]
Fe(II), Mn(II), Fe(III), Zn(II), Ni(II), Co(II)	Azo dyes	[62]
Fe(III)	Oxalic acid	[55]
Ce(III)	Phenol	[63]
Mn(II), Mo(VI), Fe(II), Cu(II), Ni(II)	Benzoic acid	[64]

1.9.2 Heterogeneous catalytic ozonation and its mechanisms

In the heterogeneous catalytic process, ozone decomposition is catalysed by solid catalysts. Several materials have been used as heterogeneous catalysts and among the most widely used are metal oxides (such as Al_2O_3, MnO_2, TiO_2, FeOOH and CeO_2), metals (Cu, Ru, Pt, Co) on support (such as SiO_2, Al_2O_3, TiO_2, CeO_2 and activated carbons), zeolites modified with metals and activated carbons. Following are some important catalysts and their mechanisms.

1.9.2.1 Metal oxides as catalysts

In the ozonation process several metal oxides have been successfully used as heterogeneous catalysts. Among them are Al_2O_3, TiO_2, MnO_2 and FeOOH. Some of the metal oxides and organic pollutants are presented in Table 1.6.

Table 1.6: Heterogeneous catalytic ozonation-metal oxides

Catalyst	Organic compound	References
Al_2O_3	Carboxylic acids, NOM, dimethylphthalate, chloroethanol,	[1, 3, 17, 65-67]
MnO_2	Carboxylic acids (oxalic, pyruvic, sulfosalicylic, propionic, glyoxalic), phenol, NOM	[55, 59, 68-70]
γ-Al_2O_3	Pharmaceuticals (diclofenac, sulfamethoxazole, 17α-ethlystradiol), methylisoborneol	[2, 18]
ß-Al_2O_3	Pyruvic acid	[71]
α-Al_2O_3, γ-Al_2O_3, γ-AlOOH	2,4,6-trichloroanisole	[19]
TiO_2	Carbamazepine, naproxen, nitrobenzene, clofibric acid, oxalic acid	[6, 72-74]
TiO_2/ γ-Al_2O_3	Oxalic acid	[75]
Fe_2O_3/Al_2O_3	Oxalic acid	[55]
TiO_2/AC	Methylene blue	[76]
MgO	Dye	[77]
NiO/CuO	Dichloroacetic acid	[78]
NiO/Al_2O_3	Oxalic acid	[79]
ZnO	p-chlorobenzoic acid	[80]
CuO/Al_2O_3	Alchlor, oxalic acid, substituted phenols	[59, 81, 82]

Among the metal oxides alumina has been selected in this work and its mechanism has been investigated and compared with ZSM-5 zeolites.

1.9.2.1.1 Mechanism of ozonation in the presence of alumina

The chemistry of alumina is described in section 1.10. Alumina is one of the widely studied catalysts in the catalytic ozonation process. It has been applied in both aqueous and gaseous phases but unfortunately its mechanisms are largely unknown and there are conflicting reports on the mechanism of ozonation in the presence of alumina. Oyama et al [83] studied the decomposition of ozone in the gaseous phase on various materials such as Al_2O_3, MnO_2, CoO_4 and Fe_2O_3. However, he reported alumina as an inactive material. Since then it has been used mainly as catalyst support.

Cooper at al [13] reported that aqueous ozone is decomposed by alumina. It was observed that the efficiency of ozonation in the presence of alumina is higher when compared with ozonation alone when the degradation of oxalic acid, chloroethanol and chlorophenol were investigated. However, no adsorption studies in above mentioned work make it difficult to understand the mechanism of the process. The catalytic activity of alumina is certainly questionable and there are contradictory reports in the literature. Some authors reported that alumina can remove some organic pollutants however others reported that alumina is not effective for some pollutants. It has been reported by Kasprzyk-Hordern et al [15] that alumina is not a good catalyst for the removal of hydrocarbons and no catalytic activity of alumina was observed for aromatic hydrocarbons such as cumene, chlorobenzene and ethers [4, 15]. Interestingly, in the same work it was reported that aqueous ozone decomposition is higher in the presence of alumina when compared with ozonation alone. It was suggested that adsorption of organic compounds is one of the important steps in catalytic ozonation. As ethers and hydrocarbons do not adsorb on alumina therefore this catalyst does not show high efficiency in their removal.

Furthermore, Kasprzyk-Hordern et al [3] studied the removal of natural organic matter (NOM) during the ozonation in the presence of alumina. It was reported that alumina has high efficiency for NOM removal when compared with ozonation alone. Additionally, high adsorption capacity of alumina was reported towards NOM. It was therefore suggested that adsorption of pollutants on the surface of the catalyst is important for their effective degradation.

Recently, Guzman-Perez et al [16] studied the removal of 2, 4-dichlorophenoxylacetic (2,4-D) acid ozonation in the presence of alumina. It has been reported that the adsorption of a pollutant plays an important role in the catalytic ozonation process. The ozonation in

the presence of alumina showed considerably high mineralization of total organic carbon (TOC) when compared with ozonation alone. Additionally, the removal of 2, 4-D was found to increase with the increase in pH.

Ernest et al [17] studied the removal of organic acids such as oxalic acid, succinic acid and formic acid by ozonation on γ-Al_2O_3. In this investigation the highest removal was obtained for succinic acid and it was reported that the acid which adsorbs to the lowest extent (succinic acid) had the highest removal when compared with others. Furthermore, it was hypothesized that alumina generates hydroxyl radicals in the solution that react with organic pollutants present in the solution (Fig. 1.8).

According to this mechanism the superoxide ion radical and $^{o}O_2H$ radicals can be produced by the interaction of aqueous ozone with the surface hydroxyl groups of alumina as shown in Figure 1.8b. This radical reacts subsequently with another ozone molecule to generate an O_3^- radical (Fig. 1.8c). Finally, the ozonide radical decomposes to oxygen and hydroxyl radical. The formed hydroxyl radicals decompose organic pollutants. Unfortunately there has been no direct proof provided by Ernest et al [17] that confirms the formation of active oxygen species in the catalytic ozonation process.

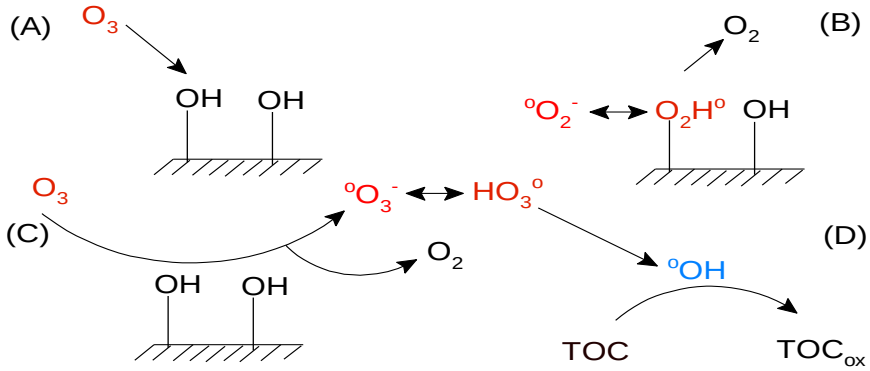

Figure 1.8: Mechanism of aqueous ozone decomposition by alumina [17].

Beltran et al [84] observed the similar results for the removal of oxalic acid by alumina ozonation in water. Additionally, experiments were performed in the presence of phosphates and it was reported that the catalytic activity of alumina was reduced in the presence of phosphate buffer.

In contrast to the above study Lin et al [21] reported that aqueous ozone is not decomposed by alumina. However, Chen et al [18], while studying the degradation of 2-methylisoborneol by γ-Al_2O_3, observed high efficiency of catalytic process when compared with ozonation alone. In the same investigation, it was reported that the pH of solution plays an important role in the mechanism of catalytic ozonation. It was observed that at pH of solution close to the point of zero charge (pzc) of the material, the catalyst has the highest activity. Additionally, the removal of 2, 4, 6-trichloroanisole was also studied by the same group by using alumina oxides (γ-Al_2O_3, γ-AlOOH, and α-Al_2O_3). It was suggested that the highest density of surface hydroxyl groups and strongest surface bronsted acidity of catalyst are responsible for aqueous ozone decomposition. Similar results were obtained by Qi et al [19, 20] and reported that the highest activity of alumina is at pH = pH_{pzc} and suggested that surface hydroxyl groups of alumina in their neutral form are more reactive to decompose aqueous ozone. However, in the above reports it has not been proven that decomposition of ozone occurs on the surface of alumina. In contrast, Pocastales et al [2] investigated the removal of pharmaceuticals (diclofenac, sulfamethoxazole and 17α-ethynylstradiol) in the presence of γ-Al_2O_3/O_3 and $Co_3O_4/Al_2O_3/O_3$. It was reported that degradation of pharmaceuticals may be due to their adsorption on the surface of the catalyst and their reactions with adsorbed ozone and hydroxyl radicals in bulk solution.

As discussed above that Qi et al [20] studied the ozone decomposition catalysed by different forms of alumina. It was observed that γ-Al_2O_3 shows high catalytic activity as compared with α-Al_2O_3. The density of surface hydroxyl groups of γ-Al_2O_3 was found to be higher when compared to α-Al_2O_3. Therefore, it was assumed that high catalytic activity of γ-Al_2O_3 was due to the higher availibity of active sites (surface hydroxyl groups). Therefore, in the current investigation γ-Al_2O_3 alumina has been selected.

The above discussion indicates that further in-depth analyses are required to understand the processes occurring during the ozonation of pollutants in the presence of alumina. Additionally, pathways of aqueous ozone decomposition in catalytic ozonation processes are not clear and as literature review indicates there are several mechanisms possible. The major question is whether the removal of pollutants occurs via direct attack of ozone on the catalyst surface or ozone is decomposed by the catalyst leading to the production of hydroxyl radicals. Furthermore, the understanding of the role of the adsorption of pollutants on the surface of the catalyst is vital to an understanding of the mechanism of catalytic ozonation on alumina. It is important to study variables such as the effect of pH of a solution and the effect of natural water constituents such as phosphates, carbonates, bicarbonates, sulphates and natural organic matter.

1.9.2.1.2 Mechanism of ozonation in the presence of other metal oxides

Among the metal oxides MnO_2 is one of the most frequently used catalysts. It is reported that MnO_2 can most efficiently decompose ozone in gas phase [83]. The activity in aqueous media is known to increase with a decrease in pH of the solution [85]. Unfortunately, there is a lack of understanding of the mechanism of catalytic ozonation on MnO_2 and there are conflicting reports about its mechanism. It was reported by Tong et al [86] that adsorption of both ozone and organic compounds on the surface of MnO_2 is

important. However, Dong et al [87] reported high catalytic activity of β-MnO_2 nano wires for the removal of phenol and observed that the amount of adsorbed phenol was only 8% therefore it was suggested that adsorption of pollutants is not important for the catalytic degradation of pollutants on MnO_2.

Another catalyst that has been used effectively is FeOOH. Granulated forms of iron have been used as an adsorbent of As(V) [88]. Park et al [89, 90] used commercially available goethite for the removal of natural organic matter from water. It has been reported that FeOOH decomposes aqueous ozone, which leads to the generation of ^{o}OH radicals. Surface hydroxyl groups of FeOOH play an important role in ozone decomposition. Furthermore, higher decomposition of natural organic matter was observed at basic pH values. Additionally, Park et al [91] successfully removed p-chlorobenzoic acid (p-CBA) by catalytic ozonation on FeOOH and it has been hypothesized that surface reactions are important for the effective removal of pollutants. However, it was reported that decomposition of p-CBA is independent of TBA which may suggest that hydroxyl radicals do not have any role in the decomposition of p-CBA. Similar findings were reported by Beltran et al [92] and it was observed that TBA does not have a significant effect on the removal of oxalate by Fe_2O_3 /Al_2O_3/ O_3. It was suggested that both ozone and organic compounds adsorb on the surface of the catalyst and reactions of molecular ozone on the surface lead to the degradation of oxalic acid.

However, Zhang et al [93] studied the removal of nitrobenzene by FeOOH/O_3 and found that FeOOH effectively remove nitrobenzene from water. It was observed that nitrobenzene does not adsorb on the surface of the catalyst. Furthermore, the catalytic ozonation process was found to proceed via a hydroxyl radical mechanism as shown in the Fig. 1.9. Figure 1.9 illustrates that ozone molecules can combine with the surface hydroxyl

groups of the catalyst, as its O and H are nucleophilic and electrophilic respectively. The combined species decompose to produce HO_2^- ion. This ion may further react with the ozone molecule to produce hydroxyl radicals and superoxide ion radicals. It was assumed that superoxide ion can further react with ozone to produce hydroxyl radicals [93]. Additionally, Sui et al [94] investigated the removal of oxalic acid by $FeOOH/O_3$ and reported that degradation of oxalic acid took place via radical mechanism.

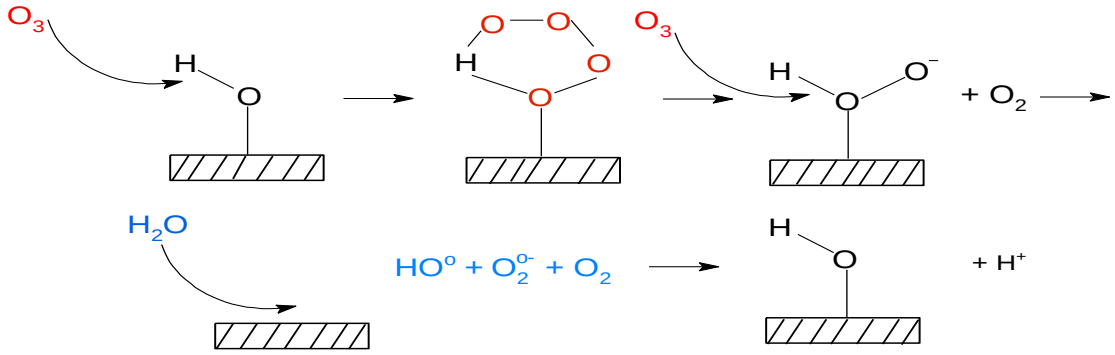

Figure 1.9: Scheme of mechanism of ozone decomposition by FeOOH [93].

Titania (TiO_2) is a well-known catalyst in photo catalysis [95]. It has been used successfully in ozonation systems as an effective catalyst. Beltran et al [6] used TiO_2 in the ozonation process for the removal of oxalic acid in water. It was reported that both the ozone and organic molecules adsorbed on to the surface of the catalysts which result in the degradation of oxalic acid.

It was reported by Yang et al [5] that nano-TiO_2 is active in the form of rutile and not anatase in the removal of nitrobenzene. Furthermore, Ye et al [96] studied the degradation of 4-chloronitro benzene (CNB) during the photo catalytic and catalytic ozonation in the presence of TiO_2. It was observed that both processes have similar efficiency in the removal of CNB.

Titania has also been used in the removal of pharmaceuticals such as carbamazepine and naproxen from water [72]. It was reported that TiO_2 decomposes aqueous ozone leading to the generation of hydroxyl radicals. Furthermore, Rosal et al [73] studied the catalytic ozonation of clofibric acid on titania. It was suggested that adsorption of both ozone and pollutants on the surface of catalyst are important for an effective removal of organic pollutants by catalytic ozonation on TiO_2. Additionally, TiO_2 was also used in combination with activated carbon for the removal of methylene blue. It was reported that $TiO_2/Ac/O_3$ has higher efficiency when compared with Ac/O_3. Furthermore, it was hypothesized that enhanced removal in $TiO_2/Ac/O_3$ may be due to the generation of hydroxyl radicals. Colombo et al [97] studied the removal of bisphenol by the photocatalysis, catalytic ozonation, ozonation and combination of processes by using TiO_2 as catalyst. It has been reported that the combined process of catalytic ozonation and photocatalysis show the highest degradation of bisphenol when compared with other processes. It was further assumed that hydroxyl radicals formed during the process are responsible for bisphenol degradation. The above discussion indicates that there a conflicting reports about the mechanisms of catalytic ozonation in the presence of metal oxides and further investigations are required to understand the mechanism of the catalytic ozonation process.

1.9.2.2 Other catalytic ozonation processes and catalysts: mechanisms

In the catalytic ozonation process different types of materials have been tested as heterogeneous catalysts and supports. Among them are metals on support, activated carbons, minerals and non polar systems etc. Table 1.7 presents types of catalysts and organic molecules studied in the process of catalytic ozonation.

Table 1.7: Heterogeneous catalytic ozonation–metals on supports, activated carbons, minerals and non polar systems

Catalyst	Organic compound	References
Metals on Support		
Rh-CeO_2	Pyruvic acid	[98]
Ru-CeO_2/TiO_2,Cu-ZrO_2/Al_2O_3	Pyruvic acid, succinic acid	[99]
Ru (2%)/CeO_2	Succinic acid	[100]
Ru (2%)/CeO_2-TiO_2	Chloroacetic and succinic acid	[101]
PdO/CeO_2	Oxalate	[102]
V_2O_5/Al_2O_3, SiO_2, TiO_2	1, 2-dichlorobenzene	[103]
Activated carbons		
AC	Phenolic compounds	[104]
AC	Organic acid	[9]
AC	Pharmaceuticals	[105, 106]
MnO_2/GAC	Nitrobenzene	[107]
Minerals		
Ceramic honeycomb (2MgO-2Al_2-$O_3$5-SiO_2)	Nitrobenzene	[108, 109]
Al_2O_3, TiO_2 On SiO_2 and NaX	Phenol	[110]
Natural brucite ($Mg(OH)_2$, 94.7%;SiO_2, 2.9%)	Phenol	[111]
Raw bauxite, Iron modified bauxite	2,4,6-trichloroanisol	[112, 113]
Alumina silicates	Pesticide dichlorvos	[114]
Non polar systems		
High silica zeolites	Trichlorotoluence, Phenol	[11, 23]
Perfluorinated alumina, perfluorinated MCM-41	Aromatic hydrocarbons, ethers, NOM, dyes, Humic acids	[4, 15, 115-119]
Polydimethylsiloxane	Phenol, chlorophenols, nitrobenzene	[120, 121]

Metals on supports have been used in catalytic ozonation reactions. Among them are ZrO_2/Al_2O_3, CeO_2, CeO_2/TiO_2 or Al_2O_3. The mechanisms of catalytic ozonation in the presence of metals on support are not clear. It has been reported that hydroxyl radicals are not formed in this process and adsorption of pollutants on the surface of the catalysts is important for their effective removal.

Activated carbons have also been successfully used in catalytic ozonation reactions. They have been used successfully to remove colour, dyes [122, 123], phenols [104], pharmaceuticals [105] and organic acids [9] from water. However, the mechanisms of catalytic reactions are not well understood and similar controversies appeared, as discussed previously in the case of metal oxides. For example it is not clear whether activated carbons decompose aqueous ozone leading to the generation of hydroxyl radicals or direct ozone attack is responsible for the degradation of organic pollutants from water. Some reports suggested that activated carbons promote radical formation [105]. Lui et al [124] studied the catalytic ozonation of oxalic acid in the presence of multi-walled carbon nanotubes (MWCNT) and proposed a free radical mechanism. It involves both surface reactions and bulk reactions between the active species and oxalic acid. In this work TBA has been used to identify the radical mechanism.

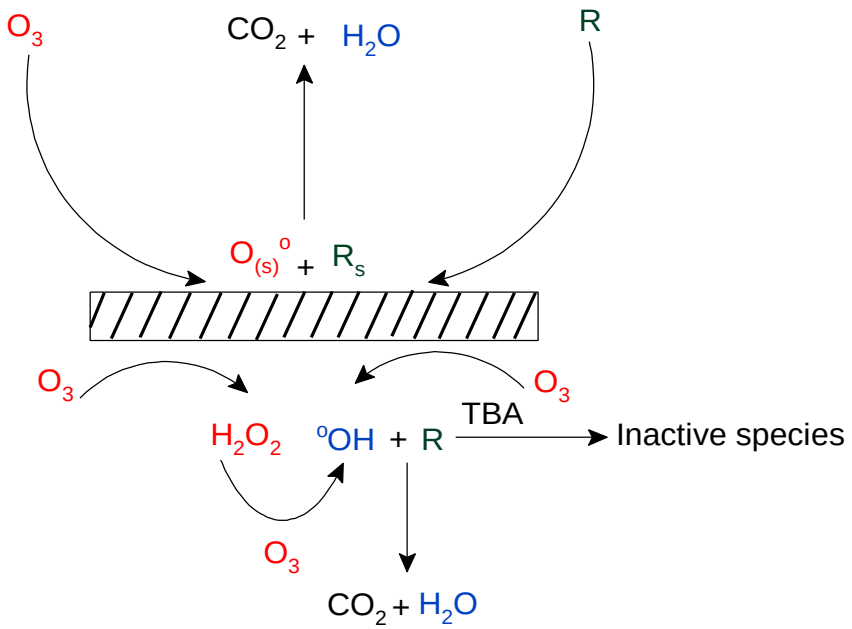

Figure 1.10: Scheme of catalytic ozonation of oxalic acid in the presence of MWCNT (R-oxalic acid; $O_{(s)}$- surface oxygenated chemicals; R_s-adsorbed oxalic acid [124].

The mechanism in the Figure 1.10 shows that hydroxyl radicals can be formed in two ways. One, in which ozone reacts with the surface of MWCNT to generate H_2O_2, which further reacts with O_3 to produce ^{o}OH radicals. The other hypothesized possibility is that ozone interacts with the surface of MWCNT to generate hydroxyl radicals. It has been further reported that ozone may interact with the catalyst's surface to produce singlet oxygen which then reacts with the adsorbed oxalic acid to produce CO_2 and H_2O. However, others are opposed to it and suggested the direct reactions of ozone on the surface of activated carbons [125]. Some of the organic compounds used in ozonation in the presence of activated carbons are listed in the Table 1.7.

The minerals such as cordierite, perovskite and zeolites, pure or modified with metals and metal oxides have been tested in the ozonation process. Their mechanisms are also not well understood and further research is required to understand the process. Some of the minerals and the compound used in ozonation process are presented in Table 1.7.

The non polar systems have also been used in the catalytic ozonation process because of the nonpolar nature of ozone. The ozone has a dipole moment of 0.46D, which indicates that the ozone molecule is non-polar hence it can be suggested that ozone has a high solubility in non-polar solvents [126]. In contrast, its solubility in polar solvents such as water is very low and it decreases with an increase in the pH of water. The solubility of ozone was found to be approximately 10 times higher in perfluorinated hydrocarbons (nonpolar solvents) than that of water [127, 128]. Therefore, hydrophobic materials and materials bonded with non-polar organic compounds have been implied in ozonation systems. It is assumed that oxidation of organic pollutants in the two phase non polar ozonation systems takes place via molecular ozone reactions. However, Gromadzka et al [129] studied the degradation of clofibric acid by ozonation in the presence of

perflorinated solvents, and it was observed that the degradation of clofibric acid took place via hydroxyl radical mechanism and was further reported that ozonation efficiency was decreased in the presence of TBA. A significant increase in the efficiency of pollutants removal such as ethers, humic acids, hydrocarbons, natural organic matter and organic dyes have been reported in ozonation in the presence of two phase non polar systems such as alumina or MCM-41 modified with perfluorooctanoic or perfluorooctadecanoic acids [4, 15, 115-119]. The other systems such as silica gel [130] and high silica zeolites (HSZ) [11, 23, 131] have been successfully used in ozonation systems. However, the mechanism of ozonation in the presence of high silica zeolites is still not well understood. The Figure 1.11 shows the mechanism of nonpolar alumina bonded phase. It was hypothesized by Kasprzyk-Hordern et al [1, 3, 4] that the catalytic activity of perfluorinated catalysts mainly depends upon the hydropohbicity of catalysts and adsorption of organics on the surface of catalysts. The surface reactions between the adsorbed ozone and organic pollutants play a significant role in the removal of pollutants.

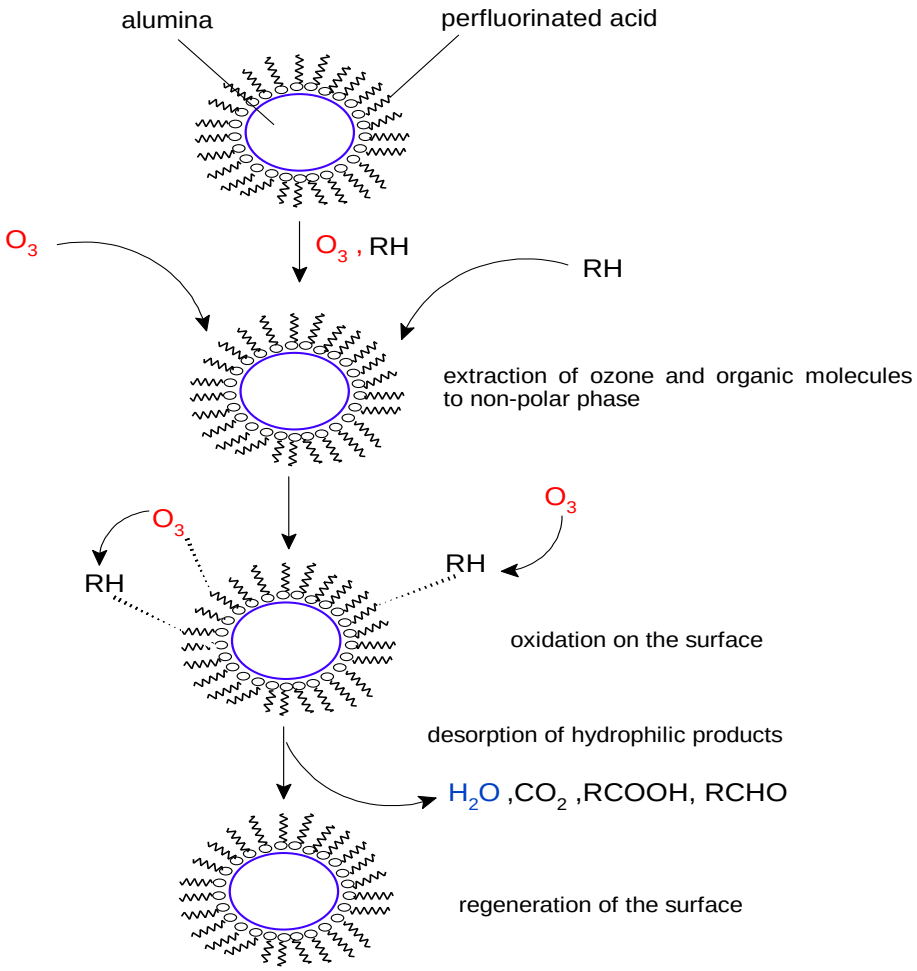

Figure 1.11: Mechanism of ozonation in the presence of non-polar alumina bonded phase [1].

The idea of the using non-polar media in ozonation is promising; however, further investigations are required to understand the mechanism. Some of the two-phase ozonation systems and target organic pollutants are presented in Table 1.7.

1.9.2.3 ZSM-5 zeolites in ozonation process: mechanisms

The ZSM-5 zeolites have been recently used in ozonation systems for the removal of some organic pollutants. Fujita et al [22] investigated the adsorption of water dissolved ozone on high silica zeolites and found that ZSM-5 zeolites can adsorb aqueous ozone and stabilize it. Additionally, it was reported that silica to alumina ratios of zeolites are

important and observed that the higher the silica to alumina ratio the higher the adsorption of water dissolved ozone will be. The ZSM-5 zeolites have been successfully used in the ozonation process for the removal of organic pollutants such as phenol, n-hexadecane and trichloroethene [11, 23, 24]. Amin et al [23] studied the removal of phenol and chemical oxygen demand (COD) on four different types of zeolites (H-ZSM-5, H-Beta, H-Mordenite and H-USY). It was reported that these zeolites successfully removed phenol and COD from water. Additionally, among the zeolites, ZSM-5 was found to be the most effective catalysts. Based on the adsorption results it was assumed this may be because of the hydrophobicity of ZSM-5 zeolites that adsorbe phenol to higher extent and promote surface reactions. Therefore, in current study ZSM-5 zeolites have been selected to investigate the mechanism. However, it is important to to emphasis that other types of zeolites should be investigated in further research.

Furthermore, the process was found to be pH dependent and zeolites were found to be a better catalyst at low pH values. It was hypothesized that this may be due to less stability of ozone at basic pH values. It was further hypothesized that both ozone and phenol adsorbed on the surface of zeolites and their reactions with each other results in the formation of oxidative products of phenol, CO_2 and H_2O (Fig. 1.12). However, no direct proof of this mechanism has been provided.

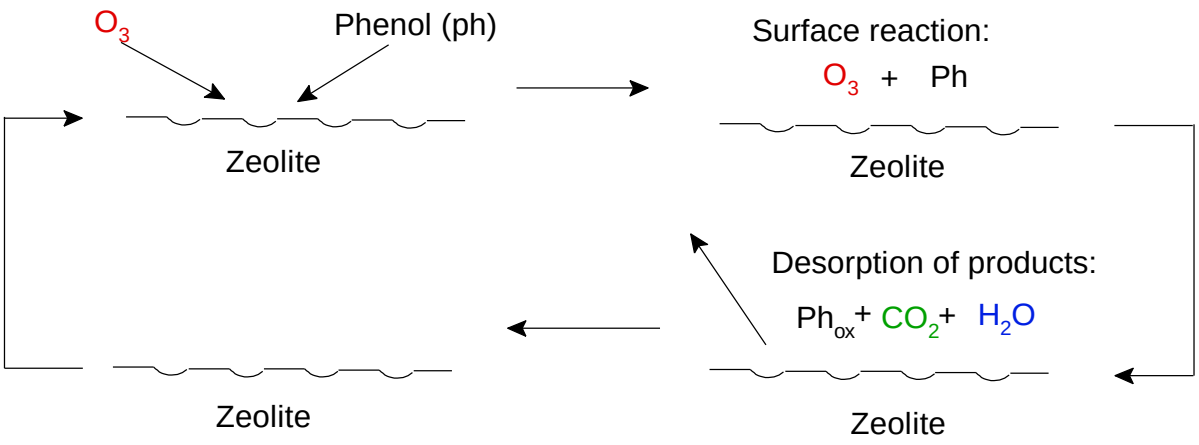

Figure 1.12: Mechanism of phenol removal during the ozonation in the presence of zeolites [23].

In opposed to above hypothesis, Valdes et al [26] reported that Lewis and Bronsted acid sites of zeolites may decompose the aqueous ozone leading to the generation of hydroxyl radicals. Unfortunately, no extensive investigation has been undertaken in order to understand the process occurring during the ozonation in the presence of ZSM-5 zeolites. Based on the previous reports, study on an understanding of zeolites mechanism (in ozonation process) is rather new and their application in water treatment requires the understanding of their mechanisms.

The chemistry of zeolites, classification and their important parameters has been discussed in section 1.11.

1.9.2.4 Discussion

The above literature indicates that the mechanisms of heterogeneous catalytic ozonation processes are not well understood. There are many questions that have to be answered in order to understand the process. One of the major question is whether the catalysts (metal oxides and others) reacts with aqueous ozone leading to the generation of hydroxyl radicals or direct attack of ozone on the surface of catalysts is responsible for the

degradation of pollutants. It is important to notice here that although some reports [18-20] support the radical mechanisms however, ozonation in the same catalysts with some other pollutants have not been successful [4, 15]. The role of adsorption, surface properties of catalysts, effect of pH etc is important to understand the catalytic ozonation processes. In this research work an effort has been made to understand the catalytic ozonation process. For this purpose two different types of materials have been selected. Alumina is one of the widely used metal oxides in catalytic processes as heterogeneous catalysts and as support therefore it has been selected among the metal oxides. The catalytic ozonation process on alumina was compared with several ZSM-5 zeolites. Furthermore, in this work the catalytic ozonation of different type of pollutants such as VOCs, ibuprofen and acetic acid has been performed, this study may help to understand the role of adsorption and surface reactions in catalytic processes.

1.10 Chemistry of Alumina

Due to the growing applications of alumina in drinking and wastewater purification, it is important to know the structure of alumina and its possible interactions with water. The properties of metal oxide surfaces in aqueous media, including sorptive capacity and surface charging are determined by the nature of their functional groups. It is assumed that surface properties of metal oxides play an important role in the mechanism of catalytic ozonation [18-20]. It is therefore important to understand the chemistry of alumina.

1.10.1 Classification of Alumina

The Haber (European) and American classifications of alumina have been provided in the Table 1.8.

Table 1.8: Classification of alumina [132]

Chemistry	α-group	ß-group	γ-group
Haber classification			
Al_2O_3	corundum	-	gamma oxide
Al_2O_3 H_2O	diaspore	-	boehmite (bauxite)
Al_2O_3 $3H_2O$	does not exist	-	gibbsite
American classification			
Al_2O_3 H_2O	boehmite	diaspore	-
Al_2O_3 $3H_2O$	gibbsite	bayerite	nordstrandite

It was reported by Stumpf et al that apart from the α-Al_2O_3, another six crystal structures of alumina occur: γ, δ, κ, ή, ί and χ-Al_2O_3. The sequence of particular type formation under the thermal processing of diaspore, boehmit, bayerite and gibbsite is as follows [132].

$$\text{Diaspore} \xrightarrow{450^oC} \alpha\text{-}Al_2O_3$$

$$\text{Boehmite (AlOOH)} \xrightarrow{450^oC} \gamma\text{-}Al_2O_3 \xrightarrow{600^oC} \delta\text{-}Al_2O_3 \xrightarrow{1050^oC} \theta\text{-}Al_2O_3 \xrightarrow{1200^oC} \alpha\text{-}Al_2O_3$$

$$\text{Bayerite (Al (OH)}_3) \xrightarrow{230^oC} \acute{\eta}\text{-}Al_2O_3 \xrightarrow{850^oC} \theta\text{-}Al_2O_3 \xrightarrow{1200^oC} \alpha\text{-}Al_2O_3$$

$$\text{Gibbsite (Al (OH)}_3) \xrightarrow{250^oC} \chi\text{-}Al_2O_3 \xrightarrow{900\ ^oC} \kappa\text{-}Al_2O_3 \xrightarrow{1200^oC} \alpha\text{-}Al_2O_3$$

There have been other classifications proposed by Munster et al and Lippens et al. All these structures are based on more or less closed packed oxygen lattice with alumina ions in the octahedral and tetrahedral interstices. Furthermore, the low temperature aluminas are characterized by cubic closed packed oxygen lattices; however the high temperature aluminas are characterized by hexagonal close-packed lattices [132]. The crystal structure

of corundum (α-Al_2O_3) consists of closed packed planes (A and B) of oxygen anions stacked in the sequence as shown in Figure 1.13. Figure 1.14, shows the complete stacking sequence of oxygen and alumina layers will form A-a-B-b-A-c-B-a-A-b-B-c-A.....[133].

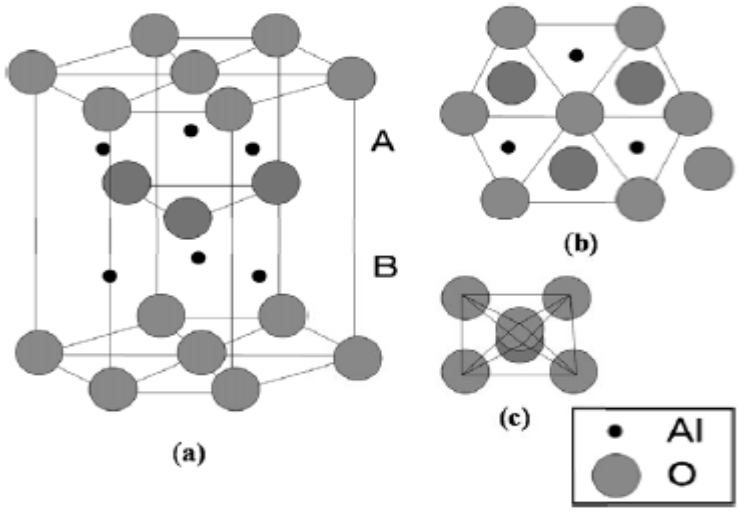

Figure 1.13: (a) Corundum structure in α- Al_2O_3 , (b) top view of the corundum structure, and (c) octahedral structure of α- Al_2O_3 [133].

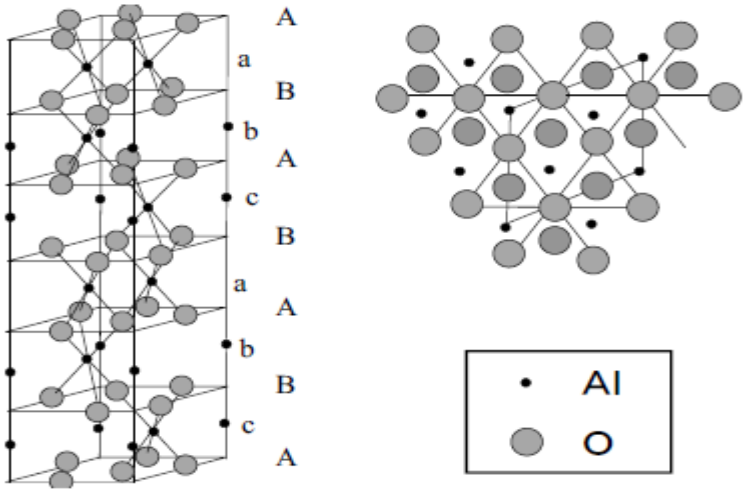

Figure 1.14: Structure of α-Al_2O_3 [133].

In terms of catalytic activity the low temperature aluminas are more active than that of high temperature ones. This may be due to the lower surface area and different population

of surface active sites of high-temperature aluminas when compared with low-temperature ones [132].

1.10.2 Surface of Alumina

The surface chemistry of alumina may play an important role in the catalytic process. It is important to know the active sites of catalysts in order to understand the mechanism of the process. The two main parameters determining the catalytic properties of alumina are acidity and basicity. Lewis acidity-basicity is the ability to accept-donate electron pairs. Bronstead acidity-basicity is the ability to accept and donate protons. The alumina can adsorb water molecules, depending on the temperature, yields to chemisorption or physisorption as dissociated form with the formation of surface hydroxyl groups. The surface hydroxyl groups of alumina are formed at higher temperatures and gradually expelled as H_2O. However, even at higher temperature (800ºC-1000ºC) and in vacuum, some tenths of a percent of water are still retained in the alumina. The hydroxyl groups formed on the surface of alumina behave as Bronstead acid sites. Furthermore, the degradation of two neighbouring hydroxide (OH^-) ions causes the formation of strained oxygen bridges on the surface of alumina (Fig. 1.15). The Lewis and Bronstead acid sites of alumina are considered to be the catalytic centres. Furthermore, it has been reported that surface hydroxyl groups of alumina (Bronstead acid sites) can interact with the ozone, leading to the formation of hydroxyl radicals [132].

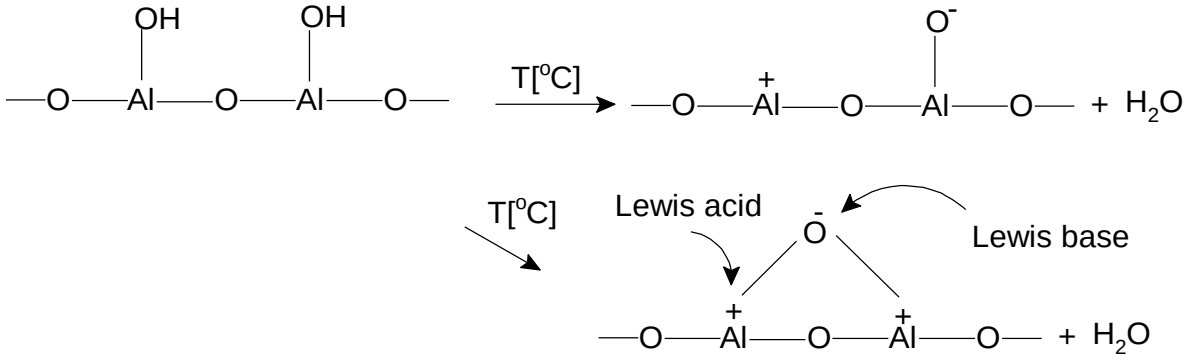

Figure 1.15: Scheme of mechanism of ozone decomposition by [132].

1.10.3 Surface hydroxyl groups of alumina and pH effect

It has been reported that the surface hydroxyl groups of alumina can decompose aqueous ozone [18-20]. Therefore, in order to understand the mechanism of catalytic ozonation, it is very important to know the nature of surface hydroxyl groups on alumina in aqueous solutions.

In aqueous solutions there would be greater complexity in the surface hydroxyl groups of alumina, as water molecules interact with the surface hydroxyl groups of alumina. The pH of water and the point of zero charge of alumina (pH_{PZC}, point of zero charge, the pH value at which the net surface charge is zero) are also important to consider. Additionally, in aqueous solutions an electric double layer at the solid - liquid interface is formed as a result of the electrostatic interactions between the ions in the solution and the charged alumina ions. These interactions also depend upon the pH of the solution, as the concentration of positive (H^+) and negative (OH^-) ions changes with the change in pH of the solution. The properties of the surface of alumina strongly depend on the pH value. In acidic medium, below the point of zero charge of alumina, the surface is positively charged. In a basic medium ($pH > pH_{pzc}$) the surface is negatively charged as shown in Figure 1.16 [132].

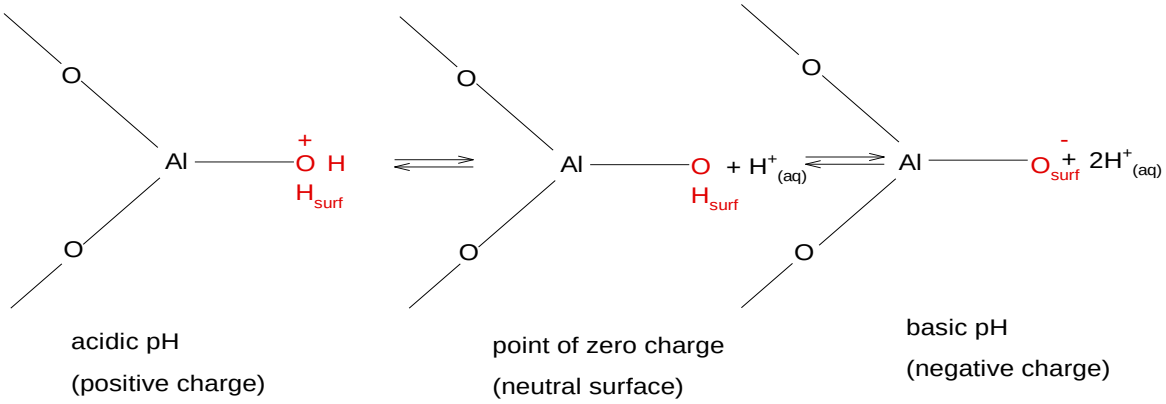

Figure 1.16: The surface of alumina and pH of solution [132].

1.11 Zeolites: an introduction

Zeolites are crystalline aluminium silicates with an open, three dimensional frameworks constituting of tetrahedral SiO^{4-}_4 and AlO^{5-}_4 units linked through shared oxygen in a continuous array (Fig. 1.15) [134, 135]. In the eighteenth century a Swedish mineralogist, Cronstedt discovered zeolites. Zeolites can be classified as synthetic and natural zeolites. The synthetic zeolites are usually prepared in a media containing bases and cations. The principal raw materials used are silica and alumina. Furthermore, they can be manufactured according to desired structures. The examples are ZSM-5, ZSM-11 and silicate. The synthetic zeolites are not only applied in powder form but also as pellets and beads, which are manufactured by mechanical means after the addition of binders. Natural zeolites are formed as a result of a chemical reaction between volcanic glass and saline water for 50,000 years.

In zeolites frameworks the tetrahedral coordination of alumina atoms generates charge deficiency, which is balanced by cations. These cations are not an integral part of the framework. The zeolites may adsorb water molecules depending upon their silica to alumina ratios. The greater the silica to alumina ratio the lesser will be the adsorption of

water molecules [136, 137]. The water can be removed thermally at around 400 ^{o}C to 500 ^{o}C and this leaves the zeolite in its active state. When the zeolite is dehydrated, the cations become highly mobile and can be replaced by ion exchange to varying degrees, depending on the zeolite structure and exchanging cations [138]. The type and number of cations may affect the catalytic properties of zeolites.

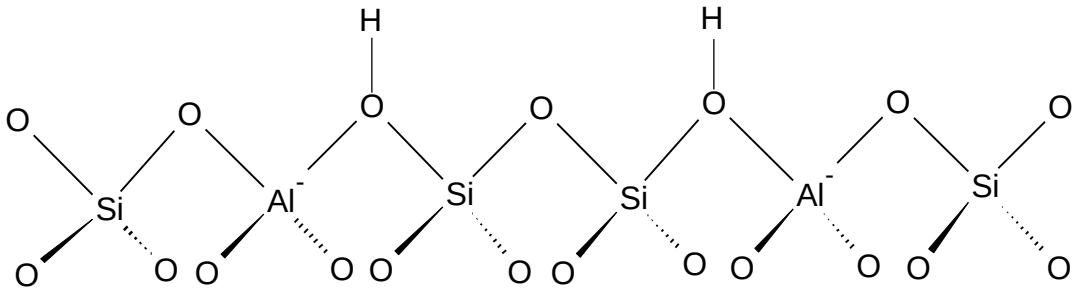

Figure 1.17: Schematic representation of a zeolite in the H form [139].

1.11.1 Classification of molecular sieves

The molecular sieves are classified on the bases of their pore size into macro porous, mesoporous and micro porous as shown in the Table 1.9 [140, 141]. The micro porous molecular sieves can be further divided into ultra large, large, medium and small openings depending on their channel size as shown in Table 1.9 [140, 141].

Table 1.9: Classification of molecular sieves on the basis of pore size [140, 141]

Definition	Example	Pore size (Å)
Macro porous	Porous glasses	> 500
Mesoporous	MCM-41	20-200
	MCM-48	20-200
Micro porous		
Ultra large	UTD-1	7.5
	VPI-5	12.1
Large	Zeolite-β	6.4-7.6
	ZSM-12	5.5-5.9
	Zeolite Y	7.4
Medium	ZSM-5	5.3-5.5
	ZSM-48	5.3-5.6
Small	Zeolite-A	4.1

1.11.2 Adsorption and separation

Zeolites have been used for adsorption and separation of different type of compounds. The shape selective properties of zeolites are also the basis of their use in molecular adsorption. Their ability to exclude some molecules and adsorb certain molecules makes them a unique adsorbent [142]. The hydrophobic zeolites preferentially adsorb non-polar organic compounds. The cation containing zeolites are extensively used as desiccants due to their high affinity to adsorb water. Thus zeolites can separate molecules based on differences in shape, size and polarity.

1.11.3 Significance of silica to alumina ratio

The silica to alumina ratio (Si/Al) of zeolites plays an important role in their catalytic behaviour, ion exchange capacity and their ability to adsorb polar and non-polar molecules. The molecules can adsorb on external and internal surfaces, the relative

polarities of the solvent, adsorbent and solute play a significant role in the adsorption. The polarities depend upon the silica to alumina ratios [142, 143].

The zeolites with low Si/Al ratio, having high concentrations of balancing H^+ ions are hydrophilic in nature and they possess strong affinity for polar molecules. The zeolites with high Si/Al ratio are hydrophobic and can adsorb hydrophobic compounds. The stability of zeolites crystal frame work also depends upon Si/Al ratio and increase with the increase of silica to alumina ratios [143].

The polarity of zeolites pores is an important property and it depends on the alumina content in zeolites. The hydrophobicity/hydrophilicity is related to the polarity of zeolites pores. The zeolites without alumina in the frameworks are more hydrophobic. The zeolites molecules may adsorb water molecules to some extent and zeolites with more polarity can adsorb more water molecules. These water molecules generate Bronstead acid sites on zeolites that are important in catalytic processes [136, 137].

1.11.4 Acid properties of zeolites

1.11.4.1 Bronsted acid sites

Pure siliceous zeolites are electrically neutral. By replacing their silicon (tetrahedrally coordinated with oxygen atoms; having a formal charge of 4^+) with aluminium (formal charge 3^+) in the zeolite lattice, results in a negatively charged tetrahedron. The counter ions (such as Na^+, K^+, H^+ etc.) compensate the negative charge. The Bronsted acid sites have been created when counter ions are H^+. The protons (H^+) are formally assigned to be bonded to the bridging oxygen of a Si-O-Al bond to form hydroxyl groups that act as Bronsted acid sites. Furthermore, the strength of these sites depends upon the structure of zeolites and their chemical composition [144]. These acid sites may be important to an understanding of the mechanism of catalytic process. It has been reported that Bronsted

acid sites in zeolites may decompose aqueous ozone [26]. In this work ZSM-5 zeolites with different composition and counter ions have been used to investigate this effect.

1.11.4.2 Lewis acid sites

Lewis acid sites are related to the formation of positively charged oxide clusters or ions within the porous structures of zeolites. These species are typically silica/alumina or alumina. They may be formed by the extraction of aluminium from the lattice, or metal ions exchanging for the protons of acid sites. It has been reported by Valdes et al [26] that in the case of natural zeolites the Lewis acid sites may generate at basic pH values in water ($pH > pH_{PZC}$), and these sites may decompose aqueous ozone. However it is reported that in aqueous solutions water molecules adsorb on zeolites and block Lewis acid site [136, 137].

1.11.5 Zeolites as catalyst

Zeolites can act as catalysts for chemical reactions, which take place within the internal cavities. They are a useful catalyst for several reactions involving organic compounds and an important reaction is that involving hydrogen exchange zeolites, whose framework-bound protons give rise to very high acidity. Metal loaded zeolites have also been used as catalysts for example titanium loaded ZSM-5 zeolites have been used in the production ε-caprolactam and copper loaded zeolites have been used in NO_x decomposition [145, 146]. The zeolites have been implied in crude oil cracking, isomerisation and hydrocarbon synthesis [147]. Zeolites can promote a wide range of reactions such as acid-base and metal induced reactions. Additionally, these reactions can take place within the pores of zeolites that allows a greater degree of product control. The zeolites pore size and shapes are important and can exert a steric influence on the reactions. The zeolites are often considered to act as shape selective catalysts [147].

1.11.5.1 ZSM-5 zeolites as catalysts

ZSM-5 is a synthetic heterogeneous catalyst developed by Mobil Oil. It belongs to three-letter zeolites structure code MFI, family. The secondary building units in ZSM-5 zeolites are 5-1 rings (Fig. 1.18a). The ZSM-5 zeolites are constructed from pentasil units that are linked together to form pentasil chains as shown in figure 1.18c.

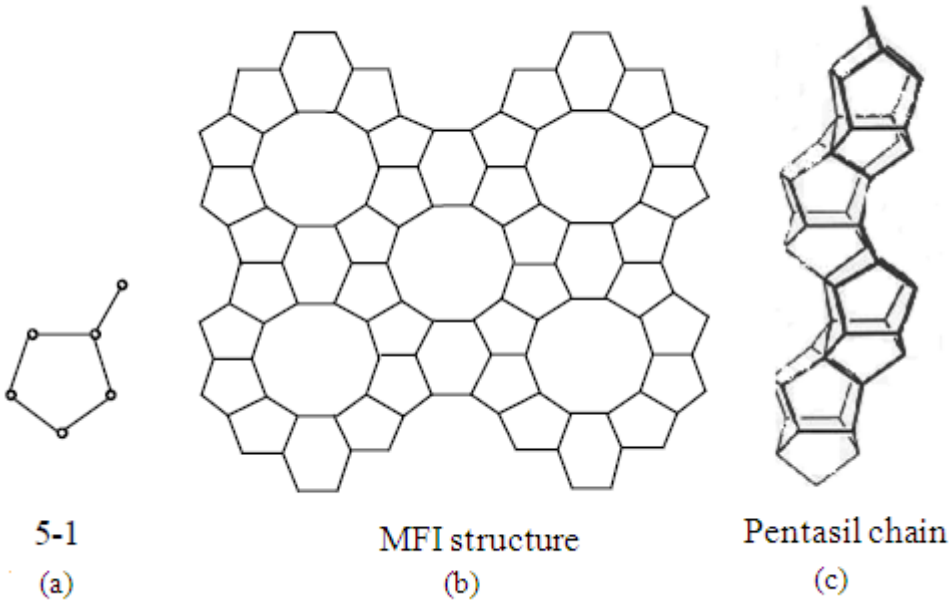

Figure 1.18: (a) 5-1 secondary building unit, (b) the MFI structure and (c) pentasil chain

It is a high silica zeolite (HSZ); the high silica content makes it hydrophobic in nature [120, 121]. The hydrophobicity of these materials makes them good adsorbents of hydrocarbons. When the silica ion is substituted by alumina, an extra positive charge is required to balance the overall charge. In aqueous solutions the water molecules are adsorbed on zeolites and form Bronstead acid sites and strength of these acid sites depends upon the alumina content of HSZ [136, 137].

1.12 Factors affecting the mechanism of catalytic ozonation

Various factors such as pH of solution, adsorption of pollutants on catalyst surface, effect of hydroxyl radical scavengers (t-butanol), and the effect of inorganic ions (e.g. phosphates, carbonates, bicarbonates, sulfates) play an important role in an understanding of the mechanism of the catalytic ozonation process. In current research, the effect of above mentioned factors has been studied in ozonation over ZSM-5 zeolites and alumina.

1.12.1 Effect of pH

The pH of a solution plays an important role in the study of the mechanisms of catalytic ozonation, since it affects ozone decomposition. Furthermore, it determines the surface properties of the catalysts and properties of the analytes being oxidised. Ozonation reactions at different pH follow different mechanisms. It is well-known that the presence of OH^- ions in water leads to ozone decomposition and the generation of hydroxyl radicals (^oOH), which then react with organics in a non-selective way [36]. The pH of a solution could also affect the surface properties of catalysts such as metal oxides. Alumina is a good example. At basic pH ($pH > pH_{PZC}$) the surface of alumina is negatively charged (no surface hydroxyl groups present), at acidic pH ($pH < pH_{PZC}$) its surface is positively charged, while at $pH = pH_{PZC}$ the surface of alumina is neutral (surface hydroxyl groups with no charge) [132].

The pH of solutions may also change the surface properties of zeolites. For example, Valdes et al [27, 28] reported that the pH of a solution can affect the aqueous ozone decay rates in the presence of zeolites. It was stated that at $pH > pH_{PZC}$ zeolites are negatively charged and Lewis acid sites may be responsible for ozone decay. On the other hand at $pH < pH_{PZC}$ the surface will be positively charged and Bronsted acid sites on zeolites may be responsible for aqueous ozone decay and generation of hydroxyl radicals [26, 27]. It has to

be however noted here that zeolites (and aluminas) do not exhibit Lewis acidity in the presence of water as Lewis sites hydrate and becomes Bronsted sites [136, 137]. It is therefore important to investigate the effect of pH in order to understand the mechanism of catalytic ozonation processes.

1.12.2 Effect of adsorption of pollutants

An investigation of adsorption of pollutants on the surface of catalyst is an important factor, since it can affect the mechanism of the catalytic ozonation process. Furthermore, comparison between the efficiency of the removal of pollutants by adsorption alone, ozonation alone and catalytic ozonation can be used to determine the extent of removal of pollutants by catalytic effect. Some reports suggested that adsorption of pollutants on the surface of the catalyst is important. In contrast, some reports indicate that adsorption is not important in the catalytic ozonation process.

Ernst et al [17] studied the degradation of organic acids by ozonation in the presence of alumina and observed that the organic acid which adsorbed least had better degradation rate when compared with others. It was suggested that the degradation of pollutants occurs in the solution rather than on the surface of the catalyst.

Kasperzyk-Hordern et al [15] studied the removal of hydrocarbons (cumene, chlorobenzenes) and observed that alumina did not adsorb these pollutants. Additionally, it was reported that alumina did not show any significant removal of pollutants by catalytic ozonation. In the same investigation alumina bonded with perfluorooctanoic acid showed higher catalytic activity and had higher adsorption of hydrocarbons on catalyst.

The natural organic matter (NOM) has been removed by ozonation in the presence of alumina [3]. It was reported that alumina has high adsorption of natural organic matter and

it showed the catalytic effect. Therefore, it was hypothesized that surface reactions are important in catalytic ozonation and adsorption of pollutants plays an important role in catalytic ozonation.

The organic molecules differ in the nature of the functional groups, they have different molecular weights and molecular sizes, therefore their sorption mechanism are diverse. The pH of the solution can affect the surface charging of organic compounds that have acidic, basic and amphoteric properties; they may be present in the form of cations or anions. The organic compounds may form stable complexes with metal cations and therefore, may result in the chemical dissolution of adsorbents. [132].

Apart from the functionality, the hydrophobicity and hydrophilicity of both organic molecule and adsorbent are important in the adsorption process. The metal oxides (e.g. Al_2O_3) are hydrophilic in nature therefore non-ionic, hydrophobic organic compounds such as chlorobenzenes, alklybenzenes and polycyclic aromatic hydrocarbons interact weakly and non-specifically with mineral surfaces [132].

An understanding of the adsorption of carboxylic acids on metal oxide surfaces is vital since these compounds are commonly present in the treated water. They are also the main oxidation by-products, which are resistant to ozone. The –COOH groups comprise a significant part of natural organic matter, which is a typical component of natural water. The adsorption of carboxylic acids on alumina is thought to occur via ligand exchange reaction, which results in the replacement of surface hydroxyl groups of alumina (Fig. 1.19b) or by the esterification mechanism (Fig. 1.19a) [148].

According to Karaman et al [148] surface coordination, or ligand exchange model, the anions of carboxylic acids replace the surface hydroxyl groups of alumina. The nature of

the interactions between the surface hydroxyl groups of alumina and carboxylic acids have been studied by several groups [132] and it is believed that carboxylic groups adsorb on the alumina surface by replacing the surface hydroxyl groups of alumina [4, 18-20]. It is therefore important to know the effect of carboxylic acids in ozonation process.

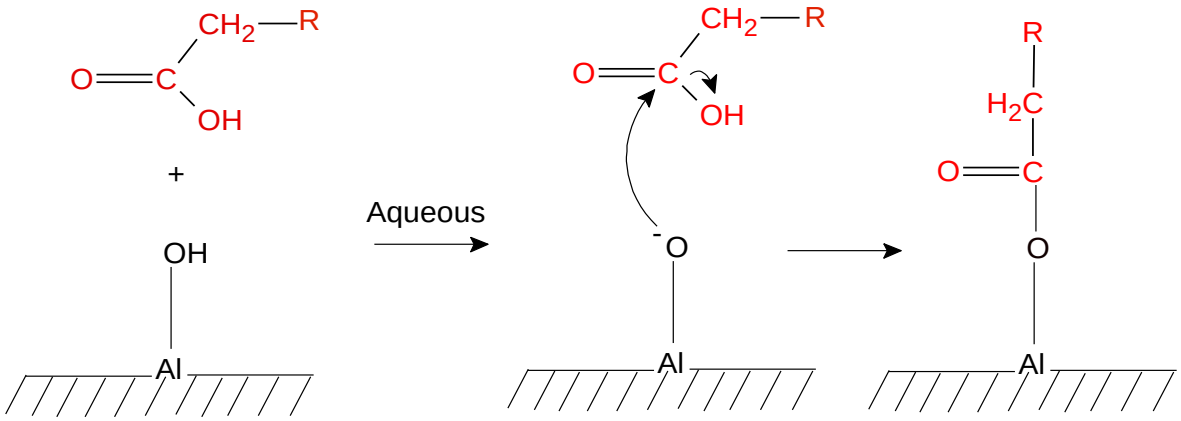

(a) Esterification mechanism

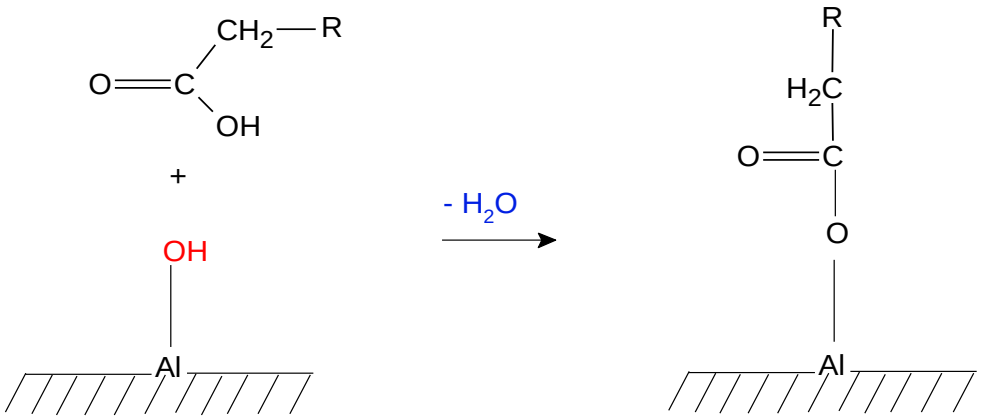

(b) Ligand exchange reaction

Figure 1.19: The esterification and ligand exchange mechanisms between hydroxyl groups on the alumina surface and carboxylic acids [148].

The adsorption of pollutants on zeolites depends upon various factors such as, composition, surface area, pore size, size of adsorbents and silica to alumina ratio. The zeolites have been used for the adsorption and separation of many types of organic

compounds such as nucleosides, nucleotides [142], and hydrocarbons [149] etc. The silica to alumina ratios, porosity and surface areas are found to be among the important factors that can affect adsorption.

The ZSM-5 zeolites are hydrophobic in nature and they have high adsorption capacity towards non polar compounds rather than polar organic compounds. They have been found to be good adsorbent of hydrocarbons [149]. It is therefore, important to investigate the effect of adsorption of different types of organic pollutants on the catalytic ozonation process.

1.12.3 Effect of phosphates

Inorganic ions such as phosphates (PO_4^{3-}), carbonates (CO_3^{2-}) and sulphates (SO_4^{2-}) may be present in natural waters. These ions may adsorb on the catalyst surface and poison it [132]. It is therefore important to know the effect of these ions on the catalytic reactions. In this study phosphates have been selected, since they are harder bases than carbonates and sulphates and have the strongest affinity to adsorb on the surface of alumina [132]. It is known that the adsorption of phosphates occurs through the ligand exchange, which results in the replacement of surface hydroxyl groups of alumina and the deprotonation of phosphates [150]. It is a well-known fact that different forms of phosphates exist at different pH ranges (these are H_3PO_4, $H_2PO_4^-$, HPO_4^{-2} and PO_4^{-3}). Concentration of protonated forms of phosphates are highest at acidic pH, hence the surface hydroxyl groups of alumina may be rapidly replaced at acidic pH as phosphate adsorption was considered to occur through exchange via replacing the surface hydroxyl groups of alumina [150]. Ligand exchange can also take place in the presence of water molecules and other easily displaced ligands coordinatively bonded to the sites [151]. Additionally, it was reported that the catalytic activity of alumina was greatly reduced in the presence of

phosphates [84]. Therefore ozonation experiments in the presence of phosphates have been conducted in order to verify the importance of hydroxyl groups present on the surface of alumina in ozone decomposition and to understand the possible influence of phosphates on ozonation in the presence of ZSM-5 zeolites, since the effect of phosphates on ozonation in the presence of ZSM-5 zeolites has not been investigated previously.

1.12.4 Effect of hydroxyl radical scavengers (t-butanol)

Tertiary butanol (TBA) has been used in ozonation reactions in order to understand the mechanism of the process. t-butanol is a hydroxyl radical scavenger and reacts with hydroxyl radicals (^{o}OH) with a rate constant of 6×10^{8} $M^{-1}s^{-1}$ [152]. It reacts directly with ozone with a rate constant of 3×10^{8} $M^{-1}s^{-1}$ [153]. The ^{o}OH radicals react with t-butanol by abstracting an H-atom mainly from the carbon (95%) and to a much lesser extent, from oxygen (Equations 1.15, 1.16) [154].

$$^{o}OH + (CH_3)_3COH \rightarrow H_2O + {}^{o}CH_2C(CH_3)_2OH \quad (1.15)$$

$$^{o}OH + (CH_3)_3COH \rightarrow H_2O + (CH_3)_3CO^{o} \quad (1.16)$$

TBA has been used in the ozonation process to understand whether the process involves hydroxyl radicals or direct attack of ozone decomposes the organic pollutants. The decrease in degradation rate of certain pollutants in the presence of TBA indicates the radical mechanism.

1.13 Reactive oxygen species

Reactive oxygen species (ROS) are highly reactive molecules containing oxygen. It has already been described (see 1.6.2) that aqueous ozone reacts with hydroxide ions in water leading to the production of ROS. Among them are superoxide radical ($^{o}O_2^{-}$), molecular oxygen (O_2), hydroxyl radicals (^{o}OH), hydrogen peroxide (H_2O_2) and their conjugates. In

this research work formation of the superoxide radical ($^{o}O_2^-$), hydroxyl radicals (^{o}OH) and hydrogen peroxide (H_2O_2) have been investigated during the ozonation and catalytic ozonation process.

1.13.1 Superoxide anion radical ($^{o}O_2^-$) and its reactions

The superoxide anion ($^{o}O_2^-$) has both anionic and radical character. As described before (see 1.6.2) superoxide may exist in $^{o}O_2^-$ form or in the form of its conjugate acid (hydroperoxy radical, HOO^{o}), depending on the pH of the water. Therefore, with regard to the superoxide anion, it is important to take into account the reactions of its conjugate acid. The reactivity of $^{o}O_2^-$ depends on its basicity and nuleophilicity in the reacting systems. It can be argued that the basicity of the superoxide anion would be greater in a aprotic medium than in a protic medium. This may be because $^{o}O_2^-$ is more basic without a solvation shell than when it is solvated. However, it is important to note that in the case of the reactions of superoxide with ascorbic acid and α-tocopherol, the reactivity is unexpectedly higher in aqueous solutions than in an aprotic solvent, dimethylformamide (DMF) [155]. This is because in the aprotic medium, the basicity of the proton donors is increased even more than that of superoxide anion. Hence, deprotonation by superoxide anion in aqueous solution is faster [155]. Therefore, basicity of superoxide ion doesn't only depend on the pka value, but also on the solvent system and acidity (or basicity) of the proton donor).

The reactions of the superoxide anion as a nucleophile have been reported in aprotic media. However, there is little evidence indicating the nucleophilic activity in protic media [156]. This may be due to the strong solvation of superoxide anion by the protic solvents. On the other hand, superoxide anion is a strong nucleophile in aprotic media. It reacts with acyl halides, alkyl halides, esters and acyl anhydrides to produce peroxy

radical intermediates through nucleophilic substitution reactions as presented in Figure 1.20 [155]. In these reactions superoxide anion undergoes an addition reaction with carbonyl groups and form radical anion intermediates.

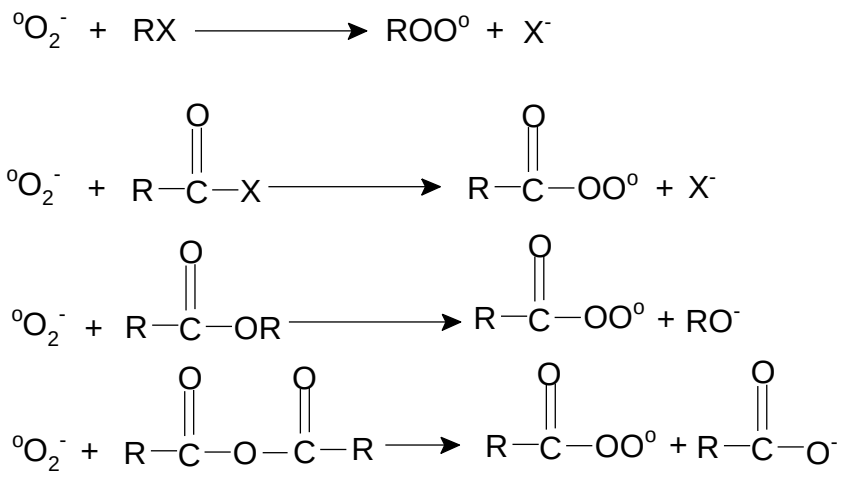

Figure 1.20: The reactions between superoxide anion and an alkyl halide, an acyl halide, an ester and anhydride in aprotic media [155].

It has been reported that the superoxide anion can add to positively charged carbon-carbon double bonds (Fig. 1.21). Similar mechanism has also been suggested for carbon-nitrogen double bond containing compounds [157].

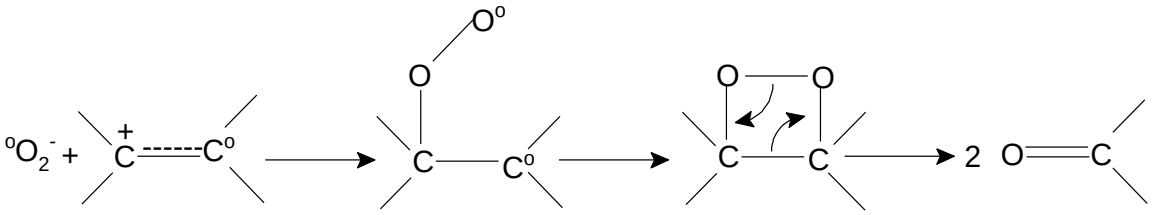

Figure 1.21: The addition reaction between superoxide anion and unsaturated radical cation [157].

In the case of hydrogen abstraction mechanisms superoxide anion reacts by abstracting a proton from the organic compound, as indicated by the reaction of hydroxylquinone (Fig. 1.22).

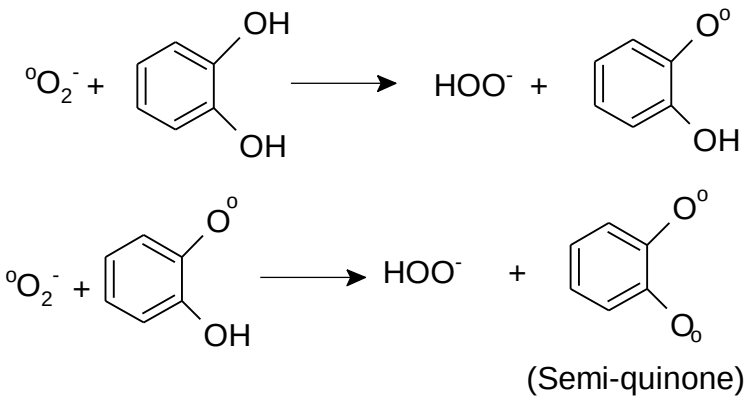

Figure 1.22: Mechanism of formation of semi-quinone by the reaction between superoxide anion and catechol [157].

The superoxide anion can also undergo on electron transfer reactions with many organic compounds. Many aromatic compounds can undergo one-electron transfer reactions, such as nitro compounds (Fig. 1.23) and guinone, [158]. These reactions have been reported in both protic and aptotic media.

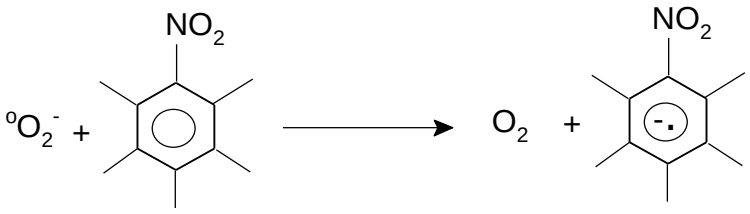

Figure 1.23: Electron transfer reaction of superoxide anion with nitro compounds [158].

1.13.2 Hydroxyl radical (^{o}OH) and its reactions

The hydroxyl radicals are one of the most important ROS. They are known as the most reactive member of the radical family and are an important oxidant in the advanced

oxidation process. The reactions involving hydroxyl radicals are similar in both the aqueous and gas phase. There are three main mechanisms by which hydroxyl radicals react with organic compounds such as, hydrogen abstraction, electrophilic addition and electron transfer reactions.

The hydrogen abstraction reactivity of hydroxyl radicals depends on the strength of the R-H bond in the substrate which can be defined by the difference between the bond formation of the product (HO-H) and bond dissociation energies of the substrate (R-H) [156, 159]. These reactions can occur in aldehydes, ketones, esters, alcohols, alkanes, haloalkanes, carboxylic acids, thiols, amines and hydroperoxides [159].

The hydroxyl radicals react with alcohols via the hydrogen abstraction mechanism. The hydrogen abstraction can occur at both C-H and O-H. However, due to the lower bond dissociation energy of C-H bond than that of the O-H bond, it will be dominant at C-H bond. The reactions of primary, secondary and tertiary alcohol are presented in Figure 1.24.

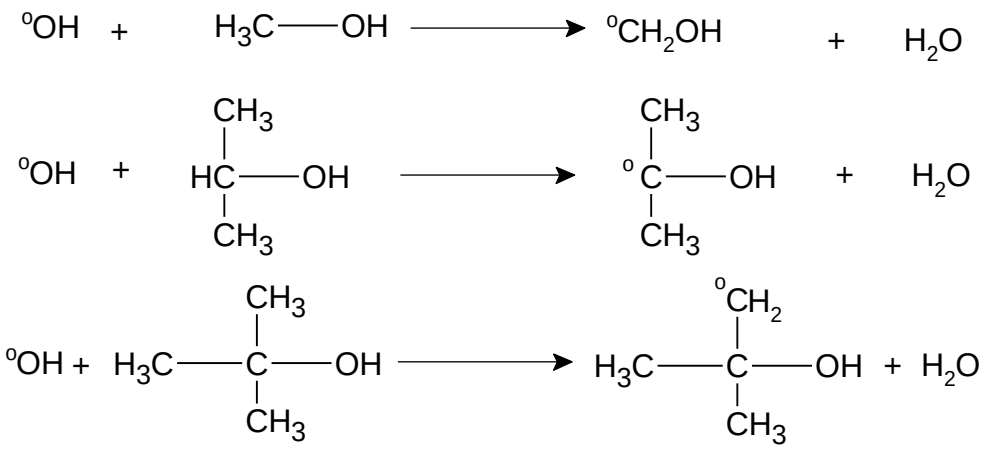

Figure 1.24: Hydrogen abstraction mechanism of hydroxyl radicals from methanol, 2-propanol and 2-methyl-2-propanol [159].

In the case of aliphatic aldehydes, hydrogen atom abstraction by hydroxyl radicals occurs at the hydrogen attached to the carbonyl group [159]. Figure 1.25 indicates the hydrogen abstraction mechanism in the case of formaldehyde.

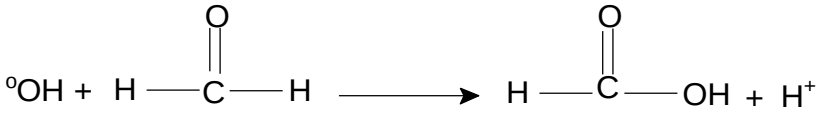

Figure 1.25: Hydrogen abstraction mechanism of hydroxyl radicals with formaldehyde [159].

The hydrogen abstraction mechanism also occurs when hydroxyl radicals react with alkanes. For example, hydrogen abstraction occurs in the case of 2-methylpentane (Fig. 1.26). The reactivity of the tertiary C-H is higher because of the lower bond dissociation energy. Hydroxyl radicals also react with carboxylic acids via the hydrogen abstraction mechanism. Usually, the hydrogen abstraction occurs in the furthest position from the –COOH group. However, α-hydroxy acids tend to react with hydroxyl radicals by α-hydrogen abstraction [159].

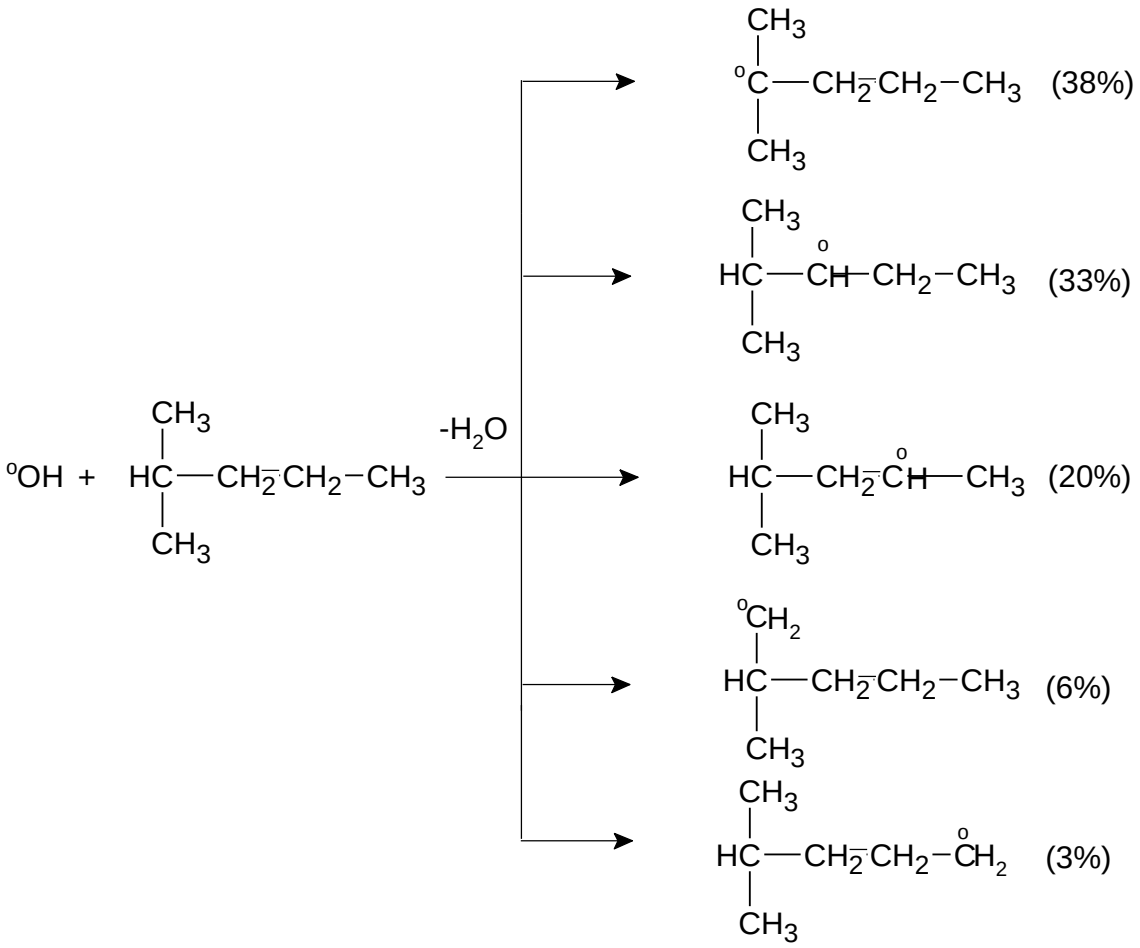

Figure 1.26: Hydrogen abstraction mechanism of hydroxyl radical from 2-methylpentane [159].

Another important mechanism by which hydroxyl radicals react with organic compounds is the electrophilic addition reaction. This reaction occurs in the organic compounds where the bond dissociation energy of C-H is too high to allow abstraction of hydrogen atoms. Among the organic compounds that react via electrophilic reactions are alkenes, alkynes, aromatic compounds and thiols. Following are some examples of these types of reactions. The reactions of unsaturated alkenes (Fig. 1.27) occurs by the addition of hydroxyl radical to the C-C double bond having less substituted carbon atoms [159]. Another example of the electrophilic addition reaction of hydroxyl radicals is their reactions with

aromatic compounds (Fig. 1.27). The conjugated π-system provides a relatively stable OH-adduct radical by delocalization.

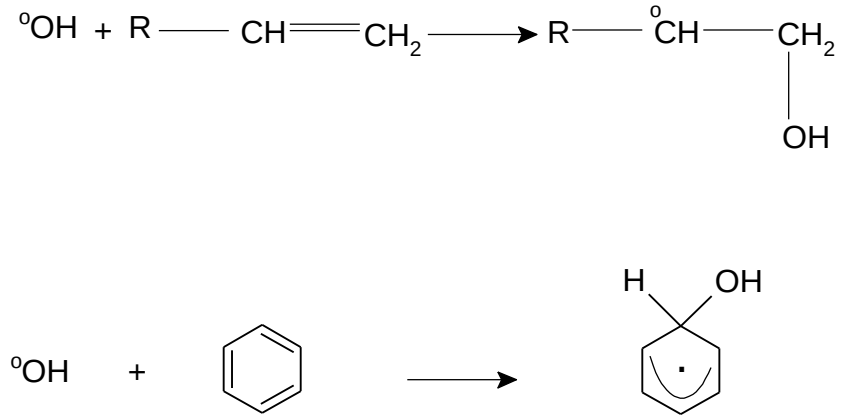

Figure 1.27: Electrophilic addition reactions of hydroxyl radicals [159].

The aromatic compounds may react with hydroxyl radicals by electron transfer reactions. For example, the electrons transfer pathways in the p-dimethoxybenzene (Fig. 1.28).

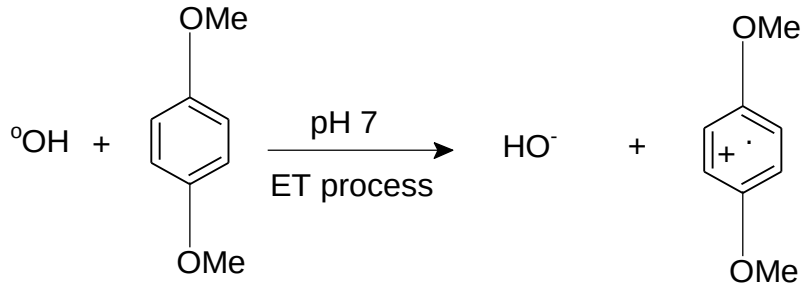

Figure 1.28: Reaction of hydroxyl radical and p-dimethoxybenzene by electron transfer mechanism [160].

1.13.3 Hydrogen peroxide (H_2O_2) and its reactions

The hydrogen peroxide is one of the stable ROS. It has both nuleophilic and electrophilic properties. The electrophilic character arises from the fact that the bond between the two oxygen atoms can be easily polarized [161]. Hydrogen peroxide being a weak oxidant has limited ability to react with organic compounds such as olefins and aromatic hydrocarbons

[161]. In aqueous solutions the hydrogen peroxide dissociates into its derivatives depending on the pH. Under basic conditions it can be turned into hydroperoxy anion (HOO^-) and in acidic media it turns into hydroxyl cation ($O_2H_3^+$). Furthermore, in the presence of ultraviolet light or transition metals it turns to hydroxyl radicals [161] as shown in the Figure 1.29.

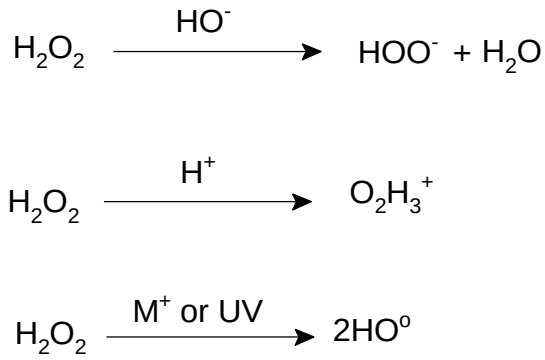

Figure 1.29: Direct activation modes of hydrogen peroxide [161].

The hydrogen peroxide can react with carboxylic acids and its derivatives to produce proxy acids as shown in Figure 1.30.

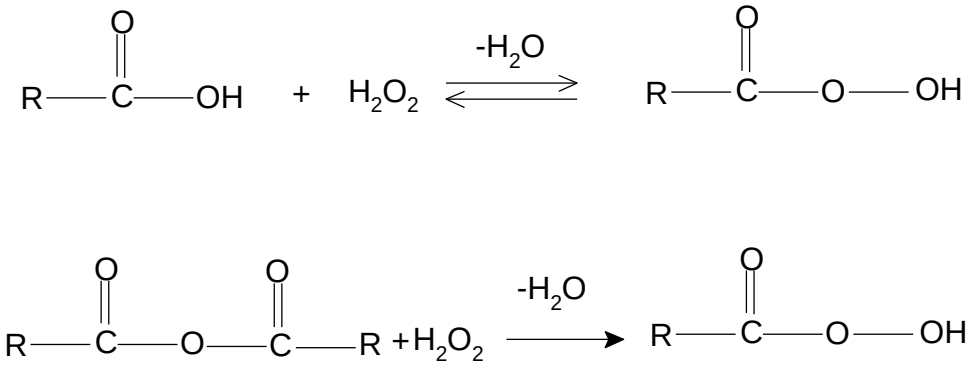

Figure 1.30: Reactions of hydrogen peroxide with carboxylic acids and esters [162].

The reactions of hydrogen peroxide with transition metals are very important since they results in the formation of hydroxyl radicals through Fenton-type reactions according to the following reaction:

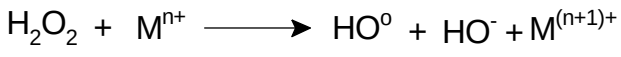

Figure 1.31: Reactions of hydrogen peroxide with transition metals.

In alkaline conditions hydrogen peroxide is in equilibrium with hydroperoxy anion, which is a strong nucleophile, and can react with aldehydes, unsaturated ketons and quinines to form epoxides as shown in Figure 1.32 [162]. Furthermore, hydrogen peroxide reacts with aromatic aldehydes and ketones at basic pH and undergoes rearrangement reactions (Fig. 1.33).

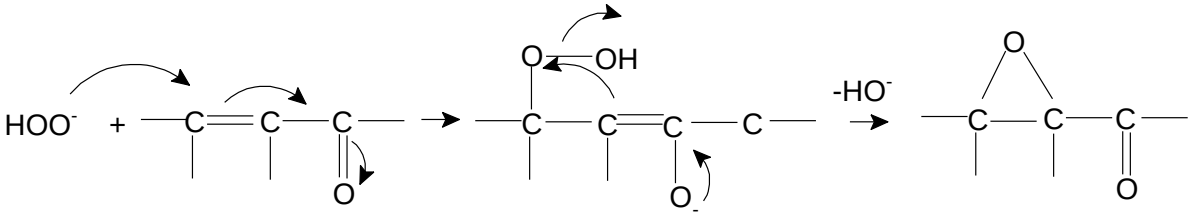

Figure 1.32: Epoxidation of unsaturated aldehydes or ketones by hydrogen peroxide in alkaline conditions [162].

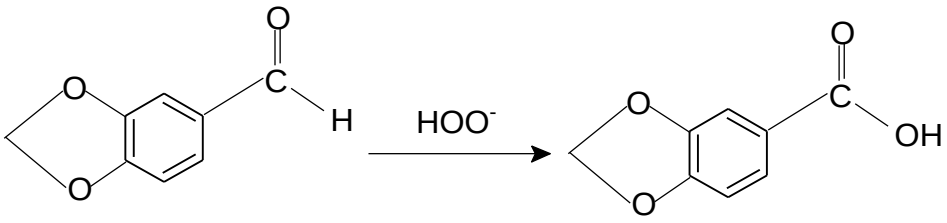

Figure 1.33: Oxidation of aromatic aldehyde by hydrogen peroxide in alkaline conditions [161].

1.13 Spectroscopic probes for the detection of reactive oxygen species

The detection and measurement of reactive oxygen species (ROS) are vital in order to understand the mechanism of AOPs as described before. The probe-assisted spectroscopy

(spectrophotometry, electron spin resonance, fluorescence and luminescence) is the main tool for the detection of ROS. The probes are the compounds that selectively react with ROS to produce specific products that can be easily detected. They have been used in aqueous and biological assays for the detection of ROS. Despite the use of spectroscopic probes in ozonation and biological assays have some disadvantages. These include: the low stability of probes and their products [163]. However, the use of spectroscopy probes has many advantages as they provide an easy, economical and simple means for the detection and quantification of ROS production. Additionally, by detecting ROS from different catalytic processes the mechanisms can easily be understood. The spectroscopic probes have been successfully used in the ozonation and catalytic ozonation processes for an investigation of ROS [48, 163-165].

The spectroscopic probes include the spin traps, hydroxylamines, spectrophotometric probes, luminescence probes and fluorescence probes. Among them fluorescence probes have wide range of advantages. For example, they have low background fluorescence, linear response to a wide range of ROS concentrations, higher sensitivity and have low detection limits [166]. Some of the probes that have been used to detect ROS in aqueous and biological assays have been listed in the Table 1.10.

Table 1.10 Spectroscopic probes for the detection of reactive oxygen species

Probe	ROS
Hydroxylamines	
1-Hydroxy-4-phosphonooxy-2,2,6,6-terramethylpiperidine (pp-H)	$^{o}O_2^-$ [167]
1-Hydroxy-2,2,6,6-terramethyl-4-oxo-piperidine (Tempone – H)	$^{o}O_2^-$ [168]
Spin traps	
5,5-Dimethyl-1-5pyrroline N-oxide (DMPO)	^{o}OH radicals [163]
5-Diethoxyphosphoryl-5-methyl-1-pyrroline N-oxide (DEPMPO)	$^{o}O_2^-$ [169]
Spectrophotometric probes	
Nitro Blue Tetrazolium (NBT)	$^{o}O_2^-$ [170]
2,3-Bis(1-methoxy-4-nitro-5-sulphophenyl)-5-[(phenylamino)carbonyl]-2H-tetrazolium hydroxide (XXT)	$^{o}O_2^-$ [171]
4-Chloro-7-nitrobenzo-2-oxa-1,3-diazole (NBD-Cl)	$^{o}O_2^-$ [172, 173]
N,N-Diethyl-p-phenylenediamine (DPD)	H_2O_2 [174]
Fluorescence	
Coumarin (COU)	^{o}OH radicals [175, 176]
4-Chloro-7-nitrobenzo-2-oxa-1,3-diazole (NBD-Cl)	$^{o}O_2^-$ [172, 173]
Amplex red	H_2O_2 [177]
Terephthalic acid	^{o}OH radicals [178]
Luminescence probes	
5-Amino-2,3-dihydroxy-1,4-phthalayineidone (luminal)	$^{o}O_2^-$ [179]
2-Methyl-6-(p-methoxyphenyl)-3,7-dihydroimidazol(1,2-)pyrazin-3-one (MCLA)	$^{o}O_2^-$ [180]

CHAPTER 2- EXPERIMENTAL

"This chapter is divided into two parts. The purpose of the first part (experimental) is to provide the procedures of the experiments performed in this work and to provide the information for each type of technique and the chemicals used in this work. In the second part (method development and validation) the method development and validation is described".

2.1 PART 1 - Experimental

2.1.1 Reagents and chemicals

All the experiments were undertaken with ultrapure deionized water. The ZSM-5 zeolites with different silica to alumina ratios and counter ions (Z1000H:SiO_2/Al_2O_3 = 1000, Z900Na:SiO_2/Al_2O_3 = 900, Z25H:SiO_2/Al_2O_3 = 25 and Z25Na:SiO_2/Al_2O_3 = 25) and γ-alumina has been used as catalysts in the present work. The zeolites were obtained from Zeochem, Switzerland and γ-alumina was obtained from Alcoa Inc, USA.

For the determination of aqueous ozone, analytical grade potassium indigo trisulfonate (purity, 99 %), sodium dihydrogen phosphate (purity, 99 %) and concentrated phosphoric acid were purchased from Sigma-Aldrich, U.K. For ozone dose experiments (gas-phase ozone), analytical grades potassium iodide (KI) and sodium thiosulfate ($Na_2S_2O_3$) were obtained from Fisher Scientific, U.K. The concentrated H_2SO_4 and starch were purchased from Sigma-Aldrich, U.K.

Coumarin and 7-hydroxy coumarin have been used in an investigation of hydroxyl radicals in ozonation in the presence of alumina and ZSM-5 zeolites. Both the coumarin and 7-hydroxy coumarin were of HPLC grade (purity, 99 %). The GC grade 99.7 % pure tert-butanol was used to investigate the scavenging effect of hydroxyl radicals. The phosphates effect has been investigated by using sodium di-hydrogen phosphate (Analytical grade; Purity, 99 %). Amplex red and resorufin (HPLC grade; purity 99) have been implied to investigate the formation of hydrogen peroxide in the ozonation and catalytic ozonation processes. The 4-chloro-7-nitrobenzo-2-oxa-1, 3-dizole (NBD-Cl) and potassium superoxide (analytical grade; purity, 99%) have been used for an investigation

of superoxide ion radical. All the above mentioned chemicals were purchased from Sigma-Aldrich, U.K.

For the ozonation and catalytic ozonation of VOCs, cumene and dichlorobenzene used were of GC grade with 99.9% purity and were purchased from Sigma-Aldrich U.K. The 1,2,4-trichlorobenzene was purchased from Across Organics, USA is having 99% purity. HPLC grade hexane (for liquid-liquid extractions), ibuprofen (purity, 99%), organic acids such as oxalic acid, succinic acid, formic acid and acetic acid (99% pure; ACS reagent grade), tetra butyl ammonium hydroxide (1M in water; ion chromatography grade) and heptaflourobutyric acid (purity 99.5%; GC grade) were purchased from Sigma-Aldrich, U.K.

2.1.2 Equipments

Table 2.1: Summary of techniques, instruments used and their applications

Techniques	Instrument	Applications
UV-Vis spectroscopy	Shimadzu UV-160A UV-Visible spectrophotometer	To analyse coumarin, NBD-Cl and aqueous ozone.
Fluorescence spectroscopy	Hitachi F-4500 Fluorescence Spectrophotometer	To analyse 7-hydroxy coumarin, resorufin and NBD-Cl product for the determination of hydroxyl radicals, hydrogen peroxide and superoxide ion radicals respectively in water.
Corona discharge ozone generation	Azco HTU-5000GE-120 ozone generator in line with moisture absorbing column	To produce ozone from pure oxygen, which is used in ozonation and catalytic ozonation experiments.
Flow control	Watson Marlow, 323 peristaltic pump	To have a uniform flow of ozone at a fixed rate, during the ozonation and catalytic ozonation experiments.
Gas chromatography-mass spectrometry	Agilent GC-MS; J&W Scientific, HP-5MS 19091S-431column	To analyse of VOCs (cumene, 1,2-dichlorobenzene, 1,2,4-trichlorobenzene).
Ion chromatography	Dionex, DX-120 ion chromatograph	To investigate organic acids
	1. Ion Pac- ICE-ASI 9X250 mm column; AMMS-TCE 300 anion micro membrane suppressor	To investigate phosphates
	2. Ion Pac As14 analytical column (4×250 mm); Ion Pac AG14 guard column (4×250 mm); ED-50A electrochemical detector	
High-performance liquid chromatography	Gilson 307 HPLC/UV equipped with Phenomenex Kintex 2.6μ C_{18} 100A (100× 4.60) column	To analyse ibuprofen.
Fourier transform spectroscopy	Nicolet, 380 FTIR spectrophotometer	Catalysts characterization.
Scanning electron microscopy	JEOL JSM-6060 scanning electron microscope	To observe the surface morphology of catalysts.

2.1.3 Methods

2.1.3.1 Characterization of catalysts

The physicochemical properties such as surface areas and porosities of the studied catalysts were determined either by the manufacturers or by our group in previous work [4]. They were measured by nitrogen adsorption at 77K. Surface areas were determined from the desorption isotherms applying the BET equation and porosities were determined from the adsorption isotherms using the Kelvin equation and the BJH method. The surface morphology of catalysts has been characterized by scanning electron microscopy (SEM). The SEM studies were carried out using a JEOL JSM-6060 microscope. The images were taken with 100 μA emission current by a tungsten filament and 12 KV of accelerator voltage. The catalysts were secured onto brass stubs with carbon conductive tape; sputter coated with gold, and viewed the surface under JEOL JSM-6060 microscope. The pre-treatment of catalysts was done by coating with an evaporated Au film in a Polaron Sc 7620 sputter coater metallization to increase the catalyst electric conductivity. The characterization of functional groups of catalysts has been done with the use of Nicolet 380 FTIR spectrophotometer. For this purpose first of all a background spectrum was collected, after that spectrum of the sample was collected by placing small amount of sample on the sample plate and applied the plunger to press the sample firmly against the plate. Finally, the sample key on the keypad was pressed to collect the spectrum.

The points of zero charge of different catalysts were determined by the mass titration method as described by Preocanin et al [181]. In the case of mass titration, subsequent portions of materials are added to an electrolyte solution (NaCl), and the pH of equilibrated dispersion is measured. The pH of the system changes gradually and approaches to a constant value, which is equal to the point of zero charge. The counter ion

association shifts the pH either to the acidic region (cations adsorption) or to the basic region (anion). Mass titration method therefore enables the detection of the association of both anions and cations [181]. Before the measurement, the materials were washed with deionised water and dried in an oven at 108 ^{o}C. Subsequently, catalysts (0.1 g) were added to 25 mL of 10^{-3} mol/dm^3 electrolyte solution (NaCl) with continuous stirring. After each portion of the catalyst was added to the solution, the pH of the equilibrated dispersion was measured. The pH of the solution changed gradually and become constant at a certain point and that pH was identified as the point of zero charge (pH_{PZC}). It is important to note that experiments have been performed at initial pH 4.0 and 9.8.

For the X-ray diffraction (XRD) studies, dry catalyst samples were grounded with the help of mortar and pestle. The fine power catalysts were packed on the sample holder. The diffraction pattern measurements were recorded in the high angle 2θ range of 2-80^{o}. The scan speed and step were 0.5^{o} min^{-1} and 0.02^{o}, respectively**.**

2.1.3.2 Ozonation experiments

The ozonation experiments have been performed in semi-batch (Fig. 2.1) and semi-continuous (Fig. 2.2) reactors. The experiments aiming to investigate the formation of hydroxyl radicals, superoxide ion radical and hydrogen peroxide have been performed in a semi-batch reactor. The ozonation of selected pollutants such as VOCs, ibuprofen and acetic acid were performed in semi-continuous reactor.

2.1.3.2.1 Ozonation experiments in semi-batch reactor

The ozonation experiments in the semi-batch reactor (Fig. 2.1) have been performed in order to investigate the formation of hydroxyl radicals, superoxide ion radical and hydrogen peroxide during the ozonation and catalytic ozonation processes, for this

purpose probes such as coumarin, NBD-Cl and amplex red have been used respectively. The procedures are as follows.

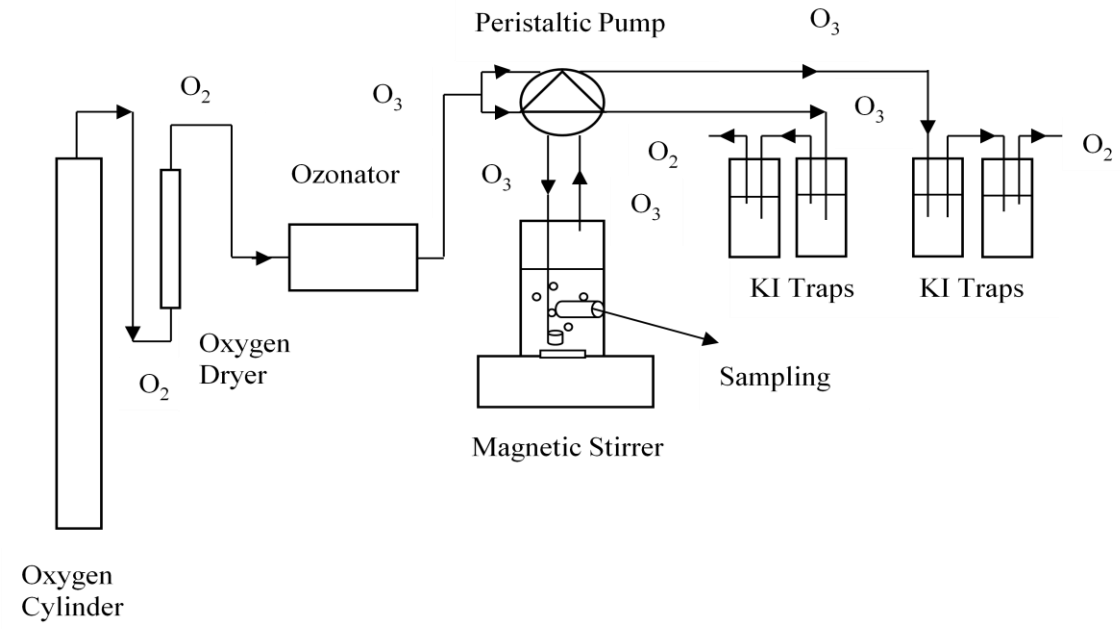

Figure 2.1: Scheme of semi-batch ozonation system.

2.1.3.2.1.1 Ozonation of coumarin, NBD-Cl and 7-hydroxy coumarin

Aqueous solution (190 mL) of either NBD-Cl or 7-hydroxy coumarin (20 ppm) was transferred to the reactor containing 2.0 g of the catalysts and was subsequently stirred (at 200 rpm) over a period of 30 minutes (temperature; 25^{o}C). Ozone was generated from pure oxygen by an HTL-500GE/20 ozone generator (Azon, Canada) and was continuously introduced to the column by means of a ceramic sparger (flow rate: 0.6 mg/min). Samples were collected at 5 minute intervals and were quenched with 0.025M Na_2SO_3 in order to remove any residual ozone and were filtered (PTFE 0.45 µm syringe filter). All the experiments were performed in the dark and the samples were analysed immediately after collection.

In the case of 7-hydroxy coumarin the collected samples during the ozonation (7HC) experiments were diluted with ultrapure water (1 mL of sample was diluted to 25 mL) and were analysed with a Hitachi F-4500 fluorescence spectrophotometer.

2.1.3.2.1.2 Ozonation to determine hydrogen peroxide

The ozonation experiments aiming to investigate the hydrogen peroxide have been performed by using amplex red as a probe. All experiments were conducted according to the procedure described above but with one exception: the ultra-pure deionized water (190 mL) was ozonated without the addition of amplex red. After filtration, 1 mL of the sample was immediately added to 3 mL of the solution of amplex red (20 mg/L) and left for 30 minutes (optimum time of H_2O_2 reaction with amplex red) and then analysed with an F-4500 Fluorescence Spectrometer (Hitachi, Japan). All the experiments were performed in triplicate and were performed in the dark (the reactor was covered with aluminium foil during the experiments).

2.1.3.2.1.3 Ozonation to investigate TBA and phosphates effect

The ozonation experiments in the presence of tertiary butyl alcohol (TBA) and phosphates have been performed as described above by adding either phosphates (sodium dihydrogen phosphate) or TBA (50 mg/L) to the aqueous solutions placed in the semi-batch reactor just before the ozonation process.

2.1.3.2.1.4 Ozonation to investigate the effect of catalyst amount

In order to investigate the effect of catalyst amount on the efficiency of catalytic ozonation, experiments were performed by undertaking ozonation experiments in the presence of various amounts of selected catalysts (2.0-8.0 g) according to the procedure described in section 2.1.3.2.1.1.

2.1.3.2.1.5 Kinetics of aqueous ozone decay

Ozone decay rates were investigated in pure water (in the absence of pollutants) in the semi-batch reactor (Fig. 2.1) and over pH range 3-13. The pH was adjusted using concentrated HCl or concentrated NaOH solution. A saturated solution of ozone was prepared with water (190 mL) by introducing ozone at a rate of 1.5 mg/min for 1 hour in the semi-batch reactor. 0.95 g of catalyst (alumina, ZSM-5 zeolites) was added into 190 mL of ozone saturated solution (initial ozone concentration: 1.5-3.0 mg/L, the variable initial ozone concentration is due to the different initial pH of solution), and the mixed suspension was stirred continuously for a period of one hour (temperature: 25^{o}C). Samples were collected every 10 min, filtered (PTFE 0.45 µm syringe filter), quenched with indigo reagent and analysed for aqueous ozone by indigo method. Aqueous ozone decay was also studied in experiments in which ozonation was used alone without the addition of a catalyst. The aqueous ozone decay was found to follow first order kinetics, as the graphs between ln [A] vs time (A = the concentration of aqueous ozone at time t) were linear in ozonation and ozonation in the presence of catalysts. Therefore, first order rate constants for ozone decomposition were determined using ln $[A]_{conc}$ /time plots and the value of rate constant was determined from the slope of the graph. Similar experiments were performed in the presence of 50 mg/L of TBA. All experiments have been performed three times and average rates of reactions have been determined.

2.1.3.2.2 Ozonation experiments in semi-continuous reactor

The ozonation experiments in the semi-continuous reactor (Fig. 2.2) have been performed in order to investigate the removal of pollutants such as VOCs, ibuprofen and acetic acid during the ozonation and catalytic ozonation processes. Additionally, experiments aiming

to investigate the effect of TBA, phosphates and tap water have also been performed in the semi-continuous reactor.

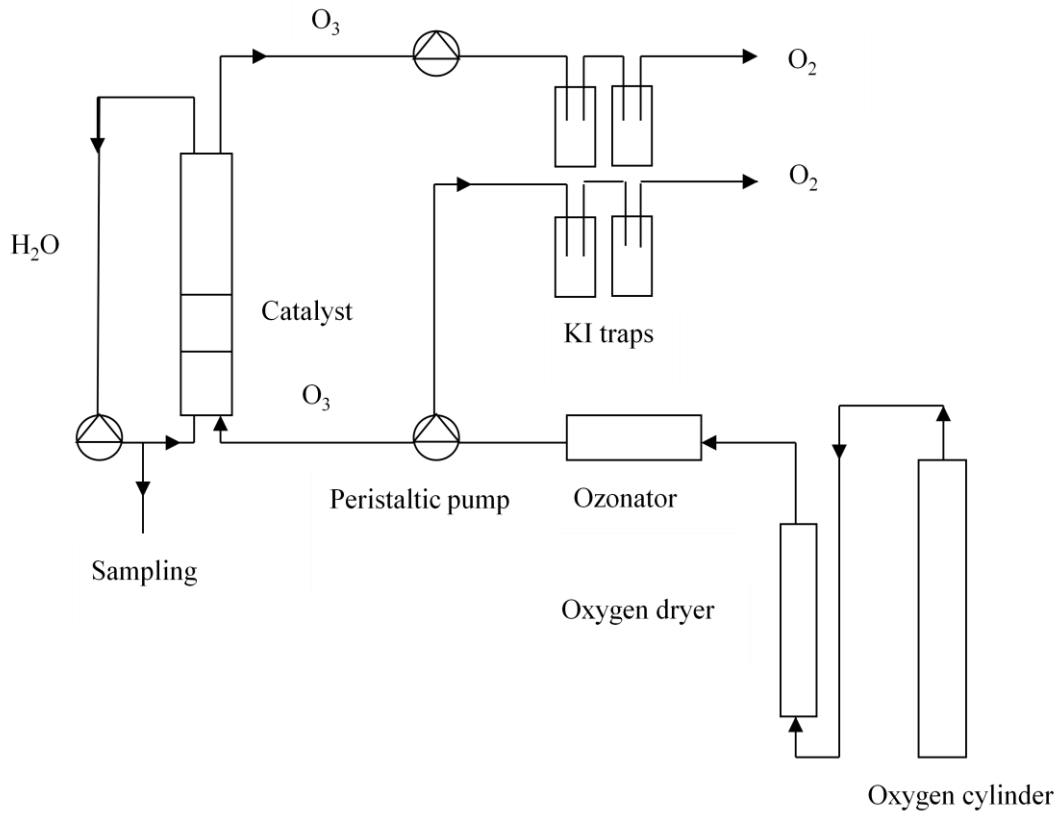

Figure 2.2: Scheme of semi-continuous ozonation system.

2.1.3.2.2.1 Ozonation of VOCs, ibuprofen and acetic acid

The ozonation experiments were conducted at room temperature (20^{o}C) in a semi-continuous mode as shown in Figure 2.2 (column length, 70 cm; width, 31 mm). Aqueous solution (490 mL) saturated with pollutants (20 mg/L), was transferred to the column containing 5.0 g of the catalyst. The water was recirculated over the period of 30 minutes with a flow rate of 15 mL/min. Ozone was generated from pure oxygen by AZCO HTU-5000GE-120 ozone generator and was continuously introduced to the column by means of a ceramic sparger, and a flow rate of 0.1 mg/min for VOCs ozonation and 0.5 mg/min for

ibuprofen and acetic acid ozonation. The samples were collected at 5 minute intervals and were quenched with 0.025M Na_2SO_3 in order to remove any residual ozone. All the samples were filtered (PTFE 0.45 µm syringe filter) prior to the analysis.

In the case of VOCs, the loss of VOCs due to volatization was determined by adding 490 mL of VOCs solution to the reaction column and re-circulated for 30 minutes. All the experiments were performed in triplicate at room temperatures.

In the case of the VOCs experiments it is important to mention that before the ozonation experiments the saturated solution of VOCs was prepared by directly spiking the appropriate volumes of VOCs required to prepare 1000 mg/L solution in a flask containing ultra pure water. The volumetric flask was filled up to the 1000 mL mark and the solution was poured into a glass stoppered bottle, shacken manually for 5 minutes and placed in a dark place for 24 hrs. After 24 hrs 500 mL of saturated solution was pumped out from the middle portion of bottle using a Watson Marlow 323 pump and that solution was used in the ozonation and catalytic ozonation experiments.

2.1.3.2.2.2 Ozonation to investigate TBA and phosphates effect

The ozonation experiments in the presence of tertiary butyl alcohol (TBA) and phosphates have been performed as described above by adding phosphates (sodium dihydrogen phosphate) and TBA (50 mg/L) to the semi-continuous reactor and following the above procedure.

2.1.3.2.2.3 Ozonation in the presence of drinking water

The efficiency of ozonation in the presence of ZSM-5 zeolites and alumina has been investigated by formally contaminating tap water with pollutants (VOCs and ibuprofen). The solutions were ozonated as described earlier (section 2.1.3.2.2.1). The aim of this

investigation was to find whether the naturally present substances like sulphates, phosphates, carbonates and bicarbonates in drinking water can cause a decrease in the efficiency of ozonation in the presence of zeolites and alumina. In order to remove any residual chlorine in the tap water, 500 mL of the sample was taken in a glass bottle and was shaken manually and placed in a dark place for 24 hours, and then the solution of pollutants was prepared as described above. The amount of residual chlorine was determined by the iodometric method [182].

2.1.3.2.2.4 Reuse performance of catalyst

The reuse performances of catalyst for the removal of VOCs and ibuprofen have been investigated in the semi-continuous reactor (Fig. 2.2). For this purpose 5.0 g of catalyst was added in the 490 mL solution containing pollutants (VOCs; 19 mg/L, 3.5 mg/L and 0.5 mg/L of cumene, dichlorobenzene and trichlorobenzene respectively and ibuprofen; 20 mg/L). The ozonation time was fixed to 30 minutes and experiments were performed for 6 hours, after every 30 minutes a fresh solution of pollutants was introduced in a semi-continuous reactor.

2.1.3.3 Adsorption experiments

The adsorption experiments have been performed in order to compare the removal of organic compounds with catalytic ozonation and adsorption only. For this purpose the experiments have been performed in both the semi-batch (Fig. 2.1) and the semi-continuous reactors (Fig. 2.2). The adsorption of phosphates and humic acid on zeolites and alumina has also been determined. Furthermore, adsorption capacities of pollutants on zeolites and alumina have been determined using glass tubes.

2.1.3.3.1 Adsorption experiments in semi-batch reactor

The adsorption of the probe molecules and phosphates has been performed in the semi-batch reactor (Fig. 2.1). The procedures are as follows

2.1.3.3.1.1 Adsorption of probes

The adsorption experiments have been conducted in the semi-batch reactor (Fig. 2.1) in order to investigate the adsorption of the probe molecules (coumarin, NBD-Cl, 7HC) over ZSM-5 zeolites and alumina. The extent to which COU, NBD-Cl were removed from the aqueous solution by physical adsorption on the catalysts was measured, so that this effect could be separated from the removal of these compounds by ozonation. For these measurements 2.0 g of the catalysts were added to 190 mL of probe solution (20 mg/L) and stirred for 30 minutes (rate, 200 rpm). Experiments were performed at 25^{o}C temperature. The samples were collected every 5 minutes and were filtered (PTFE 0.45 µm syringe filter). All the experiments were performed in the dark and samples were analysed immediately after collection with the use of Shimadzu UV-160A UV-Visible spectrophotometer. It is important to note here that the experiments were performed separately for each compound to investigate its adsorption on ZSM-5 zeolites and alumina.

2.1.3.3.1.2 Adsorption of phosphates

The adsorption of phosphates (50 mg/L) on the catalysts has been investigated in the semi-batch reactor. The ozonated samples in the presence of phosphates (50 mg/L) were collected every 5 minutes and were filtered (PTFE 0.45 µm syringe filter). The samples were analysed with the use of the Dionex DX-120 system. The experiments in semi-batch reactor were performed by using 2.0 g of catalysts. All the experiments were carried out at 25^{o}C temperature.

2.1.3.3.2 Adsorption experiments in semi-continuous reactor

The adsorption experiments have been conducted in the semi-continuous reactor in order to investigate the adsorption of VOCs, ibuprofen and acetic acid on zeolites and alumina. Additionally, the adsorption of phosphates and humic acid has also been investigated in semi-continuous reactor (Fig. 2.2). The procedures are as follows

2.1.3.3.2.1 Adsorption of pollutants

The adsorption experiments of selected pollutants such as VOCs (cumene, chlorobenzenes), ibuprofen and acetic acid have been performed in the semi-continuous reactor. For this purpose 5.0 g of the catalysts were added to 490 mL of saturated VOCs solution (cumene, 19.1 mg/L; 1,2-dichlorobenzene, 3.5 mg/L; 1,2,4-trichlorobenzene, 0.5 mg/L), ibuprofen (20 mg/L) and acetic acid (20 mg/L) solutions. The solutions were recirculated for 30 minutes (flow rate, 15 mL/min). The samples were collected after every 5 minutes and were filtered (PTFE 0.45 µm syringe filter) prior to the analysis.

2.1.3.3.2.2 Adsorption of humic acid

The experiments aiming to understand the extent of adsorption of humic acid on the ZSM-5 zeolites and alumina have been performed in the semi-continuous reactor. The experiments were performed by adding 5.0 g of the catalyst to 490 mL of humic acid solution (7 mg/L). The solution was recirculated for 30 minutes (flow rate, 15 mL/min). The samples were collected after every 5 minutes, filtered and were analysed with Shimadzu UV-160A UV-Visible spectrophotometer.

2.1.3.3.2.3 Adsorption of phosphates

The experiments in the semi-continuous reactor have been performed using 5.0 g of catalysts. The ozonated samples in the presence of phosphates were collected every 5

minutes and were filtered (PTFE 0.45 µm syringe filter). The samples were analysed with the use of the Dionex DX-120 system. All the experiments were carried out at ambient temperatures.

2.1.3.3.3 Determination of adsorption capacities

The adsorption capacities of VOCs and ibuprofen on ZSM-5 zeolites and alumina have been determined using glass test tubes of 25 mL capacity. The procedures are as follows.

2.1.3.3.3.1 Determination of adsorption capacities of catalysts towards VOCs

In order to undertake the adsorption capacity experiments the optimum time of adsorption was determined (equilibrium time) by shaking the test tubes containing 25 mL of VOCs solutions (closed, no headspace) for 2.5 hours and after every 30 minute sample was removed and analysed. The adsorption capacity of alumina and zeolites towards VOCs was determined by using varying amounts of materials (0.1 g to 2.0 g) added to 25 mL of saturated solution of VOCs in a test tube without headspace but with continuous shaking over the period of 1 hour (equilibrium time), with Gallenkemp flask shaker. The experiments were performed at room temperature (20^{o}C) and an initial pH of 6.2. The adsorption data were found to fit the Langmuir adsorption model (linear Langmuir adsorption isotherms). Therefore, adsorption capacities were determined from Langmuir isotherms. The Langmuir isotherm can be described by following equation [183].

$1/q = 1/q_m.b\ (1/c_e) + 1/q_m$

Where q = sorbed concentration (mass adsorbate/mass adsorbent)

q_m = maximum capacity of adsorbent for adsorbate

c_e = aqueous concentration of adsorbate at equiblirium (mass/ volume)

b = measure of affinity of adsorbate for adsorbent

The graph between $1/q_e$ vs $1/C_e$ indicated the straight line, hence the adsorption capacity was determined from the intercept ($1/q_m$) [183].

2.1.3.3.3.2 Determination of adsorption capacities of catalysts towards ibuprofen

The adsorption capacity of alumina and zeolites towards ibuprofen has been determined by adding 1.0 g of catalyst to 25 mL of ibuprofen solution with various initial concentrations in a test tube without head-space, but with continuous shaking (Gallenkemp flask shaker, Gallenkemp, UK). The samples were filtered and were analysed after 4 hours (optimum time). The experiments were performed at room temperatures (20^oC). The initial pH of the solution was adjusted to 7.2 with NaOH and HCl. The data was found to best fitted in the Langmuir adsorption model.

The Langmuir adsorption model can be represented as follows [183].

$C_e/q_e = 1/bq_m + C_e/q_m$

Here, C_e, q_m, q_e and b have been described in above section.

The adsorption capacities were calculated by plotting a graph between C_e/qe vs C_e and the maximum adsorption capacity q_m was determined from the slope of the graph [183].

2.1.3.4 Analytical procedures

2.1.3.4.1 Ozone Dose (ozone in gas phase)

Iodometric method [182] has been used for the determination of ozone in the gas phase. Gaseous ozone in in-gas and off-gas was continuously introduced to two sets of glass bottles, each filled with 200 mL of 2% KI, through a ceramic sparger (Fig. 2.1, Fig. 2.2). After acidification of 200 mL of the 2% KI solution with 10 mL of 1N HCl, the liberated iodine was titrated with standard 0.005N $Na_2S_2O_3$ using a starch indicator. The volume of titrant was noted and ozone dose was calculated by following formula:

Here A= the volume of titrant used in trap A

B = volume of titrant used in trap B

N = normality of titrant

T = total time of ozonation

Following are the procedures used to prepare reagents which have been used in the determination of ozone dose.

2.1.3.4.1.1 Starch indicator solution

In order to prepare the starch indicator solution, 5.0 g of starch was added to a little cold water and grounded in a mortar to a thin paste. It was poured into 1L of deionised water; stirred and left to settle overnight. The clear supernatant was used and was preserved with 1.25 g salicylic acid and 4.0 g zinc chloride.

2.1.3.4.1.2 Standardization of $Na_2S_2O_3$

Standard solution of sodium thiosulfate (0.1N) was prepared and standardized by titrating with potassium dichromate (normality, 0.1N).

Normality of $Na_2S_2O_3$ = 1/mL $Na_2S_2O_3$ consumed.

2.1.3.4.1.3 Preparation of calibration curve

The calibration curve has been prepared by passing ozone gas through a KI trap for a fixed interval of times (1, 2, 3, 4, 5, 6 minutes) in 250 mL volumetric flask containing a known volume (200 mL) of 2 % KI solution and the rest of the procedure is described above. A calibration curve was prepared between ozone concentractions and ozonation time.

2.1.3.4.2 Aqueous ozone (Indigo colorimetric method)

The concentration of ozone dissolved in the aqueous phase was determined by the indigo method [182]. The difference in absorption of light at 600 nm between blank and sample was measured with a Shimadzu UV-160A UV-Visible Spectrophotometer. The calibration curve was established before analysis. The concentration of ozone was determined by the following calculations:

mg O_3/L = 100×ΔA/f×b×V

ΔA = difference in absorbance between sample and blank
b = path length of cell, cm.

v = volume of sample in mL

f = constant = 0.42

Following procedures have been used to prepare reagents which were used in aqueous ozone studies.

2.1.3.4.2.1 Indigo stock solution

In order to prepare indigo stock solution, 500 mL of distilled water and 1mL of concentrated phosphoric acid was added to a 1L volumetric flask. Then 770 mg potassium of indigo trisulfonate was added and the flask was filled with deionized water to the mark. A 1:100 dilution exhibits an absorbance of 0.20 ± 0.01 cm at 600 nm [182].

2.1.3.4.2.2 Indigo reagent I

The indigo reagent I was prepared by adding 20 mL indigo stock solution to a 1L volumetric flask, 10.0 g of sodium dihydrogen phosphate (NaH_2PO_4) and 7 mL concentrated phosphoric acid was added and diluted up to the mark. The indigo solution I is used for ozone concentrations ranges 0.01 to 0.1 mg O_3/L [182].

2.1.3.4.2.3 Indigo reagent II

The indigo reagent II was prepared by following the procedure as an indigo solution I with the exception of adding 100 mL indigo stock solution instead of 20 mL. The indigo solution II is used for ozone concentrations greater than 0.1 mg O_3/L [182].

2.1.3.4.2.4 Calibration curve

The calibration curves have been prepared by ozonating deionized water for fixed intervals of time (1, 2, 3, 4, 5, 6 minutes), and then indigo reagent II and sample were mixed in 10: 90 ratios. The sample was put into 1 cm glass cell and absorbance at 600 nm has been determined by Shimadzu UV-160A UV-Visible Spectrophotometer. The calibration curve has been established between absorbance vs. ozone concentration.

2.1.3.4.3 Analysis of coumarin

Coumarin concentration was measured through absorbance at 277 nm (Shimadzu UV-160A UV-Visible Spectrophotometer) in a 1.0 cm cell following filtration of the working solution, and using a suitable calibration curve.

2.1.3.4.4 Analysis of 7-hydroxy coumarin

The concentration of 7HC was determined by fluorescence intensity at 455 nm (excited at 332 nm) using a Hitachi F-4500 Fluorescence Spectrometer. Both the emission and excitation slits were set to 5.0 nm. A calibration curve was prepared over the appropriate concentration range. Samples were filtered (PTFE 0.45 μm syringe filter) prior to the analysis [175, 176, 184].

2.1.3.4.5 Analysis of resorufin

The concentration of H_2O_2 was determined from its fluorescence emission spectrum (excited at 563 nm) of resorufin with the use of F-4500 fluorescence spectrometer

(Hitachi, Japan). Both the emission and excitation slits were set to 5.0 nm. Fluorescence at 587 nm was recorded [177] and the calibration curves were established by reacting hydrogen peroxide (concentration ranges 0 – 170 µg/L of H_2O_2 formed from 30% aqueous solution of H_2O_2) with amplex red reagent (20 mg/L) for 30 minutes. Due to the fact that amplex red reaction with H_2O_2 is pH dependent, calibration curves were established at different pH values: 6.2, 8.8 and 13.0.

2.1.3.4.6 Analysis of NBD-Cl

The 4-chloro-7-nitrobenzo-2-oxa-1, 3-dizole (NBD-Cl) was analysed with the use of Shimadzu UV-160A UV-Visible Spectrophotometer by recording the absorption at 343 nm. This was obtained by plotting absorbance at 343 nm against NBD-Cl concentration. All samples were filtered through a PTFE 0.45 µm syringe filter, placed in 1 cm silica cells and were analysed.

2.1.3.4.7 Analysis of NBD-Cl Product

An identification of NBD-Cl product (reaction product of superoxide ion and NBD-Cl [172, 173] was conducted by recording fluorescence emission spectrum (excited at 470 nm) with an F-4500 fluorescence spectrometer (Hitachi, Japan). Both the emission and excitation slits were set to 5.0 nm during the measurements. Fluorescence at 550 nm was recorded [173]. The formation of NBD-Cl product was confirmed by reacting KO_2 (source of superoxide) and NBD-Cl. The amount of superoxide ion radical was quantified by plotting fluorescence at 550 nm against $^{\bullet}O_2^-$ concentration (using 100 µM of NBD-Cl and different concentrations of KO_2 that are in the range of 0 – 100 µM and the calibration curves have been established at pH values, 3.0, 6.2, 8.8 and 13.0.). All the aqueous samples were mixed with acetonitrile prior to the analysis (1 mL of an aqueous solution of

NBD-Cl product with 2 mL of acetonitrile) [173]. All the samples were filtered (PTFE 0.45 µm syringe filter) prior to the analysis.

2.1.3.4.8 Analysis of VOCs

The concentrations of cumene and chlorobenzenes have been determined by Agilent gas chromatography coupled with mass spectrophotometry (GC/MS). After liquid-liquid extraction (hexane: water, 1:5, extraction time, 1min) 1µL of the extractant solution was injected using an auto sampler and a split-less mode. The temperature programme used was as follows: column oven temperature was 50^{o}C for 4 minutes then 50^{o}C per minute to 200 ^{o}C. The carrier gas flow rate was 1.3 mL/min, the scan mode was selected ion storage with mass range of 50-500 and mass transfer line temperature was 280^{o}C.

2.1.3.4.9 Analysis of ibuprofen

The concentration of ibuprofen has been determined by Gilson 506C HPLC equipped with UV-visible detector. The column used for the elution was Phenomenex Kinetex 2.6 µm C_{18} 100 Å column (100 × 4.60 mm). After collecting samples from ozonation and catalytic ozonation experiments 30 µL of the solution was injected using an auto sampler. The mobile phase used was methanol/ water (70: 30 v/v) and 1% acetic acid (pH 3). It was passed through the column at a flow rate of 0.4 mL /min. The calibration curves have been established before analysis.

2.1.3.4.10 Analysis of humic acid

Humic acid concentration was measured through absorbance at 254 nm with the use of Shimadzu UV-160A UV-Visible Spectrophotometer. The sample was placed in a 1.0 cm cell following filtration of the working solution, and using a suitable calibration curve [3].

2.1.3.4.11 Analysis of phosphates

Phosphate concentrations were determined by ion chromatography using a DIONEX DX-120 system with Ion Pac As14 analytical column (4 × 250 mm) and Ion Pac AG14 guard column (4 × 250 mm) coupled to an ED-50A electrochemical detector (Dionex, USA). Analyses were performed using an isocratic method at a flow rate of 0.82 mL/min and a constant temperature of 30^{o}C. The mobile phase used was a mixture of the 3.5 mM sodium carbonate and 1.0 mM sodium hydrogen carbonate (0.742 g sodium carbonate was added in 2 L deionised water and 0.168 g sodium hydrogen carbonate in 2 L deionised water (Both solutions have been mixed together). The injection volume of the sample was 25 µL. The calibration curve was established before analysis.

2.1.3.4.12 Analysis of organic acids

The organic acids have been analysed with the use of Dionex DX-120 ion chromatograph, equipped with Ion Pac- ICE-ASI 9 x 250 mm column and AMMS-TCE 300 anion micro membrane suppressor. Heptafluorobutyric acid (1.0 mM) was used as eluent and tetra butyl ammonium hydroxide (5 mM) was used as regenerant. The injection volume was 25 µL; cell temperature, 30^{o}C; eluent flow rate, 0.82 mL/min and regenerant flow rate was 5 mL/min.

2.1.3.4.13 Determination of residual chlorine

For the determination of residual chlorine 500 mL of tap water sample was taken and adjusted with 5 mL of acetic acid to reduce the pH (3.0-4.0). After this, 1.0 g of KI was added and the sample was titrated with 0.01 N $Na_2S_2O_3$ from a burette until yellow colour. At this stage 1 mL of starch solution was added and was further titrated until the blue colour disappeared. A blank titration was performed using ultra-pure deionised water. This

is performed in order to determine the contribution of oxidizing or reducing impurities. The blank also compensates for the concentration of iodine bond to starch at the end point [182]. All the experiments were performed three times and the concentration of residual chlorine was calculated by using following relationship:

mg of Cl/L = (A - B) × N ×35450/mL of sample

A = mL of titration for sample
B = mL of titration for blank
N = normality of $Na_2S_2O_3$

2.2 PART 2 – Method development and validation

Part 2 of chapter 2 describes the development and validation of methods that have been used in this study. A suitable method is important for the analysis of probes and organic pollutants in the bulk and in aqueous solutions. It is indeed important to develop a simple, sensitive, accurate, precise and reproducible method for the determination of organic compounds. The methods have been developed and validated for the analysis of volatile organic chemicals (VOCs; cumene, dichlorobenzene, trichorobenzene) with gas-chromatography-mass spectrometry (GC/MS), ibuprofen with high-performance liquid chromatography coupled by UV-visible detector (HPLC/UV), organic acids with ion chromatography coupled with electrochemical detector (IC/ECD), coumarin (COU), 4-chloro-7-nitrobenzo-2-oxa-1,3-dizole (NBD-Cl) concentrations with UV-visible spectrophotometer and 7-hydroxy coumarin and resorufin with fluorescence spectrophotometer.

2.2.1 Analysis of coumarin, NBD-Cl with UV-Vis spectrophotometer

2.2.1.1 Preparation of stock solutions of COU and NBD-Cl

The 500 µg/mL stock solution of COU and NBD-Cl was prepared by dissolving (separately) 50 mg of analytes in 50 mL ultrapure deionised water, transferred them to 100 mL volumetric flasks and volumes were made up to the mark with ultrapure deionised water. The solution pH was adjusted to pH 6.2 with NaOH or HCl.

2.2.1.2 Verification of maximum absorbance of COU and NBD-Cl

In order to determine λ_{max} values of COU and NBD-Cl, standard solutions of appropriate concentrations have been prepared from the stock solutions by diluting the stock solutions. The maximum absorbance (λ_{max}) was determined for COU and NBD-Cl by placing the standards in 1 cm silica cells and analysed with Shimadzu UV-160A UV-vis spectrophotometer in wavelength scan mode. The (λ_{max}) values were found to be 277 nm and 343 nm for COU and NBD-Cl respectively (Fig. 2.3).

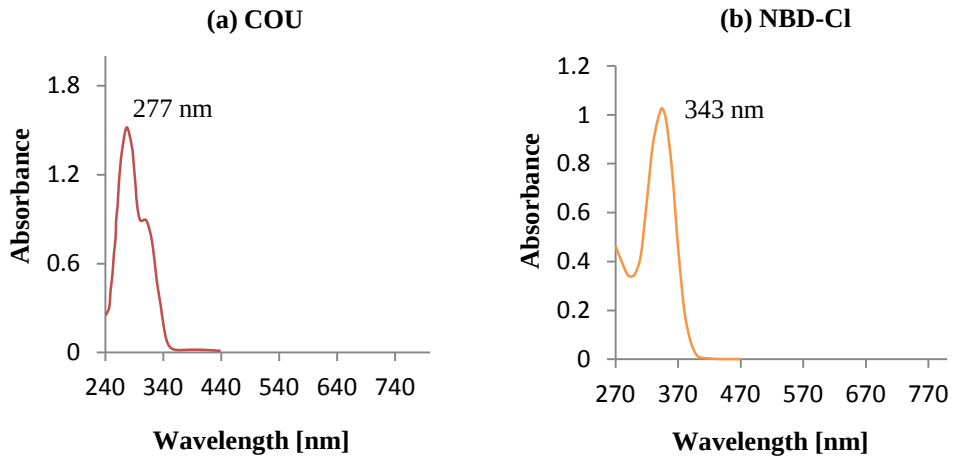

Figure 2.3: UV-vis scans of (a) coumarin and (b) NBD-Cl.

2.2.1.3 Method validation for COU and NBD-Cl

First of all calibration curves were prepared by preparing known standards from stock solutions in suitable concentration range and an average of such 3 sets were prepared. The

standards were analysed with Shimadzu UV-160A UV-vis spectrophotometer at λ_{max} values of COU and NDB-Cl. The calibration curves were drawn by plotting a graph between absorbance and concentrations, for COU and NBD-Cl. The relationship between the concentrations and absorbance was found to be linear for both COU and NBD-Cl (concentration range: 0 – 20 mg/L). The linear regression coefficant (R^2) values were 0.9914 and 0.9994 for COU and NBD-Cl respectively.

The above described methods have been validated in term of their linearity, precision and accuracy. Additionally, the limit of detections (LODs) and quantifications (LOQs) have been determined. The followings are the procedures and results of validation.

2.2.1.3.1 Linearity

The linearity of the method was determined by using three sets of calibration standards and calibration curves were prepared. The average correlation co-efficient and regression line equation was determined.

2.2.1.3.2 Accuracy

The accuracy of the assay was calculated by spiking known amounts of compounds in ultrapure deionised water and their response was recorded from the instrument. The concentrations were calculated from calibration curves and the accuracy was determined as a percentage of the amount obtained.

2.2.1.3.3 Precision

The precision of the assay was determined by using three sets of concentrations. Three standards were prepared for each concentration and were analysed at three different times of points in the same day for intra-day precision. The inter-day precision was determined

by analysing samples at three different time of point on three different days. The % RSD was calculated. The precision in λ_{max} values has also been determined.

2.2.1.3.4 Limit of detection and limit of quantification

The limits of detection (LOD) and limit of quantification (LOQ) were determined by using signal to noise method. The limit of detection of each compound was determined by considering the concentrations at which the signal (S) to noise (N) ratio, S/N $\geq$ 3. The limit of quantification was taken as five times the limit of detection [185].

2.2.2 Analysis of 7HC and resorufin with fluorescence spectrophotometer

The analysis of 7HC and resorufin has been performed by Hitachi F-4500 fluorescence spectrophotometer [175, 177].

2.2.2.1 Preparation of stock solutions of 7HC and resorufin

The stock solutions of 7HC and resorufin have been prepared as described in section 2.2.1.1.

2.2.2.2 Emission wavelength values of 7HC and resorufin

In order to determine the values of emission wavelength (at which maximum fluorescence values may be obtained for 7HC and resorufin), standard solutions of suitable concentrations have been prepared from the stock solutions by diluting the stock solutions. The emission wavelengths were determined for 7HC and resorufin by placing the standards in glass cells and analysed with Hitachi F-4500 fluorescence spectrophotometer in scan mode. The maximum fluorescence values have been obtained at 455 nm and 563

nm for 7HC and resorufin respectively (Fig. 2.4).

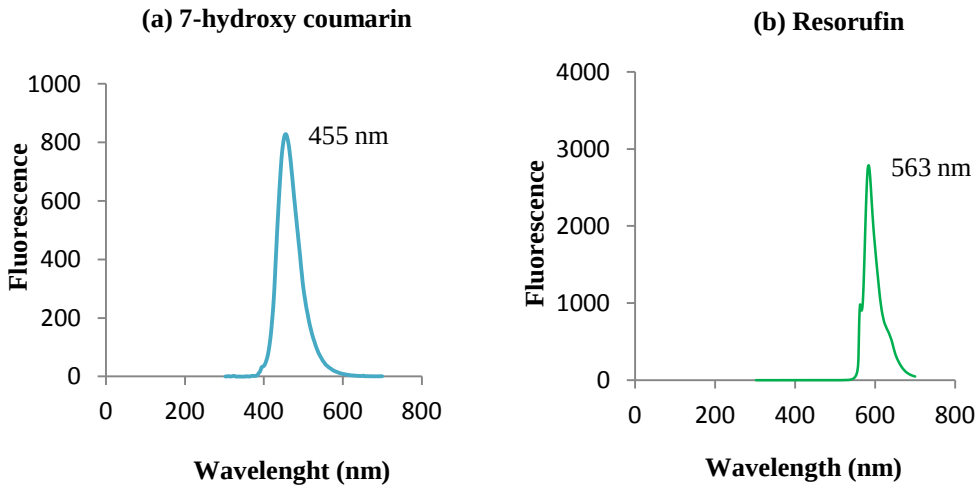

Figure 2.4: Fluorescence scans of (a) 7HC and (b) resorufin.

2.2.2.3 Method validations for 7HC and resorufin

The calibration curves of 7HC and resorufin have been prepared by analysing the standards with Hitachi F-4500 fluorescence spectrophotometer in photometric mode using emission wavelengths of 455 nm and 563 nm for 7HC and resorufin respectively. The standards have been prepared from stock solutions in a suitable concentration range. The results indicate a linear relationship between the concentration of analytes and fluorescence in a concentration range: 0 - 20 mg/L. The linear regression (R^2) values were found to be 0.9997 and 0.9777 for COU and NBD-Cl respectively. Finally the method has been validated in terms of linearity, accuracy and precision as described in section 2.2.1.3.

2.2.3 Analysis of VOCs with gas chromatography-mass spectrometry

The method has been developed for the analysis of VOCs such as cumene, 1,2-dichlorobenzene and 1,2,4-trichlorobenzene with the use of Agilent GC-MS equipped with J&W Scientific HP-5MS 19091S-431 column.

2.2.3.1 Preparation of stock solutions of VOCs

For the method development, 1000 ppm stock solutions of VOCs have been prepared by spiking appropriate volumes (11.6 µL, 7.7 µL and 6.9 µL for cumene, dichlorobenzene and trichlorobenzene respectively) of VOCs necessary to make a 1000 ppm solution in hexane using 10 mL volumetric flask and was filled up to the mark.

2.2.3.2 Method development

The key parameters for the method development for VOCs analysis are the column oven's temperature, the carrier gas flow rate and the inlet conditions. 1µL of VOCs solution was injected using split-less mode. The temperature programme used was as follows: the column oven temperature was 50^{o}C for 4 minutes then 50^{o}C per minute to 200 ^{o}C. The carrier gas flow rate was 1.3 mL/min, on MS the scan mode was set to selected ion storage with mass range of 50-500 and mass transfer line temperature was 280^{o}C. The chromatogram obtained by this method is shown in Figure 2.5.

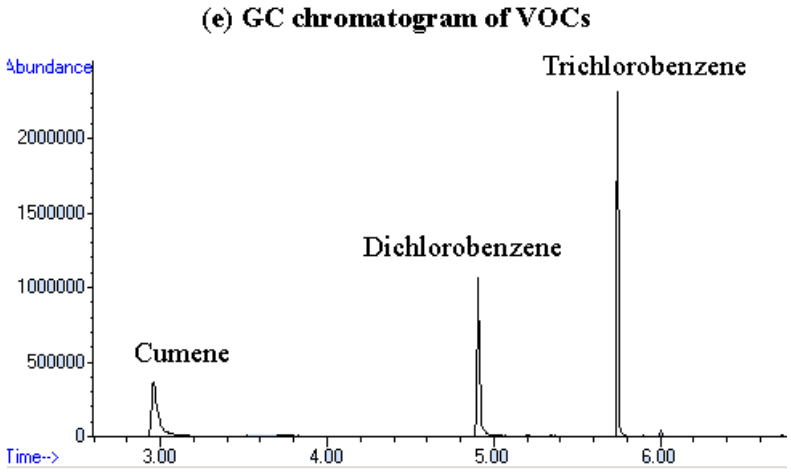

Figure 2.5: Gass chromatograms of VOCs (cumene, dichlorobenzene and trichlorobenzene).

2.2.3.3 Method validations for VOCs

First of all calibration curves of VOCs have been prepared from the stock solution containing the mixture of VOCs. For this purpose the stock solution is diluted necessary to prepare standard solutions in the concentration range of 10 – 100 ppm. The standards were injected to the GC/MS and calibration curves have been drawn by plotting a graph between peak areas and concentrations of VOCs. The relationship was found to be linear as indicated by the linear regression values, which are 0.9937, 0.9970 and 0.9961 for cumene, dichlorobenzene and trichlorobenzene respectively. Finally, method has been validated in term of accuracy, linearity and precision as described in section 2.2.1.3. The retention times have also been validated.

2.2.4 Analysis of ibuprofen with high-performance liquid chromatography

The concentrations of ibuprofen have been determined by developing a method on Gilson 506C HPLC equipped with UV-visible detector. The column used for elution was Phenomenex Kinetex 2.6 µm C_{18} column (100 × 4.60 mm).

2.2.4.1 Method development

The method has been developed for the determination of ibuprofen with HPLC/UV. The key parameters varied were flow rate and composition of the mobile phase. The mobile phase used was methanol/ water (70: 30 v/v) and was passed through the column at a flow rate of 0.4 mL /min. The pH of the mobile phase was adjusted to 3.0 by using acetic acid. The retention time of the method was 12.16 minutes.

2.2.4.2 Method validation for ibuprofen

The stock solution of ibuprofen was prepared by dissolving 100 mg of ibuprofen in 100 mL of deionized water (concentration, 1000 mg/L). From the stock solution standards of known concentrations have been prepared (0 – 100 mg/L). The calibration curves have

been drawn by plotting a graph between concentrations of ibuprofen vs peak area. The results show a linear relationship as indicated by the R^2 value, 0.9990. The accuracy and precision were determined as described before.

2.2.5 Analysis of organic acids with ion chromatography

The organic acids have been analysed with the use of Dionex DX-120 ion chromatograph, equipped with Ion Pac- ICE-AS1 9 × 250 mm column and AMMS-ICE 300 anion micro membrane suppressor. The method has been developed for acetic, formic, succinic and oxalic acid. Heptafluorobutyric acid (1.0 mM) was used as eluent and tetra butyl ammonium hydroxide (5 mM) was used as regenerant. The injection volume was 25 μL; cell temperature, 30^{o}C; eluent flow rate, 0.82 mL/min and regenerant flow rate was 5 mL/min.

2.2.5.1 Preparation of eluent and regenerant

The stock solution (1 M) of heptaflurobutyric acid (eluent) was prepared by diluting 130.5 mL (calculated from mass/density) of heptaflurobutyric acid to 1 liter by adding deionized water. Then 1 mL of stock solution was taken and diluted to 1 liter to prepare 1.0 mM heptafluorobutyric acid eluent. To prepare 5 mM solution from 1 M solution of tetra butyl ammonium hydroxide 5 mL of 1 M solution was diluted to 1000 mL.

2.2.5.2 Preparation of acid solutions

The stock solutions (1000 ppm) of acids (oxalic acid, succinic acid, formic acid and acetic acid) have been prepared by directly adding their appropriate quantities (95.3 μL, 81.97 μL, 0.1g and 0.1g for acetic, formic, succinic and oxalic acid respectively) in 100 mL volumetric flask and then were filled up to mark with ultra-pure water.

2.2.5.3 Method development

The conditions of the developed method were as follows.: (i) the eluent, 1mM heptafluorobutyric acid; (ii) flow rate, 0.82 mL/min; (iii) regenerant's flow, 5 mL/min; (iv) injection volume, 25 µL and (v) cell temperature, 30^{o}C. A chromatogram of all acids separated with the developed method is presented in Fig. 2.6.

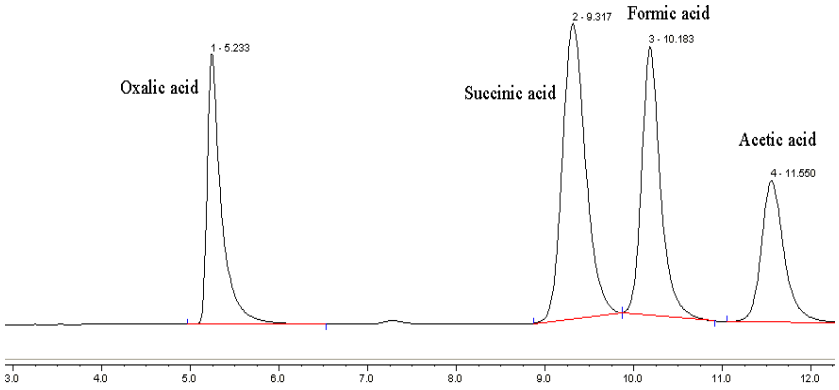

Figure 2.6: Ion chromatogram of organic acids (oxalic acid, succinic acid, formic acid, acetic acid).

2.2.5.4 Validations

First of all calibration curves of organic acids have been prepared by dilution stock solution to produce standards from 0 – 100 mg/L. Then these standards were analysed on IC. Each standard was injected three times and the average peak area was used for the preparation of calibration curves. The calibration curves were drawn between concentration vs peak areas. The relationship was found to be linear for all studied acids in the concentration range of 0 – 100 mg/L. The linear regression values were 0.9720, 0.9985, 0.9959 and 0.9978 for oxalic, succinic, formic and acetic acid respectively. Finally, linearity, precision and accuracy have been determined as described in section 2.2.1.3. The limits of detection and quantifications have been determined as described in section 2.2.1.3.

2.2.6 Analysis of phosphates with ion chromatography

Phosphate concentrations were determined by ion chromatography using a DIONEX DX-120 system with Ion Pac As14 analytical column (4 × 250 mm) and Ion Pac AG14 guard column (4 × 250 mm) coupled to an ED-50A electrochemical detector (Dionex, USA).

2.2.6.1 Method Development

The method has been developed by using ion chromatography. The main variable was the mobile phase flow rate, following method has been developed. Analyses were performed using an isocratic method at a flow rate of 0.82 mL/min and a constant temperature of 30^{o}C. The mobile phase used was a mixture of the 3.5 mm sodium carbonate and 1.0 mM sodium hydrogen carbonate (0.742 g sodium carbonate was added in 2 L deionised water and 0.168 g sodium hydrogen carbonate in 2 L deionised water. The retention time of the phosphate peak was 8.1 minutes (Fig. 2.7).

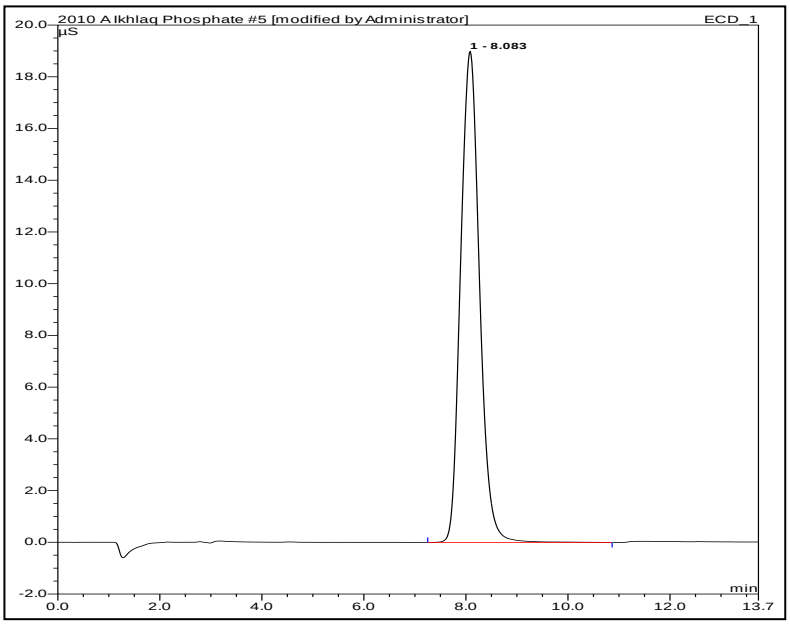

Figure 2.7: Ion chromatogram of phosphates (concentration, 100 mg/L).

2.2.6.2 Method Validations

Firstly calibration curve has been prepared by using standard solutions (0 – 100 ppm) prepared from 1000 ppm stock solution. The relationship between concentration of phosphates and average peak areas was found to be linear (R^2, 0.9972; concentration range: 0 -100 mg/L). Finally, precision, linearity and accuracy have been determined as described in section 2.2.1.3.

2.2.6 Results and discussion of method validation

The result shows that the precision of the methods and instruments (discussed in method development), both inter-day and intra-day are very good, as all RSD values for respective compounds are less than 1% (Table 2.2). The results show that the calibration data (Table 2.3) of all analytes were found to be linear. A representative plot, described by the equation $y = mx + c$, show that detectors responses were found to be linear over the concentration ranges with $R^2 > 0.99$. The precision data for both intra-day and inter-day analysis indicate that the precision is acceptable, as % RSD is less than 5%. Intra-day precision were in the ranged from 0.5 – 3.5% (Table 2.3) and the % RSD for inter-day ranged from 1.3 to 4.9%. The studies further revealed that the methods are highly accurate as accuracy was found to be 97- 99%. The results indicated that all the methods were precise and accurate therefore can be implied for further studies.

Table 2.2: Intra-day and inter-day precision results for λ_{max} (UV), Emission wavelength (Fluorescence) and retention times (GC/MS, HPLC/UV, IC)

Compounds	**% RSD intra-day**	**% RSD inter-day**
Coumarin	0.099	0.996
NBD-Cl	0.064	0.762
7-hydroxy coumarin	0.087	0.987
Resorufin	0.997	0.155
Cumene	0.129	0.213
Dichlorobenzene	0.185	0.365
Trichlorobenzene	0.102	0.288
Ibuprofen	0.098	0.998
Oxalic acid	0.079	0.970
Succinic acid	0.186	0.330
Formic acid	0.055	0.066
Acetic acid	0.687	0.176
Phosphates	0.129	0.239

Table 2.3: Method validation data (n = 3)

Method/technique	Analytes	Regression line equation	Correlation coefficient (R^2)	Accuracy (%)	Precision (%RSD)		LOD (mg/L)	LOQ (mg/L)
					Intra-day	Inter-day		
UV-vis spectroscopy	coumarin	y = 0.0725x-0.007	0.9914	99	2.0	3.1	0.06	0.3
	NBD- Cl	y = 0.045x-0.0215	0.9994	99	1.5	1.3	0.07	0.35
Fluorescence spectroscopy	7HC	y = 8745x+65.69	0.9997	98	1.2	2.5	0.02	0.1
	resorufin	y = 10.956x+82.38	0.9777	97	3.5	3.8	0.005	0.025
Gas chromatography- mass spectrometry	cumene	y = 77006x-234542	0.9937	98	3.3	4.5	0.2	1.0
	dichlorobenzene	y = 119559x+44388	0.9970	98	2.2	4.9	0.5	2.5
	trichlorobenzene	y = 146528x+39492	0.9961	99	2.1	4.2	0.3	1.5
High-performance liquid chromatography	ibuprofen	y = 163146x+41948	0.9990	99	0.5	1.1	0.3	1.5
Ion chromatography	oxalic acid	y = 0.0622x-0.5902	0.9720	97	0.5	2.5	5	25
	succinic acid	y = 0.0606x-0.0045	0.9985	99	1.3	2.1	0.15	0.75
	formic acid	y = 0.0457x-0.0566	0.9959	98	0.5	0.9	0.13	0.65
	acetic acid	y = 0.02862x-0.0144	0.9978	99	1.1	1.5	0.10	0.5
	phosphates	y = 0.062x-0.0448	0.9972	98	1.1	4	0.5	2.5

CHAPTER 3 - CHARACTERIZATION

"In this chapter the results of characterization of ZSM-5 zeolites and γ-Al_2O_3 have been provided. The information about surface areas, pore size and composition of catalysts has been obtained from the manufacturers. In addition, the catalysts have been characterised by mass titration, FTIR, SEM and XRD techniques".

3.1 Introduction

The aim of this chapter is to characterize the ZSM-5 zeolites and γ-alumina, which have been used as catalysts in the present work. The catalyst composition, pore size, surface morphology and nature of active sites are vital in the catalytic process. For example the silica to alumina ratios of zeolites play a significant role in the catalytic process, since they can affect the extent of adsorption of hydrophilic and hydrophobic compounds on the catalyst surface [149]. The Bronsted (surface hydroxyl groups) and Lewis acid sites of the catalyst may affect the aqueous ozone decomposition [19, 20, 26]. It has been reported that the strength of surface hydroxyl groups of alumina can affect the aqueous ozone decomposition [20]. It is therefore important to characterize the surface hydroxyl groups of the catalysts. The point of zero charge is another important property of catalysts. It is the pH at which the net charge on the surface of the material equals zero (surface is electrically neutral)**.** It has been reported by some authors that the highest catalytic activity of alumina is at its point of zero charge (pH_{pzc}) [18, 19]. Additionally, it was assumed that point of zero charge is an important property that can affect the mechanism of ozonation in the presence of zeolites [26]. Therefore, it is important to determine the point of zero charge of the catalysts. The surface morphology of catalysts may also be helpful to an understanding of catalytic process. The SEM images have been used previously to compare the surface of alumina before and after reuse performance experiments for the degradation of natural organic matter in drinking waters. It was hypothesized that the significant change in the surface of the catalyst may be due to the adsorption of inorganic carbon on alumina [132]. The ZSM-5 zeolites and γ-alumina have been characterized by various techniques such as scanning electron microscopy (SEM), X-ray diffraction (XRD) and the Fourier transformed infrared spectroscopy (FTIR). These techniques have been

used to understand surface morphology, surface hydroxyl groups and elemental composition respectively.

3.2 Results

3.2.1 Physicochemical properties of catalysts

The physicochemical properties of the studied catalysts are presented in Table 3.1. Surface areas and porosities were determined either by the manufacturers or by our group in previous work [4]. They were measured by nitrogen adsorption at 77K. Surface areas were determined from the adsorption isotherms applying the BET equation and porosities were determined from the desorption isotherms using the Kelvin equation and the BJH method.

Table 3.1: Physicochemical properties of ZSM-5 zeolites and alumina

Material	SiO_2, wt%	Al_2O_3, wt. %	Na_2O, wt.%	SiO_2/Al_2O_3 mol ratio	Surface area (m^2/g)	Average pore size (Å)	Crystal size (µm)
Z900Na	98	0.2	1.3	900 ± 5	300	5.3	2-5
Z25Na	90	6.1	3.7	30 ± 5	300	5.3	<1
Z1000H	99	0.1	0.04	1000 ± 5	300	5.3	<1
Z25H	96	5.4	0.1	30 ± 5	300	5.3	<1
Alumina	0	100	0	-	190	47.8	-

The surface areas and porosities of the four zeolites are, as expected, essentially the same, and are substantially greater than the surface area of the alumina which, in line with this, exhibits very much larger pores than the zeolites.

3.2.2 Point of zero charge

The pH_{PZC} values for zeolites (Z1000H: SiO_2/Al_2O_3 = 1000, Z900Na: SiO_2/Al_2O_3 = 900, Z25H: SiO_2/Al_2O_3 = 25 and Z25Na: SiO_2/Al_2O_3 = 25) and alumina are consistent with compositions, with the zeolites in acid form showing lower values than the sodium forms and the alumina (Fig. 3.1). The Zeolites were characterized by different pH_{PZC} values. Z25H was found to have the lowest pH_{PZC}, which denoted 5 ± 0.2, Z1000H was characterised by pH_{PZC} of 7.5 ± 0.2. On the other hand, Z900Na and Z25Na had pH_{PZC} within the range of 9.2 - 9.5. The point of zero charge of γ-alumina was found to be 8.9 ± 0.1 (Fig. 3.1). The pH_{PZC} values of γ-alumina have been reported in the range of 8.0 – 9.7 [132]. From the Figure 3.1 it can be seen that in the case of initial pH 4.0, by the addition of alumina the pH of the solution increases and becomes constant after some time. The increase in pH is due to the adsorption of H^+ ions from the solution on alumina surface (Fig. 1.16). The decrease in pH in the case of experiments at initial pH 9.8 may be due to the release of H^+ ions from alumina surface in the solution (Fig. 1.16). In the case of zeolites the initial variation in pH by adding catalysts may be due to the exchange of Na^+ and H^+ ions, depending upon the initial pH of the solution.

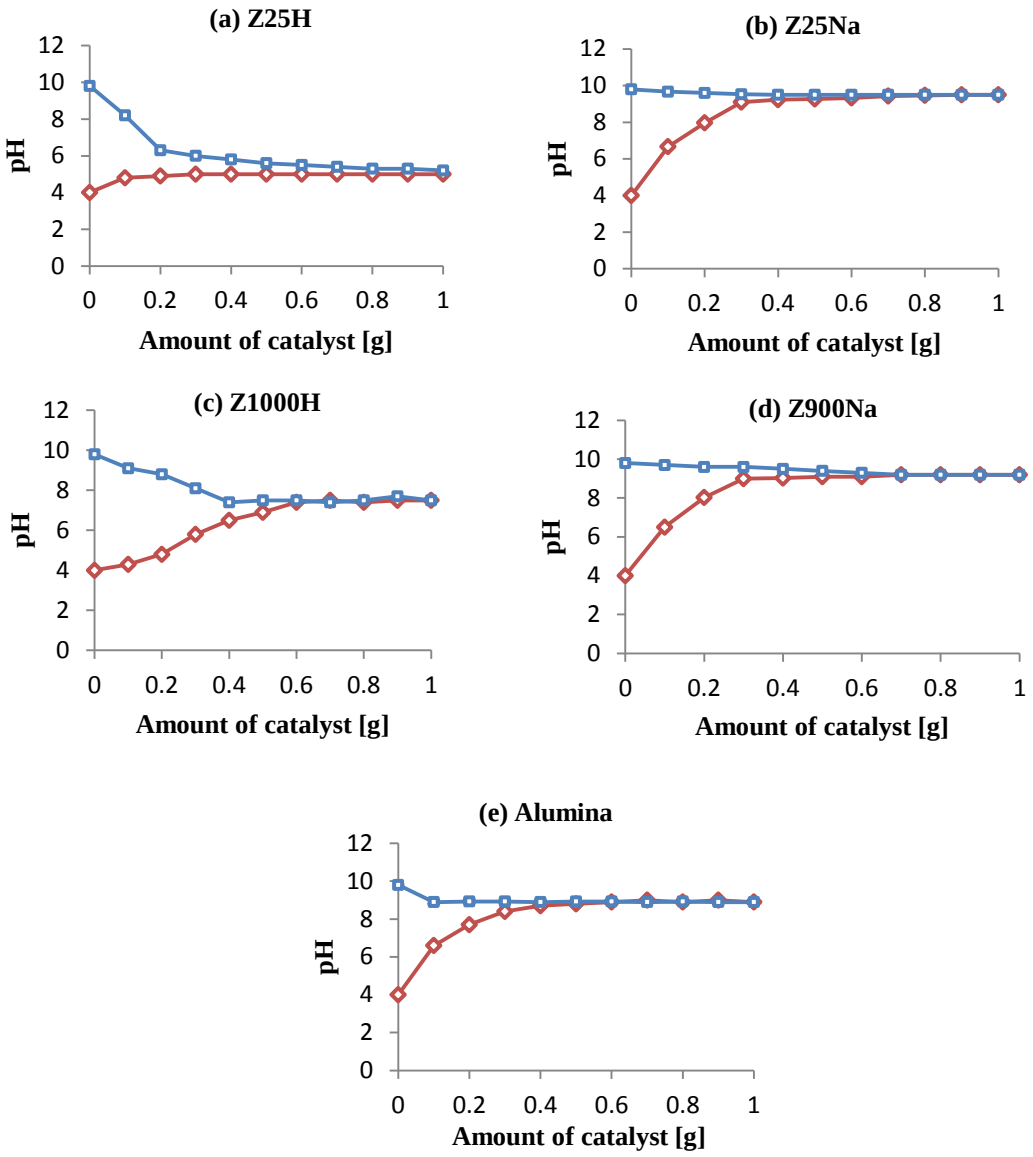

Figure 3.1: Point of zero charges (pH_{PZC}) of ZSM-5 zeolites and alumina (catalyst = 0.1 - 1.0 g; T = 25^{o}C; electrolyte NaCl = 10^{-3} mol/dm^{3}; V = 190 mL; SD ± 0.15).

3.2.3 FTIR studies

The IR region in the range of 3000 - 3700 cm^{-1} is important to assign, it gives important information about the surface hydroxyl groups present in the catalyst that are considered to be active catalytic sites [18, 20]. The IR spectra of ZSM-5 zeolites and alumina are shown in the Figure 3.2. The IR region in the range of 3000 - 3700 cm^{-1} (Fig. 3.2) can be assigned to the hydroxyl groups. The alumina shows strong bands in

this region when compared with ZSM-5 zeolites. This is because of the surface hydroxyl groups in alumina. Qi et al [20] investigated the density of surface hydroxyl groups of different forms of alumina by using Grignard method. The results indicated that γ-Al_2O_3 has high density of surface hydroxyl groups then that of α-Al_2O_3; these are 3.17×10^{-5} mol/m^2 and 0.27×10^{-5} mol/m^2 for γ-Al_2O_3 and α-Al_2O_3 respectively.

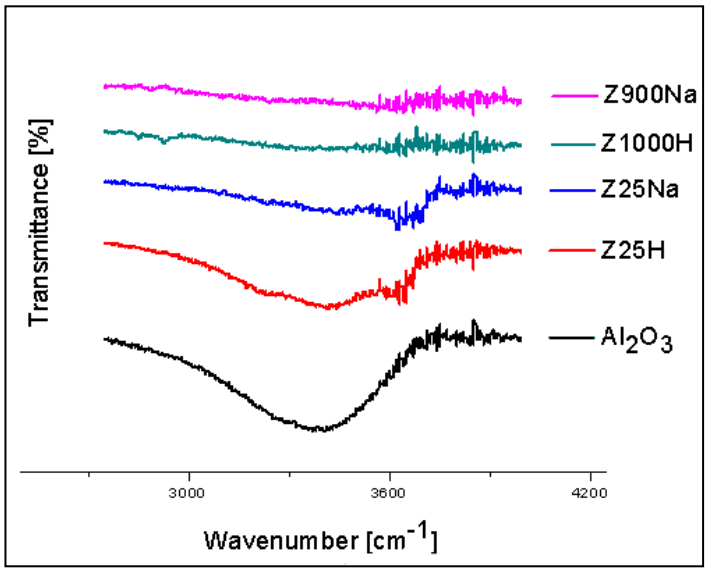

Figure 3.2: FT-IR spectra of ZSM-5 zeolites and γ-alumina.

The ZSM-5 zeolites (Z1000H, Z900Na, Z25H) show very weak bands around 3000 - 3700 cm^{-1} (Fig. 3.2). These may be assigned to the internal hydrogen bonded silanol groups [186].

3.2.4 SEM studies

The surface morphology of ZSM-5 zeolites and alumina has been characterized by SEM (Fig. 3.3). The SEM analyses are not conclusive and indicate that catalysts are not very well defined in morphology. Therefore, it is important to do XRD to investigate the nature of catalysts.

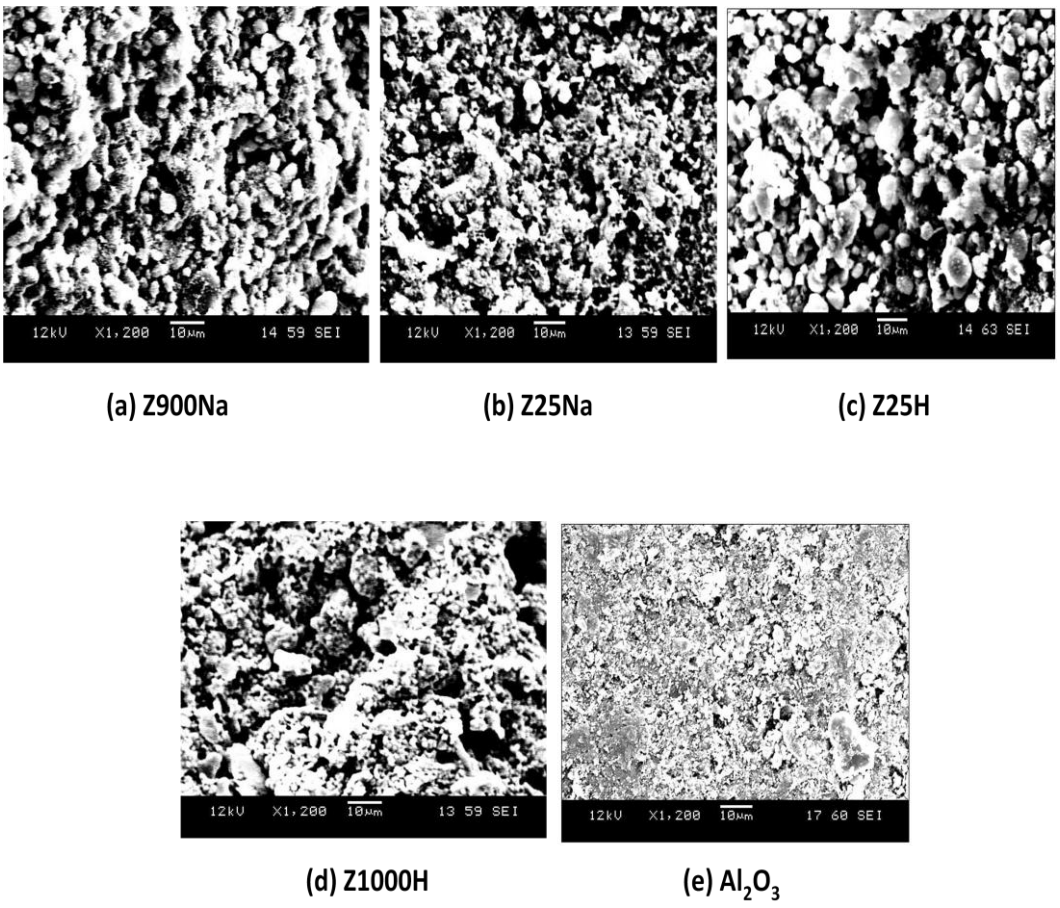

Figure 3.3: SEM images of ZSM-5 zeolites and alumina.

3.2.5 X-Ray diffraction studies

XRD patterns of ZSM-5 zeolites and alumina are presented in figure 3.4. The peaks at 2θ 7-10 and 22-25 confirmed ZSM-5 zeoliters [187]. The patterns further indicate the crystalline nature of ZSM-5 zeolites and amorphous nature of alumina.

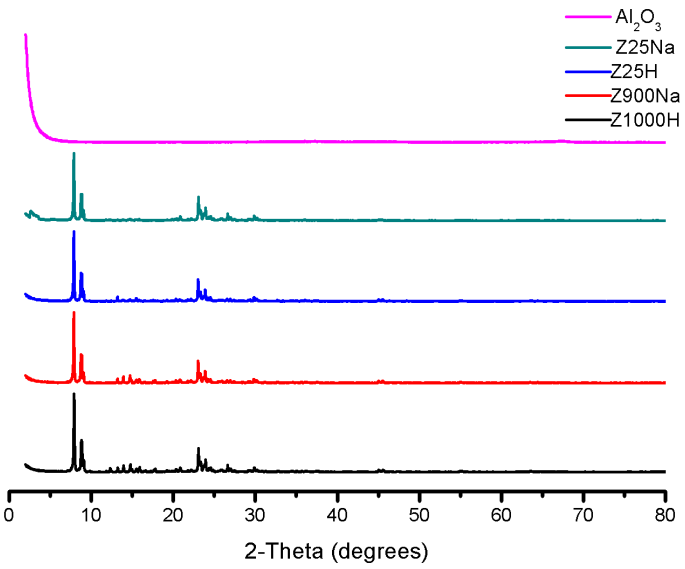

Fig. 3.4 XRD patterns of ZSM-5 zeolites and alumina

3.3 Summary of results

The ZSM-5 zeolites have been characterized by similar pore size and surface areas with different silica to alumina ratios and counter ions (Z1000H:SiO_2/Al_2O_3 = 1000, Z900Na:SiO_2/Al_2O_3 = 900, Z25H:SiO_2/Al_2O_3 = 25 and Z25Na:SiO_2/Al_2O_3 = 25). The catalysts have been characterized by using SEM, XRD and FTIR techniques. The points of zero charges (pH_{PZC}) have been determined by mass transfer method. The H-forms had low pH_{PZC}. The Z25H has the lowest pH_{PZC} (5.5) which is consistent with the composition of zeolites. The pH_{PZC} of alumina was found to be 8.9. The ZSM-5 zeolites show weak bands around 3000 – 3700 cm^{-1} region. However, alumina shows the strong bands, which indicate the highest density of surface hydroxyl groups in the case of alumina. The scanning electron microscopy (SEM) pattern indicates that all the catalysts are porous in

nature. The XRD patterns indicated that all zeolites are crystalline in nature and alumina was found to have amorphous nature.

3.4 Conclusions

1. The zeolites have a high surface area as compared with alumina.
2. The FT-IR studies show that alumina has stronger bands of surface hydroxyl groups as compared with zeolites.
3. The zeolites with H-forms have low point of zero charge values (pH_{PZC}) as compared with sodium forms.
4. The XRD patterns indicate the crystalline nature of ZSM-5 zeolites and amorphous nature of alumina.

CHAPTER 4 -MECHANISMS OF CATALYTIC OZONATION

"In this chapter the results of an investigation of active oxygen species such as hydroxyl radicals, hydrogen peroxide and superoxide ion radical formation in ozonation process on ZSM-5 zeolites and alumina have been presented. The coumarin, amplex red and NBD-Cl were used as probe molecules for an investigation of hydroxyl radicals, hydrogen peroxide and superoxide ion respectively".

4.1 Introduction

Ozone in water is unstable and undergoes reactions with some water matrix components. The decomposition of ozone in water leads to the formation of reactive oxygen species (ROS), which include the super oxide ion ($^{\bullet}O_2^-$), hydroxyl radicals ($^{\bullet}OH$) and hydrogen peroxide (H_2O_2). An investigation of the formation of ROS may give relevant information to understand the mechanism of the catalytic ozonation process.

The aim of this study has been to investigate the mechanism of catalytic ozonation (and in particular the formation of hydroxyl radicals, super oxide ion and hydrogen per oxide) on several ZSM-5 zeolites and alumina. Coumarin (COU), 4-chloro-7-nitrobenzo-2-oxa-1,3-dizole (NBD-Cl) and amplex red have been used as probe molecules as these are known to react with hydroxyl radicals, super oxide ion and hydrogen peroxide respectively, leading to the formation of fluorescent products. In this study the catalytic properties of alumina are compared with those of a series of silicalite ZSM-5 zeolites with different silica to alumina ratios and with both sodium and hydrogen counter ions (Z1000H:SiO_2/Al_2O_3 = 1000, Z900Na:SiO_2/Al_2O_3 = 900, Z25H:SiO_2/Al_2O_3 = 25 and Z25Na:SiO_2/Al_2O_3 = 25).

This chapter is focussing on the production of fluorescence products (7-hydroxycoumarin, resorufin and NBD-Cl product) as indicators of a radical mechanism. Further experiments have been performed in the presence of tert-butyl alcohol (TBA), which is a known radical scavenger. They have also been performed in the presence of phosphate ions, which may adsorb on the catalyst surface and replace the surface hydroxyl groups of alumina that may be responsible for ozone decomposition [18-20]. Therefore, the effect of phosphates may help to understand the role of surface hydroxyl groups of alumina in catalytic processes and their possible effect on ozonation in the presence of ZSM-5.

4.1.1 An investigation of hydroxyl radicals formation

According to the traditional catalytic ozonation theory, molecular ozone can oxidize organic substances via a direct route or can undergo decomposition via a chain reaction mechanism (chapter 1) leading to the formation of ROS. The hydroxyl radicals are one of the most important ROS. Therefore, the measurement of hydroxyl radicals is useful to investigate the mechanisms of catalytic ozonation processes. In this work coumarin (COU) has been used as a probe molecule as it is known to react with hydroxyl radicals leading to the formation of fluorescent 7-hydroxycoumarin (7HC) (Fig. 4.1). Coumarin is also a reasonable representative of the constituents in natural organic matter typically found in water [188-190]. Furthermore, it is used in the pharmaceutical industry as a precursor molecule in the synthesis of anticoagulant pharmaceuticals [191].

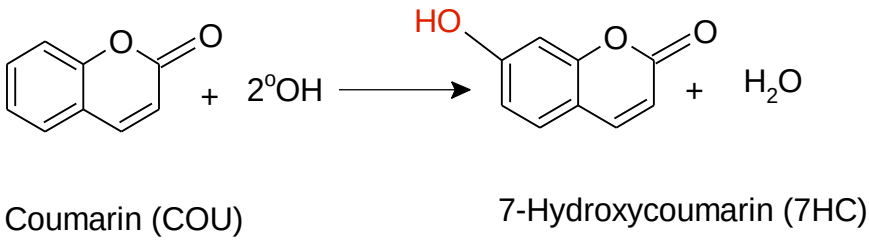

Figure 4.1: Formation of 7-hydroxycoumarin in the reaction of coumarin with hydroxyl radicals.

In this research coumarin was used as a radical probe, to investigate whether the mechanism for the degradation of pollutants on alumina and ZSM-5 zeolites involved the formation of hydroxyl radicals.

4.1.1.1 ^{o}OH radicals formation during the ozonation of water

It is well-known that aqueous ozone reacts in water, leading to the production of ROS such as hydroxyl radicals. The mechanism of ozone decomposition, leading to the formation of hydroxyl radicals has been discussed in chapter 1 (section 1.6.2). The

formation of ^{o}OH radicals depends on the pH of water and their concentration increases with the increase of pH. This may be due to the increase in hydroxide ions in the water as discussed in chapter 1.

4.1.1.2 ^{o}OH radicals formation during the catalytic ozonation

The formation of hydroxyl radicls during the catalytic ozonation processes has been investigated for many years in order to differentiate between radical and non radical mechanism. There have been several reports indicating the formation of hydroxyl radicals in various catalytic ozonation systems as discussed in chapter 1. It is not clear whether ozonation in the presence of alumina results in the formation of hydroxyl radicals, some reports indicated the ^{o}OH radicals formation [18-20] and others opposed it [21]. Usually, TBA has been used to differentiate between the radical and non radical mechanism in the ozonation in the presence of alumina [18-20]. However, there has been no direct proof of the formation of hydroxyl radicals. Similarly, the formation of ^{o}OH radicals in the presence of ZSM-5 zeolites is not well known therefore it is important to investigate the formation of hydroxyl radicals during the catalytic ozonation processes in the presence of alumina and ZSM-5 zeolites.

4.1.1.3 Methods for ^{o}OH radicals determination

Previously, various spin traps coupled with transient absorption in UV-Vis range and electron paramagnetic resonance (EPR) detection have been successfully applied for the detection of hydroxyl radicals during the ozonation process. Other methods such as luminescence [192], UV-Visible absorption [193] and fluorescence [194], have also been applied to measure hydroxyl radicals. Recently, it has been proved that several molecules such as terephthalic acid [195] and coumarin [196-199] produce strong luminescent compounds with hydroxyl radicals. Hence coumarin has been used for the first time as a

probe molecule for detecting and measuring hydroxyl radicals formed during the ozonation in the presence of alumina and ZSM-5 zeolites.

4.1.2 An investigation of hydrogen peroxide formation

Hydrogen peroxide is the only stable active oxygen species in the AOPs; the formation of hydrogen peroxide may give relevant information on the radical reactions taking place. Furthermore, hydrogen peroxide is one of the important oxidants and is often used as an agent to generate hydroxyl radicals in an advanced oxidation process [200]. Hydrogen peroxide also acts as a hydroxyl radical scavenger and is generated by the combination of two hydroxyl radicals [201]. Thus the measurement of H_2O_2 concentrations has been useful to evaluate and analyse AOP mechanisms. In this research work amplex red has been used as a probe to investigate the formation of hydrogen peroxide since amplex red has been known to react selectively to form highly fluorescent resorufin (Fig. 4.2).

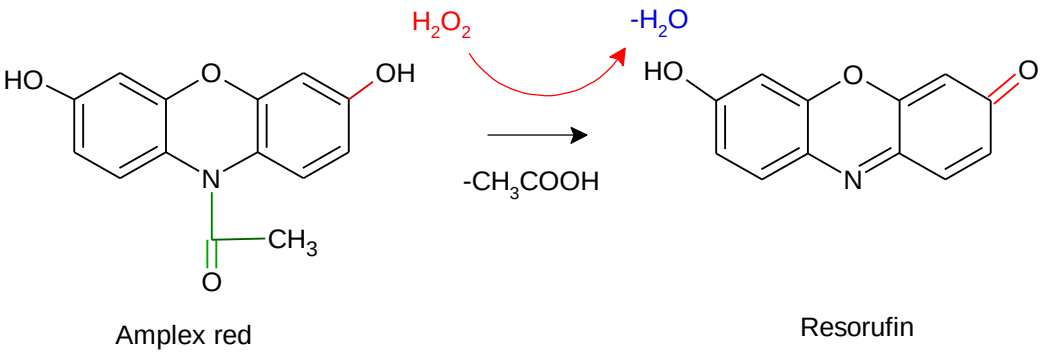

Figure 4.2: Formation of resorufin in the reaction of amplex red with hydrogen peroxide.

4.1.2.1 H_2O_2 formation during the ozonation of water

Staehellin et al [36, 201] studied ozone decomposition in water and found out that the aqueous ozone may react with hydroxide ions (OH^-) or organic molecules to generate reactive oxygen species. Hydrogen peroxide formation can result from O_3 decomposition or from the ozonation of organic compounds. In the first case ozone reacts with OH^- ions

in aqueous solutions to generate H_2O_2 (Equations 4.1 and 4.2). The stability of forming H_2O_2 depends upon the pH of the solution and it decreases with the increase in pH (Equation 4.2) [36]. It is worth mentioning here that H_2O_2 also reacts with O_3, but only when present in the ionized form (pH > 11.6) (Equation 4.3) [36]. The reaction leads to the generation of hydroxyl radicals and superoxide ion [36]. The superoxide ion ($^{o}O_2^-$) reacts with ozone to form $^{o}O_3^-$ ion, which then reacts with water molecules to form hydroxyl radical (Equations 4.4-4.5) [36, 201]:

$$O_3 + OH^- \rightarrow HO_2^- + O_2 \quad (4.1)$$

$$H_2O_2 \rightleftharpoons HO_2^- + H^+ \quad pKa = 11.6 \quad (4.2)$$

$$O_3 + HO_2^- \rightarrow OH^{o} + {}^{o}O_2^- + O_2 \quad (4.3)$$

$$O_3 + {}^{o}O_2^- \rightarrow {}^{o}O_3^- + O_2 \quad (4.4)$$

$$^{o}O_3^- + H_2O \rightarrow HO^{o} + OH^- + O_2 \quad (4.5)$$

The hydroxyl radicals can then interact further with O_3:

$$HO^{o} + O_3 \rightarrow HO_2^{o} + O_2 \qquad k = 3.0 \times 10^9\ M^{-1}s^{-1} \quad (4.6)$$

However, scavengers (carbonates, phosphates and bicarbonates) compete for the hydroxyl radicals [36]:

$$HO^{o} + CO_3^{2-} \rightarrow OH^- + {}^{o}CO_3^- \qquad k = 4.2 \times 10^8\ M^{-1}s^{-1} \quad (4.7)$$

$$HO^{o} + HCO_3^- \rightarrow OH^- + HCO_3^{o} \qquad k = 1.5 \times 10^7\ M^{-1}s^{-1} \quad (4.8)$$

$$HO^{o} + HPO_4^{2-} \rightarrow OH^- + {}^{o}HPO_4^- \qquad k = 5 \times 10^6\ M^{-1}s^{-1} \quad (4.9)$$

Two hydroxyl radicals may also combine to form H_2O_2 [201]:

$$HO^{o} + HO^{o} \rightarrow H_2O_2 \qquad k = 5 \times 10^9\ M^{-1}s^{-1} \quad (4.10)$$

Furthermore, H_2O_2 may also be formed as a result of the reaction of O_3 with organic solutes;

$$O_3 + M \rightarrow M_{oxid} + H_2O_2 \quad (4.11)$$

The reactions of hydroxyl radicals with organic molecules (M) can initiate a radical chain reaction [36]:

$HO^{o} + M \rightarrow R^{o}$ (4.12)

$R^{o} + O_2 \rightarrow ROO^{o}$ (4.13)

$ROO^{o} \rightarrow M_{oxid} + HO_2^{o}$ (4.14)

4.1.2.2 H_2O_2 formation during the catalytic ozonation

The formation of H_2O_2 in catalytic ozonation processes has been reported by some authors and such phenomena have been observed during the aqueous ozone decomposition in the presence of granular activated carbon [202] and catalytic ozonation of nitrobenzene in the presence of modified ceramic honeycomb [203]. Alvarez et al [202] reported that H_2O_2 formed in ozonation on granular activated carbon was due to the interaction of ozone with the surface of the catalyst. However, it was reported by Zhao et al [203] that the formation of H_2O_2 in catalytic ozonation of nitrobenzene on a ceramic honeycomb was due to the reactions of adsorbed O_3 and nitrobenzene. Furthermore, H_2O_2 formation was higher in catalytic ozonation when compared with ozonation alone [203]. It has been reported by Zhang et al that H_2O_2 formed during the ozonation in the presence of ZSM-5 zeolites. However, the formed hydrogen peroxide was less than ozonation alone [204]. It is therefore important to study the formation of H_2O_2 in ozonation on other catalysts such as alumina and ZSM-5 zeolites in order to understand the mechanism of the catalytic ozonation process.

4.1.2.3 Methods for H_2O_2 determination in water

Various methods have been used to measure H_2O_2 in AOPs. Among them are spectrophotometric methods employing N, N–diethyl-p-phenylenediamine (DPD) [174], using copper (II) ion with 2,9-dimethyl-1,10-phenanthroline (DMP) [205] and a

fluorometric method employing p-hydroxylphenyl acetic acid (POHPAA) [206]. Amplex red has been used before as an effective probe in biological assays [166, 177, 207]. This is because it selectively reacts with H_2O_2, which then leads to the formation of fluorescent resorufin [166, 177, 207]. Based on the previous reports it has been considered that other ROS may not interfere with the reaction between amplex red and hydrogen peroxide. In this work amplex red has been used as a probe for detecting and measuring hydrogen peroxide formed during the ozonation alone and ozonation in the presence of alumina and ZSM-5 zeolites with different silica to alumina ratios (Z1000H:SiO_2/Al_2O_3 = 1000, Z900Na:SiO_2/Al_2O_3 = 900, Z25H:SiO_2/Al_2O_3 = 25 and Z25Na:SiO_2/Al_2O_3 = 25).

4.1.3 An investigation of superoxide ion radical formation

The high reactivity of ozone molecule gives rise to different reactions with some water matrix components. These reactions lead to the formation of ROS. The superoxide ion is an important and short-lived entity, constituting the fundamental part of AOPs. Hence the formation of superoxide ion may give the relevant information on the radical reactions taking place.

4.1.3.1 $^{o}O_2^-$ formation during the ozonation of water

The ozone in water may react with hydroxide ions (OH^-) leading to the formation of ROS [36]. The superoxide ion is one of these species and may be formed as described below. Two hypotheses were presented to describe the formation of $^{o}O_2^-$ in water as a result of the reaction between ozone and hydroxyl ions (OH^-). In the first hypothesis, ozone reacts with OH^- ions in aqueous solutions to generate $^{o}O_2^-$ (Equations 4.15, 4.16). The formation of $^{o}O_2^-$ depends upon the pH of the solution and decreases with the decrease in pH of the solution (Equation 4.16) [36]. It is worth mentioning here that $^{o}O_2^-$ also reacts with O_3,

leading to the formation of $^{o}O_3^-$ which then react with water molecules to form hydroxyl radicals (Equation 4.17, 4.18) [36].

$$O_3 + OH^- \rightarrow HO_2^{o} + {}^{o}O_2^- \quad (4.15)$$

$$HO_2^{o} \rightleftharpoons {}^{o}O_2^- + H^+ , \text{pKa} = 4.8 \quad (4.16)$$

$$O_3 + {}^{o}O_2^- \rightarrow {}^{o}O_3^- + O_2 \quad (4.17)$$

$$^{o}O_3^- + H_2O \rightarrow HO^{o} + OH^- + O_2 \quad (4.18)$$

In the second hypothesis, O_3 reacts with OH^- ions to form HO_2^- ions which further react with ozone to form OH^o radicals , O_2 and $^{o}O_2^-$ (Equation 4.1, 4.3). Furthermore, the H_2O_2 may also be formed and its stability depends upon the pH of the solution (which is when pH > 11.6) [36]. The $^{o}O_2^-$ may further react with O_3 to form $^{o}O_3^-$, which reacts with water to form hydroxyl radicals (Equation 4.4, 4.5).

4.1.3.2 $^{o}O_2^-$ formation during the catalytic ozonation

The formation of superoxide ion radical ($^{o}O_2^-$) in catalytic ozonation processes has been reported in the presence of modified FeOOH [93]. Additionally, it was hypothesized by Zhang et al [93] that the reaction of ozone with the surface hydroxyl groups of FeOOH results in the formation of $^{o}O_2^-$ anion and hydroxyl radicals. Ernst et al [17] hypothesized that $^{o}O_2^-$ may form in the catalytic ozonation of alumina leading to the generation of hydroxyl radicals however no proof of the formation of superoxide ion radical was provided in that investigation. Staehelin et al [36] hypothesized that the production of highly O_3 selective $^{o}O_2^-$ anion promotes the reaction to produce hydroxyl radicals (HO^o). It is therefore important to study the formation of superoxide ion ($^{o}O_2^-$) in the ozonation on alumina and ZSM-5 zeolites in order to understand the mechanism of the catalytic ozonation process.

4.1.3.3 Methods for $^{o}O_2^-$ determination

The concentration of $^{o}O_2^-$ has been determined by various methods in aqueous and biological systems. Among the frequently used methods is the electron paramagnetic resonance (EPR) spin trapping [208] and spectrophotometric methods employing nitro-substituted aromatics such as nitroblue tetrazolium (NBT) [209]. In this research 4-chloro-7-nitrobenz-2-oxa-1,3-diazole (NBD-Cl) was used as a probe molecule for the first time to detect $^{o}O_2^-$ in the ozonation process in the presence of ZSM-5 zeolites and alumina. The NBD-Cl has been used before as an effective probe in aqueous systems and biological assays [172, 173]. The reason to select NBD-Cl (Fig. 4.3) as a probe had been due to its selective reaction with $^{o}O_2^-$ leading to the formation of the fluorescent product at 550 nm which can be detected at low levels by fluorescence spectroscopy [166, 172, 173].

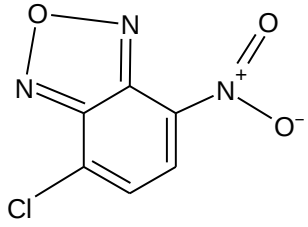

4-chloro-7-nitrobenz-2-oxa-1,3-diazole
(NBD-Cl)

Figure 4.3: Structure of NBD-Cl.

4.2 Results and discussion

The results have been divided into three main sections. The first part describes the results obtained in catalytic ozonation of coumarin on zeolites and alumina. The second part describes an investigation of hydrogen peroxide and in the final part the results of the superoxide ion radical investigation have been presented. Furthermore, experiments have been performed to study the influence of the main variables affecting the mechanism of

the catalytic ozonation process (i.e. solution pH, presence of ^{o}OH scavenger tert-butyl alcohol, presence of phosphates and the effect of catalyst dose).

4.2.1 PART 1 – An investigation of hydroxyl radical formation

4.2.1.1 Adsorption of coumarin on Al_2O_3 and ZSM-5 zeolites in the absence of ozone

The data presented in Figure 4.4 as the percentage of total coumarin concentration removed from the solution with time in the reactor, at various pHs. The data show clearly that the four zeolites adsorb coumarin to a similar extent and more effectively than alumina. There is relatively little dependence of adsorption capacity on solution pH. After 30 minutes, the zeolites typically adsorb 25 % (2.5 mg/g) of the coumarin at pH 3.0 and 15 % (1.5 mg/g) at pH 13.0, whereas the alumina adsorbs 5% or less at both pHs. It is worth noting that adsorption of 5% of the coumarin corresponds to only 0.5 mg coumarin per gram of catalyst. Referring to the Figure 4.4, the rate of coumarin adsorption on ZSM-5 zeolites and alumina is consistent to some extent over the pH range 3.0-8.8, but in all cases, show a dramatic fall at pH 13.0. It is likely that the surface is fully populated with OH^- ions at this pH therefore it is suggested that it might be this that reduces the rate of adsorption of coumarin.

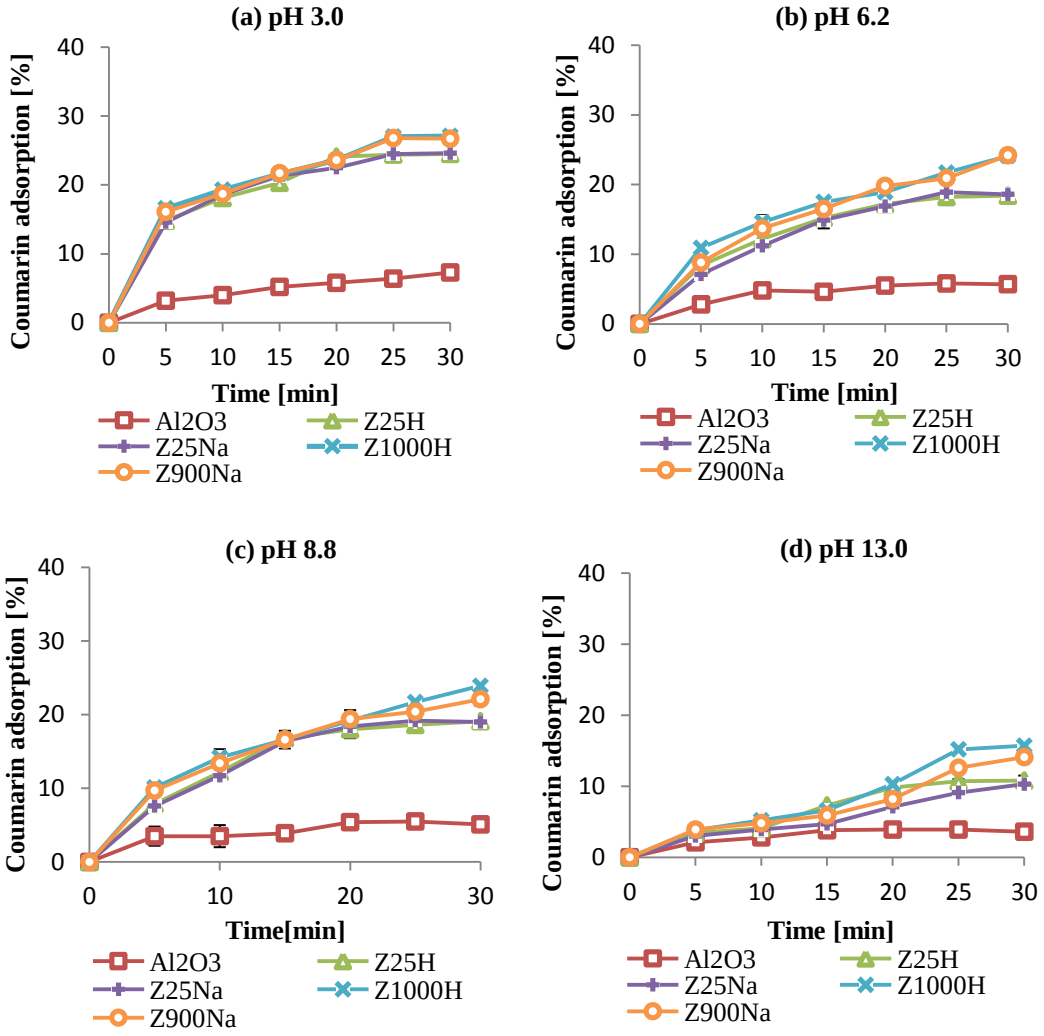

Figure 4.4: Removal of coumarin by adsorption ($C_{o\,(COU)}$ = 20 mg/L; T =25 ^{o}C; pH = 3.0, 6.2, 8.8 and 13.0; adsorbent = 2.0 g; V = 190 mL; SD ± 1.5%).

4.2.1.2 Catalytic ozonation of coumarin and the effect of pH

Figure 4.5 shows the percentage removal of coumarin with time for the same catalysts and at the same pH values but in the presence of ozone. Data is also shown in the percentage removal under the action of ozone alone. The first thing to note is that at pH 13.0, ozonation is effective in decomposing coumarin, producing 60% removal after 30 minutes, but the presence of the catalysts does not affect the extent of decomposition. At lower pH the catalytic effect is observed. By considering the difference between ozonation

alone and ozonation in the presence of a catalyst, alumina is most effective at pH 8.8 (Fig. 4.5e, t = 30 minutes). The zeolites have a relatively small effect at this pH, with the low silica zeolites having almost no effect and the high silica zeolites have a similar effect to the alumina. As the pH reduces the activity of the zeolites increases and at pH 3.0 all the zeolites lead to complete removal of the coumarin after 30 minutes compared with ozonation alone and ozonation/alumina (which leads to only 30-40% removal).

It is possible to rationalise these results to some extent. At pH 13.0, none of the catalysts shows activity. This is most likely because they are all well above their pH_{PZC} and their surfaces are essentially covered with hydroxide ions. It is known that hydroxide ions promote the decomposition of ozone so any reaction of coumarin with ozone on the surface of the catalysts would be unlikely.

Alumina shows its highest activity at pH 8.8, close to its pH_{PZC} of 8.9. This suggests that the most active surface for catalytic ozonation is the one dominated by neutral hydroxyl groups. The O of protonated surface hydroxyl group is weaker in nucleophilicity than the O of a neutral state hydroxyl group. Therefore, the protonation of the surface hydroxyl group will be a disadvantage to the surface binding of ozone [210]. This pH dependence of alumina's activity has been noted before [18-20].

It is important to note that over the time scale of the experiments the zeolites will equilibrate with the external pH, for example at pH 3.0 the Na-form of the zeolites will go to acid form. However, 30 minutes may not be that long so there may not be much exchange, the results further support is assumption as there was no significant change in the pH was obserbed, during the adsorption, ozonation and catalytic ozonation experiments. Therefore, Na-form and H-forms can be compared to some extent.

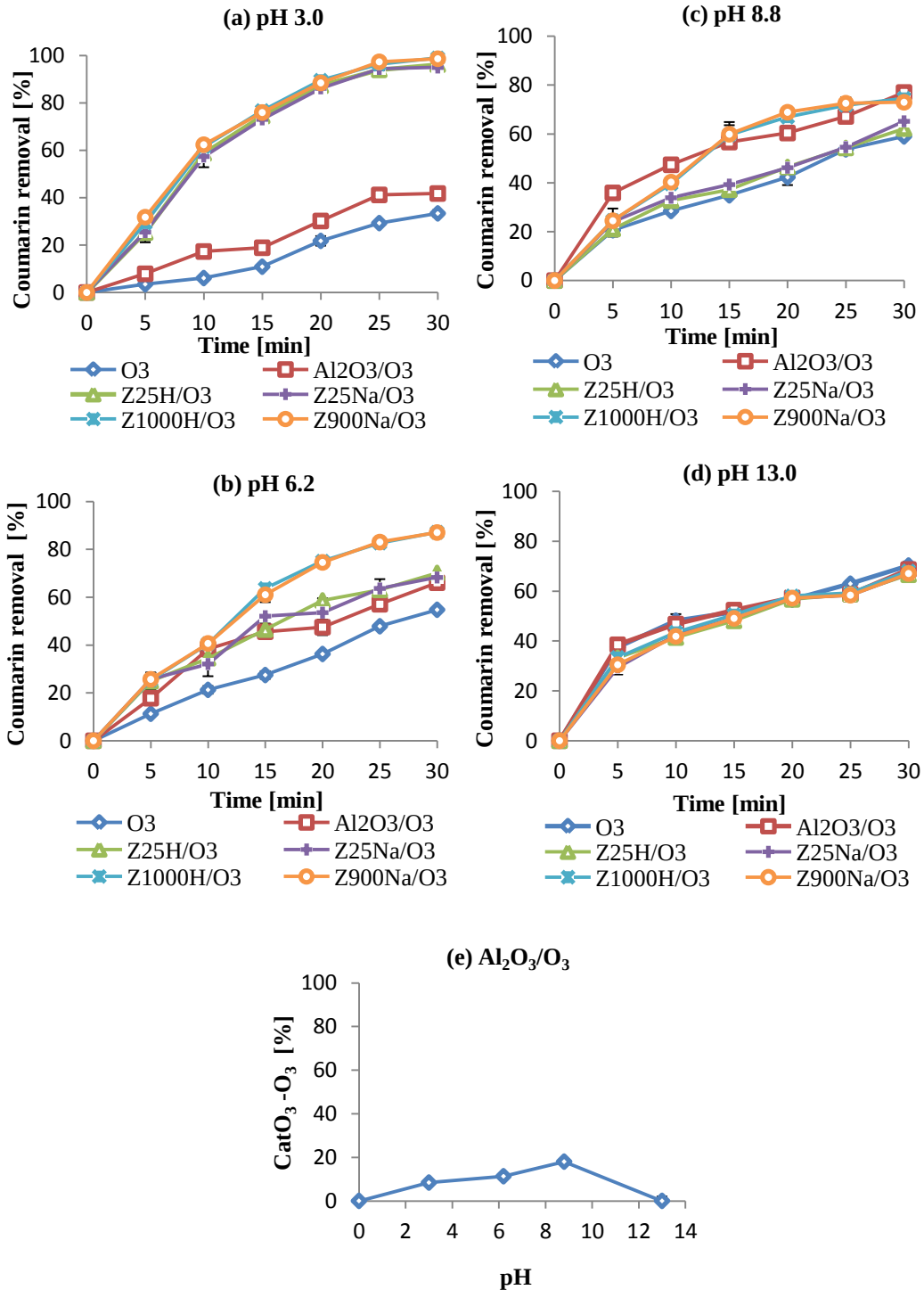

Figure 4.5: Removal of coumarin by ozonation alone and ozonation in the presence of Al_2O_3 and ZSM-5 zeolites ($C_{o\,(COU)}$ = 20 mg/L; T = 25 ^{o}C; pH = 3.0, 6.2, 8.8 and 13.0; O_3 = 0.6 mg/min; t = 30 minutes; catalyst = 2.0 g; V = 190 mL; SD ± 5 %).

The zeolites appear to be most active at acidic pH. For example the removal of COU on studied zeolites was 90% at pH 3.0 and only 68% at pH 13.0 (Fig. 4.5). It has been suggested by others that Bronsted acid groups on zeolites might promote ozone decay and even lead to the generation of hydroxyl radicals. This possibility is investigated in the following experiments. It is also worth noting that the pH of the solution did not change significantly (± 0.1) after 30 min ozonation with and without catalysts.

4.2.1.3 Formation of 7-hydroxycoumarin

The formation of 7HC, a hydroxylated transformation product of COU, was monitored during the ozonation of coumarin. This product is thought to be an indicator of a radical mechanism of decomposition. The data presented in Figure 4.6, shows that, at pH 3.0, almost no 7HC is formed with any of the catalysts. The results at pH 3.0 are not conclusive in terms of radical and non radical mechanism since 7HC is not the only hydroxylated product formed during ozonation and catalytic ozonation process, Other researchers have detected following isomers 3HC, 4HC, 5HC, 6HC and 8-hydroxycoumarin [197]. At pH 6.2 and 8.8, alumina results in the significant 7HC generation, in contrast to the zeolites which result in negligible amounts of the product. This strongly suggests that alumina does indeed promote decomposition of coumarin by a radical mechanism, at least at a pH close to the pH_{PZC}. Based on several reports [196-199], it is assumed that superoxide ion, HO_2^o and H_2O_2 do not interfere with the reaction between hydroxyl radicals and COU to produce 7HC. Additionally, in this work a mixture of 5 mL of 30% H_2O_2 and 195 mL of 20 mg/L COU was treated in a semi-batch reactor for 30 min and no significant fluorescence was observed.

The 7HC concentration profiles shown in Figures 4.6b and 4.6c indicated that in the case of alumina the 7HC concentration rises over the first 10-15 minutes and then decreases. It

seems likely that this decrease is due to subsequent reaction of 7HC with more ozone, perhaps under catalytic action. Although we suspect that the low yield of 7HC reflects a relatively low concentration of formed hydroxyl radicals, an alternating explanation could be that negligibly low fluorescent isomers of 7HC are formed in its place. As mentioned earlier that other researchers have detected following isomers 3HC, 4HC, 5HC, 6HC and 8-hydroxycoumarin [197].

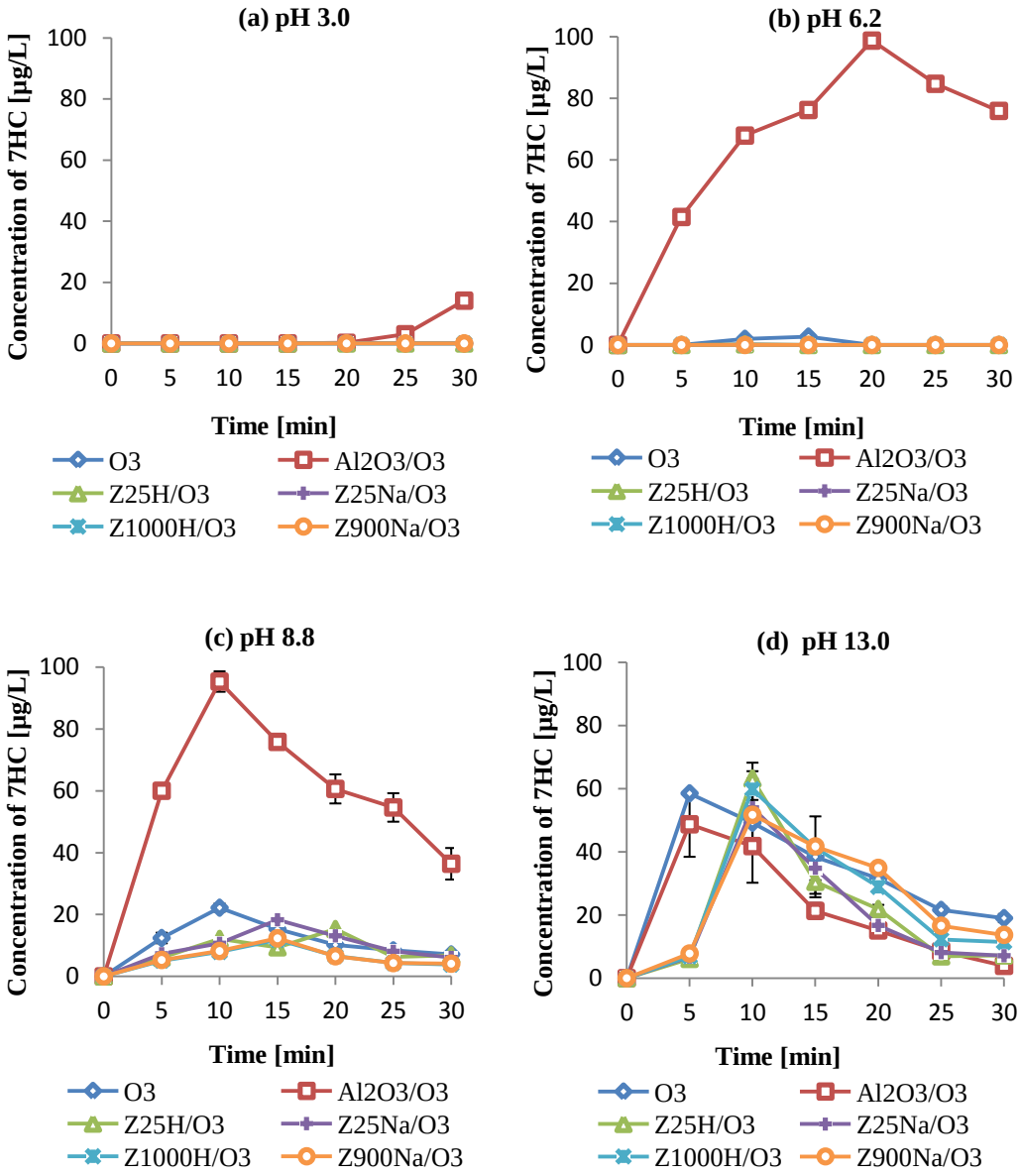

Figure 4.6: Formation of 7-hydroxycoumarin as a result of ozonation of coumarin ($C_{o\ (COU)}$ = 20 mg/L; T = 25 ^{o}C; pH = 3.0, 6.2, 8.8 and 13.0; O_3 = 0.6 mg/min; catalyst = 2.0 g;

V = 190 mL; excitation wavelength = 332 nm; emission wavelength = 455 nm; SD ± 5 μg/L).

At the highest pH of 13.0, the zeolites also appear to promote the formation of 7HC. In fact, it is likely that higher concentrations of hydroxide ions at pH 13.0 may simply be acting as precursors for hydroxyl radicals, quite independently of whether a catalyst is present.

4.2.1.4 The aqueous ozone depletion

The concentration of ozone in solution during the reaction of coumarin is shown in Figure 4.7. Monitoring of aqueous ozone concentrations in coumarin ozonation experiments undertaken at pH 3.0 and 6.2 and 8.8 revealed that the highest concentrations of aqueous ozone have been observed during the ozonation alone, decreased during the ozonation in the presence of zeolites, and were the lowest in the presence of alumina. At pH 13.0 aqueous ozone concentrations were at a similar level in all studied ozonation systems (Fig. 4.7d). Low concentrations of aqueous ozone in the presence of alumina are an indication that its decay rate is higher in the presence of alumina.

Further experiments were performed to investigate the rate at which ozone decomposition (or at least ozone removal) occurs on the alumina and zeolite studies in the absence of any organic compounds, the idea being that at least part of the ozone reduction observed as coumarin is removed might in fact be due simply to decomposition of ozone on the catalyst surface.

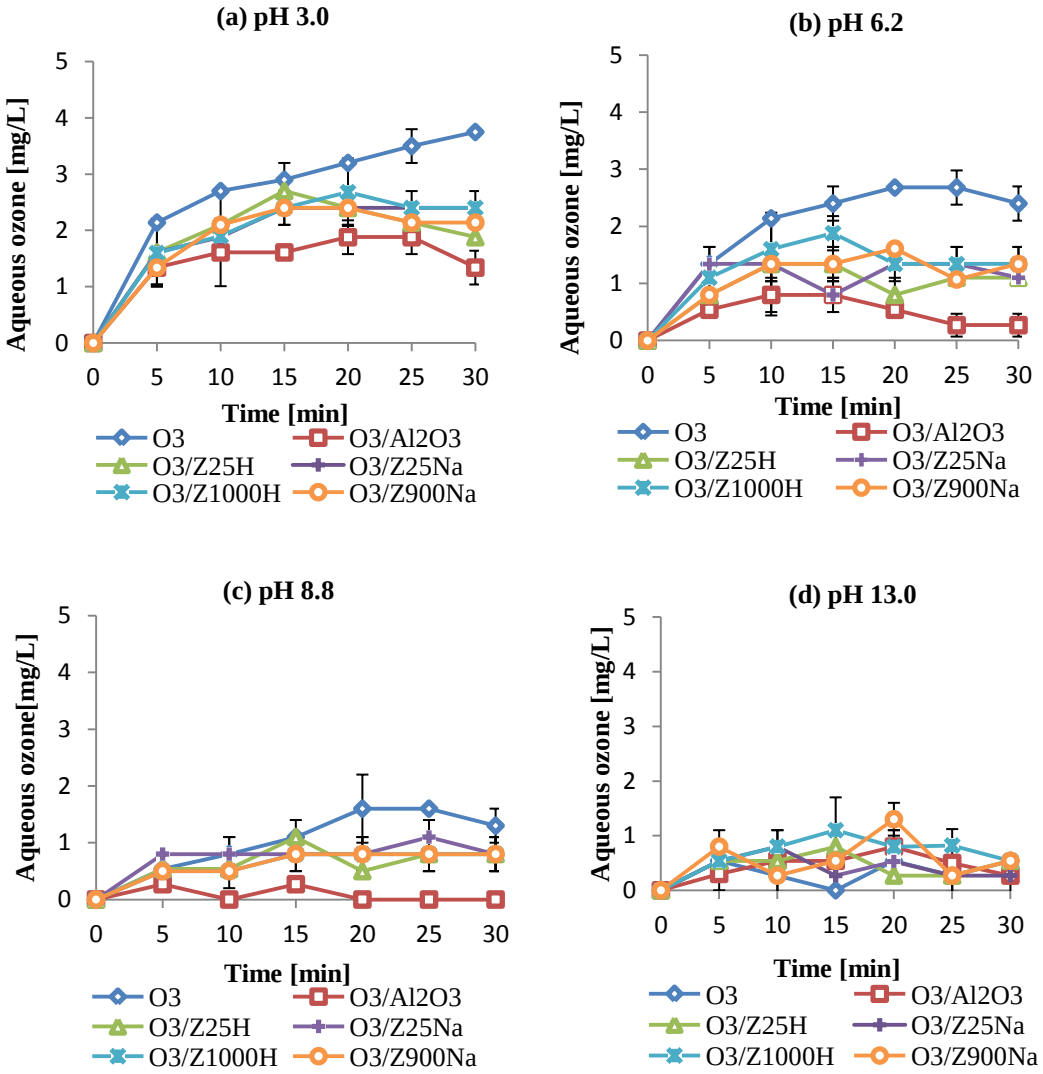

Figure 4.7: Aqueous ozone concentration during ozonation alone and ozonation in the presence of Al_2O_3 and ZSM-5 zeolites ($C_{o\,(COU)}$ = 20 mg/L; T = 25 ^oC; pH = 3, 6.2, 8.8 and 13; O_3 = 0.6 mg/min; catalyst = 2 g; V = 190 mL; SD ± 0.3 mg/L).

First order rate constants for the decomposition of ozone in the presence and absence of the five catalysts studied are shown in Table 4.1 (data is also shown for the rates of ozone decomposition in the presence of TBA, referred to later). Rate data for the decomposition reaction without TBA shows that at pHs 3.0 and 6.2 the catalysts do catalyses ozone decomposition, and alumina appears to catalyse the process more effectively than the

zeolites. At pH 13.0 the rates for all studied systems are similar. The fast decay of aqueous ozone at pH 3.0 and 6.2 in the alumina/ozone system may be due to the interaction of aqueous ozone with the surface hydroxyl groups of alumina. It is reasonable that this effect is not observed at pH 13.0, where the pH is much higher than the pH_{PZC} of alumina, and where the surface would be negatively charged.

In contrast to our results, it has been reported by Lin et al [21] that aqueous ozone is not decomposed by alumina. On the other hand other authors have observed aqueous ozone decay in the presence of alumina [3, 13, 14]. Researchers have claimed that aqueous ozone decay on alumina at pH close to the pH_{PZC} involved hydroxyl radicals, which increased the rate of ozone decay [18-20].

Table 4.1: Effect of TBA and pH of solution on the first-order ozone decay rate constants in the presence and absence of alumina and ZSM-5 zeolites

Process	***k overall* ×(10^{-3} s^{-1})**		***k overall* ×(10^{-3} s^{-1})**		***k overall* ×(10^{-3} s^{-1})**	
	pH 3.0		pH 6.0		pH 13.0	
	No TBA	With TBA	No TBA	With TBA	No TBA	With TBA
O_3	0.38 ± 0.03	0.35 ± 0.01	0.66 ± 0.01	0.51 ± 0.01	4.1 ± 0.1	3.1 ± 0.2
O_3/Alumina	0.61 ± 0.03	0.41 ± 0.01	0.98 ± 0.06	0.64 ± 0.02	4.2 ± 0.1	2.9 ± 0.2
O_3/Z 25H	0.52 ± 0.02	0.47 ± 0.08	0.86 ± 0.03	0.77 ± 0.05	4.3 ± 0.3	3.1 ± 0.3
O_3/Z1000H	0.46 ± 0.01	0.43 ± 0.01	0.77 ± 0.04	0.70 ± 0.03	4.3 ± 0.1	3.3 ± 0.3
O_3/Z25Na	0.47 ± 0.03	0.43 ± 0.01	0.76 ± 0.04	0.71 ± 0.04	4.3 ± 0.2	2.9 ± 0.2
O_3/Z900Na	0.45 ± 0.01	0.43 ± 0.01	0.75 ± 0.02	0.72 ± 0.06	4.3 ± 0.1	3.1 ± 0.3

Table 4.1 shows that the zeolite catalysts have a less pronounced effect on ozone decomposition than alumina. The previous observation that zeolites tend not to promote radical mechanisms (coumarin removal results in relatively little 7HC production) suggests that reductions in ozone concentration may be due to adsorption on the zeolite surface rather than by ozone decomposition on the surface. Indeed, Fujita et al [22] found

that high silica zeolites reduce the aqueous ozone concentrations and proposed that it may be due simply to the adsorption of ozone. Others in contrast [26] reported that acid sites on zeolites might be responsible for aqueous ozone decomposition.

Furthermore, as can be observed from Table 4.1, the effect of the radical scavenger TBA on the rate of ozone removal can be seen. The results show clearly that at pH 3.0 and 6.2, TBA reduces the rate of ozone removal on alumina but has no significant effect on ozone loss over the zeolites. This is yet more evidence for a radical ozone decomposition pathway occurring in the presence of alumina but a non-radical route in the presence of zeolites.

At the highest pH of 13.0, TBA reduces ozone loss over all catalysts and, importantly, in the absence of any catalysts, to about the same extent. This is almost certainly a consequence of the high hydroxide ion concentration in solution at this pH, which will inevitably lead to the generation of hydroxyl radicals independently of whether a catalyst is used or not.

4.2.1.5 Effect of hydroxyl radical scavengers

The evidence presented above suggests that catalytic ozonation of organic compounds on alumina takes place, at least to an extent, by a radical mechanism. On the other hand catalytic ozonation on zeolites most probably, an adsorption process of both ozone and organic molecules, which is followed by oxidative reactions between adsorbed ozone and organic compound on the catalyst surface. Further experiments to investigate this were carried out by observing the effect of the radical scavenger, TBA, on the rate of removal of coumarin and the rate of production of 7HC. The data was taken at pH 6.2 and is shown in Figure 4.8.

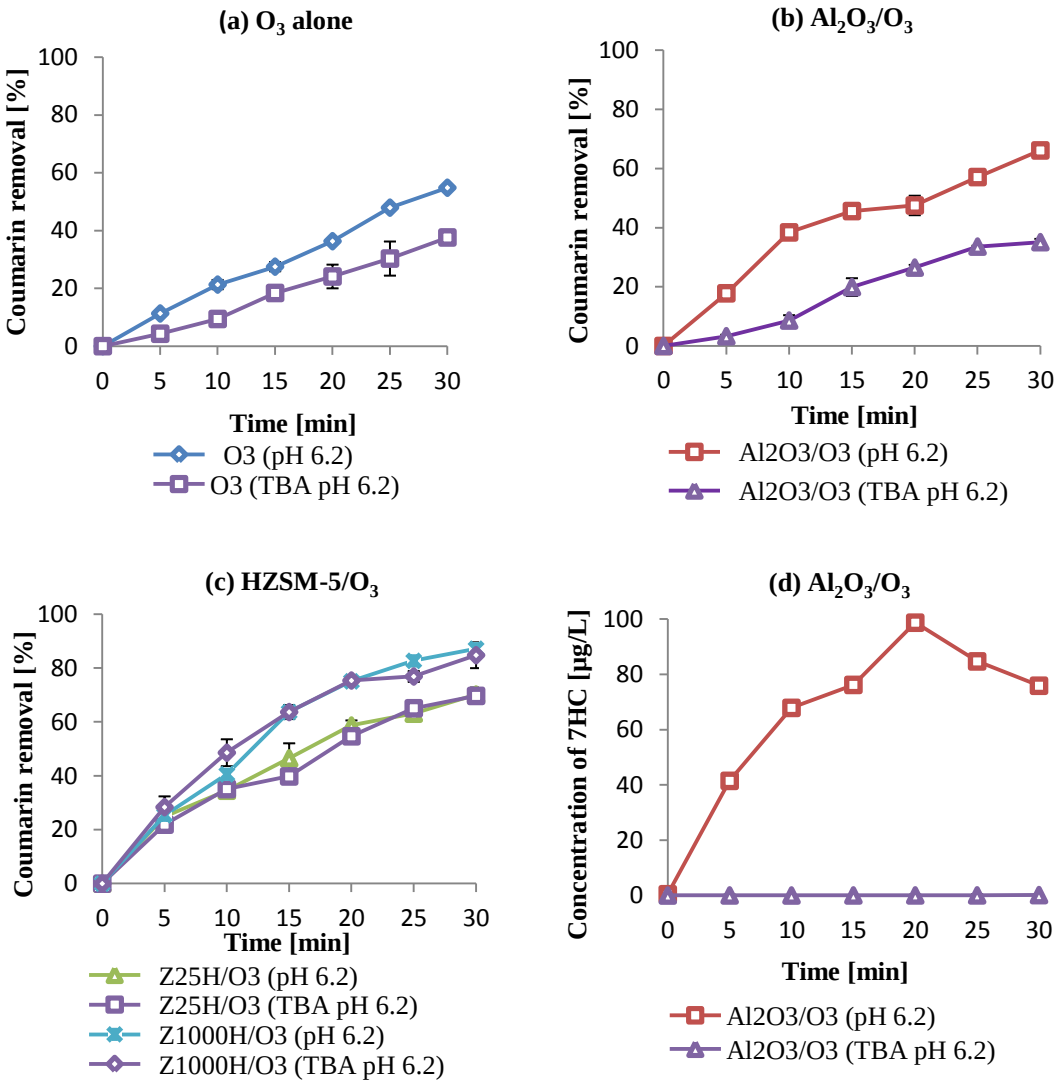

Figure 4.8: Effect of TBA on the removal of coumarin by O_3, Al_2O_3/O_3 and HZSM-5/O_3 ($C_{o\,(COU)}$ = 20 mg/L; TBA = 50 mg/L; T = 25 ^oC; pH = 6.2; O_3 = 0.6 mg/min; catalyst = 2.0 g; V = 190 mL; SD ± 5%).

The comparison of Figures 4.8a and 4.8b shows that TBA reduces the rate of removal of coumarin both under ozonation alone and under ozonation in the presence of alumina. This suggests that alumina-catalysed ozonation involves a radical mechanism. In contrast, in the presence of all four of the zeolites, TBA has a negligible effect on the rate of coumarin removal (Figure 4.8c). This data suggests strongly that alumina catalyses a

radical mechanism and the zeolites operate by a mechanism in which radical processes are not important. Figure 4.8d provides further evidence as it shows that the production of 7HC by alumina-catalysed ozonation is stopped altogether by the presence of TBA, consistent with 7HC being produced over alumina by a radical mechanism which can be suppressed by the radical scavenger.

4.2.1.6 Effect of phosphates

Experiments with added phosphate ions (50 mg/L) were carried out on the basis that phosphate ions which are hard Lewis bases can displace hydroxide ions on the surface of alumina. These ions have high affinity towards alumina ions (Al) on the surface of alumina [132] and their adsorption occurring through the exchange of surface hydroxyl groups of alumina. This may verify the importance of hydroxyl groups present on the surface of alumina in ozone decomposition and to understand the possible influence of phosphates on ozonation in the presence of ZSM-5 zeolites.

Figure 4.9 shows the effect of added phosphate ion on the rate of removal of coumarin at pH 6.2. In the presence of alumina, phosphate reduces the rate of coumarin removal (Figure 4.9a). The effect of phosphate under zeolite catalysts is considerably lower (Figure 4.9b). Consistent with this is the extent to which phosphate ion is adsorbed by alumina compared with the zeolites which adsorb almost no phosphate (Figure 4.9c). The data in Figure 4.9d shows that 7HC production over alumina is reduced by phosphate, suggesting that phosphate poisons the surface sites responsible for the radical mechanisms – presumably hydroxyl groups. Overall adsorption of coumarin by both alumina and the zeolites is not affected significantly by phosphate, suggesting that only a small fraction on the adsorbed coumarin is linked to the critical sites for radical formation (Figures 4.9e and 4.9f). This might suggest that hydroxyl groups on the surface of alumina might not be

responsible for adsorption of COU but only ozone decomposition and hydroxyl radical formation.

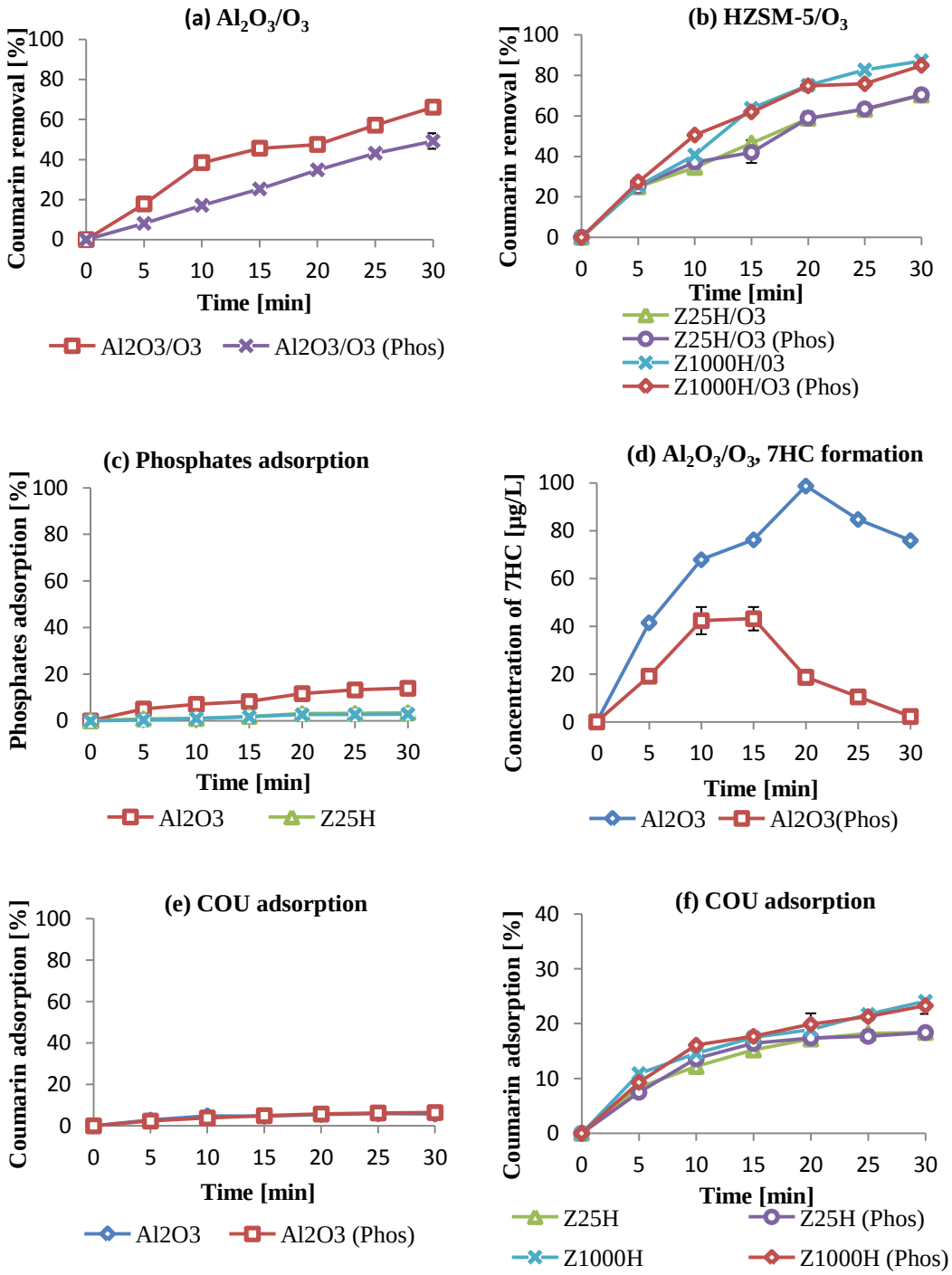

Figure 4.9: Effect of phosphates on the removal of coumarin in O_3, Al_2O_3/O_3 and ZSM-5/O_3 and adsorption of coumarin ($C_{o\,(COU)}$ = 20 mg/L; O_3 = 0.6 mg/min; T = 25°C; pH = 6.2; phosphates = 50 mg/L; catalyst = 2.0 g; V = 190 mL; SD ± 3%).

Similar results indicating the effect of phosphates on the catalytic activity of alumina have been reported by others. Beltran et al [84] observed that the catalytic activity of alumina was greatly reduced in the presence of phosphates. Alvarez et al [71] found that the presence of phosphates reduced the adsorption of pyruvic acid on the surface of alumina.

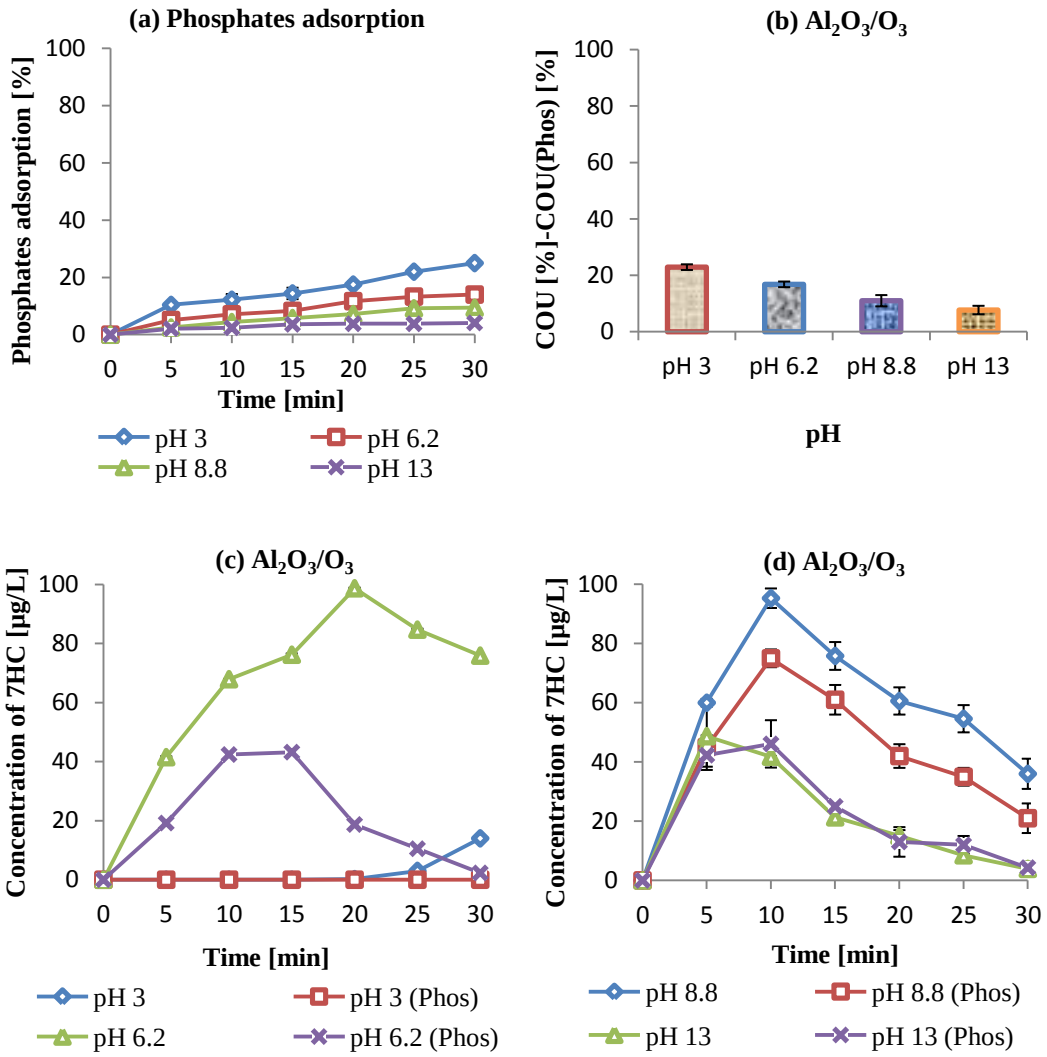

Figure 4.10: Effect of pH and phosphates on the removal of coumarin in Al_2O_3/O_3 and adsorption of coumarin ($C_{o\,(COU)}$ = 20 mg/L; O_3 = 0.6 mg/min; T = 25°C; pH = 3.0, 6.2, 8.8 and 13.0; phosphates = 50 mg/L; catalyst = 2 g; V = 190 mL; SD ± 3%).

The effect of phosphate at other pH values is shown in Figure 4.10. The adsorption of phosphates on alumina increases with a decrease in the pH of solution and is the highest

at pH 3.0 (22% on 2.0 g of alumina in 30 min). The results presented in Figures 4.10c and 4.10d show that the effect of phosphate on 7HC production over alumina is the greatest at acidic pH. It seems reasonable to propose that at the lower pH, most of the hydroxyl radicals that take part in 7HC production are generated on the alumina surface, and so added phosphate reduces the rate of 7HC production significantly. As the pH increases, two effects take hold. Firstly, the amount of phosphate adsorbed decreases and secondly because hydroxyl radicals formed from hydroxide ions in solution becomes increasingly important, adsorbed phosphate has no influence on these ions. It is important to note that the difference in efficiencies of COU removal in catalytic ozonation on alumina and ozonation alone were also the highest at pH 3 and this decreased with the increase in pH (Fig. 4.10b).

It is a well-known fact that different forms of phosphates exist at different pH ranges (these are H_3PO_4, $H_2PO_4^-$, HPO_4^{-2} and PO_4^{-3}). Concentration of protonated forms of phosphates is the highest at acidic pH, hence the surface hydroxyl groups of alumina may be rapidly replaced at acidic pH as phosphate adsorption was considered to occur through the exchange of surface hydroxyl groups of alumina [150]. The ligand exchange can also take place in the presence of water molecules and other easily displaced ligands coordinatively bonded to the sites [151]. The above results clearly indicate the importance of the effects phosphates (and other charged molecules with high affinity towards the surface of alumina) can have on the catalytic activity of materials used in catalytic ozonation of water micropollutants.

4.2.1.7 Effect of catalyst amount

In order to investigate the effect of catalyst amount on the efficiency of catalytic ozonation, HZSM-5 (Z1000H and Z25H) and alumina were studied. Ozonation experiments were performed in the presence of 2.0, 4.0 and 6.0 g of catalysts at pH 6.2.

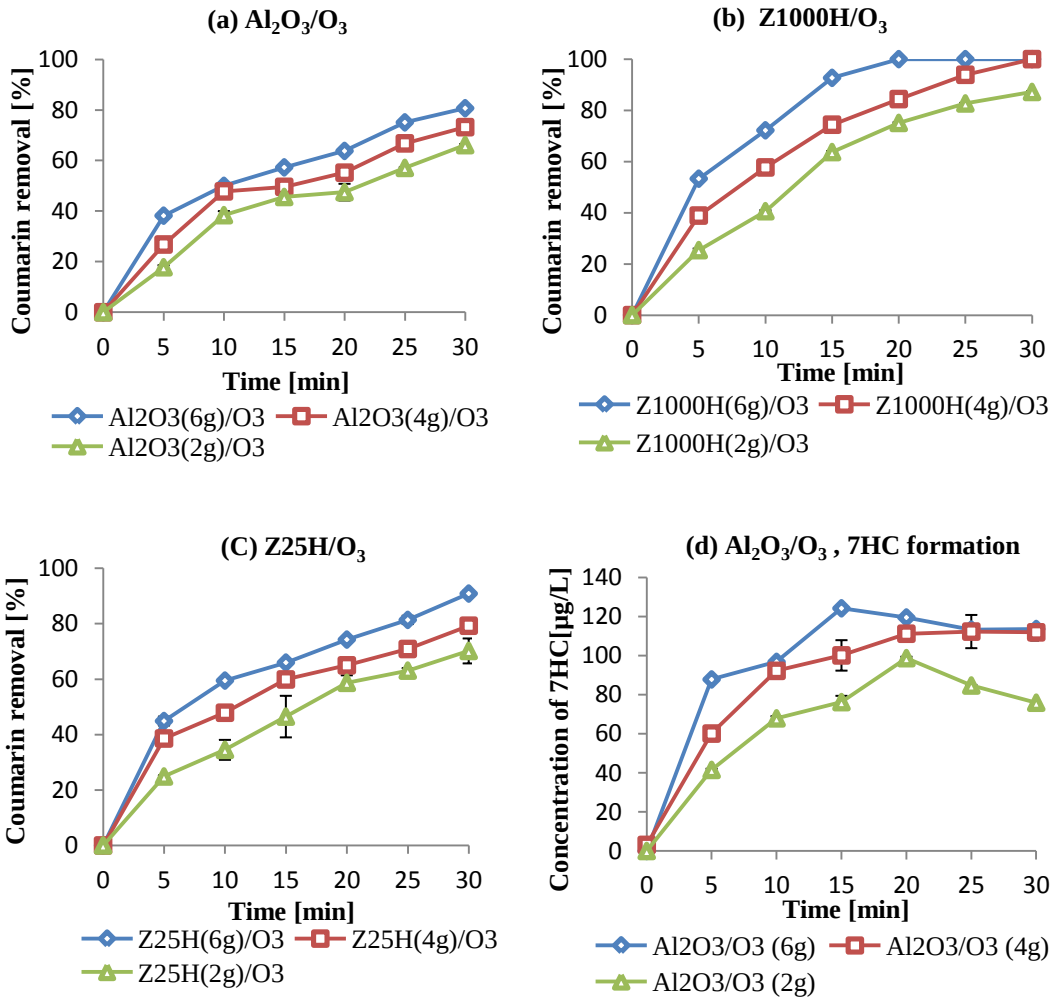

Figure 4.11: Effect of catalyst amount on the removal of coumarin by Al_2O_3/O_3 and HZSM-5/O_3 ($C_{o\ (COU)}$ = 20 mg/L; T = 25°C; pH = 6.2; O_3 = 0.6 mg/min; catalyst dose = 2.0 g, 4.0 g and 6.0 g; V = 190 mL; SD ± 4%).

The results (Fig. 4.11) show an expected increase in COU removal with the catalyst amount for both alumina and two acidic zeolites. It has not been possible to reliably

determine the rates to establish the precise link between catalyst quantity and rate of removal.

The yield of 7HC over alumina (Figure 4.11d) also increases with an increase in catalyst amount, confirming that the decomposition route involving hydroxyl radicals also takes place only on the catalyst surface at this pH. With the increase of catalyst amount there is some decrease in 7HC with time after the initial rise, and this suggests that in the presence of such a large amount of catalyst the 7HC itself can and does decompose.

4.2.1.8 7-Hydroxycoumarin ozonation

It has been mentioned above that it appears that 7HC, the product of free radical decomposition of coumarin, might be decomposed on the catalysts used in this study. We have investigated this by studying both adsorption and ozonation of 7HC in the presence of alumina, the Z25H and the Z1000H catalysts. The results are presented in Figure 4.12.

It is clear that none of these catalyst adsorbs 7HC significantly (Figure 4.12b). However, all of them promote its removal, presumably degradation, by ozonation. Ozone alone is active in degrading 7HC but all four catalyst increase the rate of decomposition, with alumina being very much more active than the two acid zeolites. This validates our earlier assumptions that decreases in 7HC concentrations after its formation from coumarin could be due to degradation by catalytic ozonation of 7HC, largely on the surface of the catalyst. The outcome of this study revealed that adsorption of coumarin and its transformation by-product, 7-hydroxycoumarin, is vital in catalytic processes and that catalytic ozonation of coumarin in the presence of alumina leads not only to the formation of its hydroxylated transformation by-products, but also its further degradation. It also explains why the observed formation of 7HC during the ozonation of COU in the presence of alumina slows down and then decreases after a specific period of time (Fig. 4.12d).

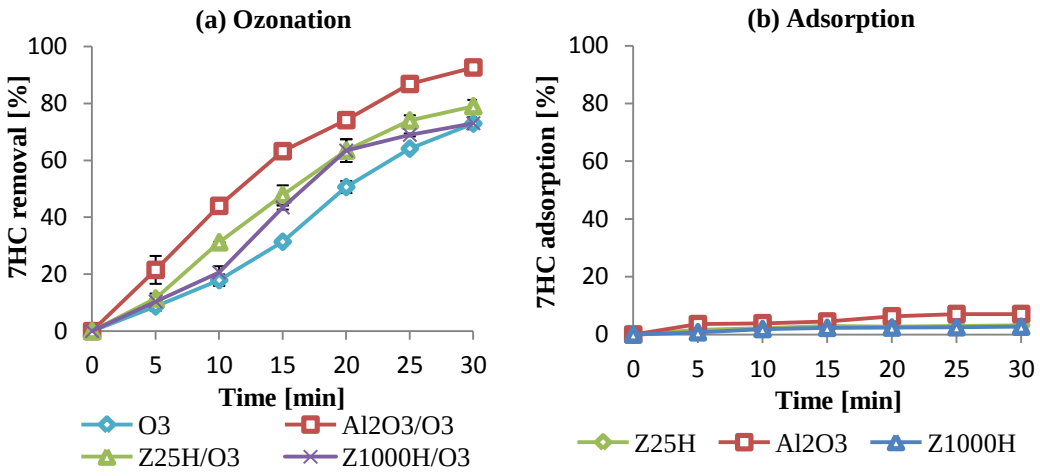

Figure 4.12: Removal of 7-hydroxycoumarin by O_3, Al_2O_3/O_3 and ZSM-5/O_3 ($C_{o\ (7HC)}$ = 20 mg/L; T = 25^{o}C; pH = 6.2; O_3 = 0.6 mg/min; catalyst = 2.0 g; V = 190 mL; SD ± 2%).

4.2.2 PART 2 – An investigation of hydrogen peroxide

4.2.2.1 The formation of hydrogen peroxide and the effect of pH

The experiments have been performed at pH values 6.2, 8.8 and 13.0 as shown in the Figure 4.13. The results clearly indicate that high concentrations of H_2O_2 are formed with Al_2O_3/O_3 at both pH 6.2 and 8.8 when compared with ozonation alone. For example, the concentration of H_2O_2 was (at pH 6.2, after 30 minutes ozonation) 234.5 µg/L for Al_2O_3/O_3 and only 114 µg/L for O_3 alone. It has been reported previously that alumina shows catalytic activity near or below its point of zero charge and when the pH becomes higher, catalytic activity is greatly reduced [18-20]. Al_2O_3 catalytic activity is directly related to its capacity to decompose ozone on its surface hydroxyl groups, which leads to the formation of hydroxyl radicals [18-20]. In contrast, at pH 13 the presence of alumina did not result in any increase in H_2O_2 production. It was therefore concluded that H_2O_2 formation in Al_2O_3/O_3 related to ozone decomposition and it was higher at pH 8.8 than 6.2 in the first 5 to 10 minutes of ozonation (Fig 4.13a, b). This is because the catalytic

activity of alumina is the highest near its point of zero charge. Furthermore, it was observed that at pH 6.2 H_2O_2, production was very rapid for the first 10 to 15 minutes (Fig. 4.13a) and then slowed. This may be due to adsorption and decomposition of H_2O_2 on alumina [211]. It was also observed that at basic pH (Fig. 4.13b, c), the rate of H_2O_2 formation in the first five minutes was high and then it decreased for both ozonation and catalytic ozonation process. This may be because of the low stability of H_2O_2 at basic pH values [36]. Furthermore, H_2O_2 may further adsorb and decompose on the catalyst surface [211]. Additionally, it is hypothesized that resorufin (the product of the reaction between H_2O_2 and amplex red) may be decomposed by the oxidative species (such as ozone and hydroxyl radicals) in the system.

The results for ZSM-5 zeolites clearly indicate that no significant increase in H_2O_2 formation was observed at any pH when compared with ozonation alone. It is therefore assumed that ZSM-5 zeolites mainly act as adsorbents of ozone and do not decompose aqueous ozone leading to the formation of free reactive oxidative species such as hydrogen peroxide or hydroxyl radicals.

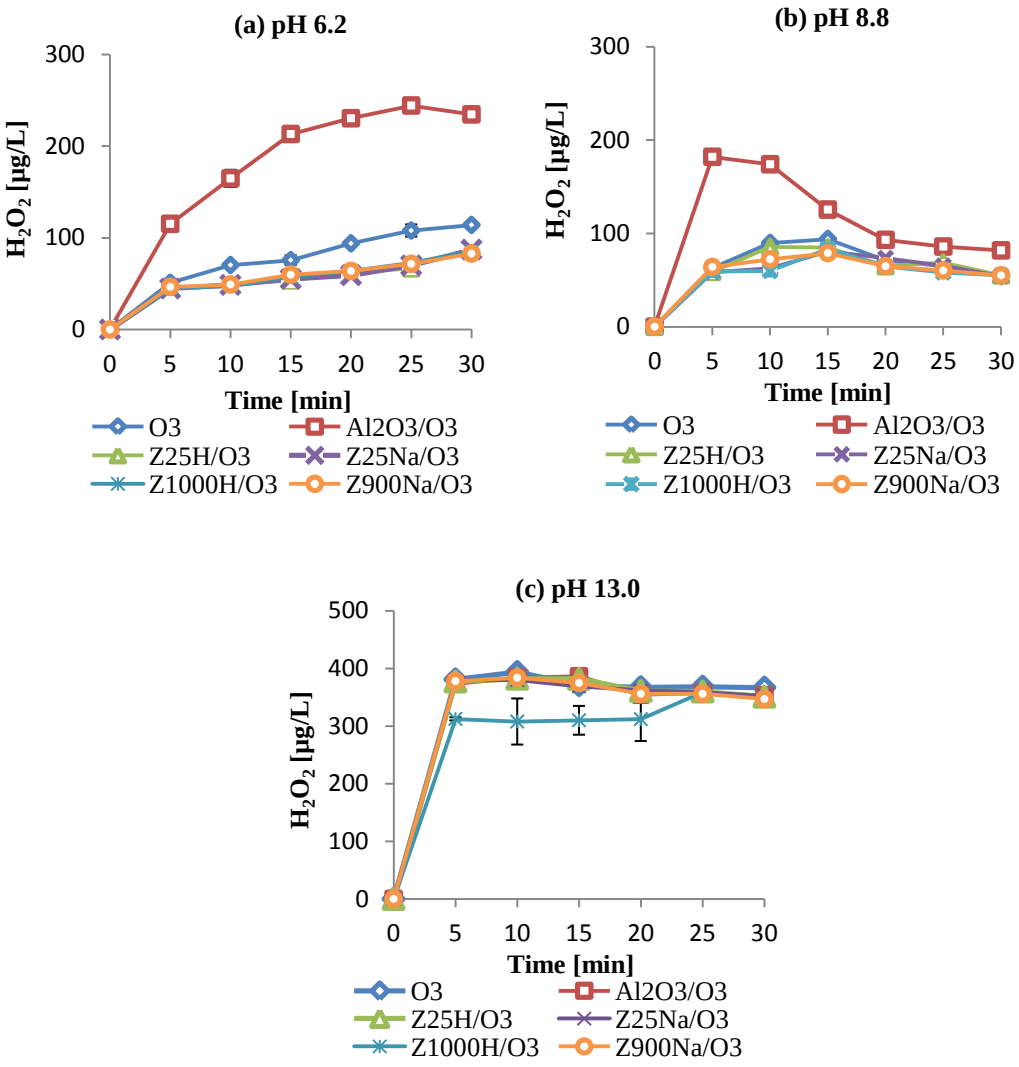

Figure 4.13: Formation of hydrogen peroxide in ozonation alone and catalytic ozonation (C_{0Amp} = 20 mg/L; O_3 = 0.6 mg/min; T = 25^{o}C; pH = 6.2, 8.8 and 13.0; pH_{t30min} = pH ± 0.2; catalyst amount = 2.0 g; V = 190 mL; SD ± 5 µg/L).

4.2.2.2 Effect of hydroxyl radical scavengers

The hydroxyl radicals may combine to form stable H_2O_2 [201, 211]. The formation of hydroxyl radical in the catalytic ozonation process has been investigated by the use of hydroxyl radical scavengers such as TBA. It is a well-known fact that hydroxyl radicals have a higher oxidation potential than hydrogen peroxide (H_2O_2 relative oxidation potential is 1.77eV and ^{o}OH radicals relative oxidation potential is 2.80eV) [31]. The influence of TBA on the reaction of amplex red with H_2O_2 was investigated by reacting

amplex red with H_2O_2 in the presence of TBA for 1 hour. It has been observed that TBA did not have any significant effect on the reaction between amplex red and H_2O_2 (the concentrations of resorufin with and without TBA were the same).

The results presented in Fig. 4.14b clearly indicate that in the presence of alumina, TBA inhibits the formation of H_2O_2. For example at pH 6.2 after 30 minutes ozonation time the H_2O_2 concentration was 234.5 µg/L and in the presence of TBA it was reduced to 81.9 µg/L. Furthermore, it has been observed that the decrease of H_2O_2 concentration also took place in the case of O_3 alone. As shown in the Fig. 4.14a the concentration of H_2O_2 in the ozonation alone was 114 µg/L and was reduced to 87.2 µg/L, in the presence of TBA. However, the decrease in H_2O_2 concentration in O_3 alone (in the presence of TBA) was not as great as in the case of Al_2O_3/O_3. This suggests that ^{o}OH radicals play an important role in the formation of H_2O_2 and the presence of alumina generates more ^{o}OH radicals compared with ozonation alone [18-20].

The results presented in Fig. 4.14c, d show that TBA did not have any effect on H_2O_2 formed in the presence of HZSM-5 zeolites (both Z1000H and Z25H). The amount of H_2O_2 formed in the presence of zeolites was lower than in ozonation alone. It has been already discussed that ZSM-5 zeolites may mainly act as adsorbents of both ozone and organic contaminants and do not lead to the formation of free reactive oxygen species such as hydroxyl radicals and above results further supports this view.

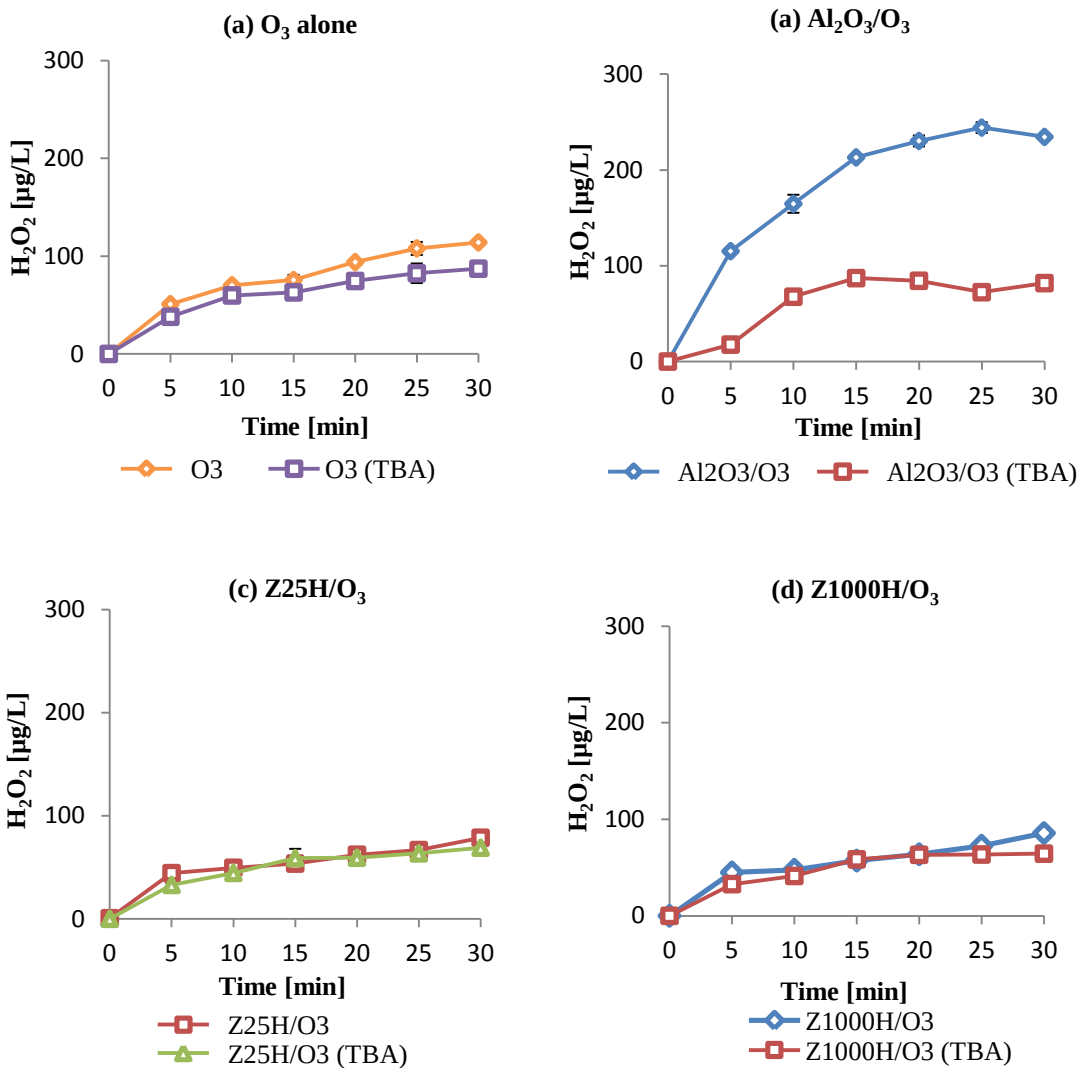

Figure 4.14: Effect of TBA on the formation of hydrogen peroxide by O_3, Al_2O_3/O_3 and HZSM-5/O_3 (C_{oAmp} = 20 mg/L; O_3 = 0.6 mg/min; TBA = 50 mg/L; T = 25°C; pH = 6.2; pH_{t30min} = 6.2 ± 0.2; O_3 = 0.6 mg/min; catalyst amount = 2.0 g; V = 190 mL; SD ± 4 µg/L).

4.2.2.3 Effect of phosphates

The effect of phosphates on the formation of H_2O_2 was studied with O_3 alone, and in the presence of HZSM-5 (Z25H and Z1000H) zeolites and alumina at pH 6.2 (Fig. 4.15). The results indicate that the presence of phosphates did not have a significant effect on H_2O_2

formed during the ozonation in the presence of HZSM-5 zeolites. On the other hand, the H_2O_2 concentration was significantly reduced during the ozonation in the presence of alumina after 30 minutes, from 234.5 µg/L to 101 µg/L at pH 6.2 (Fig. 4.15b). The presence of phosphates slightly reduced the H_2O_2 formation with O_3 alone (Fig, 4.15a). This is presumably due to the radical scavenger effect of phosphates. This effect is not seen with HZSM-5 zeolites and this may simply be because of adsorption of phosphates on zeolites, which resulted in the reduction of the concentrations of phosphates in the solution. The adsorption studies of phosphates on HZSM-5 and alumina (Fig. 4.15e) revealed that, alumina had much higher adsorption for phosphates than HZSM-5 (14.5 % on 2.0 g of alumina and 3.4 %, 3.1 % on Z25H and Z1000H respectively, in 30 min). It is therefore suggested that the decrease in H_2O_2 formation in the presence of phosphates in the case of Al_2O_3/O_3 is the result of a decrease in available surface hydroxyl groups. As discussed before, interaction of ozone with surface hydroxyl groups results in the formation of hydroxyl radicals and these hydroxyl radicals combine to form H_2O_2.

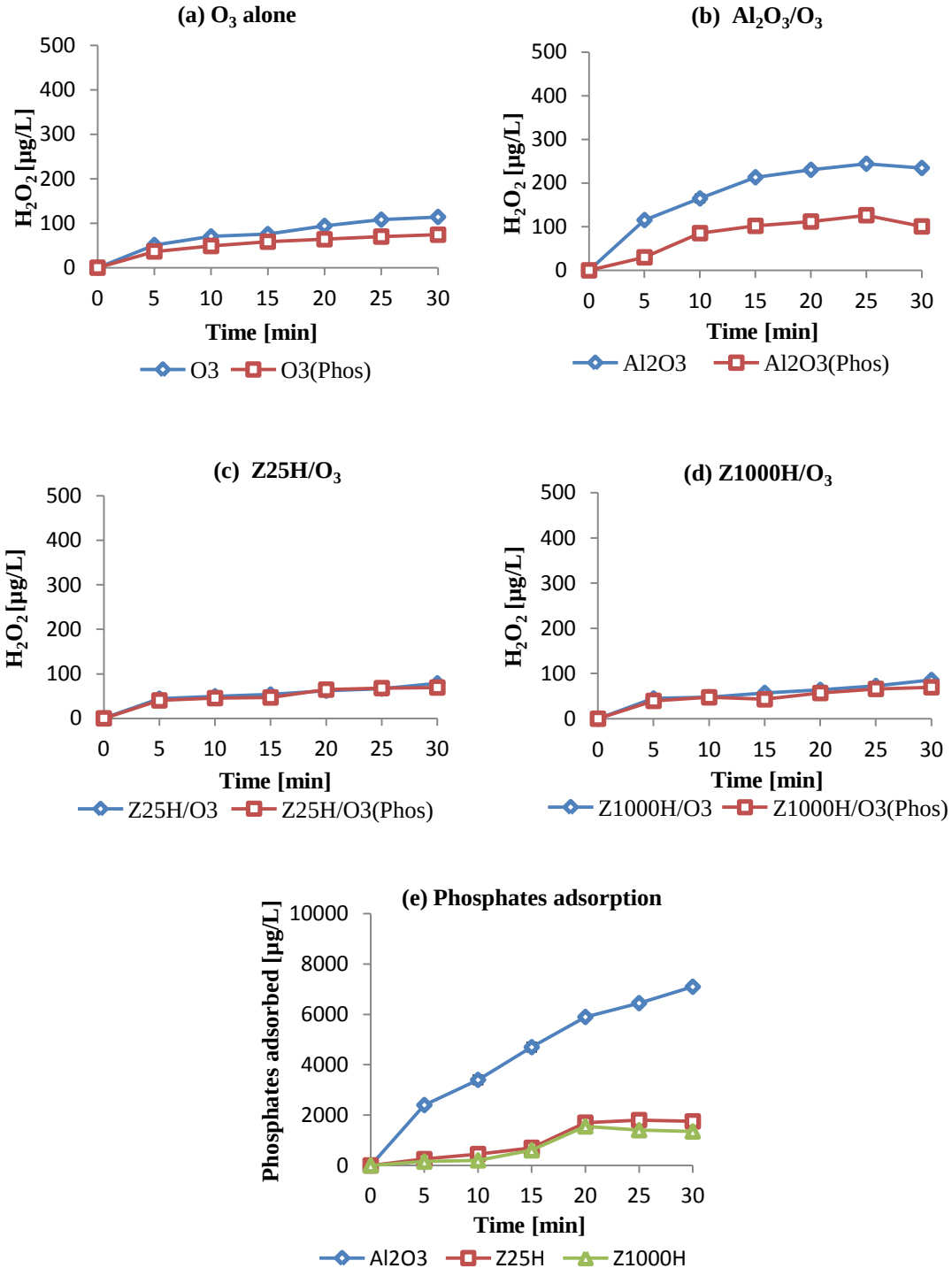

Figure 4.15: Effect of phosphates on the formation of hydrogen peroxide in O_3, Al_2O_3/O_3 and HZSM-5/O_3 (C_{oAmp} =20 mg/L; O_3 = 0.6 mg/min; phosphates = 50 mg/L; T = 25^{o}C; pH_o, 6.2; pH_{t30min} = 6.2 ± 0.2; catalyst amount = 2.0 g; V = 190 mL; SD ± 10 µg/L).

4.2.2.4 Effect of catalyst amount

The results presented in Fig. 4.16 show that with an increase in the catalyst amount the concentration of H_2O_2 formed increased in the case of Al_2O_3/O_3. This may be due to the increase in hydroxyl radical formation in line with the increase in catalyst amount, which leads to the formation of H_2O_2. Additionally, it was noticed that H_2O_2 was formed rapidly in the first 10 to 15 minutes of ozonation (Fig. 4.16a). This may be due to the adsorption and decomposition of H_2O_2 on alumina.

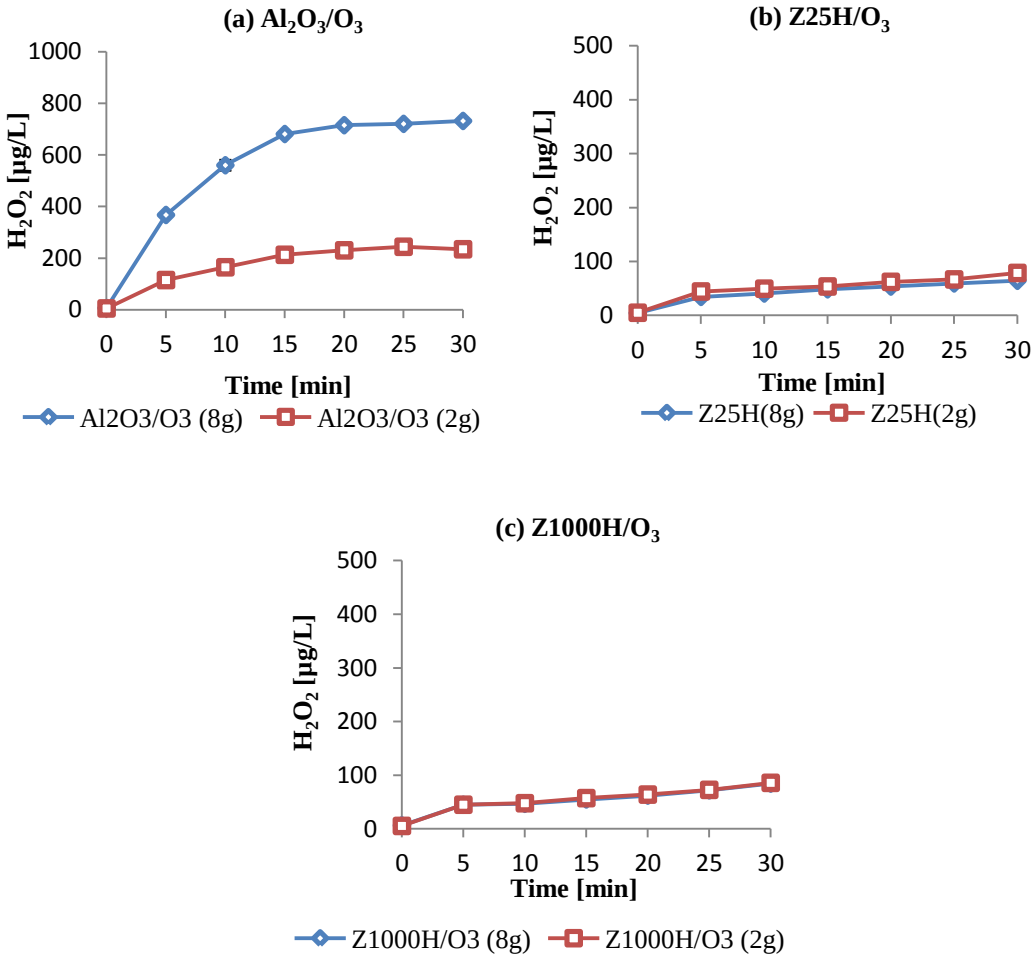

Figure 4.16: Effect of catalyst dose on the formation of hydrogen peroxide in O_3, Al_2O_3/O_3 and HZSM-5/O_3, (C_{oAmp}= 20 mg/L; catalyst = 2.0 mg/L, 8.0 mg/L; T = 25^oC; pH = 6.2; pH_{t30min} = 6.2 ± 0.2; V = 190 mL; SD ± 4 µg/L).

The experiments conducted in the presence of HZSM-5 zeolites (Fig. 4.16b, c) indicate that zeolites did not have any effect on the formation of H_2O_2. As discussed before this may be because ZSM-5 zeolites mainly act as adsorbents of ozone and do not initiate advanced oxidation mechanism that leads to the generation of free reactive oxygen species. The results presented by Fujita et al [11, 22] suggested that ozone may adsorbed on ZSM-5 zeolite surface. Additionally, Carlone et al [212] reported that interactions of ozone and zeolites on the surface of zeolites are responsible for the removal of pollutants and sorption into the pores is not important due to the speed of reaction. Therefore, further investigation is required to study the surface reactions in the presence of different types of pollutants (hydrophilic, hydrophobic).

4.2.3 PART 3 – An investigation of superoxide ion radical

4.2.3.1 Adsorption of NBD-Cl on Al_2O_3 and ZSM-5 zeolites

The adsorption data is shown in Figure 4.17 as the percentage of total NBD-Cl concentration was removed from the solution with time, at various pHs. The data shows that alumina adsorbed more effectively than zeolites. The adsorption of NBD-Cl on all catalysts was found to be very low. For example only about 4 - 5% of NBD-Cl was adsorbed on 2.0 g of alumina within 30 minutes contact time at studied pH values (3.0, 6.2, 8.8 and 13) as shown in Figure 4.17. Furthermore, the zeolites with higher alumina content (Z25H, Z25Na) had slightly higher adsorption when compared with high silica zeolites (Z1000H, Z900Na). For example about 4% of NBD-Cl was adsorbed on Z25H and Z25Na at all studied pH values. However, only 3 - 3.5% of NBD-Cl was adsorbed on Z1000H and Z900Na (Fig. 4.17). The data for experiments carried out at different pH values shows that the adsorption of NBD-Cl decreases to some extent at basic pH. It may

be because the surface is fully populated with OH^- ions at this pH and this phenomenon might result in the decrease of % adsorption of NBD-Cl.

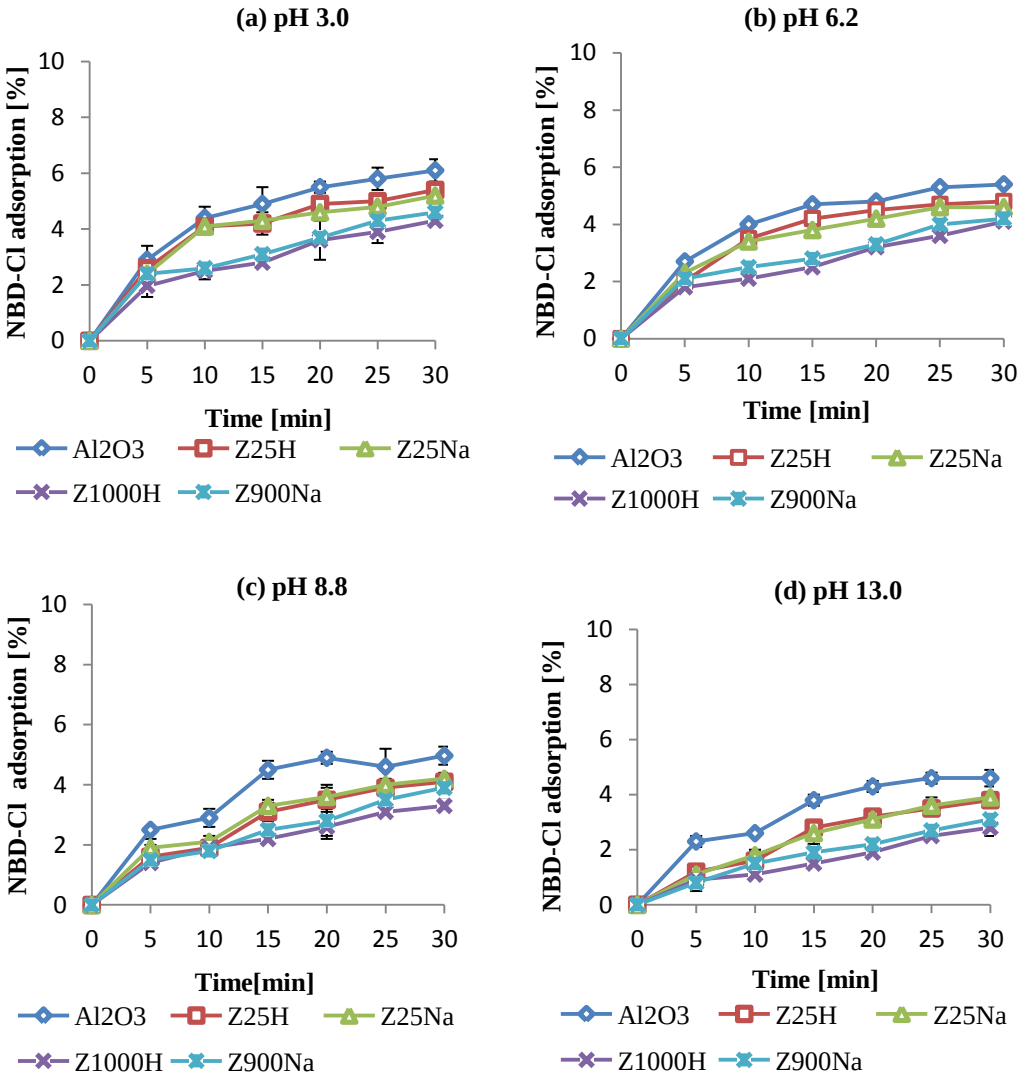

Figure 4.17: Removal of NBD-Cl by adsorption on ZSM-5 zeolites and alumina ($C_{o\ (NBD-Cl)}$ = 20 mg/L; T = 25°C; pH = 3.0, 6.2, 8.8 and 13.0; catalyst amount = 2.0 g; V = 190 mL; SD ± 0.5%).

4.2.3.2 The catalytic ozonation of NBD-Cl and the effect of pH

In the present investigation the experiments have been performed at pH values 3.0, 6.2, 8.8 and 13.0. The data in Figure 4.18 shows the percentage removal of NBD-Cl with time.

The data clearly indicated that (Fig. 4.18) catalytic ozonation of NBD-Cl in the presence of alumina shows higher removal of NBD-Cl when compared with ozonation alone and ozonation in the presence of ZSM-5 zeolites at pH 8.8 (Fig. 4.18). The efficiency of ozonation in the presence of alumina has been found to increase with the increase in pH and was the highest near point of zero charge of alumina (pH_{PZC}) as shown in Figure 4.18e. For example at pH 8.8 the NBD-Cl removal was 30% higher than ozonation alone (Fig. 4.18e). This is in contrast with the ozonation in the presence of ZSM-5 zeolites. In the case of ZSM-5 zeolites the NBD-Cl removal decrease with the increase in pH of the solution (Fig. 4.18), which indicates that ozonation in the presence of ZSM-5 zeolites may follow different mechanism than that of ozonation in the presence of alumina. Additionally, the experiments revealed that all studied catalysts were ineffective during the ozonation at pH 13.0 (had similar removal of NBD-Cl when compared with ozonation alone (Fig. 4.18d). This may be due to the high concentration of OH^- ions that are responsible for high rates of aqueous ozonation decomposition at pH 13.0 [36]. The low catalytic activity of alumina at pH 13 may be due to changes in its surface properties. As discussed before, at pH 13.0 the surface of alumina does not have protonated surface hydroxyl groups, which are believed to be responsible for ozone decomposition [20]. It is also worth noting that the pH of the solution did not change significantly (± 0.1) after 30 min ozonation with and without catalysts.

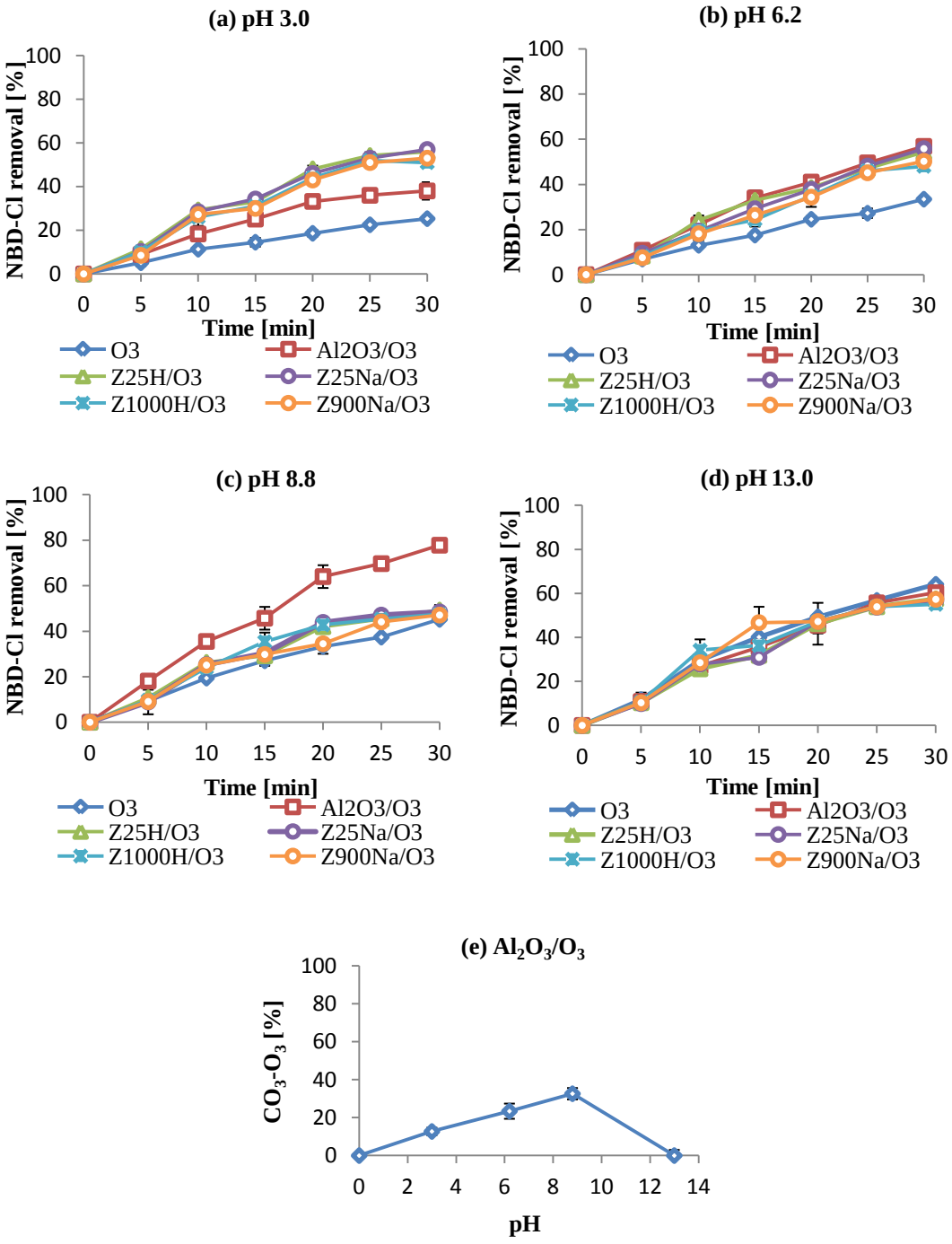

Figure 4.18: Removal of NBD-Cl by alumina and zeolites, $C_{o\ (NBD\text{-}Cl)}$, = 20 mg/L; T = 25°C; pH = 3.0, 6.2, 8.8 and 13.0; T = 30 minutes; O_3 = 0.6 mg/min; catalyst = 2.0 g; V = 190 mL; SD ± 4%.

4.2.3.3 Formation of superoxide ion radical ($^{o}O_2^-$)

The formation of superoxide ion radical has been monitored during the ozonation of NBD-Cl. The results clearly indicated that the formation of $^{o}O_2^-$ in the presence of alumina was the highest at pH = 8.8 (pH = pH_{PZC}) when compared with ozonation alone (Fig. 4.19b). It is important to note that during the first 10 to 15 minutes the $^{o}O_2^-$ formation rate increased and after about 15 to 20 minutes it decreased (Fig. 4.19b). This may be due to the reaction of NBD-Cl product with ozone and other oxidative species present in the system. Additionally, NBD-Cl may be adsorbed on the catalyst surface. It is interesting to note that there has been no significant fluorescence at pH 3.0. This may be because of low yields of $^{o}O_2^-$ as its formation is higher at basic pH value [36]. In contrast to Al_2O_3/O_3, the ZSM-5 zeolites did not show significantly higher fluorescence when compared with ozonation alone at all pH values (Fig. 4.19). This leads to the conclusion that ozonation in the presence of ZSM-5 zeolites does not result in the formation of superoxide ion radicals. It is important to note that significantly high fluorescence was observed at pH 13 in all studied ozonation systems (Fig. 4.19c). This may be due to the presence of high concentration of OH^- ions in the solution at this pH value that leading to the high aqueous ozone decomposition and formation of super oxide ion radical [36].

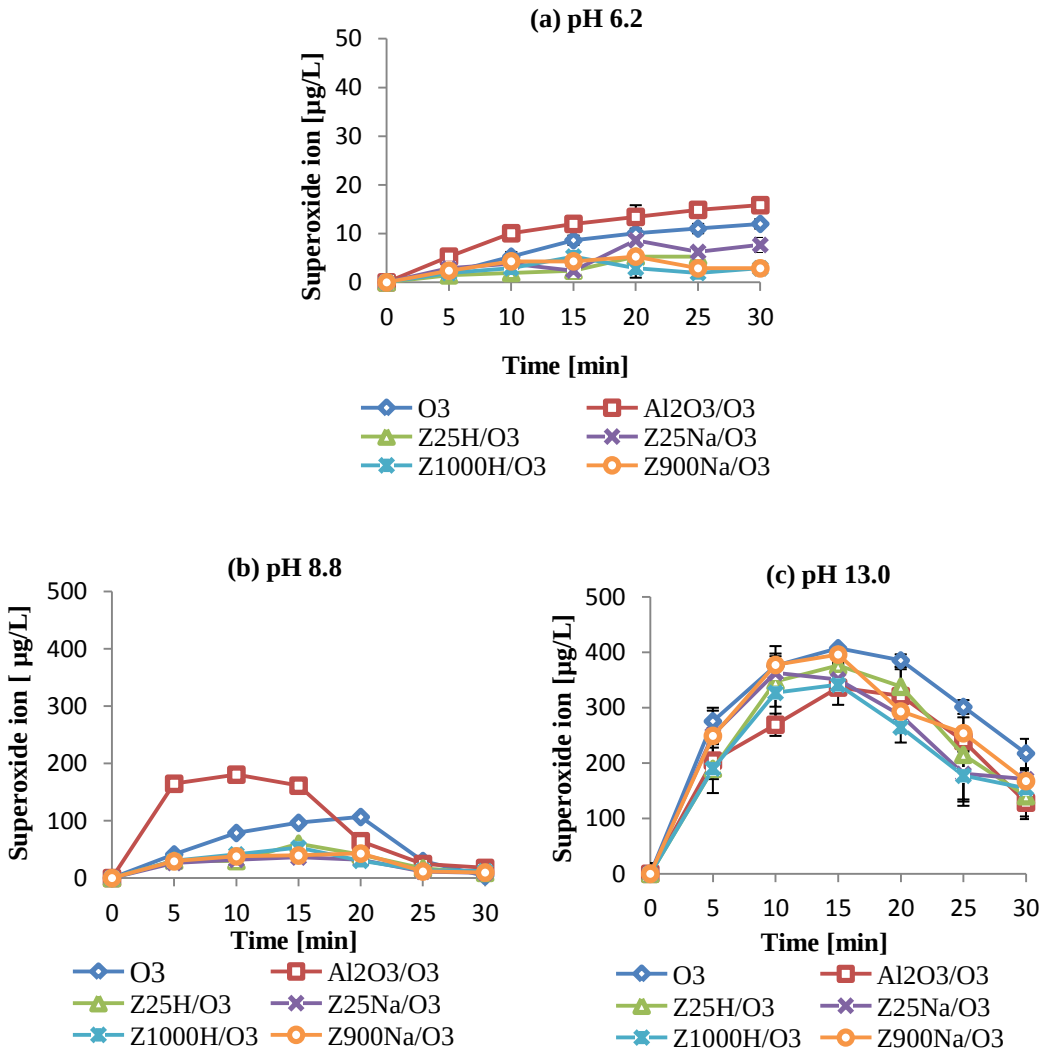

Figure 4.19: Formation of superoxide ion radical in the ozonation of NBD-Cl ($C_{o\ (NBD\text{-}Cl)}$ = 20 mg/L; T = 25^{o}C; pH = 6.2, 8.8 and 13.0; O_3 = 0.6 mg/min; catalyst = 2.0 g; V = 190 mL; excitation wavelength = 470 nm; emission wavelength = 550 nm; SD ± 5 µg/L).

4.2.3.4 Effect of hydroxyl radical scavengers

The ozonation experiments have been performed in the presence of tertiary butyl alcohol (TBA) in order to understand the role of superoxide ion radical ($^{o}O_2^-$ in the formation of

hydroxyl radicals) and to investigate the effect of TBA on the removal of NBD-Cl by catalytic ozonation on alumina and HZSM-5 zeolites. The results indicate that the presence of TBA did not have any significant effect on the removal of NBD-Cl in the presence of ZSM-5 zeolites. For example NBD-Cl removal was 50% with and without TBA when HZSM-5 zeolites have been used (Fig. 4.20c). Furthermore, no significant change in $^{o}O_2^-$ concentration was observed in the case of HZSM-5/O_3 zeolites (Fig. 4.20e) and ozonation alone (Fig. 4.20f) with or without TBA. This indicates that ZSM-5 zeolites did not generate $^{o}O_2^-$ and ^{o}OH radicals.

Furthermore, it has been observed that a small decrease in NBD-Cl concentration took place in the case of O_3 alone undertaken in the presence of TBA. For example 40% and 35% of NBD-Cl was removed after 30 minutes ozonation at pH 8.8 when ozonation was conducted with and without TBA respectively (Fig. 4.20a). Similarly, there has been some limited decrease in the NBD-Cl removal (3% after 30 min ozonation time) in the case of ozonation in the presence of alumina when TBA was added to the solution. However, it was only 3% less when compared with percentage removal without TBA in 30 minutes of ozonation (Fig. 4.20b). This may be because of $^{o}O_2^-$ scavenger effect of NBD-Cl [173]. It further suggested that superoxide ion radical plays an important role in the formation of hydroxyl radicals [36]. Therefore, it is hypothesized that in the presence of NBD-Cl formation of $^{o}O_2^-$ is restricted therefore the generation of hydroxyl radicals may also restricted. It further signifies the role of $^{o}O_2^-$ in the formation of hydroxyl radicals, in the catalytic ozonation process in the presence of alumina.

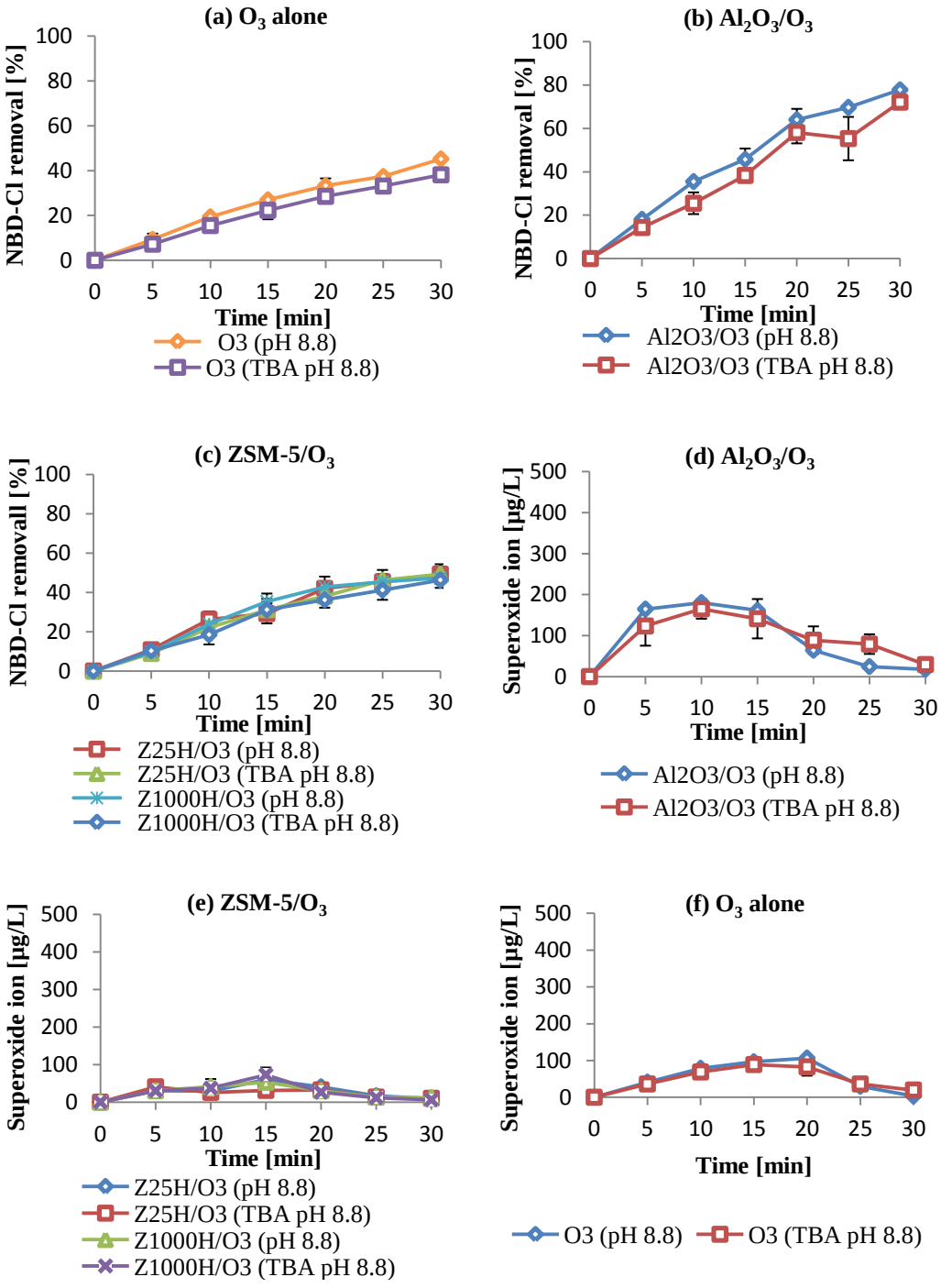

Figure 4.20: Effect of TBA on the removal of NBD-Cl and formation of super oxide ion in O_3, Al_2O_3/O_3 and ZSM-5/O_3 ($C_{o\ (NBD\text{-}Cl)}$ = 20 mg/L; O_3 = 0.6 mg/min; T = 25^{o}C; pH = 8.8; TBA = 50 mg/L; catalyst = 2.0 g; V = 190 mL; SD ± 5).

4.2.3.5 Effect of phosphates

The effect of phosphates on the formation $^{o}O_2^-$ and removal of NBD-Cl was investigated in the presence of O_3 alone, ozonation in the presence of HZSM-5 (Z25H and Z1000H) zeolites and alumina at pH 8.8 (Fig. 4.21). The results presented in Fig 4.21b indicate that the presence of phosphates did not have any significant effect on the removal of NBD-Cl in ozonation on HZSM-5 zeolites. Furthermore, no significant change in superoxide ion concentration has been observed with or without phosphates in the case of ZSM-5 zeolites (Fig. 4.21e) and ozonation alone (Fig. 4.21f). However, the formation of superoxide ion radical was significantly reduced in the presence of phosphates, when ozonation was conducted in the presence of alumina. For example 180.5 μg/L of superoxide has been formed in the case of Al_2O_3/O_3 (in the absence of phosphates) in the first 10 minutes and it was reduced to 120.5μg/L of superoxide in the presence of phosphates (Fig. 4.21c). Furthermore, the NBD-Cl removal percentage was significantly reduced in the presence of phosphates. For example (at pH 8.8, after 30 minutes ozonation time) the removal of NBD-Cl was reduced from the initial value (without phosphates) of 80% to 60% (in the presence of phosphates) (Fig. 4.21b). Similar to the results presented in part 1, the adsorption studies of phosphates on HZSM-5 and alumina (Fig. 4.21d) revealed that, as expected, at studied conditions (pH 8.8) alumina has the much higher adsorption capacity towards phosphates than HZSM-5 (8% on 2.0 g of alumina and 2.2%, 2% on Z25H and Z1000H respectively, in 30 min). It is suggested that the decrease in $^{o}O_2^-$ formation in the presence of phosphates in the case of Al_2O_3/O_3 is resulting from a decrease of available surface OH groups. As discussed before, interaction of ozone with surface hydroxyl groups results in the formation of $^{o}O_2^-$ [17]**.**

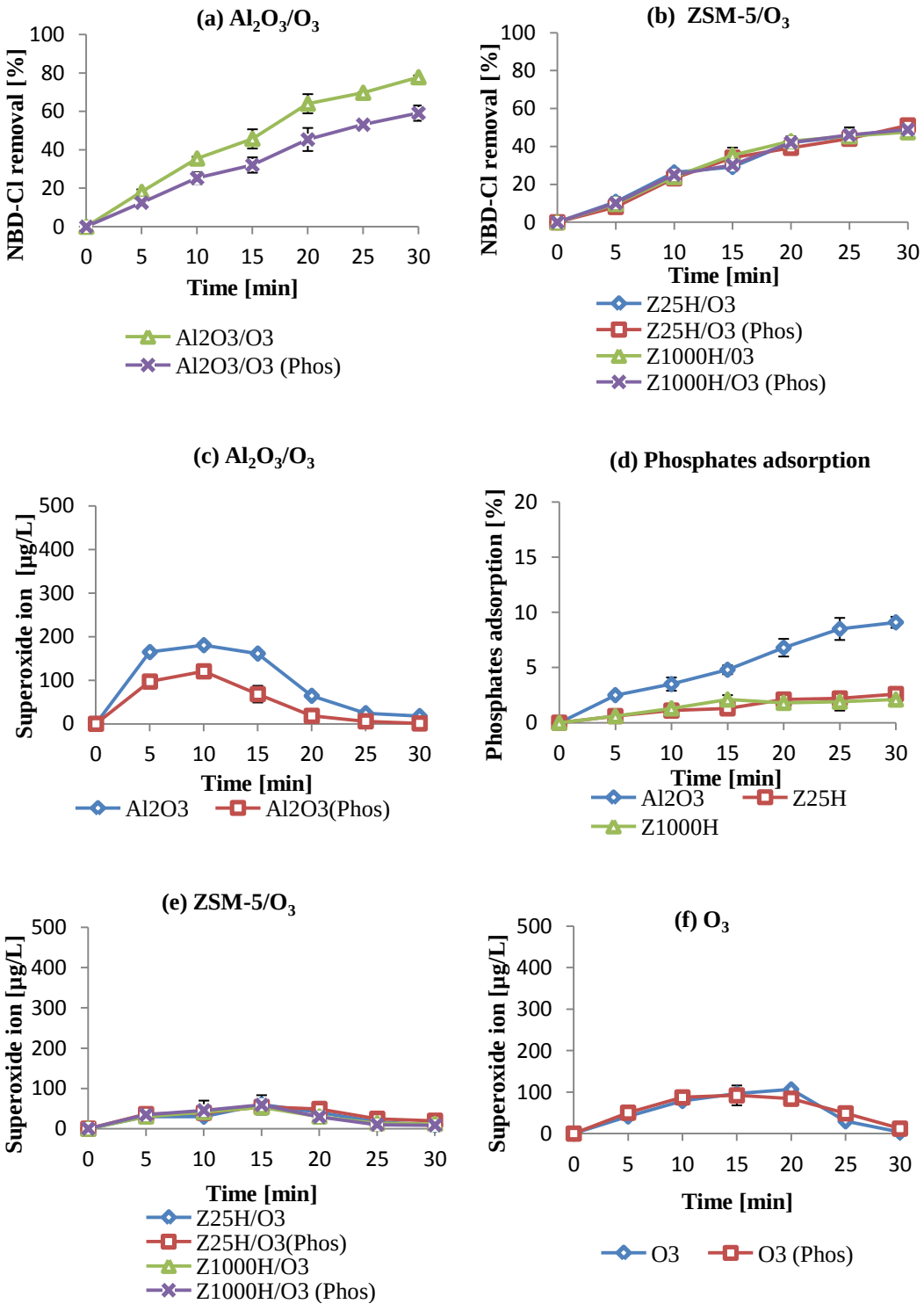

Figure 4.21: Effect of phosphates on the removal of NBD-Cl and formation of superoxide ion in O_3, Al_2O_3/O_3 and ZSM-5/O_3 ($C_{o\,(NBD\text{-}Cl)}$ = 20 mg/L; O_3 = 0.6 mg/min; T = 25^{o}C; pH = 8.8; phosphates = 50 mg/L catalyst = 2.0 g; V = 190 mL; SD ± 5).

4.2.3.6 Effect of catalyst amount

In order to study the effect of catalyst amount on the removal of NBD-Cl and formation of superoxide ion radical, HZSM-5 (Z1000H and Z25H) and alumina were selected. Experiments have been performed by using 2.0 g, 4.0 g and 8.0 g of catalysts in the semi-batch (190 mL of 20 ppm NBD-Cl solution in water) reactor at pH 8.8. The results presented in Fig. 4.22 show that with the increase in the catalyst amount the NBD-Cl percentage removal increased for both Al_2O_3/O_3 and HZSM-5/O_3. For example ozonation in the presence of 6.0 g of alumina resulted in the removal of 90% of NBD-Cl in 30 minutes and it was only 72% when 2.0 g of alumina was used (Fig. 4.22a). It is important to note here, although the removal of NBD-Cl increased in the presence of HZSM-5 zeolites when the catalyst amount is increased. However, no significant $^{o}O_2^-$ formation was observed even at a higher amount. This clearly suggests that ZSM-5 zeolites do not form superoxide ion radical. In contrast to ZSM-5 zeolites an investigation of $^{o}O_2^-$ formation revealed that in the case of Al_2O_3/O_3, the $^{o}O_2^-$ increases with an increase of the catalyst amount (Fig. 4.22d). It is worth mentioning here that the increase in $^{o}O_2^-$ formation was not linear. A sharp increase during the first 10 minutes of ozonation was observed and then it decreased. Therefore, it is assumed that the NBD-Cl product (an indicator of $^{o}O_2^-$ formation) might be degraded during the catalytic ozonation. On the other hand no significant increase in $^{o}O_2^-$ formation was observed in the case of ZSM-5/O_3 (Fig. 4.22e, f).

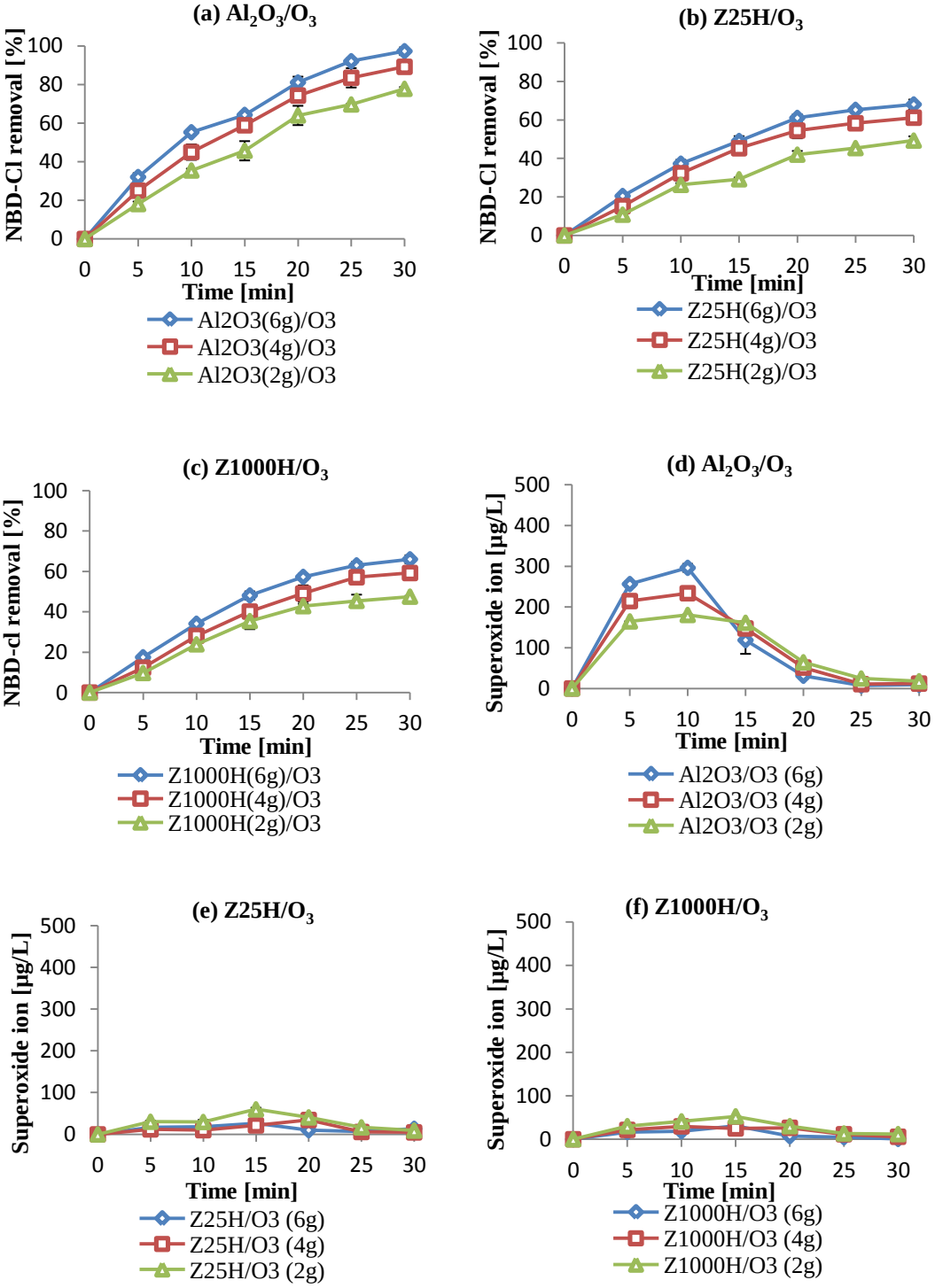

Figure 4.22: Effect of catalyst amount on the removal of NBD-Cl and formation of superoxide ion by Al_2O_3/O_3 and HZSM-5/O_3 ($C_{o\ (NBD\text{-}Cl)}$ = 20 mg/L; T = 25^{o}C; pH = 8.8; O_3 = 0.6 mg/min; catalyst amount = 2.0 g, 4.0 g and 6.0 g; V = 190 mL; SD ± 5).

4.3 Proposed mechanism of ozonation in the presence of alumina

The above results are important in explaining the mechanisms of catalytic ozonation. It is almost certain that alumina promotes the formation of hydroxyl radicals, hydrogen peroxide and superoxide ion, and it has been confirmed by using coumarin, amplex red and NBD-Cl respectively as probe molecules. Additionally, the studies of the TBA effect further support this hypothesis. The mechanism of ozonation in the presence of alumina has been proposed in the Fig 4.23. Similar mechanism has been suggested by Ernst et al [17]. However, no clear evidence has been provided in that work. On the basis of current investigation it is hypothesized that aqueous ozone interacts with the surface hydroxyl groups of alumina to promote its decomposition and this has been supported by the results of the experiments investigating the phosphates effect. The interactions of aqueous ozone with the surface hydroxyl groups of alumina result in the formation of superoxide ion radical as shown in Figure 4.23. The formation of superoxide ion during the ozonation in the presence of alumina has been confirmed in this work with the NBD-Cl probe and provides strong evidence to support this hypothesis. Furthermore, the decrease in the superoxide ion production in the presence of phosphates further supports this hypothesis (section 4.2.3.5). It has been hypothesised by some researchers that the surface hydroxyl groups of catalysts interact with the aqueous ozone leading to the formation of O_2H^o and superoxide ion radical [7, 17, 93]. This may be due to the dipole nature of ozone that reacts with the surface hydroxyl groups of catalysts to produce O_2H^o with the release of O_2.

It is further hypothesized that another O_3 molecule reacts with superoxide or O_2H^o to produce an ozonide O_3 or O_3H^o radical (Fig. 4.23) [36]. The O_3H^o radical quickly reduce to produce hydroxyl radicals. However, this process is pH dependent at basic pH (pKa,

6.2) O_3H^o exists in the form of its conjugate base $^oO_3^-$ [36]. Therefore, at basic pH $^oO_3^-$ reacts with H_2O to produce hydroxyl radicals (Fig. 4.23) [36]. The formed hydroxyl radicals may combine with one another [201, 211] to form H_2O_2. The stability and formation of H_2O_2 depends upon the pH of the solution and the concentration of hydroxyl radicals. The presence of H_2O_2 has been confirmed by the use of amplex red as a probe molecule. Additionally, the TBA effect clearly indicates that production of hydroxyl radicals is essential for the formation of H_2O_2.

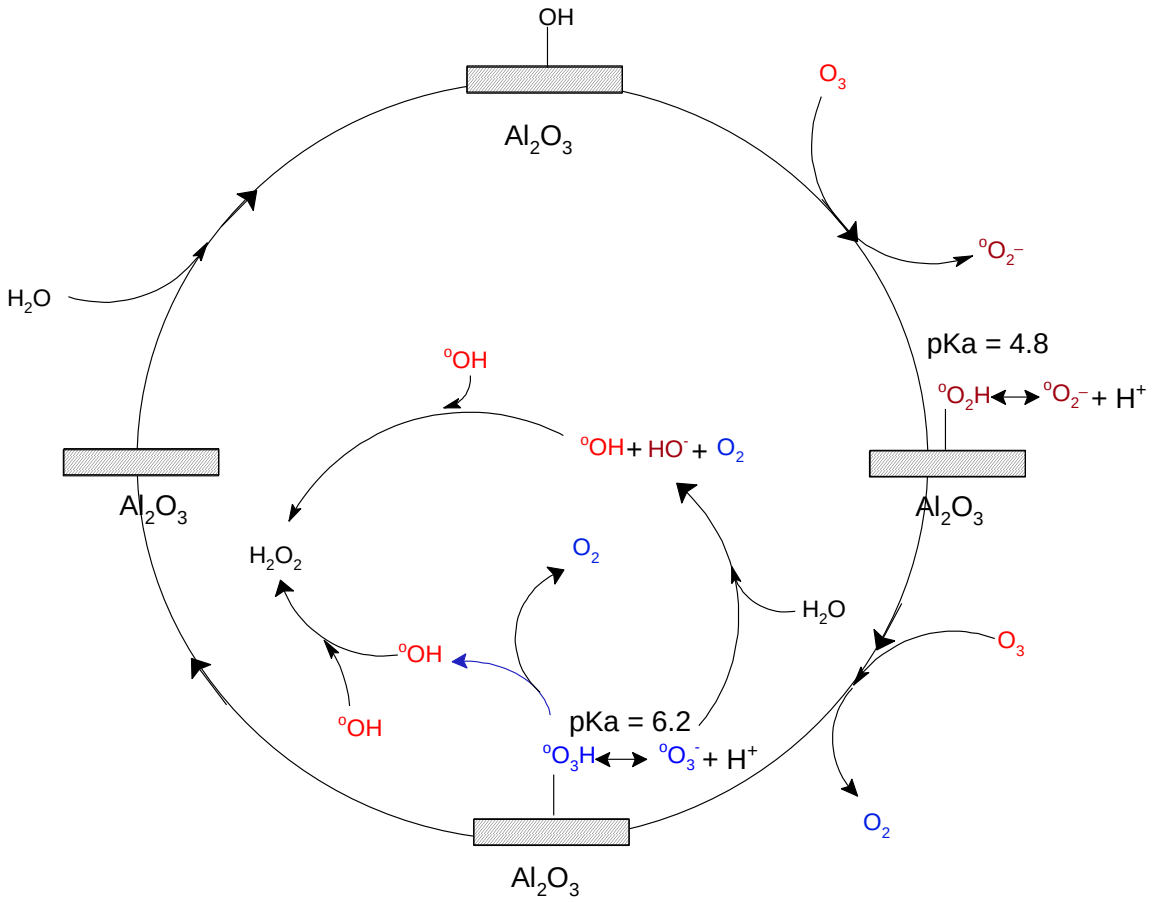

Figure 4.23: A proposed mechanism of ozonation in the presence of alumina.

4.4 Proposed mechanism of ozonation in the presence of ZSM-5 zeolites

In the case of the zeolite catalysts we found that hydroxyl radicals are not involved in the catalytic ozonation process. Additionally, zeolites do not promote the formation of hydrogen peroxide and superoxide ion radical. However, the zeolites do catalyse the ozonation of organic compounds as clearly seen from the removal of coumarin and NBD-Cl. We propose that the zeolite acts simply as a reactive surface on which the reaction between O_3 and the organic molecule can take place with reduced activation energy (Fig. 4.24). Within the family of ZSM-5 zeolites the activity of zeolites is directly related to the silica to alumina ratios. The evidence for this suggestion is strong, as indicated by their adsorption and removal of probes (P). The study of TBA effect further supports this hypothesis. The fact that the hydrogen and sodium forms of the zeolite behave indistinguishably suggests that surface acid sites are not involved in the ozonation reactions, and the ozone reaction with the organic molecule is relatively simple.

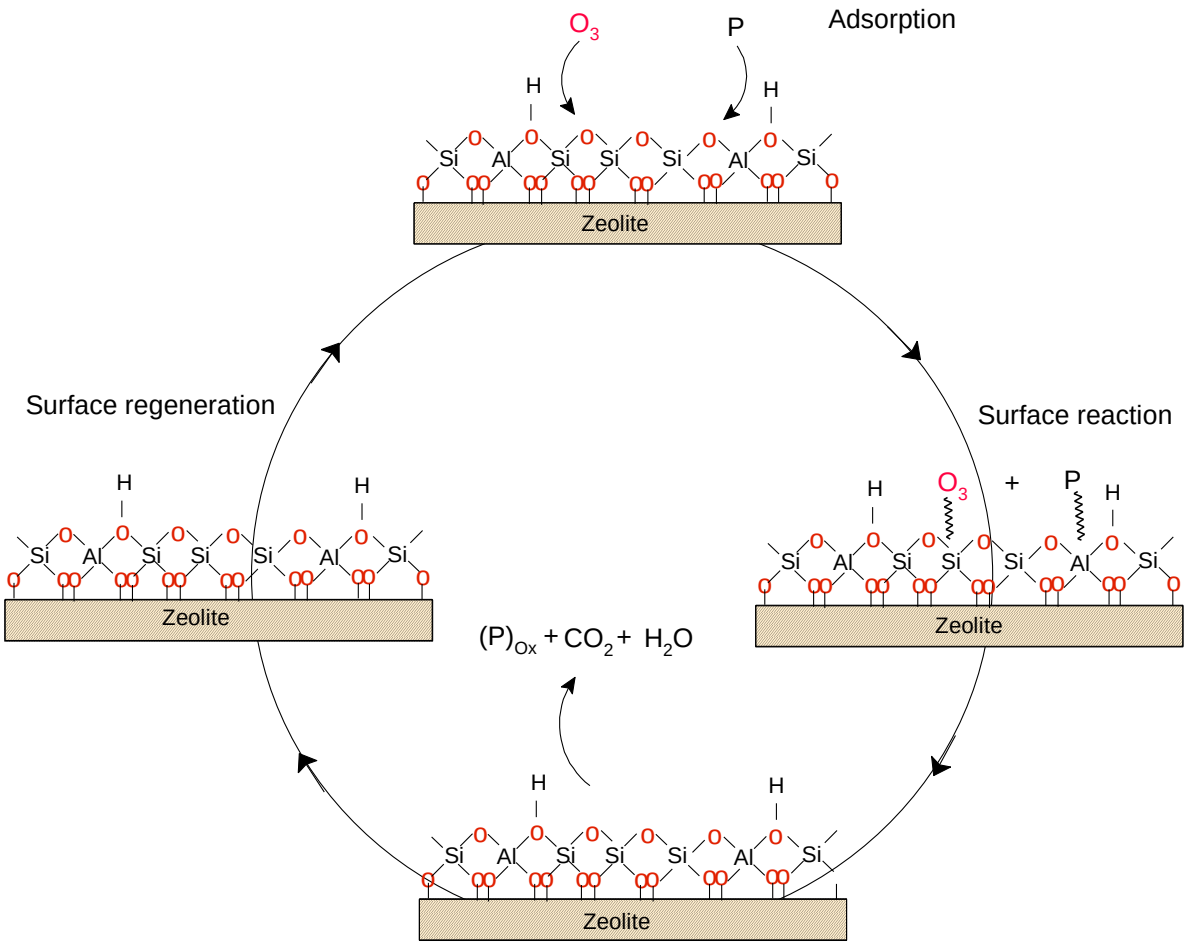

Figure 4.24: A proposed mechanism of ozonation in the presence of ZSM-5 zeolites (P = Probe molecules).

4.5 Summary of results

The mechanisms of ozonation in the presence of ZSM-5 zeolites and γ-alumina in water have been studied. The formation of reactive oxygen species (ROS) such as hydroxyl radicals (^{o}OH), hydrogen peroxide (H_2O_2) and superoxide ion radical ($^{o}O_2^-$) have been investigated in ozonation in the presence of ZSM-5 zeolites and alumina using coumarin (COU), amplex red and 4-chloro-7-nitrobenzo-2-oxa-1,3-dizole (NBD-Cl) as probes. The effect of the radical scavenger (t-butanol) and phosphates has also been used to study the possible involvement of radicals and the role of surface hydroxyl groups of catalysts. Four ZSM-5 zeolites with varying silica to alumina ratios and with both hydrogen and sodium counter ions were used in the study (Z1000H:SiO_2/Al_2O_3 = 1000, Z900Na:SiO_2/Al_2O_3 = 900, Z25H:SiO_2/Al_2O_3 = 25 and Z25Na:SiO_2/Al_2O_3 = 25). The results show that both zeolites and the alumina catalyse the removal of coumarin and NBD-Cl from aqueous solution by ozonation. The alumina is generally more active than zeolites and it catalyses a radical pathway involving ROS, showing its highest activity at pH close to the point of zero charge where surface hydroxyl groups are most susceptible to conversion of ozone to superoxide radical, hydroxyl radicals and hydrogen peroxide. The presence of phosphates and tertiary butyl alcohol (TBA) significantly reduces the formation of ROS in the case of alumina, which indicates the critical importance of surface hydroxyl groups of alumina in ozone decomposition. However, in the case of zeolites TBA and phosphates did not have a significant effect on ROS production. This is because zeolites operate through a simple adsorption process, leading to a direct reaction between adsorbed probes and adsorbed ozone. Their activity depends to an extent on the silica to alumina ratio of the zeolite but is not influenced by the nature of the zeolite counter ion.

4.6 Conclusions

The overall conclusions of the work presented in chapter 4 are as follows.

1 The ozonation in the presence of alumina involves the formation of reactive oxygen species. Ozone degradation in the presence of alumina occurs by a radical mechanism, almost certainly involving hydroxyl radicals, superoxide ion radicals and hydrogen peroxide which are formed by the decomposition of aqueous ozone due to the reaction between ozone and surface hydroxyl groups (which are most reactive at pH close to the pH_{PZC}). The hydroxyl radicals in the catalytic ozonation on alumina are responsible for the production of hydrogen peroxide.

2 The ozonation in the presence of ZSM-5 zeolites do not involve the formation of reactive oxygen species such as hydroxyl radicals, superoxide ion radical and hydrogen peroxide. However, ZSM-5 zeolites are effective in the catalytic ozonation of coumarin and NBD-Cl but they do not act through a radical mechanism. Their activity arises through their ability to adsorb ozone and probes and so promote a surface reaction between the two molecules. The activity of the zeolites is independent of their acidity, supporting this view. Activity shows some dependence on the hydrophobicity of the zeolite, with the more hydrophobic materials adsorbing more coumarin and hence showing higher activity towards its decomposition.

CHAPTER 5 - CATALYTIC OZONATION OF ORGANIC CONTAMINANTS

"In this chapter results for the catalytic ozonation of organic pollutants such as VOCs, ibuprofen and acetic acid on ZSM-5 zeolites and alumina have been presented in this chapter. The VOCs selected are cumene, 1,2-dichlorobenzene and 1,2,4-trichlorobenzene. The effect of pH, adsorption, TBA, phosphates, humic acid, reuse performance of catalyst and catalyst efficiency in tap water is described.

5.1 Introduction

The heterogeneous catalytic ozonation has been used for the degradation of organic compounds such as pharmaceuticals, pesticides, dyes, aromatic hydrocarbons and organic acids etc. Many catalysts have been successfully implied for the degradation of organic acids. Among them are, activated carbons [9], Al_2O_3 [3] and TiO_2 [6] etc. It has been reported that a catalyst may be effective for some pollutants and ineffective for others. For example, alumina has been reported as an effective catalyst for natural organic matter [3] and chlorinated organic compounds [14]. However, some reports indicate a lack of catalytic activity of alumina for hydrocarbons [15] and ethers [4]. Therefore, it is important to study the removal efficiency of catalysts in the presence of different types of pollutants.

The pharmaceuticals have been recognized as an important class of pollutants. Although they are present in trace amounts in the aquatic environment but their long term exposure is a potential risk to aquatic life and human beings, as they have been detected in drinking water [213]. In recent few years ozonation and catalytic ozonation have been successfully used for the removal of pharmaceuticals in water [2, 214, 215]. In the case of pharmaceuticals, ibuprofen (Fig. 5.1) has been selected in this study as target pollutant. The removal of ibuprofen in ozonation in the presence of ZSM-5 zeolites has not been previously studied. Therefore, it is important to investigate the removal of ibuprofen in water.

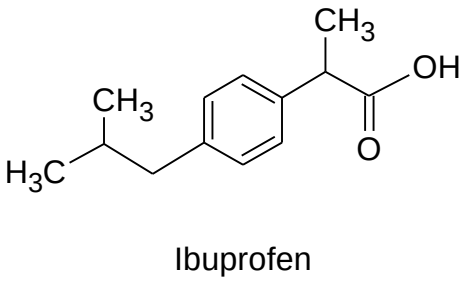

Ibuprofen

Figure 5.1: Structure of ibuprofen.

The ozonation efficiency of zeolites and alumina have also been investigated using volatile organic chemicals (VOCs) such as cumene, 1,2-dichlorobenzene and 1,2,4-trichlorobenzene (Fig. 5.2). The VOCs have been recognized as an important class of pollutants. They have been detected in drinking water [216]. The chlorinated aromatic compounds are a class of highly toxic and widely used organic pollutants that is highly resistant to ozonation [217]. Therefore, catalytic ozonation is required for the effective removal of these pollutants from water. The catalytic ozonation has been successfully used for the removal of VOCs from both aqueous media [15, 218] and air [219, 220].

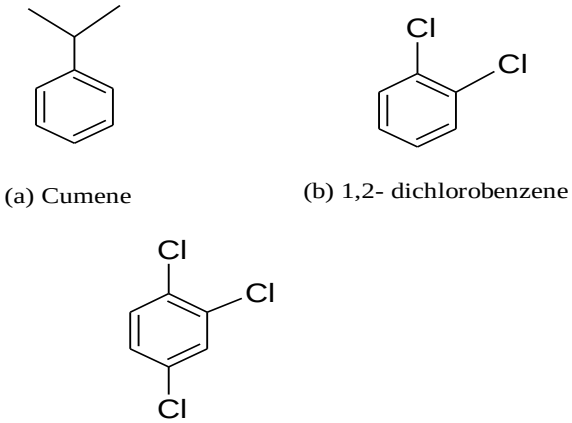

(a) Cumene (b) 1,2- dichlorobenzene

(c) 1,2,4- trichlorobenzene

Figure 5.2: Structure of VOCs.

The ozonation experiments have also been performed to study the removal of acetic acid in water in the presence of zeolites and alumina. The organic acids have been identified as one of the most common ozonation by-products and the most widely studied organic acids are acetic acid, oxalic acid, oxamic acid, formic acid and succinic acid. The short chain organic acids are highly resistant to direct ozone attack. Therefore, advanced oxidation catalysts are required for their effective removal in water. The organic acids have been found as by-products of the ozonation of VOCs and ibuprofen in the presence of ZSM-5 zeolites, therefore it is important to investigate their removal in the presence of catalysts.

In the present study, the detailed investigation of parameters such as effect of pH, adsorption, effect of inorganic ions, effect of radical scavengers and natural organic matter on the removal of pollutants have also been investigated.

The aim of this study was to investigate the efficiency of zeolites and alumina for the removal of different pollutants and to study the role of the above mentioned parameters on the mechanism of catalytic ozonation. The results presented in the chapter 4 shows that alumina follows the radical mechanism and zeolites operate through simple adsorption mechanisms. This study may further help to understand the role of adsorption, surface reactions and the nature of pollutants in the catalytic process.

5.2 Results and discussion

This selection is divided into three parts. In the first part the results of ozonation of ibuprofen in the presence of zeolites and alumina have been presented. The second part discusses the results for VOCs removal and in the final part the removal of acetic acid has been discussed.

5.2.1 Part 1 ozonation of ibuprofen in water

5.2.1.1 Adsorption of ibuprofen on Al_2O_3 and ZSM-5 zeolites

The adsorption studies of contaminants on the surface of the catalyst are vital in catalytic ozonation. The adsorption capacities of ibuprofen on alumina and ZSM-5 zeolites have been determined using Langmuir adsorption plots as described in section 2.1.3.3.3.2. The results presented in Table 5.1 indicate that the high silica zeolites have significantly lower adsorption capacities as opposed to alumina. For example, the adsorption capacity of alumina towards ibuprofen is 5.9 mg/g and it was only 2.7 mg/g in the case of Z25Na. This may be because of the hydrophobicity of zeolites. At pH 7.2, ibuprofen will be ionized and may be attracted towards hydrophilic materials.

Table 5.1: Adsorption capacities of ibuprofen on Al_2O_3 and ZSM-5 zeolites

Adsorbent	**Q (mg/g)**	**R^2**
Z1000H	0.99 ± 0.20	0.963 ± 0.02
Z900Na	0.99 ± 0.07	0.988 ± 0.03
Z25H	2.46 ± 0.35	0.975 ± 0.01
Z25Na	2.67 ± 0.35	0.973 ± 0.02
Al_2O_3	5.87 ± 0.7	0.934 ± 0.04

The results presented in Figure 5.3 show that the high silica zeolites have higher percentage adsorption of ibuprofen at pH 3.0 when compared with alumina while alumina has high adsorption at pH 7.2 and 13.0. This may be explained with respect to the ionization of ibuprofen at different pH. As the pKa of ibuprofen is 4.9, when the pH > pKa (2 units) the ibuprofen is ionized and if pH< pKa (2 units) then it will remains fully unionized, so at pH 7.2 and 13.0 ibuprofen will be ionized. Therefore, alumina has shown high adsorption at pH > 7. On the other hand, at pH lower than its pKa ibuprofen (in its protonated form) was found to show higher affinity towards ZSM-5 zeolites due to the utilisation of hydrophobic interactions. The low adsorption of ibuprofen at pH 13.0 (Fig. 5.3c) when compared with neutral pH may be due to the influence of hydroxide ions, since the surface of the catalyst will be fully populated with hydroxide ions at this pH. However, it is interesting to note here that adsorption of ibuprofen is the highest at pH 7.2 as compared with adsorption at pH 3.0 in the case of alumina. This may be due to the electrostatic forces of interaction between the positive charge alumina and negatively charged ibuprofen at this pH. Therefore, the surface charges on the catalyst and pollutants are also vital in the adsorption process.

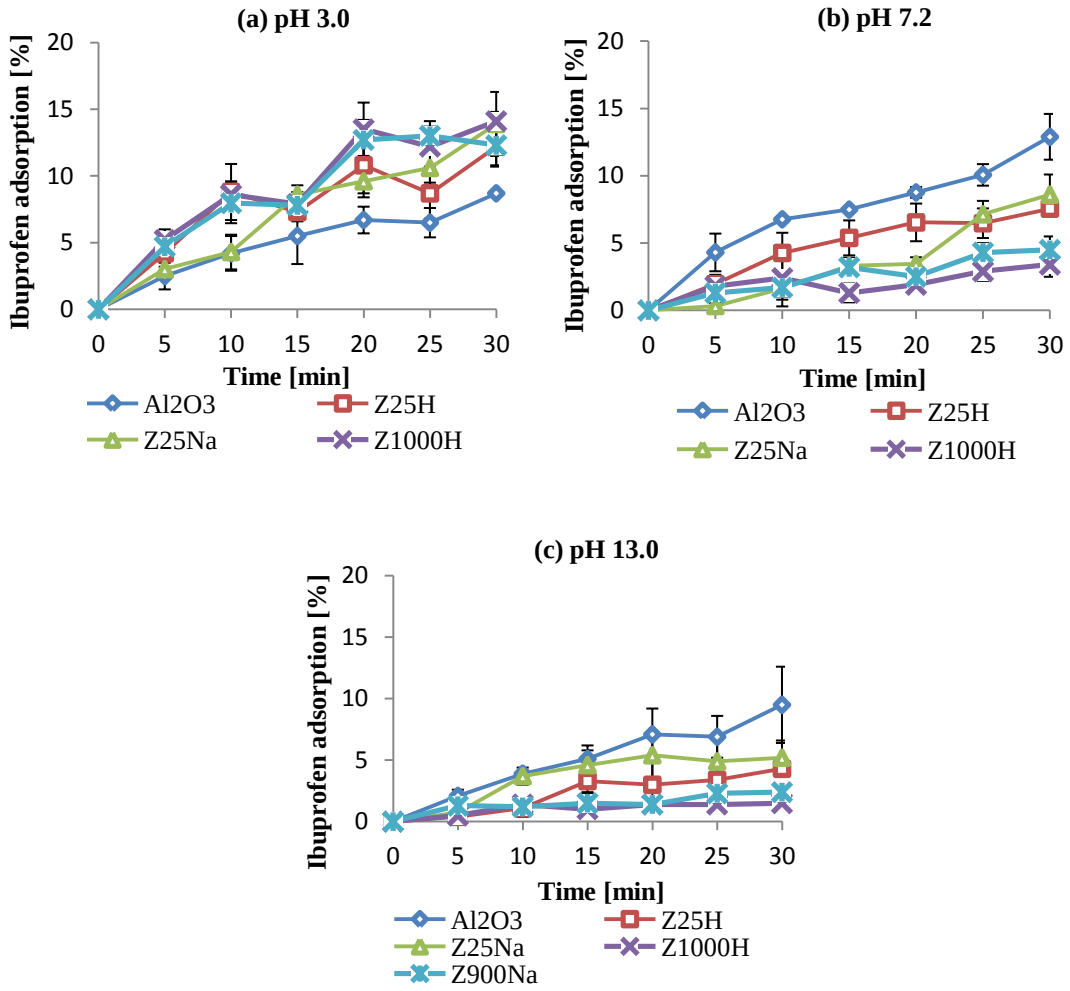

Figure 5.3: Removal of ibuprofen by adsorption ($C_{o\ (ibu)}$ = 15 mg/L; T = 20^{o}C; pH, 3.0, 7.2 and 13.0; adsorbent dose = 5.0 g; V = 490 mL).

5.2.1.2 The catalytic ozonation and the effect of pH

In this study the pH values have been selected by considering the protonated and ionised forms of ibuprofen as well as the pH values above and below the point of zero charges of catalysts. Therefore, experiments have been performed using pH 3.0, 7.2 and 13.0. In this work the pH 7.2 (instead of 6.2) is selected because the pKa of ibuprofen is 4.9, when the pH > pKa (2 units) the ibuprofen will be ionized. Therefore, by selecting these pH values

the effect of ionized and unionized forms of ibuprofen could be studied. The results presented in Figure 5.4 show that catalytic ozonation in the presence of ZSM-5 zeolites and alumina has been effective at pH 3.0 and 7.2, while at pH 13.0 the catalysts were ineffective. This may be due to the high concentration of OH^- ions that are responsible for high rates of aqueous ozonation decomposition at pH 13 [36].

At pH 13.0 (Fig. 5.4c), the surfaces of the catalysts are essentially covered with hydroxide ions. It is known that hydroxide ions promote the decomposition of ozone so any reaction of ibuprofen with ozone on the surface of the catalysts would be unlikely. The results presented in chapter 4 further support this hypothesis, since alumina and zeolites do not promote the formation of reactive oxygen species at pH 13.0 when compared with ozonation alone. An alternate explanation could be that at pH 13.0 the ibuprofen is negatively charged therefore due to the repulsive forces, the adsorption of ibuprofen on the surface of alumina may be lower. The adsorption results clearly support this hypothesis. The higher removal of ibuprofen at pH 7.2 in the presence of alumina when compared with ZSM-5 zeolites may be due to high adsorption of ibuprofen on alumina at pH 7.2. The result indicates that the catalytic activity of ZSM-5 zeolites increases with the decrease in pH and is the highest at pH 3.0. For example, at pH 3.0 the removal of ibuprofen in the presence of zeolites was 28 % (Fig. 5.4a) higher than that of ozonation alone in 30 minutes and at pH 7.2 it becomes 22 % (Fig. 5.4b). This may be due to the high adsorption of ibuprofen on zeolites at pH 3.0. Additionally, ozone is more stabilized at low pH and zeolites may favour molecular ozone reactions. The similar results have been obtained in the case of coumarin and NBD-Cl (chapter 4) removal on zeolites. In contrast to ZSM-5 zeolites the catalytic activity of alumina increases with the increase of pH. For example 83 % ibuprofen was removed at pH 7.2 (Fig. 5.4b) and at pH 3.0 the removal of ibuprofen was reduced to 58 %

in the presence of alumina. These results are consistent with an investigation of reactive oxygen species (ROS) formation in chapter 4. This suggested that with the increase in pH the generation of ROS in the presence of alumina increases and the removal of ibuprofen increases. The adsorption of ibuprofen on the alumina is also an important factor, as alumina has high adsorption of ibuprofen at pH 7.2.

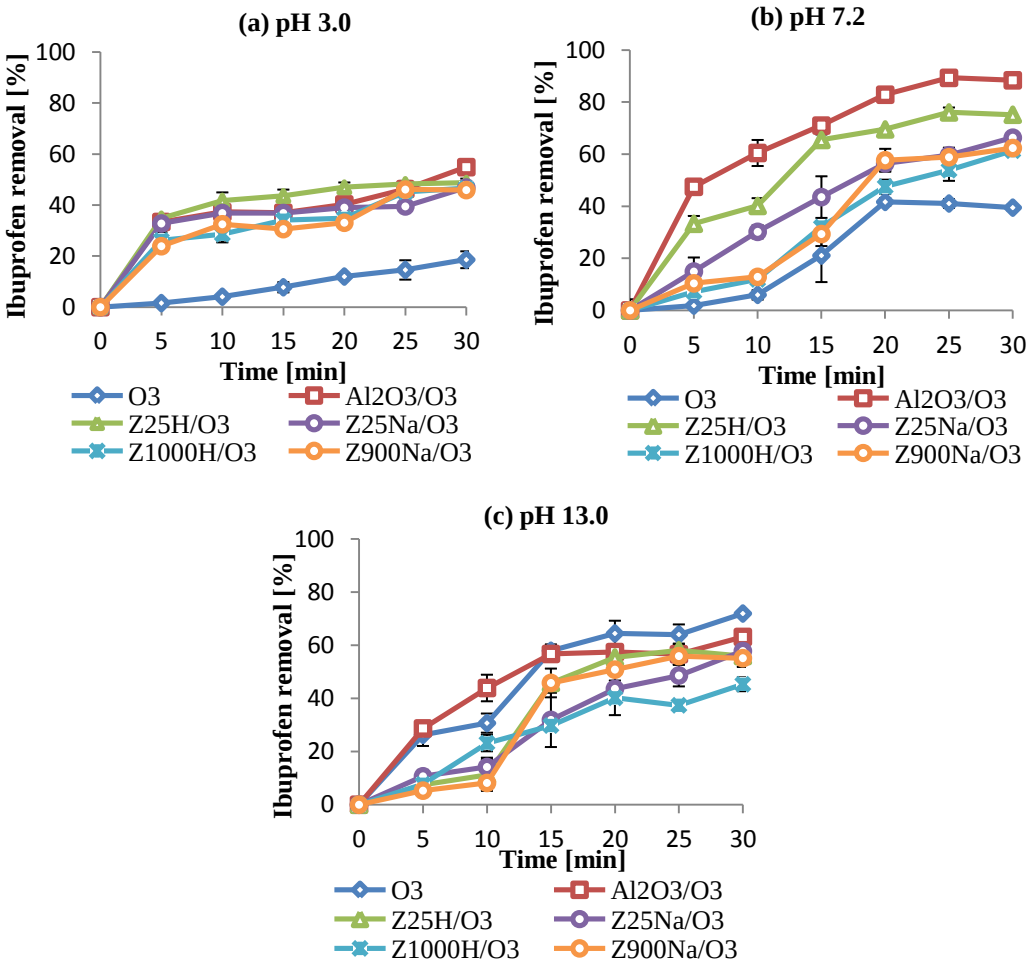

Figure 5.4: Removal of ibuprofen by ozonation alone and catalytic ozonation ($C_{o\,(ibu)}$ = 15 mg/L; O_3 = 0.5 mg/min; T = 20°C; pH = 3.0, 7.2 and 13.0; catalyst dose = 5.0 g; V = 490 mL).

5.2.1.3 Formation of organic acids

The acetic, formic and succinic acids have been identified at pH 3.0 when ZSM-5 zeolites were used as catalysts (Fig. 5.5). They have not been identified when alumina was used as catalyst. It has been hypothesized in chapter 4 that zeolites may adsorb ozone and organic compounds on their surface and their reactions with one another results in the degradation of the pollutant. Criegee mechanism [44] suggested that reactions of ozone with the organic molecules results in the formation of organic acids, as presented in chapter 1 (section 1.6.1.1). The alumina generates hydroxyl radicals as confirmed by coumarin ozonation (chapter 4). The hydroxyl radicals react also with organic acids formed in the solution. Based on the previous reports [17], it is assumed that organic acids formed due to the ozonation process further degraded by alumina. Furthermore, acidic by-products have not been observed at pH 7.2 and 13.0. This may be because of hydroxide ions in solution which can decompose aqueous ozone and can generate hydroxyl radicals.

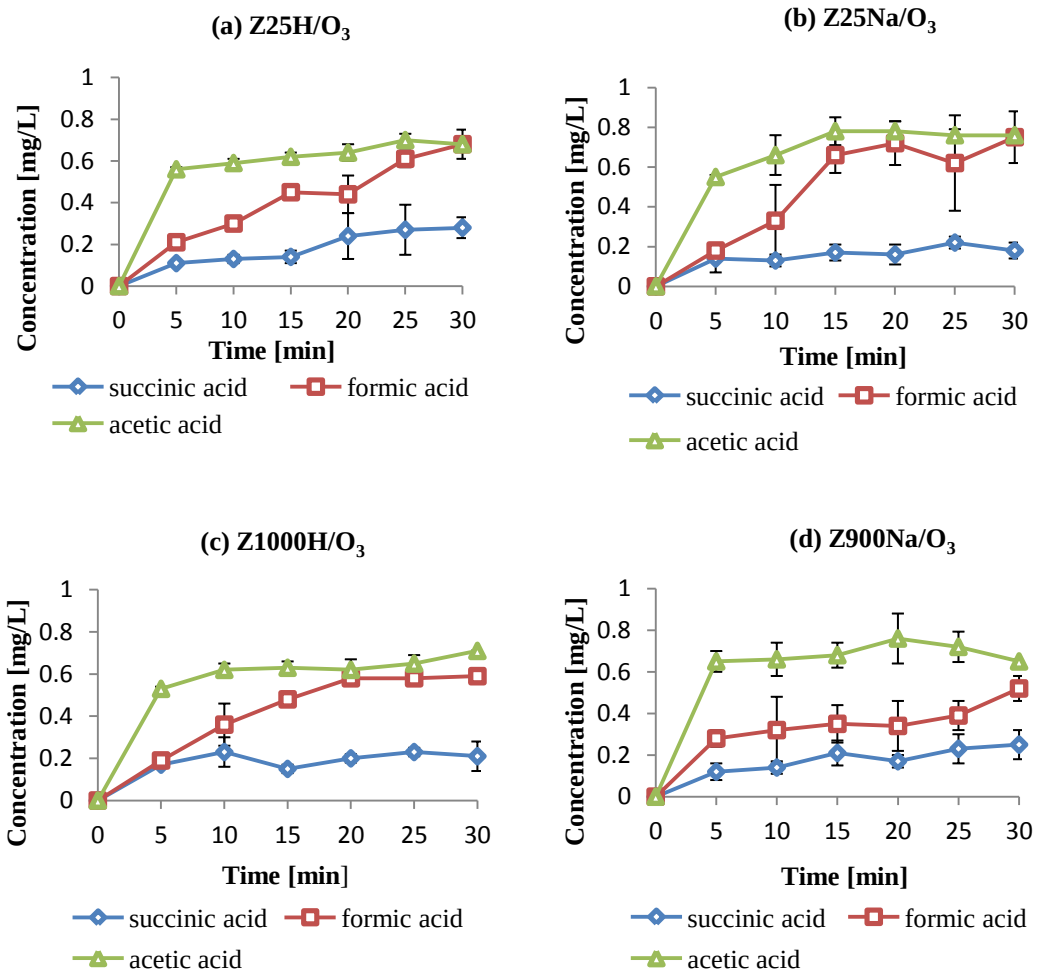

Figure 5.5: Formation of organic acids during catalytic ozonation on zeolites ($C_{o\ (ibu)}$ = 15 mg/L; T = 20^{o}C; pH = 3.0; T = 30 minutes; O_3 = 0.5mg/min; catalyst = 5.0 g; V = 490 mL).

5.2.1.4 Aqueous ozone decay

It is clear from Fig. 5.6 that the amount of aqueous ozone is lower at pH 7.2 and 3 for ZSM-5 zeolites and Al_2O_3 when compared with ozonation alone. The results presented in Figure 5.6c show that there is no significant difference in ozone decay at pH 13.0 for alumina, zeolites and ozonation alone. This is because aqueous ozone is not stabilized at this pH and is decomposed quickly into hydroxyl radicals. Furthermore, the surface of alumina is

negatively charged at this pH. The aqueous ozone decay rates presented in chapter 4 (section, 4.2.1.4) show the similar trend at different pH values. The results presented in Figure 5.6 (aqueous ozone concentration during the ibuprofen removal) can be compared to some extent with the ibuprofen removal data presented in Figure 5.4. It is interesting to note that there seems to be some relationship between ozone decay and ibuprofen removal. The Figure 5.6b has shown that at pH 7.2 the consumption of ozone is the highest in the presence of alumina and this corresponds to the highest level of ibuprofen removal (Fig. 5.6b) when compared with zeolites and ozonation alone. Additionally, it has already been investigated that as the pH approaches the point of zero charge of alumina, its activity increases (chapter 4). Therefore, higher removal of ibuprofen at pH 7.2 may be due to higher catalytic activity and more aqueous ozone decay. At pH 13.0 the ozone decay is somewhat similar in ozonation alone and catalytic ozonation (Fig. 5.6c), the ibuprofen removal studies at the same pH shows the similar removal. It has been observed that ozone decay increase with an increase in pH and this trend is similar in the case of ibuprofen removal (Fig. 5.6). The adsorption of ibuprofen may also be an important factor that cannot be ignored. The high removal of ibuprofen in the presence of zeolites when compared with ozonation alone at pH 3.0 may be due to their high adsorption. The ozone decay results also indicate that lesser aqueous ozone is present in the case of zeolites at pH 3.0 when compared with ozonation alone.

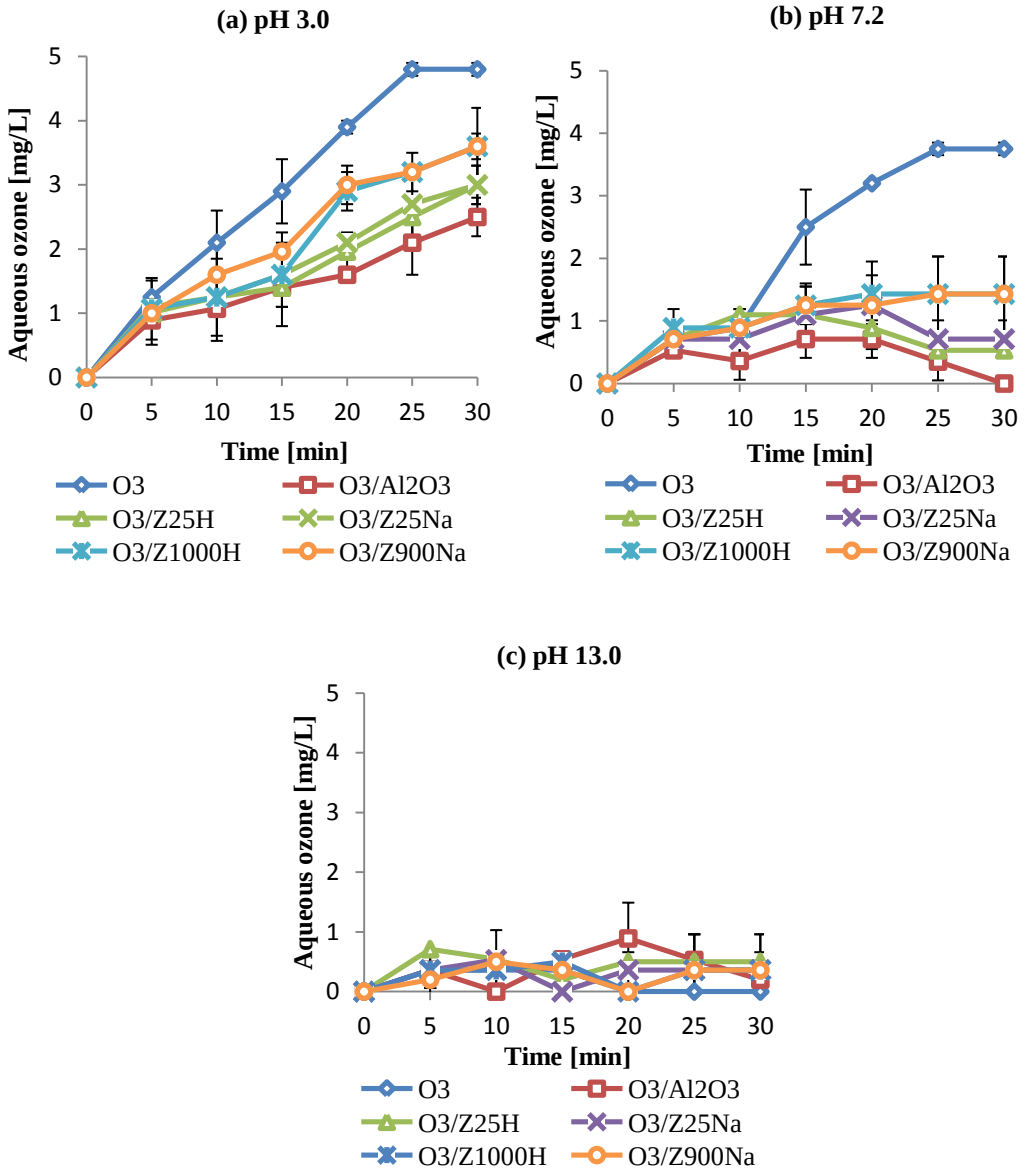

Figure 5.6: The effect of pH on aqueous ozone decay (amount of catalyst = 5 mg/L; O_3 = 0.5mg/min; T = 30 minutes; pH = 3.0, 7.2 and 13.0; T = 20^{o}C; V = 490 mL).

5.2.1.5 Effect of hydroxyl radical scavengers on ibuprofen removal

The effect of tertiary butyl alcohol (TBA) on the catalytic ozonation at different pH values has been investigated in order to understand the mechanism of ibuprofen removal by alumina and ZSM-5 zeolites. It has already been reported in chapter 4 that alumina follows the radical mechanism and zeolites do not decompose ozone to generate hydroxyl radicals.

In this study formation of radicals has been investigated in the presence of ibuprofen. The Figure 5.7 shows that TBA did not have any effect on the catalytic ozonation of ibuprofen under the investigated pH conditions when ZSM-5 zeolites were used. However, in the case of alumina TBA inhibits the removal of ibuprofen and this effect is higher with the increase in pH. For example at pH 7.2 the removal of ibuprofen was 82 % in 30 minutes and in the presence of TBA it reduced to 43 % (Fig. 5.7b). The high difference in the % removal of ibuprofen with and without TBA at pH13.0 may be due to the hydroxide ions in the solution that react with ozone to generate hydroxyl radicals. Similar effects can be observed in the case of ozonation alone at pH 13.0 (Fig. 5.7a). From the experimental data it may be assumed that hydroxyl radicals may not be the dominating active species in the ZSM-5/O3 ozonation process while ozonation in the presence of alumina follows advanced oxidation mechanism, leading to the production of hydroxyl radicals. This hypothesis is supported by the results presented in Figure 5.7. The TBA did not have any significant effect in the case of ozonation in the presence of ZSM-5 zeolites. This suggested that zeolites do not decompose aqueous ozone leading to the production of hydroxyl radicals and this has been confirmed by the previous results presented in chapter 4. The results further indicate that within the family of zeolites the nature of counter ions does not have a significant effect on the mechanism of the process.

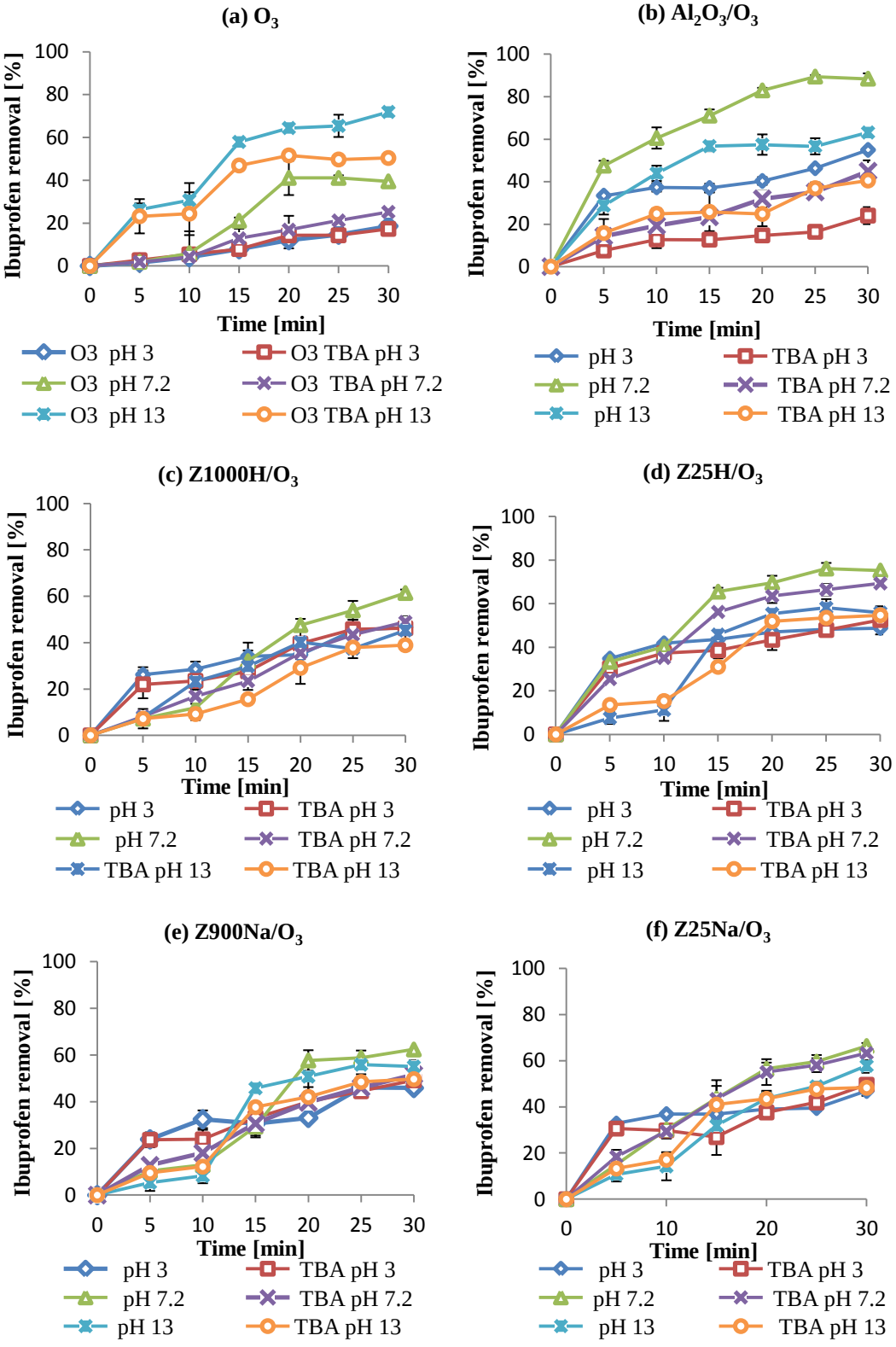

Figure 5.7: Effect of TBA on ozonation alone, ZSM-5/O_3 and Al_2O_3/O_3 ($C_{o\ (ibu)}$ =15 mg/L; T = 20^{o}C; pH = 3.0, 7.2 and 13.0; T = 30 minutes; O_3 = 0.5 mg/min; TBA = 50 mg/L; V = 490 mL).

5.2.1.6 Effect of phosphates

The results indicate that the activity of alumina was greatly reduced in the presence of phosphates especially at pH 3.0 (Fig 5.8b). These results are consistent with the findings presented in chapter 4. The presence of phosphates reduces the formation of reactive oxygen species and hence the catalytic activity of alumina is reduced.

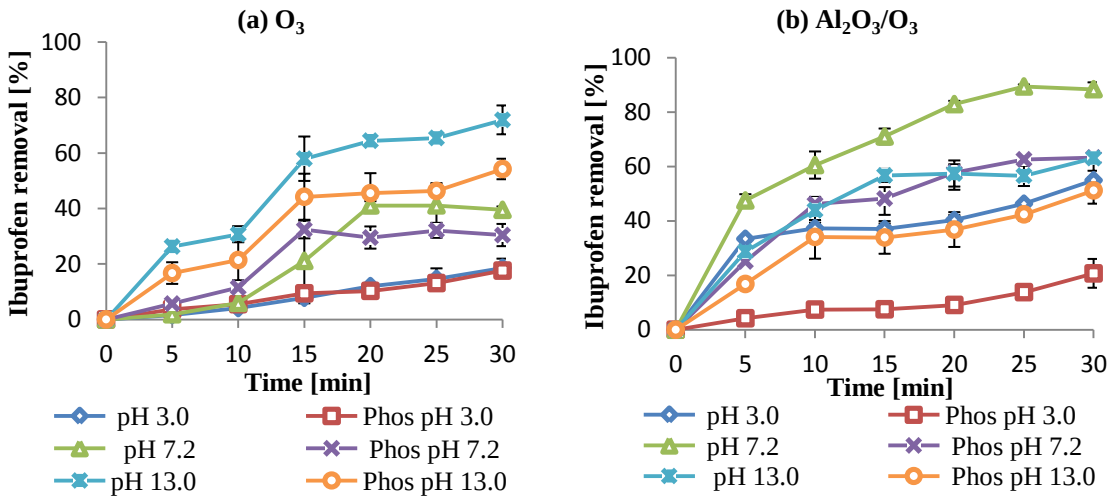

Figure 5.8: Effect of phosphates O_3 and Al_2O_3/O_3 ($C_{o\ (ibu)}$ = 15 mg/L; T = 20^{o}C; pH = 3.0, 7.2 and 13.0; T = 30 minutes; O_3 = 0.5 mg/L; phosphates = 50 mg/L; V= 490 mL).

The above Figure 5.8 clearly shows that the catalytic activity of Al_2O_3/O_3 was reduced at pH 3.0, while this effect was insignificant at pH 13.0 when compared with ozonation alone. The decrease in the ibuprofen removal for O_3 at pH 7.2 and 13.0 in the presence of phosphates may be due to the radical scavenger effect of phosphates and hydroxide ions. The adsorption studies reveal that % adsorption of phosphates onto alumina at pH 3.0 was the highest (Fig. 5.9a). For example the phosphate adsorption on alumina was 27% at pH 3.0 and at pH 13.0) and it was only 3.5%. As discussed previously (chapter 4) that phosphates adsorption is thought to occur through the ligand exchange, which results in the replacement of surface hydroxyl groups of alumina and the deprotonation of phosphates [150].

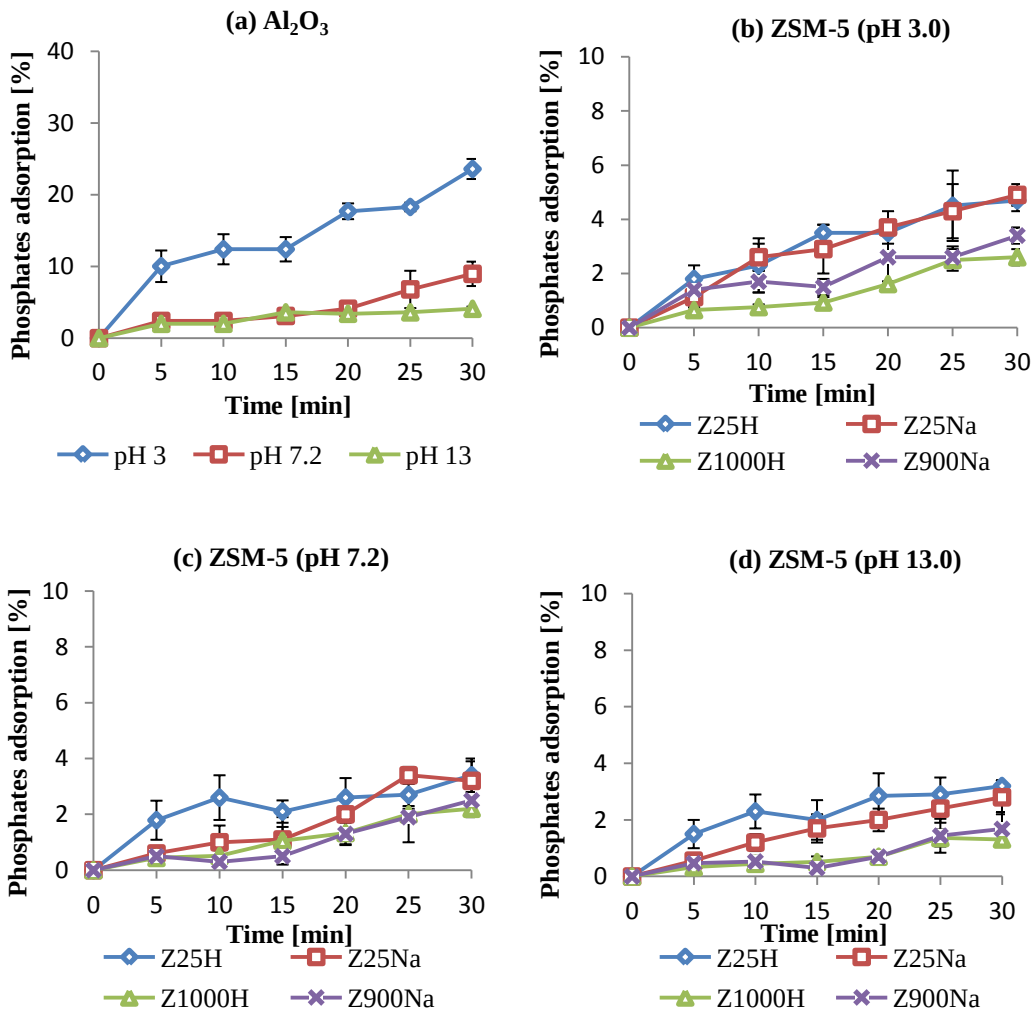

Figure 5.9: The adsorption of phosphates onto ZSM-5 zeolites and alumina (T = 20^{o}C; pH = 3.0, 7.2 and 13.0; T = 30 minutes; phosphates = 50 mg/L: adsorbent dose = 5 mg; V = 490 mL).

The phosphate adsorption on alumina and zeolites decreases with the increase in pH this is because the presences of hydroxide ions that can suppress the adsorption of phosphates as hydroxide ions are stronger base. The results show that the percentage adsorption of phosphates in the case of ZSM-5 zeolite was very low when compared with alumina. For example Z25H only adsorb 4 % phosphates at pH 3.0 (Fig. 5.9b). The zeolites with high alumina content have slightly better adsorption (Fig. 5.9b, c, d).

The data presented in Figure 5.10 clearly shows that the presence of phosphates in the water does not have a significant effect on the catalytic activity of ZSM-5 zeolites with different silica to alumina ratios and counter ions at all studied pH values. This is because phosphates do not adsorb on zeolites and do not influence catalytic process involving direct ozone reactions between adsorbed species. The alumina behaves differently to ZSM-5 zeolites as the decomposition of ibuprofen in the Al_2O_3/O_3 system is reduced in the presence of phosphates.

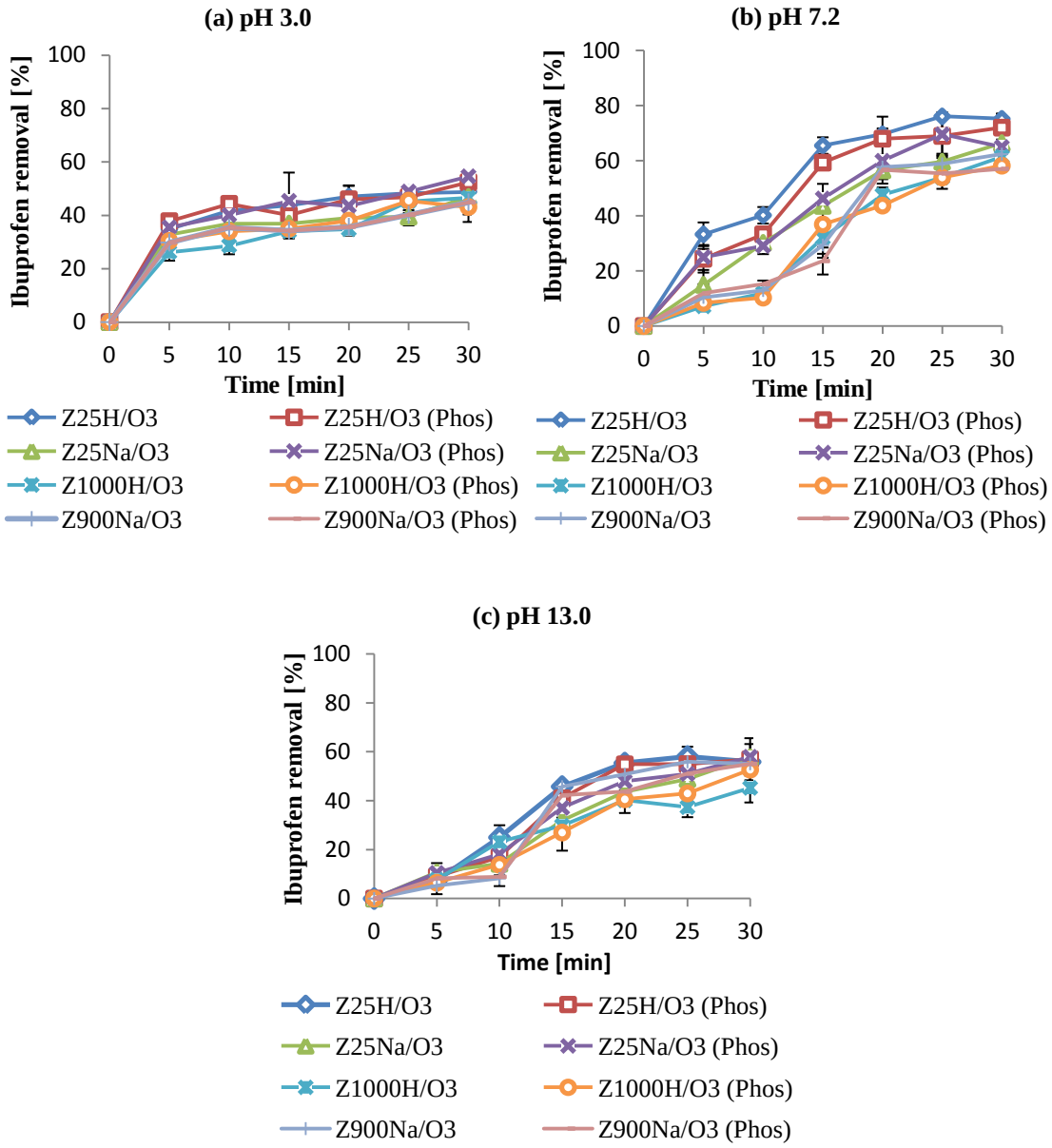

Figure 5.10: Effect of phosphates ZSM-5/O_3 ($C_{o\,(ibu)}$ = 15 mg/L; T = 20°C; pH = 3.0, 7.2 and 13.0; T = 30 minutes; O_3 = 0.5 mg/L; phosphates = 50 mg/L; V= 490 mL).

5.2.1.7 Effect of humic acid

Humic substances (HS) are an important component of natural organic matter and consist of many different classes of high molecular weight organic compounds, mainly fulvic acid (FA) and humic acid (HA). They contain both aromatic and aliphatic structural components

with carboxylic, ketonic and alcoholic functional groups. Because of the large carboxylic acid content the humic substances are negatively charged in the pH range in neutral waters (pKa_1 value is around 4 for protonation of carboxyl groups and around pKa_2 8 for protonation of phenolate groups). At basic pH a large part of phenolic and carboxylic groups are deprotonized [221] and due this reason the molecule becomes more hydrophilic. The Figure 5.11 indicates that the % removal of ibuprofen in the presence of alumina has been decreased when humic acid is present in the solution. For example the % removal of ibuprofen was 83% (reaction time, 30 minutes) in the absence of humic acid and it decreased to 60% in the presence of humic acid. In contrast, humic acids do not have a significant effect on the ozonation of ibuprofen in the presence of zeolites (Fig. 5.11c, d, e, f).

The adsorption results further reveal that alumina has high adsorption of humic acid on its surface in contrast to zeolites. This may be because humic acid at pH 7.2 is ionized, hence attracted towards the positively charged surface of alumina. Additionally, it is important to consider that the pore size of ZSM-5 zeolites is very small and due to the bigger size of humic acid, it cannot penetrate into the pores of ZSM-5 zeolites and adsorption occurs mainly on external surface of ZSM-5 zeolites. The decrease of UV_{254} absorbance to some extent is the highest in the presence of alumina when compared with ZSM-5 zeolites as indicated in the Figure 5.12a. Within the family of ZSM-5 zeolites, the zeolites with high alumina content have high adsorption of humic acids. This suggests that adsorption is one of the important steps in the catalytic ozonation process and the significant reduction in ibuprofen removal in the case of alumina may be due to the adsorption of humic acid on the surface of alumina.

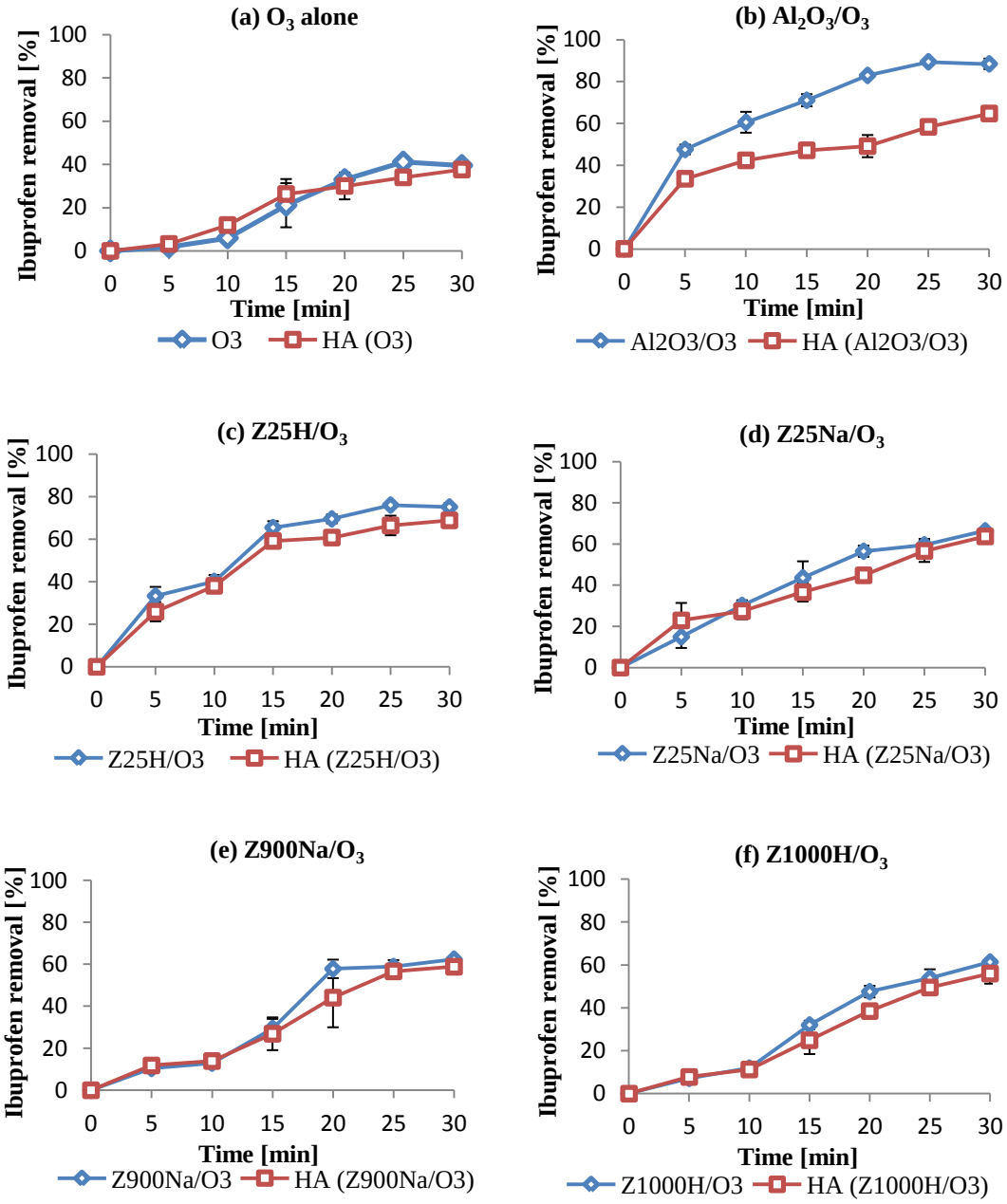

Figure 5.11: The effect of humic acid on the removal of ibuprofen by ozonation and ozonation in the presence of ZSM-5 zeolites and alumina ($C_{o\ (ibu)}$ = 15 mg/L; T = 20^{o}C; O_3 = 0.5 mg/L; pH = 7.2; C_{oHA} = 7.0 mg/L; catalyst = 5.0 g; V= 490 mL).

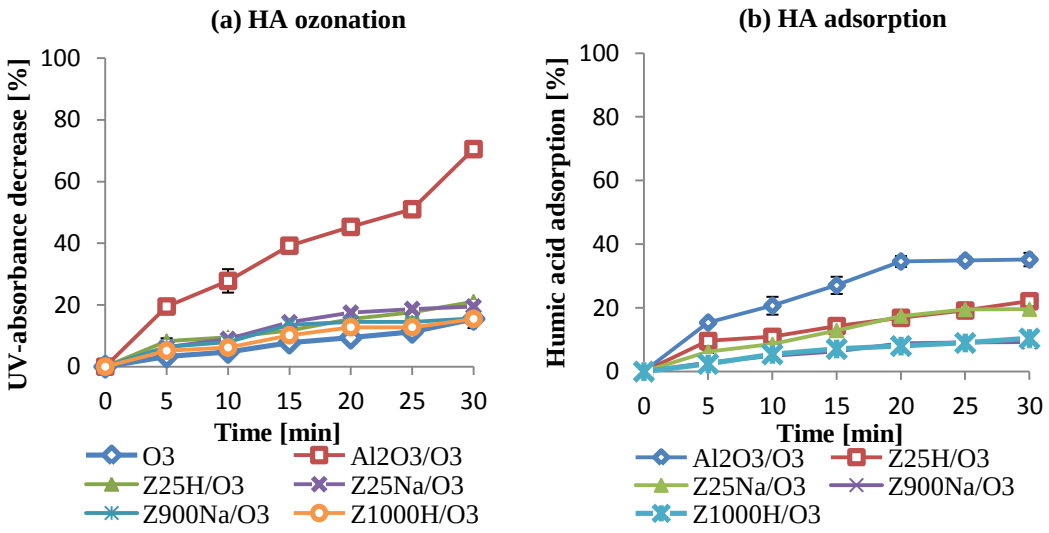

Figure 5.12: (a) Decrease of UV_{254} absorbance during ibuprofen ozoation experiments, (b) adsorption of humic acid on alumina and ZSM-5 zeolites ($C_{o\,(HA)}$ = 7.0 mg/L; T = 20°C; O_3 = 0.5 mg/L; pH = 7.2; catalyst = 5g; V = 490 mL).

5.2.1.8 Drinking water experiments

The aim of this study was to find whether the naturally present substances like phosphates, sulphates, carbonates and bicarbonates in drinking water can cause a decrease in the efficiency of ozonation in the presence of ZSM-5 zeolites and Al_2O_3. The results shown in Figure 5.13b indicate that the efficiency of ozonation of ibuprofen was decreased in the presence of alumina in tap water as opposed to deionised water. For example 83% ibuprofen was removed in 30 minutes in deionised water and it was reduced to about 60% in the tap water in 30 minutes (Fig. 5.13b). This is because tap water contains inorganic ions such as sulfates, carbonates and bicarbonates (Table 5.2) that may adsorb on the surface of alumina and replaced the surface hydroxyl groups of alumina. It has been discussed in chapter 4 that the presence of phosphates reduces the formation of ROS in ozonation in the presence of alumina. Therefore, due to the lack of catalytic activity of alumina in the presence of

inorganic ions, the removal of ibuprofen has been decreased. The comparison between the analysis in the presence of deionised water and tap water show no significant difference in the case of Z25H (Fig. 5.13a). This suggests that ZSM-5 zeolites have different mechanism for the removal of pollutants than that of alumina and since inorganic ions do not adsorb on the ZSM-5 zeolites as described in phosphate effect data, therefore the activity of ZSM-5 zeolites for the removal of ibuprofen is not affected in tap water.

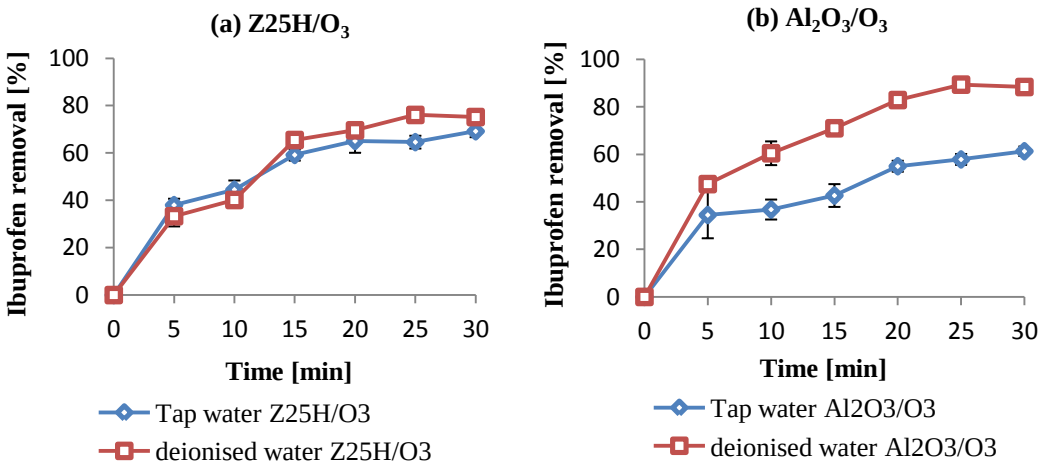

Figure 5.13: Removal of ibuprofen by ozonation in the presence of ZSM-5 zeolites and alumina in tap and deionised water ($C_{o\,(ibu)}$ = 15 mg/L; T = 20°C; O_3 = 0.5 mg/L; pH = 7.3 ± 0.2; catalyst = 5.0 g; V = 490 mL).

Table 5.2: Tap water composition of Huddersfield area obtained from Yorkshire waters [222]

Parameters	Units	Mean value
pH	-	7.3
Nitrate	mg NO_3/L	2.7
Nitrite	mg/L	0.4 <
Sodium	mg/L	9.7
Total organic carbon	mg/L	1.7
Turbidity	NTU	0.1
Calcium	mg/L	13.6
Magnesium	mg/L	2.7
Total hardness	mg/L	18.0
Sulphates	mg/L	32.1

5.2.1.9 Reuse performance

For the reuse performance experiments, among the zeolites Z25H has been selected. The results of long-time efficiency of zeolites (Z25H) and alumina in deionised and tap water (taken from University of Huddersfield) are presented in Figure 5.14. The results show that the catalytic activity of Z25H was constant in both tap and deionised water. However, ibuprofen removal decreases with the passage of time in the case of ozonation in the presence of alumina when experiments were performed in tap water. This is because of the blockage of active sites of alumina due to adsorption of natural water constituents on alumina (e.g. phosphates, sulphates, humic substances, etc.).

Figure 5.15, shows the SEM micrographs obtained from fresh alumina and alumina used in reuse performance experiments in tap water. The catalytic ozonation in drinking water and the presence of inorganic ions significantly affect the topography of the alumina surface. Based on the previous reports [3, 132], this may be attributed to the presence of inorganic ions (Table 5.2) as well as organic matter on the surface of alumina.

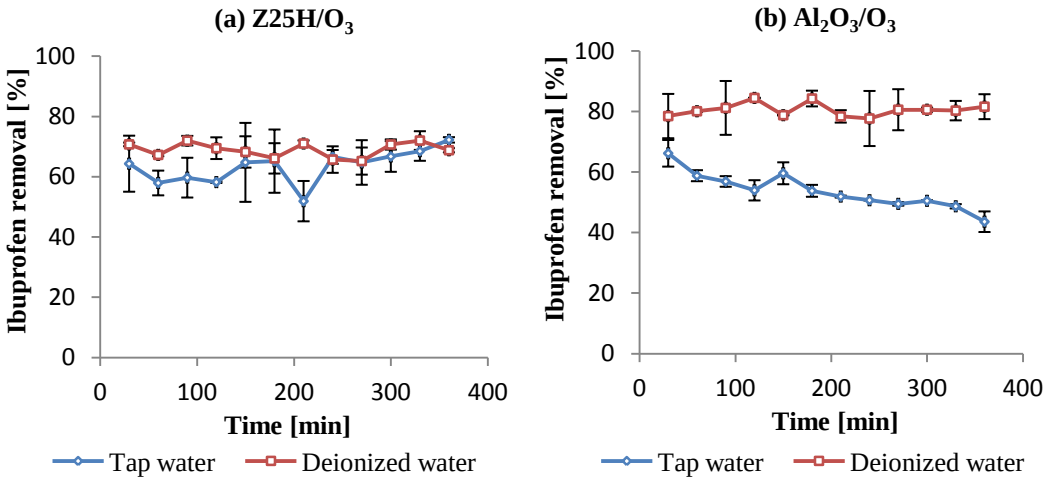

Figure 5.14: Reuse performance experiments for removal of ibuprofen by $Z25H/O_3$ and Al_2O_3/O_3 systems ($C_{o\ (ibu)}$ = 15 mg/L; T = 20°C; O_3 = 30 mg/L; pH = 7.2; catalyst = 5.0 g; V = 490 mL.

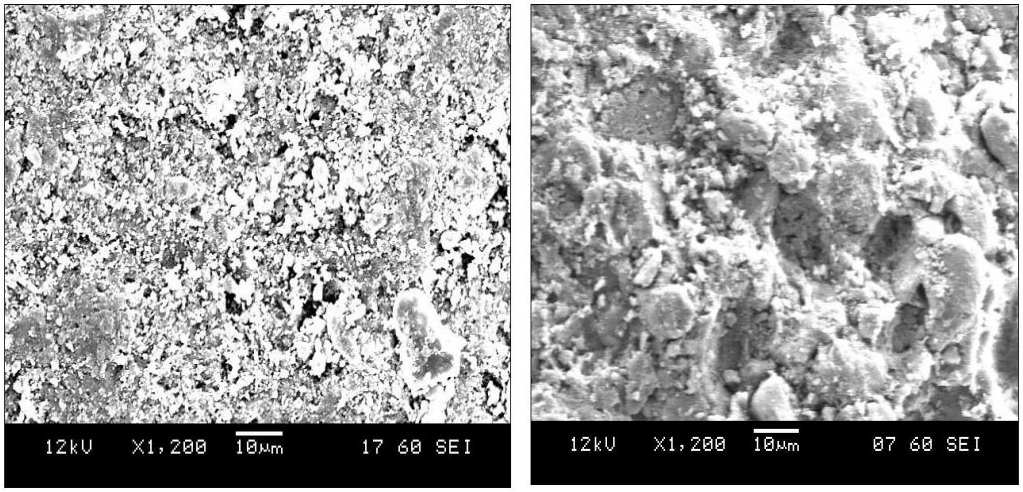

(a) Fresh Al_2O_3 (b) Al_2O_3 reused in tap water

Figure 5.15: Reuse performance experiments for removal of ibuprofen by $Z25H/O_3$ and Al_2O_3/O_3 systems ($C_{o\ (ibu)}$ = 15 mg/L; T = 20°C; O_3 = 30 mg/L; pH = 7.2; catalyst = 5.0 g; V = 490 mL.

5.2.2 Part 2 catalytic ozonation of VOCs in water

This part of the thesis contains the results of an investigation of the efficiency of VOCs removal in water on ZSM-5 zeolites and alumina. Furthermore, the parameters such as effect of pH, adsorption, inorganic ions, natural organic matter and hydroxyl radical scavengers have been investigated. Cumene and chlorobenzenes (1,2-dichlorobenzene and 1,2,4-trichlorobenzene) were used as target pollutants. Both the H-ZSM-5 and Na-ZSM-5 forms with different SiO_2/Al_2O_3 ratios and counter ions (Z1000H:SiO_2/Al_2O_3 = 1000, Z900Na:SiO_2/Al_2O_3 = 900, Z25H:SiO_2/Al_2O_3 = 25 and Z25Na:SiO_2/Al_2O_3 = 25), and γ-alumina have been used. It is important to mention here that all the experiments have been performed by using a saturated solution of VOCs (contains a mixture of VOCs).

5.2.2.1 Adsorption of VOCs on Al_2O_3 and ZSM-5 zeolites

In order to understand the role of adsorption in the ozonation of VOCs in the presence of ZSM-5 zeolites and alumina, the adsorption capacities of VOCs on alumina and ZSM-5 zeolites were determined from Langmuir adsorption isotherms and are presented in Table 5.3. The results show that high silica zeolites (Z1000H and Z900Na) have significantly higher adsorption capacities towards VOCs than alumina, Z25H and Z25Na. Adsorption capacity for Z1000H and Z900Na was 3.6 mg/g, 1 mg/g and 0.2 mg/g for cumene, 1,2-dichlorobenzene and 1,2,4-trichlorobenzene respectively. However, Z25H and Z25Na have adsorption capacities of 0.7 mg/g, 0.2 mg/g and 0.1 mg/g for cumene, dichlorobenzene and trichlorobenzene respectively and the alumina has the least adsorption capacity (0.5 mg/g, 0.1 mg/g and 0.02 mg/g for cumene, dichlorobenzene and trichlorobenzene respectively). This might be due to the higher hydrophobicity of high silica zeolites. The comparison between adsorption capacities obtained in the case of ibuprofen and VOCs indicate that within the family of zeolites, the zeolites with high alumina content adsorb more ibuprofen (ionized form) as opposed to this the zeolites with high silica content adsorb more VOCs.

This further supports the hypothesis that hydrophicity and hydrophobicity are important in the adsorption process. Zhao et al [223] studied the adsorption of cumene on mesoporous ZSM-5 zeolites with different pore sizes (22 Å to 40 Å) and surface areas (380 m^2/g to 427 m^2/g). It has been reported that adsorption of cumene follows Langmuir isotherm model, which is in agreement of the results presented in current work. The adsorption capacity of cumene was found to be 84 mg/g, which is very high as compared to the results presented in Table 5.3. This may be due to the high surface area and large pore size of ZSM-5 zeolites used by Zhao et al [223].

Kasprzyk-Hordern et al [15] studied the removal of cumene and chlorobenzenes on γ-Al_2O_3. The results indicated that alumina does not adsorb the pollutants, and it has been reported that this may be due to the hydrophobicity of pollutants. The results presented in Table 5.3 are in agreement as no significant adsorption of VOCs was observed in the case of alumina.

Table 5.3: Adsorption capacities of VOCs on Al_2O_3 and ZSM-5 zeolites

Adsorbent	Adsorption capacity (mg/g) ± S.D		
	Cumene	Dichlorobenzene	Trichlorobenzene
Z1000H	3.74 ± 0.10	1.07 ± 0.05	0.23 ± 0.04
Z900Na	3.46 ± 0.10	1.02 ± 0.05	0.20 ± 0.03
Z25H	0.70 ± 0.05	0.20 ± 0.01	0.10 ± 0.03
Z25Na	0.60 ± 0.06	0.15 ± 0.02	0.11 ± 0.03
Al_2O_3	0.50 ± 0.03	0.10 ± 0.01	0.02 ± 0.01

Further experiments have been performed at pH 3.0, 6.2 and 13.0 in the semi-continuous reactor. The data presented in Figure 5.16 was plotted between the ratios of VOCs concentrations (concentration at time t/initial concentration) versus adsorption time. The results revealed that much higher quantities of cumene, dichlorobenzene and

trichlorobenzene were adsorbed on 5.0 g of Z1000H and Z900Na when compared with Z25H, Z25Na and alumina (Fig. 5.16). As discussed earlier this may be due to the high hydrophobicity of Z1000H and Z900Na when compared with other catalysts. The results at different pH values revealed that VOCs have lower percentage adsorption at pH 13.0. This is because the surface of catalysts may be populated at this pH with hydroxide ions. Similar results have been obtained in the case of coumarin adsorption studies as discussed in chapter 4 (part 1). The results further revealed that the pH value of solution significantly affects absorption of chlorobenzenes (Fig. 5.16 g, h, i). An increase in adsorption was observed with decrease of pH of the solution. This effect was more pronounced in the case of trichlorobenzene. For example, the C/C_o ratio (the results have been presented by C/C_o ratios instead of percentage removal in the case of VOCs investigation due to the slightly variable initial concentrations of VOCs) was 0.5 of trichlorobenzene at pH 6.2, when 5.0 g of Z1000H was used and only 0.4 at 3 pH units higher. On the other hand adsorption of cumene on studied catalysts was not significantly pH dependant. This indicates that at acidic pH values there are more H^+ ions and their interactions with chloro groups would be higher at this pH value.

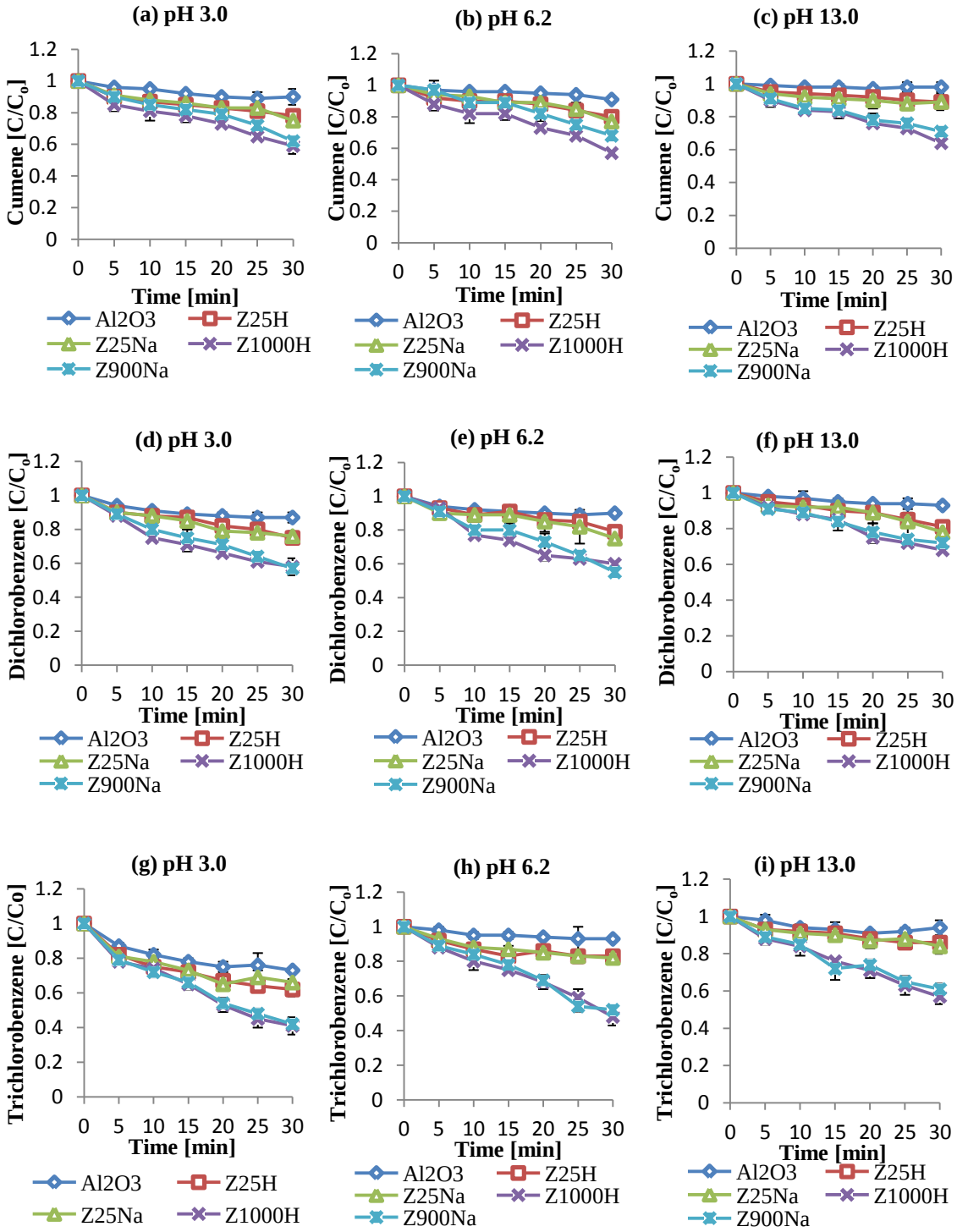

Figure 5.16: Adsorption of VOCs on ZSM-5 zeolites and alumina ($C_{o\,(cum)}$ = 19.2 ± 0.5 mg/L; $C_{o\,(DCB)}$ = 3.5 ± 0.2 mg/L, and $C_{o\,(TCB)}$ = 0.5± 0.1 mg/L; T = 20°C; pH = 3.0, 6.2 and 13.0; pH_{30min} = pH_o ± 0.3; adsorbent dose = 5.0 g; V= 490 mL).

5.2.2.2 The catalytic ozonation and the effect of pH

The catalytic ozonation of VOCs on zeolites and alumina has been investigated at selected pH values of solutions. In this study pH 3.0, 6.2 and 13.0 has been selected. In the work presented in chapter 4, the experiments have been performed at the above mentioned pHs as well as at pH 8.8. However, zeolites have not been effective at pH 8.8, therefore in this work experiments have been performed at pH 6.2 which is also closer to drinking water pH. The results shown in Fig 5.17 indicate that as the pH of the solution increases, the difference of VOCs removal in ozonation alone and ozonation in the presence of ZSM-5 zeolites decreases. For example, the difference in the ratio of the concentration in 30 minutes and the concentration at zero time ($C_{t\ 30min}/C_o$) between Z1000H/O_3 and O_3 at pH 3.0 is 0.43 and it becomes 0.14 at pH 6.2. This clearly suggested that the activity of ZSM-5 zeolites increases with the decrease of pH. These results were supported by the work of Amin et al [23] which suggested that zeolites are more active at acidic pH. This may be because aqueous ozone is more stabilized at acid pH values. The results for chlorobenzenes also show the similar correlation (Fig. 5.17). Furthermore, the results indicated that zeolites with high silica content shows better removal, that may be due to the high adsorption of VOCs on more hydrophobic ZSM-5 zeolites as indicated by the adsorption results. Fujita et al [11] studied the removal of trichloroethene (TCE) on ZSM-5 zeolites with different silica to alumina ratios and it was reported that ZSM-5 zeolites with high silica content adsorb TCE with higher efficiency and hence have the highest removal of TCE in the catalytic ozonation. These results further support the hypothesis presented in this work. The results at pH 13.0 (Fig. 5.17c, f, i) clearly revealed that zeolites are not effective at this pH value. This may be because aqueous ozone is not stabilized at this pH and free radical mechanism dominates at this pH value [36]. Similar results have been obtained when the experiments have been performed at pH 13.0 in the case of ROS investigation as well as ibuprofen study.

The results further show that alumina is not a good catalyst for VOCs this may be due to the low adsorption of VOCs on alumina. It has already been investigated in previous work (chapter 4) that alumina operates via radical mechanism and its activity is the highest near its point of zero charge. These results also support our hypothesis that adsorption of pollutants on the surface of catalyst is an important step in contrast to Ernst et al [17]. It has been reported by some researchers that surface reactions are vital for effective removal of pollutants [3, 16]. In the case of ibuprofen removal (part 1), the alumina can effectively remove ibuprofen in water as it has high adsorption on its surface, this further support this hypothesis. An alternate explanation may be that molecular ozone reactions may be favourable for the removal of VOCs, as alumina decomposes aqueous ozone leading to the generation of active oxygen species.

The results presented in Fig. 5.17 clearly indicate that high silica zeolites are good catalyst and they have a higher removal rate than that of O_3 alone. Furthermore, the rapid decrease in VOCs concentrations in the first 5 minutes in the presence of ZSM-5/O_3 may be due to the quick adsorption of VOCs on the catalyst surface. Additionally, while comparing the adsorption, ozonation and catalytic ozonation, it has been noticed that the removal of cumene at pH 3.0 in the first 5 minutes was 10 % higher in the case of catalytic ozonation than ozonation plus adsorption. This clearly suggests that ZSM-5 zeolites catalyse VOCs removal.

Among the VOCs the cumene has the highest removal as compared with chlorobenzenes. This may be due to the structure of compounds. The cumene contain aromatic ring activating group however chlorobenzenes contain electron donating groups therefore they are highly resistant to ozone attack. Therefore, ozone selectively reacts with a lesser resistant compound (cumene). This further supports our hypothesis that zeolites operate

through the direct reaction of ozone and pollutants on their surface. Since hydroxyl radicals reacts with pollutants in a non selective way.

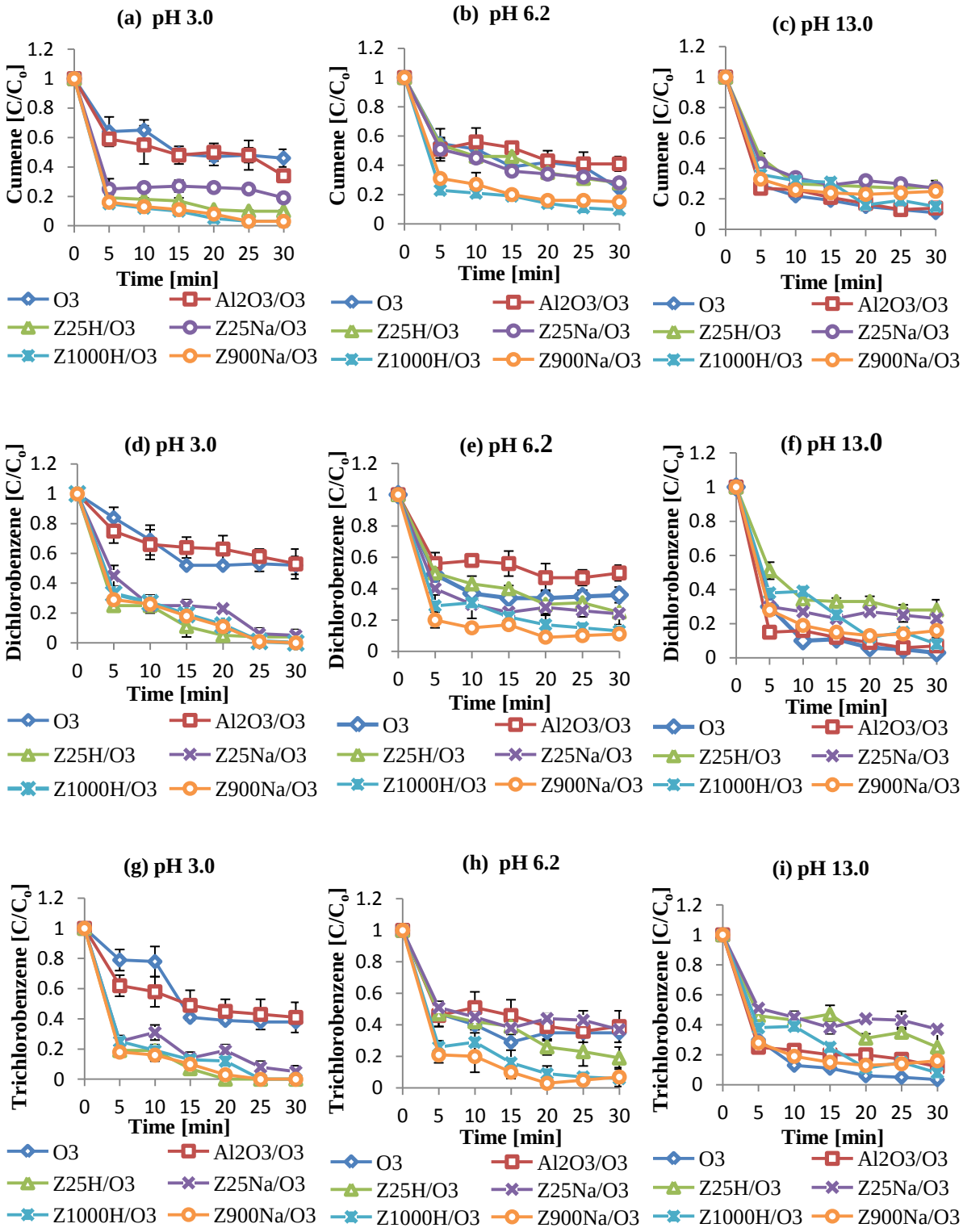

Figure 5.17: Effect of pH on VOCs removal by ozonation alone and ozonation in the presence of ZSM-5 zeolites and alumina ($C_{o\,(cum)}$ = 19.2 ± 0.5 mg/L, $C_{o\,(DCB)}$ = 3.5 ± 0.2 mg/L, and $C_{o\,(TCB)}$ = 0.5 ± 0.1 mg/L; T = 20°C; pH = 3.0, 6.2 and 13.0; pH_{30min} = pH_o ± 0.3; catalyst amount = 5 g; V = 490 mL; O_3 = 0.1 mg/min).

5.2.2.3 Formation of organic acids as by-products of reaction

The acetic and formic acids have been identified only at pH 3.0 (Fig. 5.18) and only in the case of ozonation on zeolites. This indicates that the above catalysts lead to higher degradation of VOCs when compared with other studied catalytic systems and ozonation alone. Similarly, in the case of ibuprofen removal studies the organic acids have been identified in the case of zeolites at pH 3.0. This may be because zeolites adsorbed ozone and pollutants on their surface and their direct reaction results in the formation of acidic by-products and molecular ozone does not react with these organic acids. However, in the case of alumina the hydroxyl radicals are produced that can even degrade organic acids.

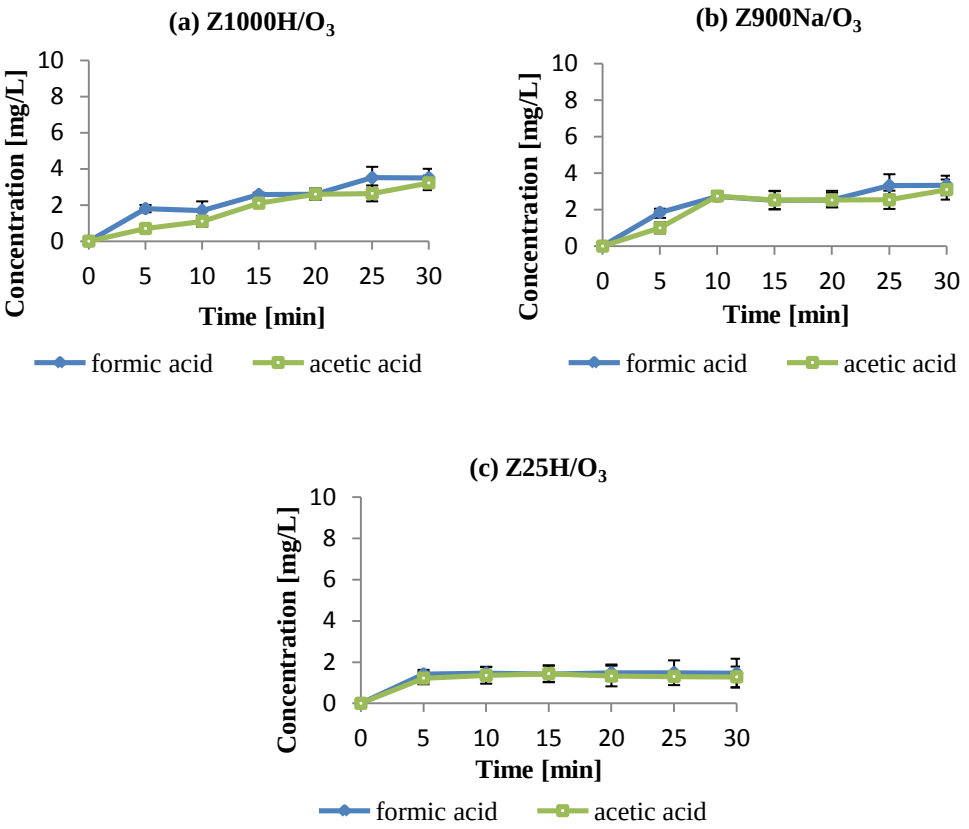

Figure 5.18: Formation of organic acids during the ozonation of VOCs in the presence of ZSM-5 zeolites ($C_{o\,(cum)}$ = 19.2 ± 0.5 mg/L, $C_{o\,(DCB)}$ = 3.5 ± 0.2 mg/L and $C_{o\,(TCB)}$ = 0.5 ± 0.1 mg/L; T = 20°C; pH_0 = 3; pH_{30min} = pH_0 ± 0.2; catalyst amount = 5 g; V= 490 mL; O_3 = 0.1 mg/min).

5.2.2.4 Aqueous ozone decay

The results presented in the Figure 5.19 show the aqueous ozone decay during the ozonation alone and ozonation of VOCs in the presence of ZSM-5 zeolites and alumina. The results indicate that ozonation in the presence of alumina and ZSM-5 zeolites show more aqueous ozone decay when compared with ozonation alone at pH 3.0 and 6.2 (Fig. 5.19a, b). However, at pH 13.0 (Fig 5.19c), the catalysts have ozone decay patterns similar to ozonation alone and this pattern is consistent with the other studies as presented in chapter 4 and part 1 of the chapter 5. It has already been suggested that this may be due to the high concentrations of hydroxide ions present at this pH that can decompose aqueous ozone leading to the production of hydroxyl radicals. The surface of catalysts may be essentially covered with hydroxide ions therefore ozone adsorption or decay by surface sites may not be possible.

The comparison of ozone decay with the VOCs removal show that ozonation in the presence of alumina has more aqueous ozone decay when compared with ZSM-5 zeolites. Despite this fact, the removal of VOCs has been found to be the lowest in the case of alumina. Similarly, the ZSM-5 zeolites with different silica to alumina ratios have almost similar ozone decay however, the high silica zeolites (Z1000H, Z900Na) show higher removal of VOCs. This can be rationalized by adsorption studies. Since the high silica zeolites have high adsorption therefore, they show more removal of VOCs. This indicates the importance of surface reactions in the catalytic ozonation process. Furthermore, the results support the hypothesis that within the family of zeolites the nature of counter ion does not play any significant role in the ozone decomposition.

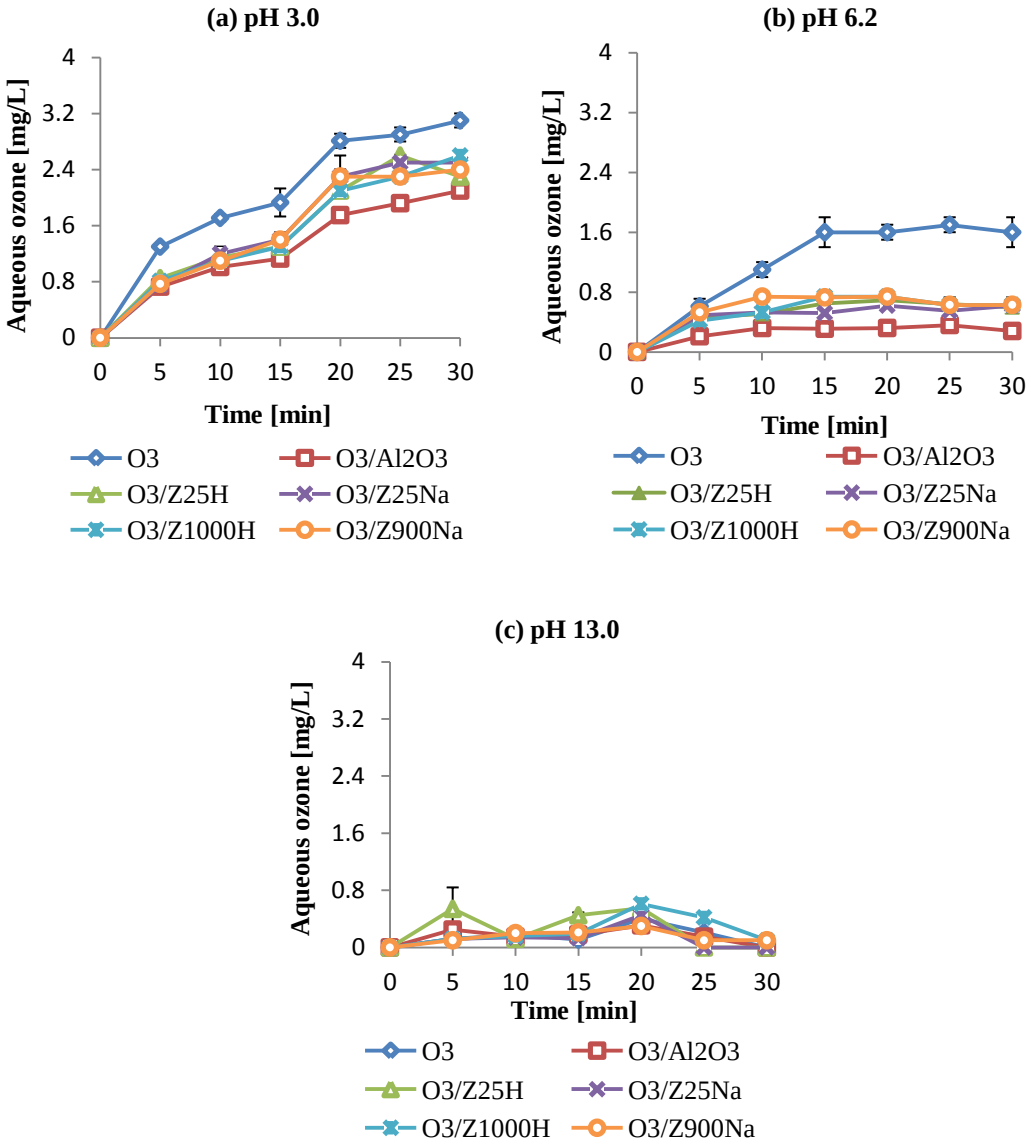

Figure 5.19: The effect of pH on aqueous ozone decomposition (amount of catalyst = 5.0 mg/L; O_3 = 0.1 mg/min; T = 30 minutes; pH = 3.0, 6.2 and 13.0; T = 20^{o}C; V = 490 mL).

5.2.2.5 Effect of hydroxyl radical scavengers

The results (Fig. 5.20a, b, c) show that in the case of ozonation alone TBA inhibition effect is more pronounced with the increase in pH and it is the highest at pH 13.0 (Fig. 5.20c). This is because at a basic pH high concentration of hydroxide ions are present and these hydroxide ions promote aqueous ozone decomposition leading to the formation of hydroxyl radicals. In the case of alumina TBA clearly inhibited the removal of cumene (Fig. 5.20d, e, f) and this effect is more significant with the increase of pH. The high inhibition effect at pH 13.0 (Fig. 5.20f) may be due to the higher radical scavenger effect of TBA in solution at pH 13.0. It is to be noted that this effect was also very high for ozonation alone (Fig. 5.20c). It has already been concluded from previous work (chapter 4) that alumina is not effective at pH 13.0 (pH > PZC). The lack of significant effect of TBA on the efficiency of catalytic ozonation on ZSM-5 (Fig. 5.21) suggests that hydroxyl radicals may not be the dominating active species. It has been already discussed in this thesis that zeolites may mainly act as adsorbent that can attract both pollutants and ozone towards their surface and oxidation of pollutants can take place on the surface of zeolites. In the case of ozonation on alumina a different mechanism is dominant and alumina can interact with ozone, which leads to the generation of hydroxyl radicals. Similarly in the case of chlorobenzenes the presence of TBA does not have any significant effect in the case of ZSM-5 zeolites.

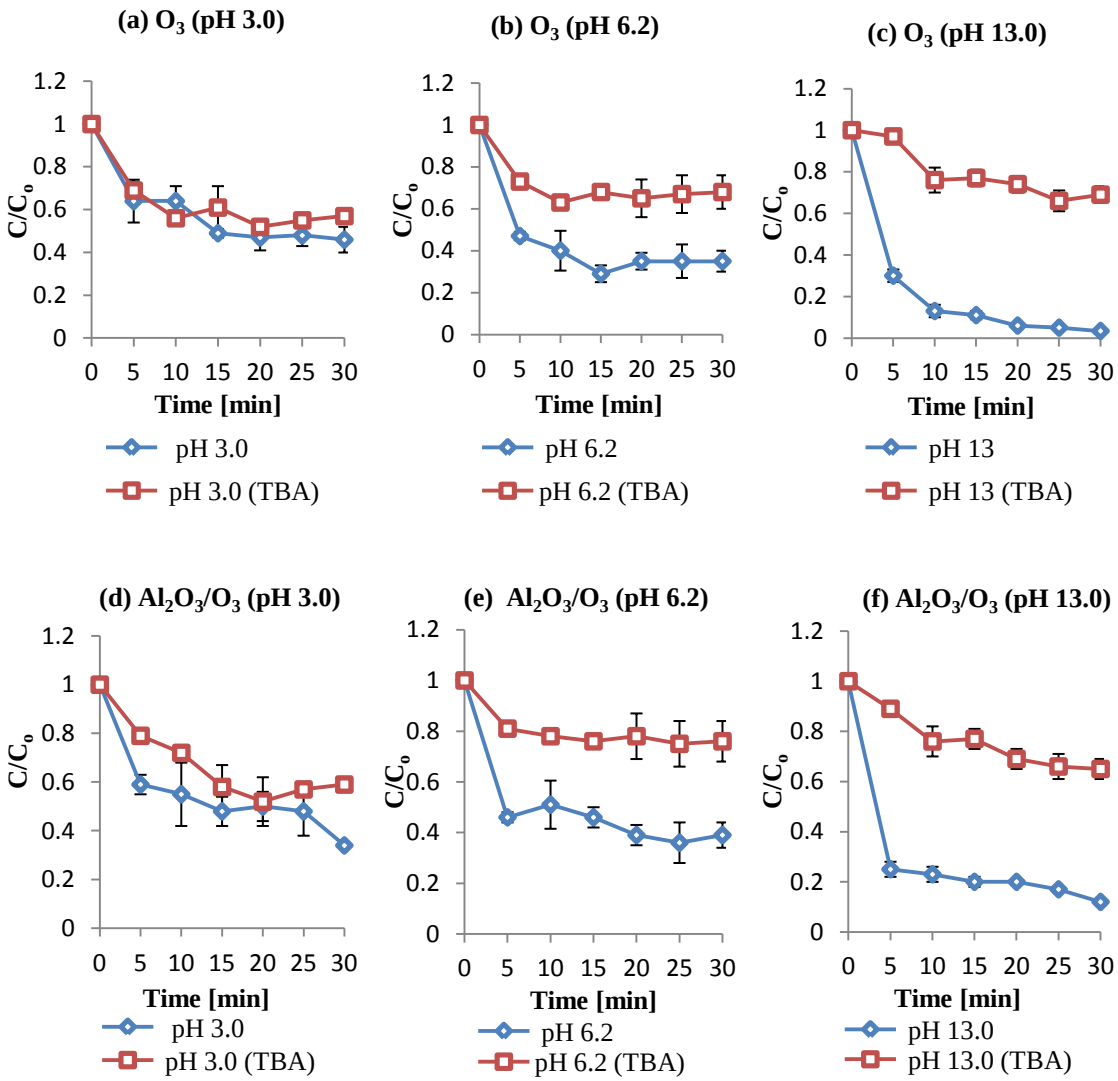

Figure 5.20: Effect of TBA on cumene removal by ozonation in the presence of alumina ($C_{o\ (cum)}$ = 19.2 ± 0.5 mg/L; T = 20°C; pH = 3, 6 and 13; pH_{30min} = pH_0 ± 0.3; TBA = 50 mg/L; catalyst amount = 5 g; V = 490 mL; O_3 = 0.1 mg/min).

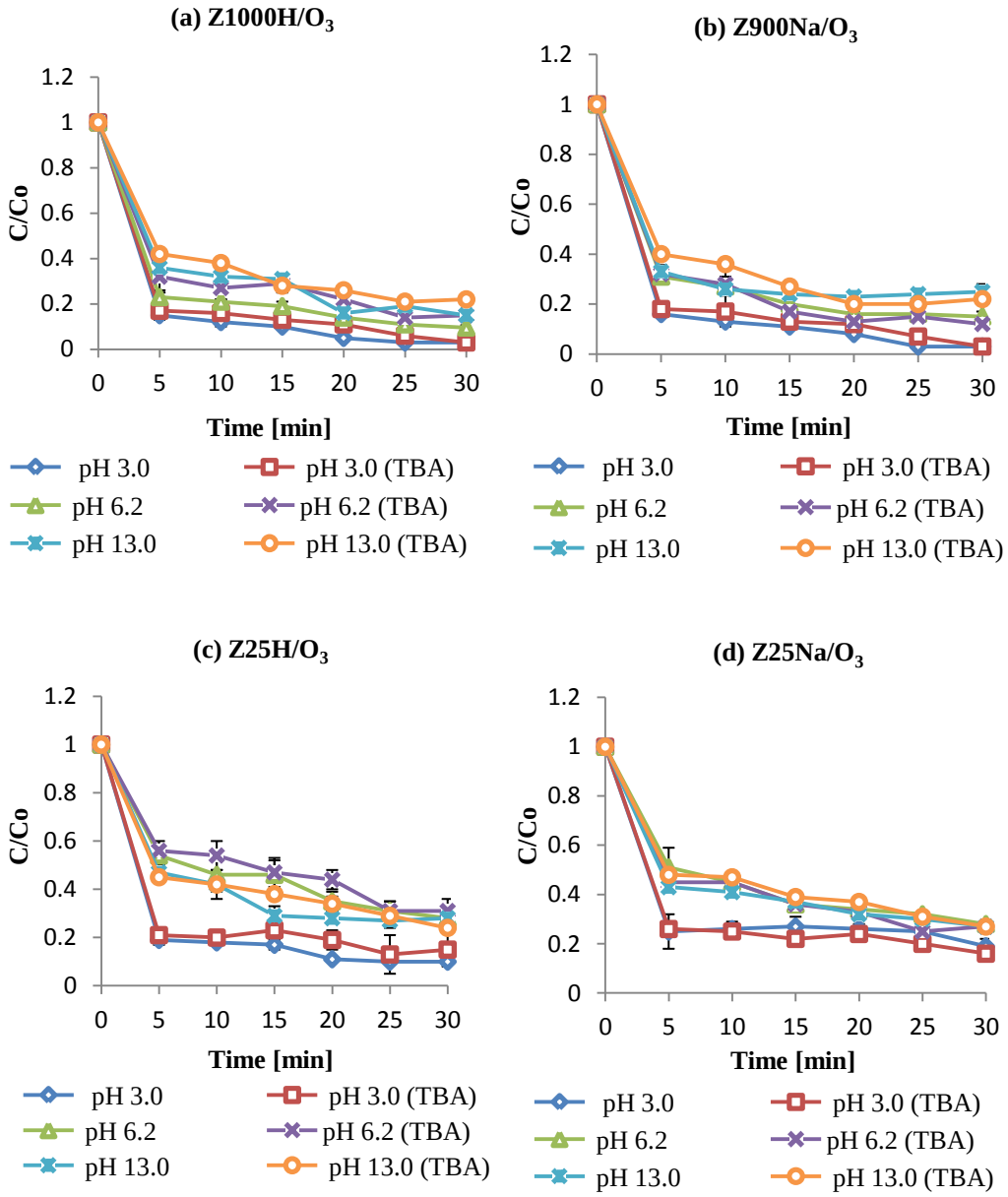

Figure 5.21: Effect of TBA on cumene removal by ZSM-5/O_3 ($C_{o\,(cum)}$ = 19.2 mg/L; T = 20^{o}C; pH = 3.0, 6.2 and 13.0; pH_{30min} = pH_o ± 0.3; TBA = 50 mg/L; catalyst amount = 5.0 g; V = 490 mL; O_3 = 0.1 mg/min).

5.2.2.6 Effect of phosphates

The adsorption experiments showed that phosphate adsorption on alumina decreases with the increase in pH this may be due to the presences of hydroxide ions that can suppress the absorption of phosphates, as hydroxide ions are stronger base [132]. For example the

phosphates adsorption was 37% in 30 minutes on alumina at pH 3.0 (Fig. 89d) and it becomes 10.3 and 4.4 at pH 6.0 and 13.0 respectively (Fig. 5.23d). The high adsorption of phosphates at pH 3.0 may also be due to the high concentration of protonated forms of phosphates at acidic pH. Hence the surface hydroxyl groups of alumina may be rapidly replaced at this pH through ligand exchange mechanism as discussed in chapter 1.

The results indicate the activity of alumina was reduced to some extent at pH 3.0 (Fig. 5.22d, e, f). This is because alumina has a high adsorption capacity towards phosphates, which increases with a decrease of pH. It has been studied that the catalytic activity of alumina was greatly reduced in the presence of phosphates (chapter 4). The decrease in catalytic activity for Al_2O_3/O_3 at pH 13.0 (Fig. 5.22d, e, f) may be due to the radical scavenger effect of phosphate [36] as similar reduction was observed in ozonation alone (Fig. 5.22a, b, c). In the case of ozonation alone the removal of cumene decreases with the increase in pH in the presence of phosphates. This is because of the radical scavenger effect of hydroxide ions at high pH values.

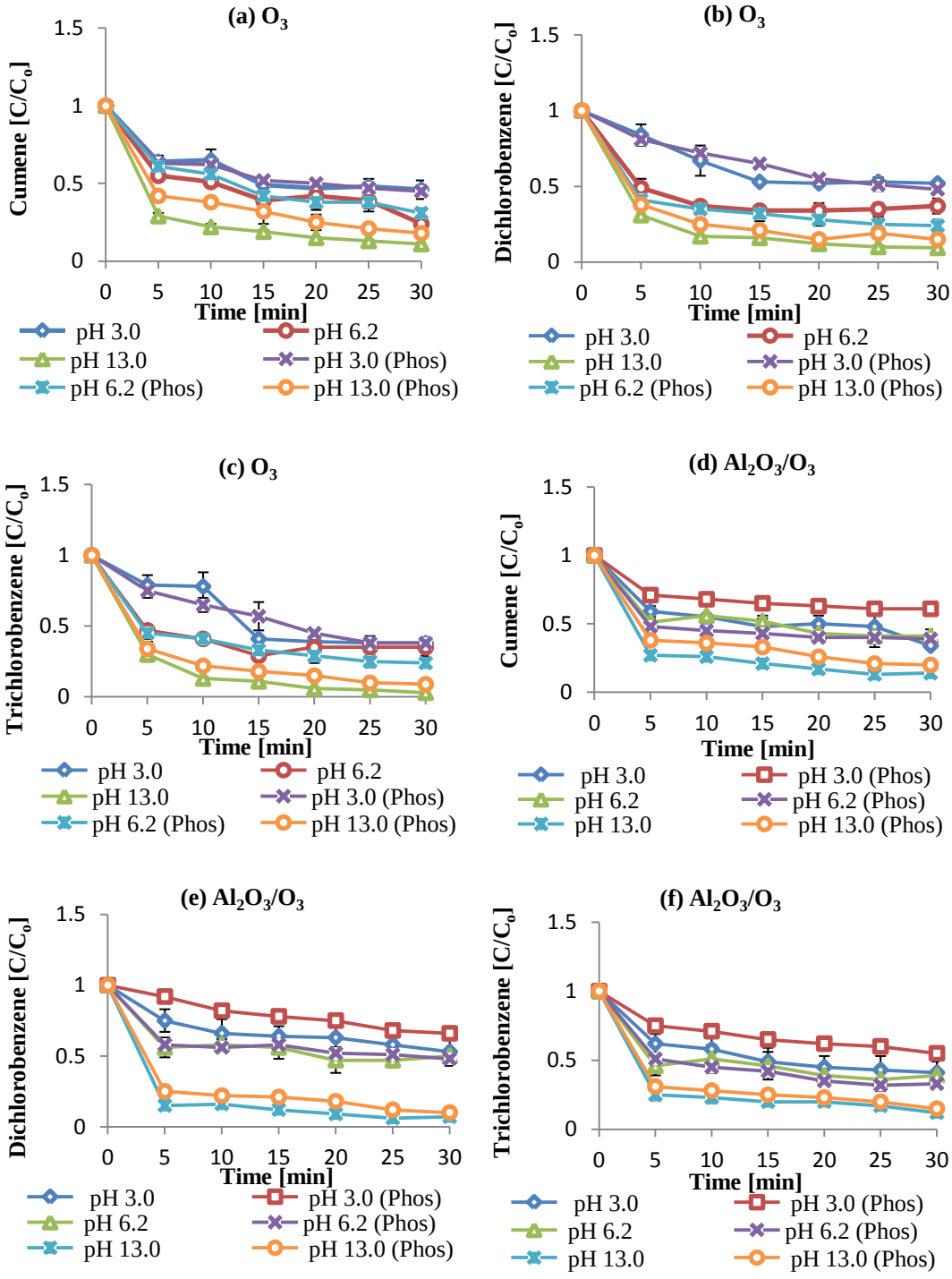

Figure 5.22: Effect of phosphates on VOCs removal by O_3 and Al_2O_3/O_3 ($C_{o\,(cum)}$ = 19.2 ± 0.5 mg/L, $C_{o\,(DCB)}$ = 3.5 ± 0.2 mg/L and $C_{o\,(TCB)}$ = 0.5 ± 0.1 mg/L; T = 20°C; pH = 3, 6 and 13; pH_{30min} = pH_0 ± 0.3; phosphates = 50 mg/L; catalyst amount = 5 g; V = 490 mL; O_3 = 0.1 mg/min).

The presence of phosphates in the water did not have a significant effect on the catalytic activity of ZSM-5 zeolites at all pH values (Fig. 5.24 and Fig. 5.25). This may be due to the lack of adsorption of phosphates on zeolites. The adsorption studies of phosphates during the catalytic ozonation process show that zeolites have very low adsorption towards phosphates at studied pH values, as shown in the Figure 5.23a, b, c.

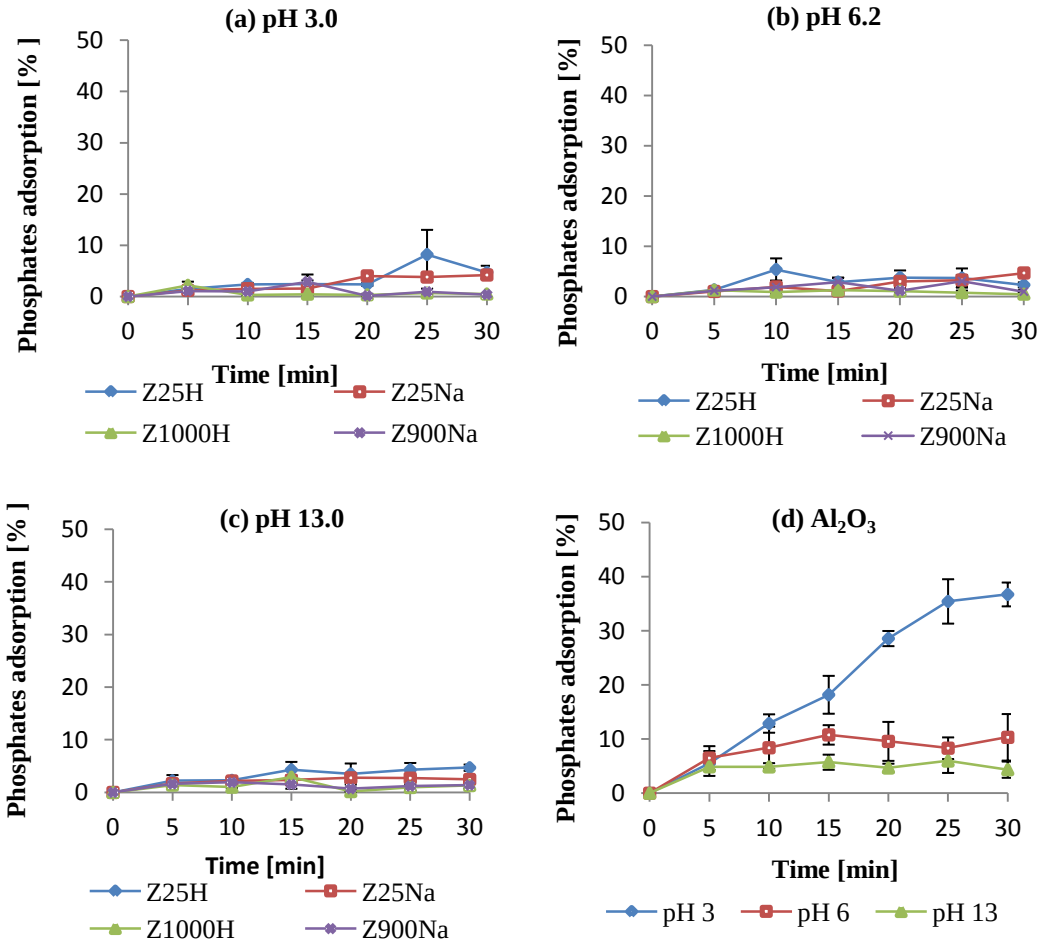

Figure 5.23: Adsorption of phosphates on ZSM-5 zeolites and alumina (T = 20^{o}C; pH = 3.0, 6.2 and 13.0; $pH_{30min} = pH_0 \pm 0.2$; phosphates = 50 mg/L; catalyst amount = 5.0 g; V = 490 mL; O_3 = 0.1 mg/min).

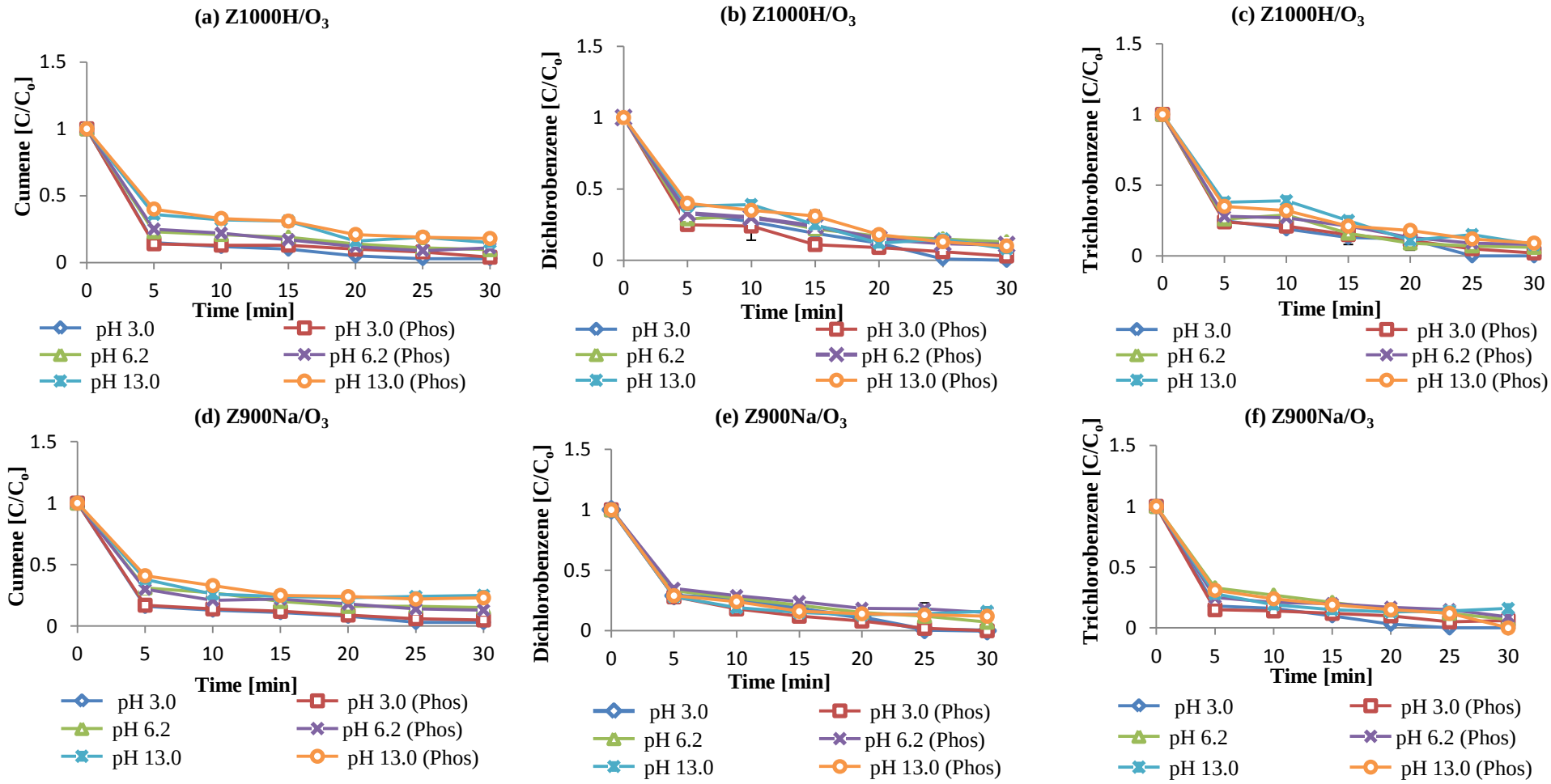

Figure 5.24: Effect of phosphates on VOCs removal by ZSM-5/O_3 ($C_{o\,(cum)}$ = 19.2 ± 0.5 mg/L, $C_{o\,(DCB)}$ = 3.5 ± 0.2 mg/L and $C_{o\,(TCB)}$ = 0.5 ± 0.1 mg/L; T = 20°C; pH = 3, 6.2 and 13; pH_{30min} = pH_0 ± 0.2; phosphates = 50 mg/L; catalyst amount = 5.0 g; V = 490 mL; O_3 = 0.1 mg/min).

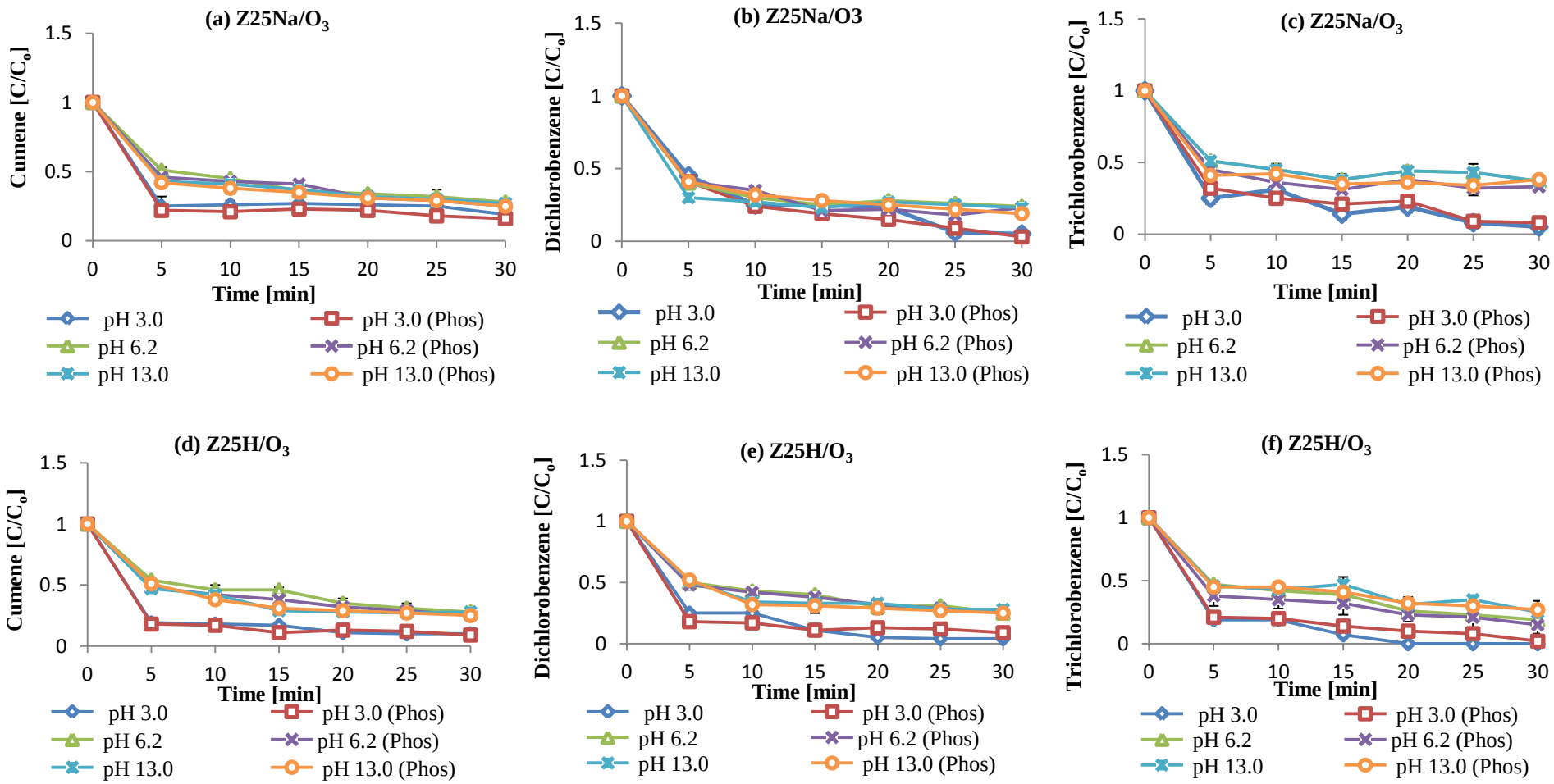

Figure 5.25: Effect of phosphates on VOCs removal by ZSM-5/O_3 ($C_{o\,(cum)}$ = 19.2 ± 0.5 mg/L, $C_{o\,(DCB)}$ = 3.5 ± 0.2 mg/L and $C_{o\,(TCB)}$ = 0.5 ± 0.1 mg/L; T = 20°C; pH = 3, 6.2 and 13; pH_{30min} = pH_0 ± 0.2; phosphates = 50 mg/L; catalyst amount = 5.0 g; V = 490 mL; O_3 = 0.1 mg/min).

5.2.2.7 Effect of humic acid

The Fig 5.26b indicates that ozonation of VOCs in the presence of alumina is reduced, for example the C/C_o ratio in the presence of HA on Al_2O_3/O_3 is 0.58 and it was 0.41 without the presence of HA. In contrast the presence of humic acid in the case of zeolites did not have any significant effect on VOCs removal (Fig. 5.26c, d, e, f). Especially, this effect is lower in the case of high silica zeolites. The adsorption results further reveal that alumina reveals high adsorption for humic acid, this may be due to the hydrophilicity of humic acid at pH 6.2, while the adsorption of HA on ZSM-5 zeolites was very low and it increases with the increase in alumina content as this increased the hydrophilicity of ZSM-5 zeolites (Fig. 5.26g). For example the adsorption was 35%, 25% and 10% on alumina, Z25 and Z1000H-Z900Na respectively.

The decrease of UV_{254} absorbance is the highest in the case of alumina as indicated in the Fig 5.26h, by the percentage decrease in UV_{254} absorbance. This suggests that adsorption is one of the important steps in the catalytic ozonation process and the slight reduction in cumene removal rate in the case of alumina is due to the adsorption of humic acid on the surface of the catalyst. However, ZSM-5/O_3 zeolites have less % UV_{254} absorbance decrease than alumina this may be due to less adsorption of HA on zeolites surface. Additionally, this effect is more pronounce in the case of Z25H and Z25Na as they have high adsorption of HA when compared with Z1000H and Z900Na. Similar results have been obtained in the case of chlorobenzenes as presented in Table 5.4.

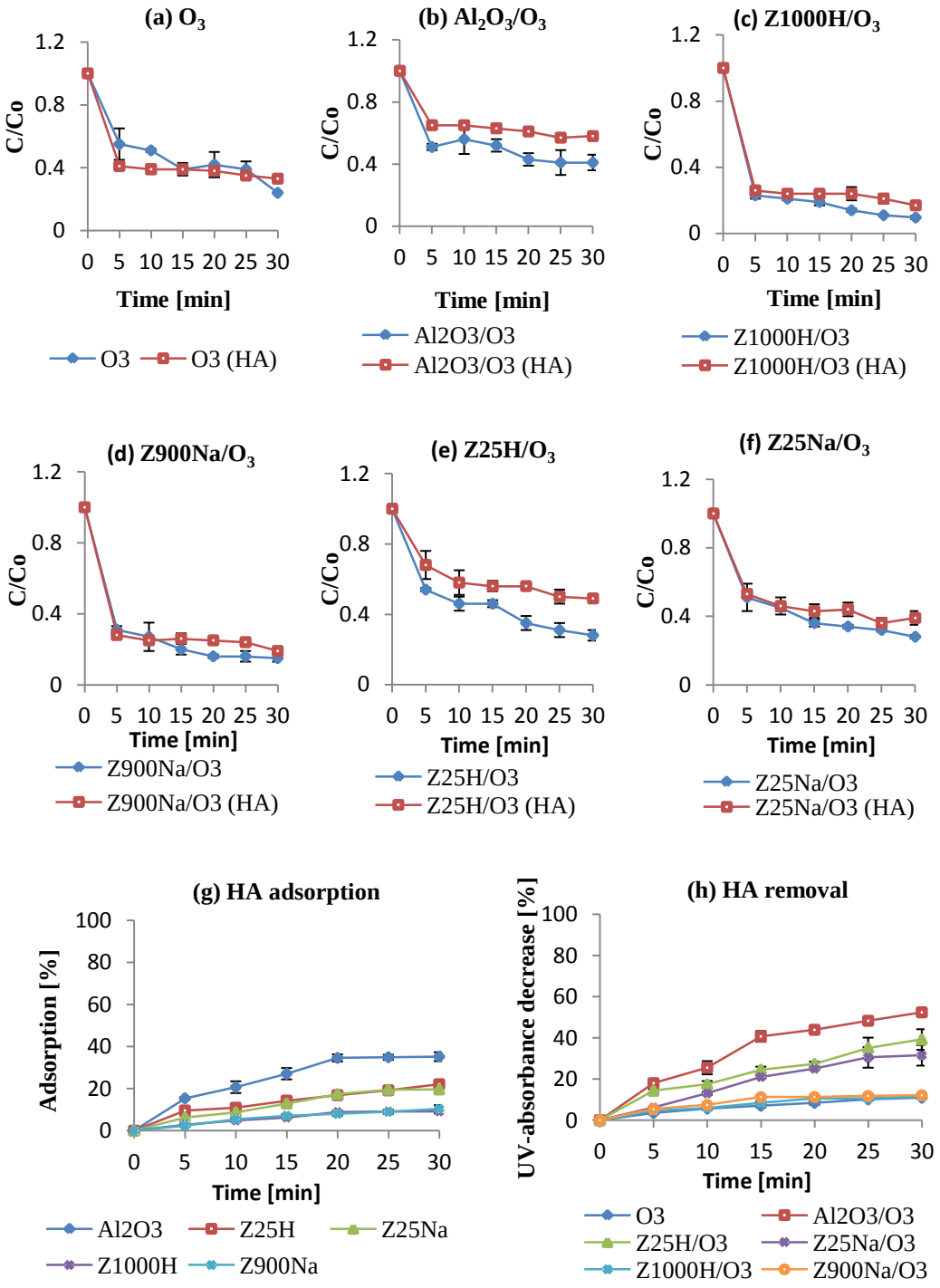

Figure 5.26: Effect of humic acid on cumene removal by O_3, Al_2O_3/O_3 and ZSM-5/O_3 ($C_{o\,(cum)}$ = 19.2 ± 0.5 mg/L; T = 20°C; pH = 6; $pH_{30min} = pH_0 \pm 0.2$; humic acid = 7 mg/L; catalyst amount, 5.0 g; V = 490 mL, O_3 = 0.1 mg/min; λ_{max} = 224 nm).

Table 5.4: Effect of humic acid on the removal of VOCs by ozonation alone and ozonation in the presence of ZSM-5 zeolites and alumina at pH 6.2 in 30 minutes (n = 3)

Sr no	Process	Amount remove (mg/L) with humic acid		Amount removed (mg/L) without humic acid	
		DCB	TCB	DCB	TCB
1	**Ozone**	1.16 ± 0.2	0.11 ± 0.09	1.57 ± 0.04	0.298 ± 0.01
2	**O_3/Z900Na**	2.48 ± 0.1	0.377 ± 0.05	2.84 ± 0.06	0.415 ± 0.04
3	**O_3/Z25Na**	1.2 ± 0.2	0.278 ± 0.06	1.70 ± 0.06	0.305 ± 0.02
4	**O_3/Z1000H**	2.88 ± 0.07	0.459 ± 0.03	3.20 ± 0.1	0.433 ± 0.01
5	**O_3/Z25H**	1.6 ± 0.2	0.328 ± 0.03	2.58 ± 0.3	0.390 ± 0.04
6	**O_3/Alumina**	0.38 ± 0.2	0.084 ± 0.04	1.23 ± 0.15	0.353 ± 0.03

5.2.2.8 Reuse performance of ZSM-5 zeolites

In this experiment Z900Na and Z1000H were selected and 5.0 g of catalyst was used in 490 mL VOCs solution that contains 19 ± 0.5 mg/L, 3.5 ± 0.2 mg/L and 0.5 ± 0.1 mg/L of cumene, dichlorobenzene and trichlorobenzene respectively. The experiments have been performed for 6 hours, it is important to note that adsorption results indicate that optimum adsorption time in the case of zeolites was 30 minutes. The experiments have been performed as described in chapter 2.

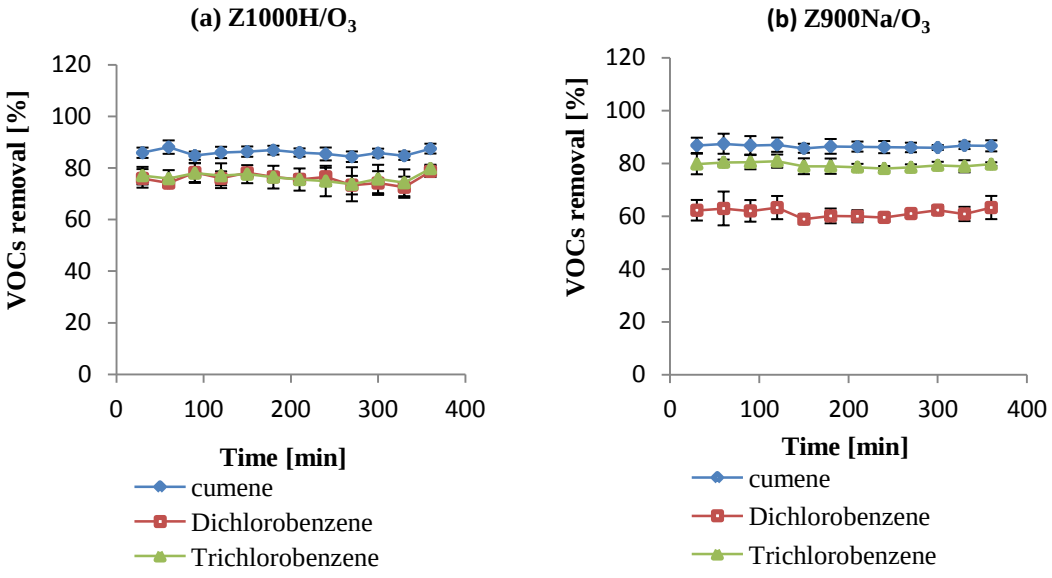

Figure 5.27: The reuse performance of Z1000H/O_3 and Z900Na/O_3 for the removal of VOCs ($C_{o\,(cum)}$ = 19.2 ± 0.5 mg/L, C_{0DCB} = 3.5 ± 0.2 mg/L and C_{0TCB} = 0.5 ± 0.1; T = 20^{o}C; pH = 6; pH_{30min} = pH_o + 0.2; catalyst amount = 5 g; V = 490 mL; O_3 = 0.1 mg/min).

The degradation of VOCs in reuse experiments is shown in Fig. 5.27. It can be seen that the catalytic activity of Z900Na and Z1000H was constant. Thus the results not only indicate the considerable potential for practical application in water treatment. Furthermore, it can be considered that the reactions of VOCs and ozone on the catalyst surface took place, as if only the adsorption of VOCs on zeolites occurs along with the

ozonation inside the solution (adsorption + ozonation), then after some time there should be decrease in overall removal since at certain stage ZSM-5 zeolites would reached to their maximum adsorption capacity.

5.2.2.9 Drinking water experiments

The Z1000H has been selected as it has the highest removal. As expected the comparison between the removal of cumene in the presence of deionised water and tap water shows similar results for ZSM-5/O_3 (Fig. 5.28) and similar results were obtained for chlorobenzenes. Since the ZSM-5 zeolites do not form hydroxyl radicals (chapter 4) and the adsorption of inorganic ions is very low as shown in section 4.5, hence the removal of VOCs is similar to deionised water. Furthermore, higher decomposition of cumene in the presence of tap water when compared with deionised water for the ozonation alone system may be due to the higher pH of tap water.

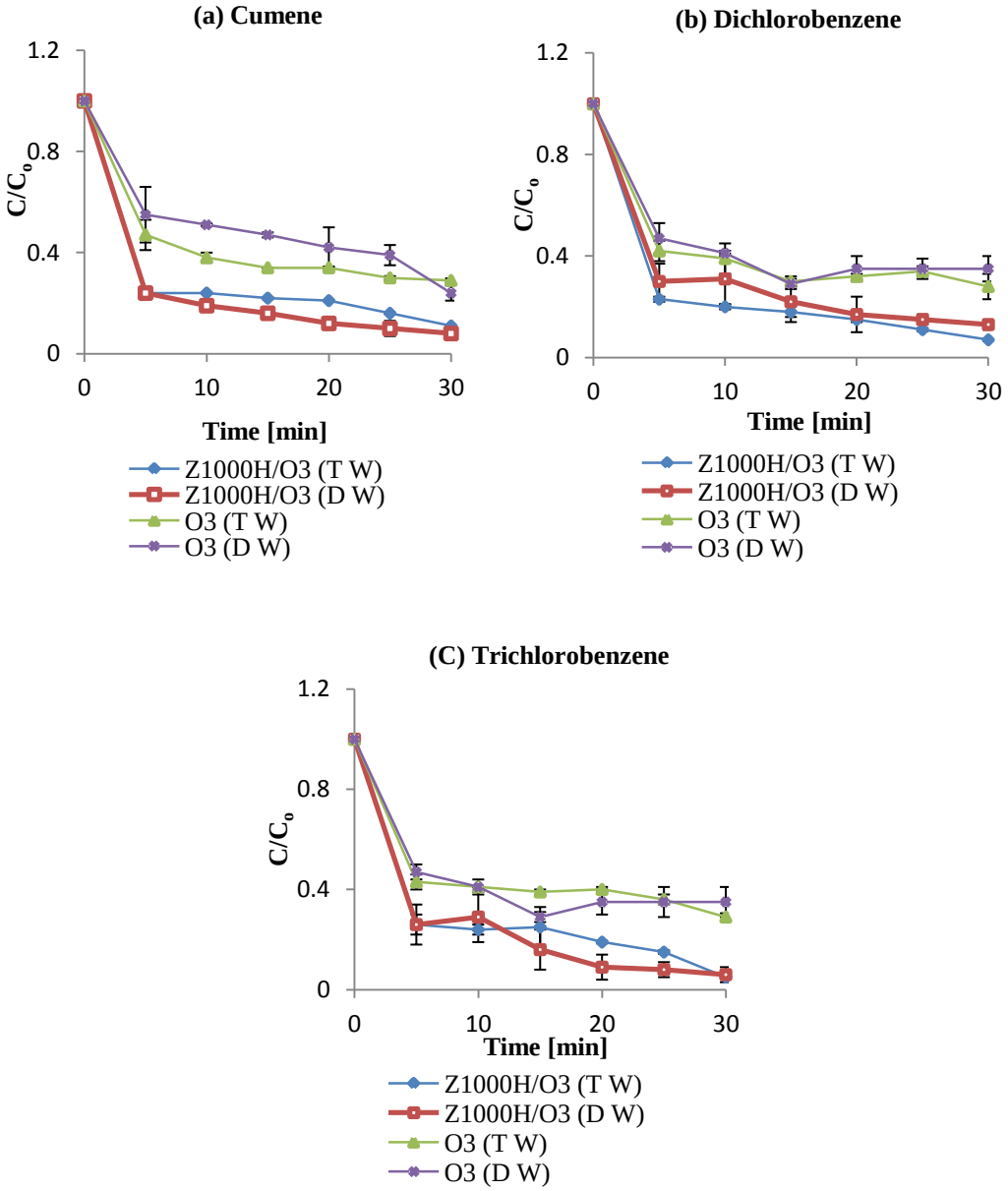

Figure 5.28: Removal of VOCs by Z1000H/O_3 in tap and deionized water ($C_{o\,(cum)}$ = 19.2 ± 0.5 mg/L, $C_{o\,(DCB)}$ = 3.5 ± 0.2 mg/L and $C_{o\,(TCB)}$ = 0.5 ± 0.1; T = 20°C; pH_{tap} = 7.3, $pH_{6.2}$; pH_{30min} = pH_o ± 0.2; catalyst amount = 5 g; V = 490 mL; O_3 = 0.1 mg/min).

5.2.3 Part 3 ozonation of acetic acid in water

This part of chapter 5 aims to show the potential of ozonation in the presence of ZSM-5 zeolites and γ-alumina for the removal of organic acids in water. The acetic acid has been selected. The result of ozonation of VOCs and ibuprofen on ZSM-5 zeolites indicates the formation of organic acids at pH 3.0. However, ozonation of pollutants in the presence of alumina does not indicate the formation of acids. Therefore, it is necessary to study the removal and adsorption of organic acids on studied catalysts. Among the ZSM-5 zeolites, Z25H has been selected for further investigations.

5.2.3.1 Adsorption of acetic acid on Al_2O_3 and ZSM-5 zeolites

The results presented in the Figure 5.29 indicate that alumina has high percentage adsorption of acetic acid when compared with Z25H. This may be due to the high hydrophilicity of alumina. The process has been found to be pH dependent and the adsorption of acetic increases with the decrease of pH. For example the % adsorption of acetic acid was 6% and 4% at pH 3.0 in 30 minutes on Al_2O_3 and Z25H respectively (Fig. 5.29) and it was reduced to 2% and 1% at pH 13.0 in 30 minutes on Al_2O_3 and Z25H respectively. It is interesting to notice here that although acetic acid is ionized at basic pH (pka, 4.7) and it should have high adsorption on alumina at basic pH due to the high hydrophilicity of alumina. Additionally, the surface of alumina is positively charged at this pH and acetic acid will be negatively charged therefore the interactions between the opposite charges lead to the higher adsorption of acetic acid on alumina. However, the adsorption was found to decrease with the increase in pH. This may be because with the increase in pH the amount of hydroxide ions increases and since hydroxide ions are harder base than acetate ions therefore they suppressed the adsorption of acetate ions on alumina. Additionally, the adsorption of organic acids on alumina occurs through the ligand exchange reaction and high exchange is more favourable in the protonated form of acetic

acid. The more adsorption of acetic acid on Z25H at pH 3.0 (Fig. 5.29b) may be due to the hydrophobicity of Z25H, as at this pH acetic acid will be unionized. Alternatively, the less adsorption of acetic acid on alumina at pH 13.0 may be explained on the bases of the charges on the catalyst and acetic acid. The acetic acid will be negatively charged at pH 13.0 (see part 1 of chapter 5) and due to the forces of repulsion between the catalyst and acetic acid its adsorption decreased.

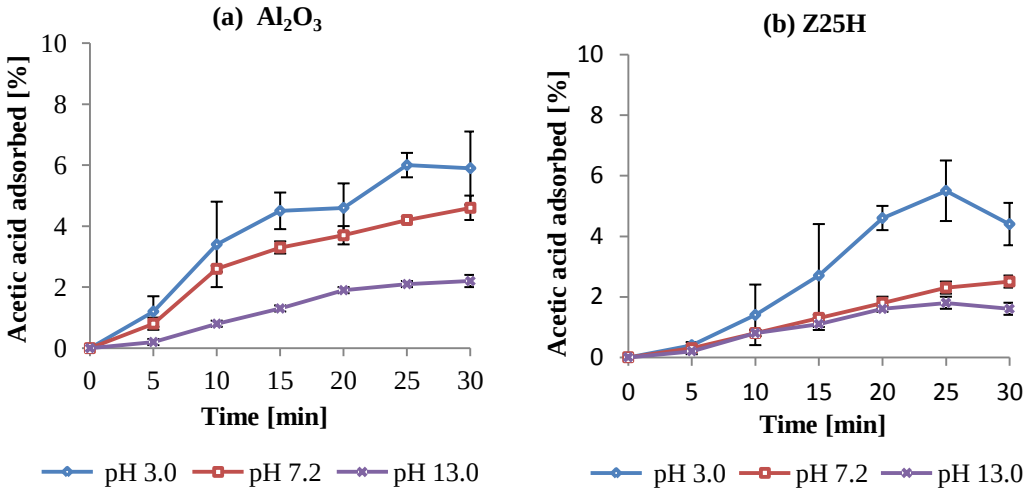

Figure 5.29: Removal of acetic acid by adsorption ($C_{o\,(Ace)}$ = 15 mg/L; T = 20°C; pH, 3.0, 7.2 and 13.0; adsorbent dose = 5.0 g; V = 490 mL).

5.2.3.2 The catalytic ozonation and the effect of pH

The results show that percentage removal of acetic acid increases with an increase in pH in the case of ozonation alone and ozonation in the presence of alumina (Fig. 5.30). The highest removal has been observed at pH 7.2 (Fig. 5.30b). For example, 19% of acetic acid was removed in 30 minutes at pH 7.2 when ozonation is performed in the presence of alumina (Fig. 5.30b). It has been reported that the activity of alumina was the highest near its point of zero charge [18-20]. Additionally, it has been reported in the current research

that ozonation in the presence of alumina promotes aqueous ozone decay leading to the production of active oxygen species (chapter. 4) and its activity increases with the increase in pH. It was observed that alumina did not show any catalytic activity at pH 13.0 (Fig. 5.30c). This is due to the change in surface properties of alumina at this pH [132].

The comparison of adsorption results of acetic acid on Al_2O_3 and catalytic ozonation revealed that the catalytic activity increases with the decrease in the adsorption of acetic acid. This may be because the acetic acid adsorbed through ligand exchange reaction [148] and poisons the active sites of alumina. Therefore, high adsorption leads to the decrease in catalytic activity.

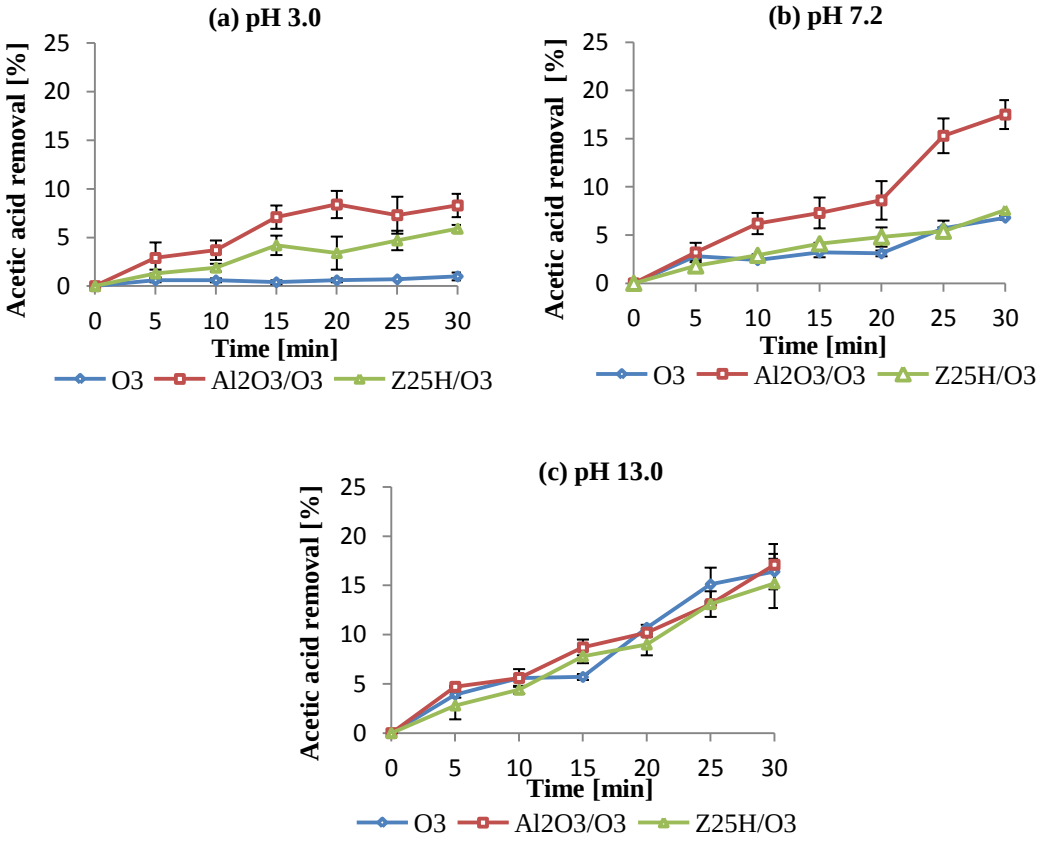

Figure 5.30: Removal of acetic acid by ozonation alone and catalytic ozonation ($C_{o\,(ace)}$ = 15 mg/L; O_3 = 0.5 mg/min; T = 20°C; pH = 3.0, 7.2 and 13.0; Catalyst dose = 5.0 g; V = 490 mL).

The results further reveal that Z25H does not show any catalytic activity for the removal of acetic acid when compared with ozonation alone. The higher percentage removal at pH 3.0 (Fig. 5.30a) when compared with ozonation alone may be due to the high adsorption of acetic acid on Z25H at pH 3.0. For example, the removal of acetic acid in the case of $Z25H/O_3$ was 5 % at pH 3.0 in 30 minutes and adsorption results indicate the similar percentage removal (Fig. 5.30). These results further support our hypothesis that ZSM-5 zeolites do not decompose aqueous ozone leading to the formation of active oxygen species (Chapter. 4) and they mainly operate through the adsorption mechanism, in which both the pollutant and ozone adsorb on the surface of catalysts and their reactions on the surface. Since acetic acid is highly resistant to direct ozone attack therefore the reactions of direct ozone with adsorbed acetic acid are potentially being very slow.

5.2.3.3 Aqueous ozone decay

The results of aqueous ozone decay during the ozonation alone and ozonation of acetic acid in the presence of Z25H and alumina show that alumina has high ozone decay when compared with ozonation alone and Z25H at pH 3.0 and 7.2 (Fig. 5.31a, b). The pH effect indicates that ozone decay increases with the increase of pH and it shows some correlation with the acetic acid removal studies in ozonation alone and ozonation in the presence of alumina. The low aqueous ozone decay at pH 3.0 (Fig. 5.31a) may be due to the less catalytic activity of alumina at acidic pH as the concentration of reactive oxygen species has been found to be low at this pH (chapter 4). Furthermore, similar trends have been obtained in the case of ibuprofen and VOCs studies. An alternative explanation could be that the high adsorption of acetic acid at pH 3.0 may poison the active sites of catalysts (surface hydroxyl groups). Therefore, less aqueous ozone decay was observed at pH 3.0 in the case of ozonation of acetic acid in the presence of alumina. The Z25H also show some ozone decay when compared with ozonation alone this may be due to the adsorption of

ozone on ZSM-5 zeolites since the ZSM-5 zeolites can adsorb and stabilize the aqueous ozone [22].

The ozone decay patterns at pH 13.0 are found to be similar for ozonation alone and ozonation in the presence of Z25H and alumina (Fig. 5.31c). It is reasonable that this effect is not observed at pH 13.0, where the pH is much higher than the pH_{PZC} of alumina, and where the surface would be negatively charged. At this pH the surfaces of catalysts are essentially covered with hydroxide ions and ozone decay patterns are found to be similar to the ozonation alone.

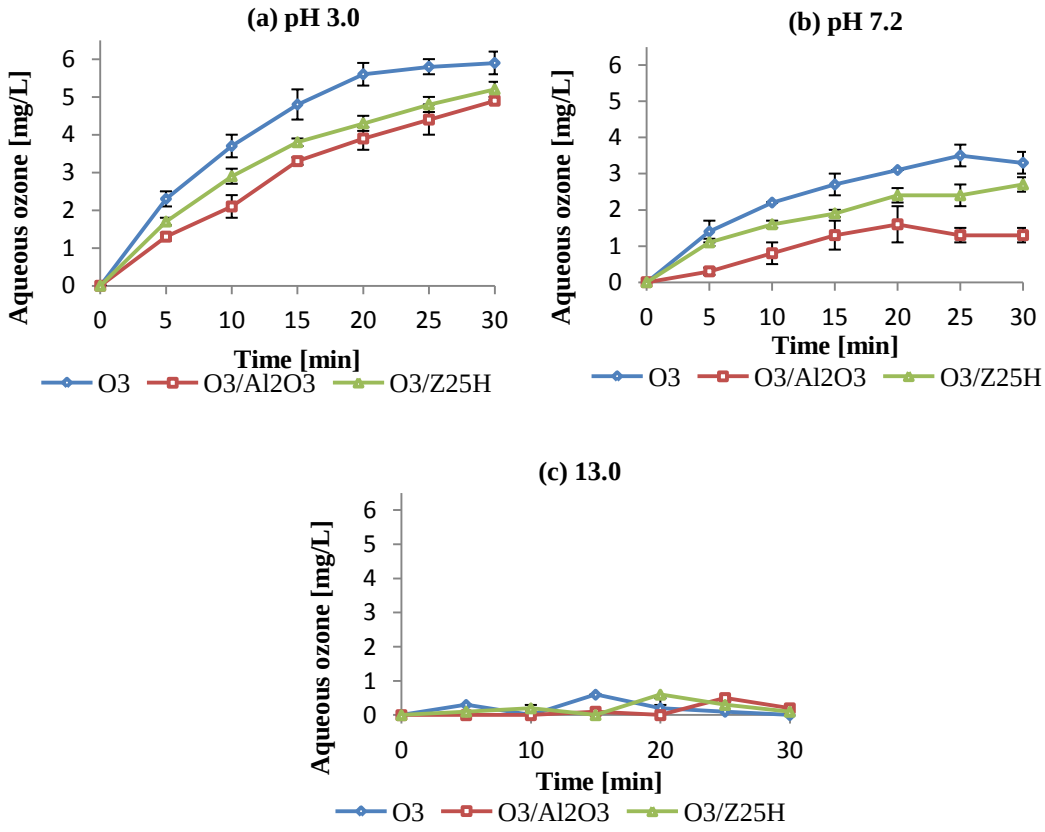

Figure 5.31: Aqueous ozone decay during the in the presence ozonation alone and catalytic ozonation of acetic acid ($C_{o\ (ace)}$ = 15 mg/L; O_3 = 0.5 mg/min; T = 20°C; pH = 3.0, 7.2 and 13.0; Catalyst dose = 5.0 g; V = 490 mL).

5.4 Suggested mechanisms

The mechanisms of ozonation in the presence of alumina and ZSM-5 zeolites have already been suggested in chapter 4. In this chapter the presented mechanisms may help to further understand the catalytic ozonation processes in the presence of some pollutants.

5.4.1 Suggested mechanism of catalytic ozonation on alumina

The mechanism of ozonation in the presence of alumina has been proposed in chapter 4; it suggested that alumina promotes aqueous ozone decomposition leading to the formation of active oxygen species such as hydroxyl radicals, hydrogen peroxide and superoxide radical. The TBA effect experiments presented in chapter 5 further support this hypothesis. Similar mechanism has been proposed by Ernst et al [17], however it was reported that surface reactions are not vital in catalytic ozonation process on alumina. The mechanism presented in chapter 4 was inconclusive in terms of highlighting the importance of surface reactions and adsorption in catalytic ozonation on alumina. The results presented in chapter 5 clearly indicate that adsorption of pollutants is vital in the catalytic ozonation process on alumina. For example, in contrast to ibuprofen the VOCs adsorb least and therefore alumina is not effective for their removal in water. It has also been reported by some researchers that adsorption of pollutants is vital in the catalytic ozonation process on alumina [3, 16].

The mechanisms of catalytic ozonation of pollutants on alumina can be rationalized to some extent on the basis of the results presented in chapter 5. The interaction of aqueous ozone with the surface hydroxyl groups of alumina results in the formation of hydroxyl radicals as confirmed in chapter 4. Furthermore, the result of phosphates and TBA effect presented in chapter 5 also supports this hypothesis. The formed hydroxyl radicals may

adsorb and desorbed quickly and reacts with the adsorbed pollutants (P) on the surface of alumina. Finally, the catalyst surface is regenerated by water molecules.

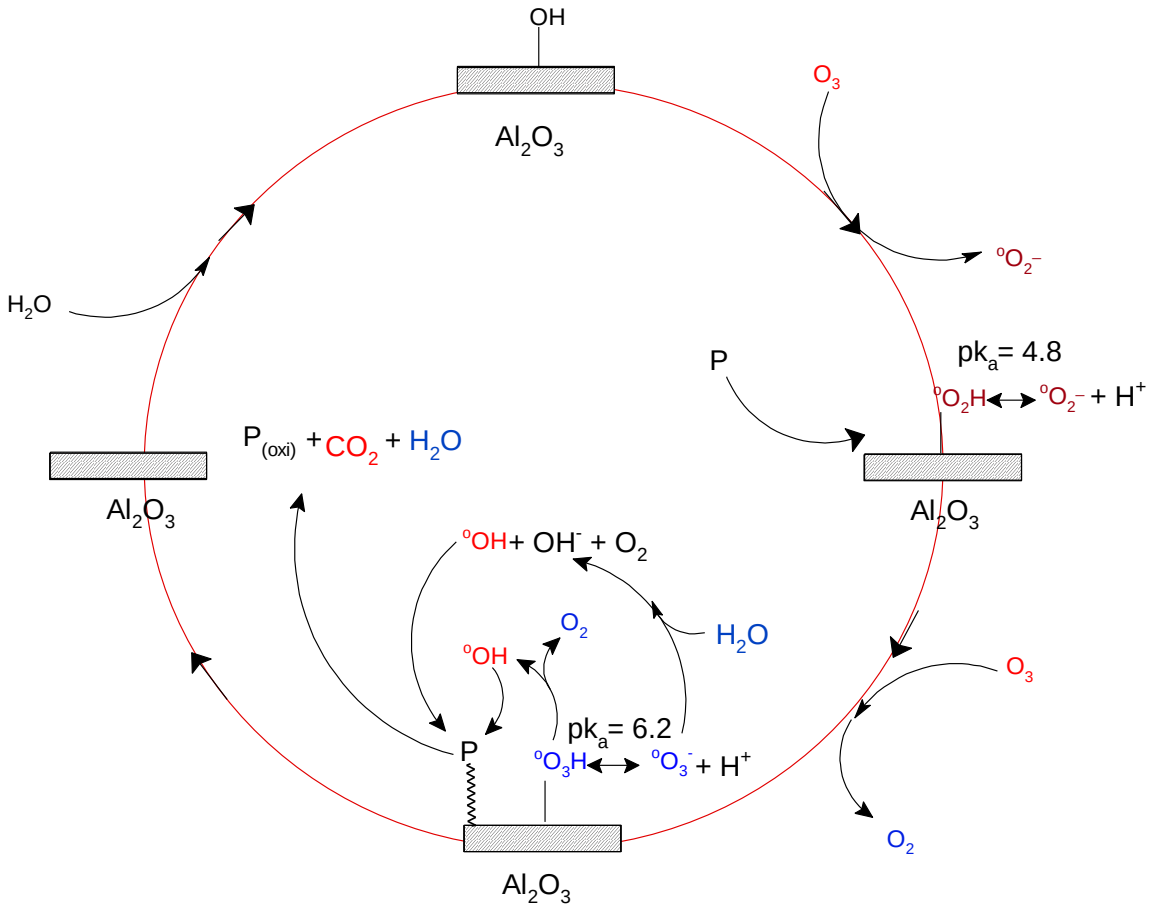

Figure 5.32: Proposed mechanism of catalytic ozonation on alumina (P = Pollutants).

5.4.2 Suggested mechanism of catalytic ozonation on ZSM-5 zeolites

The results presented in the chapter 5 indicate that catalytic ozonation on ZSM-5 zeolites is a simple process in which both the pollutants and ozone adsorbed on the surface of zeolites and their reactions resulted in the degradation of pollutants leading to the formation of oxidation by-products such as organic acids (Fig. 5.33). The mechanism presented in chapter 4 clearly suggested that zeolites do not promote the formation of hydroxyl radicals; the TBA results presented in chapter 5 further support this hypothesis.

Within the family of zeolites the silica to alumina ratio plays a significant role as clearly suggested by the adsorption and catalytic ozonation of VOCs and ibuprofen. The results of long term activity of pollutants further suggest that zeolites do catalyse the decomposition of pollutants and surface reactions are important in the catalytic ozonation on zeolites. Corlone et al [212] studied the removal of ethanol on zeolites and was concluded that due to the speed of the reaction there was no time for reactants to sorb into the pores and catalysis was on the surface of zeolites. This further supports our hypothesis that surface reactions are important in the catalytic ozonation process and adsorption of pollutants pays a significant role in the rate of reactions.

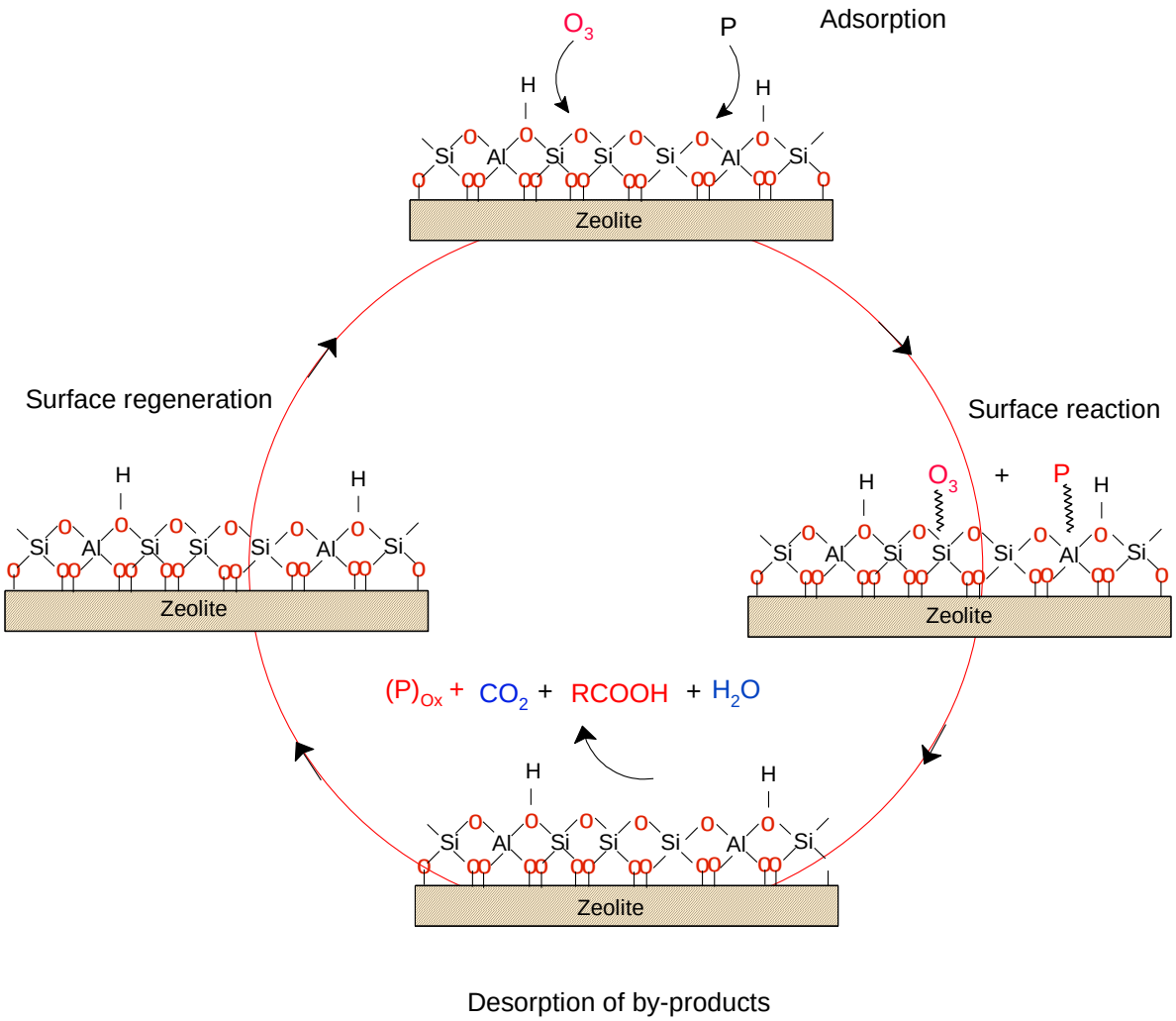

Figure 5.33: Proposed mechanism of catalytic ozonation on ZSM-5 zeolites (P = Pollutants).

5.5 Summary of results

The results presented in chapter 5 aims to show the potential of ozonation in the presence of ZSM-5 zeolites and alumina for the removal of organic pollutants in water. Both the H-ZSM-5 and Na-ZSM-5 forms with different SiO_2/Al_2O_3 ratios and counter ions (Z1000H:SiO_2/Al_2O_3 = 1000, Z900Na:SiO_2/Al_2O_3 = 900, Z25H:SiO_2/Al_2O_3 = 25 and Z25Na:SiO_2/Al_2O_3 = 25), and γ-alumina have been used. Ibuprofen and volatile organic chemicals (VOCs) such as cumene, 1,2-dichlorobenzene and 1,2,4-trichlorobenzene have been selected as target pollutants. Additionally, the ozonation experiments have been performed to study the removal of organic acids, since they have been found as ozonation by-products. For this purpose acetic acid was selected. Furthermore, the effect of parameters such as pH, adsorption, inorganic ions, hydroxyl radical scavengers and effect of natural organic matter on the degradation of pollutants have been investigated. The results show that catalytic ozonation with zeolites could substantially enhance the removal of VOCs and ibuprofen when compared with ozonation alone. The adsorption results revealed that zeolites with high SiO_2/Al_2O_3 ratios had a high adsorption capacity towards VOCs and zeolites with low SiO_2/Al_2O_3 ratios had a high adsorption capacity towards ibuprofen in its ionised form. Furthermore, the adsorption of acetic acid was found to be very low on zeolites. Within the family of zeolites the catalytic activity was found to be significantly higher with the increase in adsorption of contaminants. The activity depends on silica to alumina ratios and insensitive to the nature of counter ions. In contrast to zeolites, the alumina has been found to be more active in the removal of ibuprofen and acetic acid in their ionised forms. However, alumina was not effective for the removal of VOCs. The adsorption experiments revealed that alumina had the lowest adsorption capacity towards VOCs and the highest for ibuprofen and acetic acid when compared with zeolites. The catalytic processes have been found to be pH dependent. The catalytic

activity of alumina increases with the increase in pH. In contrast, the catalytic efficiency of zeolites is the highest at acidic pH. The presence of hydroxyl radical scavengers, phosphates and humic acid did not have a significant effect on the removal of contaminants on ZSM-5 zeolites. However, in the case of ozonation in the presence of alumina a significant reduction in the ozonation efficiency was observed. It is suggested that adsorption of pollutants on the surface of the catalyst plays a critical role in the efficiency of the catalyst to effectively remove pollutants. The mechanism of catalytic ozonation in the presence of alumina follows a radical pathway. On the other hand, ZSM-5 zeolites degrade pollutants by direct reaction of molecular ozone with pollutants on their surface.

5.6 Conclusions

1. ZSM-5 zeolites are effective especially at acidic pH in the catalytic ozonation of VOCs and ibuprofen; however they are ineffective in the removal of acetic acid. Their activity depends on their ability to adsorb pollutants and this depends upon their silica to alumina ratios and hydrophobic–hydrophilic nature of pollutants. The catalytic effect in ZSM-5 zeolites is due to their ability to promote surface reactions between the adsorbed ozone and pollutants. The presence of phosphates and humic acid has found to have no effect on the catalytic activity of zeolites, since they do not adsorb on the zeolites.

2. The alumina does promote the decomposition of ozone leading to the formation of hydroxyl radicals. The adsorption of pollutants plays an important role in the catalytic ozonation on alumina and therefore alumina is a good catalyst for ibuprofen removal and has been found to be ineffective in the removal of non-polar compounds. The surface charge on alumina and pollutants play a significant role in the adsorption process. The catalytic activity of alumina is affected in the presence of phosphates and humic acids, as they adsorb on alumina and block the active sites of catalyst

General conclusions and recommendations for future work

In this work mechanism of catalytic ozonation on ZSM-5 zeolites and alumina has been investigated. Furthermore, application of zeolites and alumina catalysts in the process of ozonation of ibuprofen, VOCs and acetic acid in pure water was examined using a laboratory-scale reaction system over a range of operating conditions. The effect of variables such as pH of the solution, the presence of radical scavenger, effect of phosphates, adsorption on catalyst, catalyst dose and presence of humic acid were investigated. The long-term efficiency of catalysts and their catalytic efficiency in drinking water have also been studied.

In general, based on the results it is concluded that aqueous ozone decay in the presence of alumina occurs by a radical mechanism, involving reactive oxygen species such as hydroxyl radicals, hydrogen peroxide and superoxide anion radical. It was found that the catalytic activity of alumina was mainly related to its ability to decompose aqueous ozone into ROS, which was notably influenced by the pH. The reaction between the aqueous ozone and surface hydroxyl groups results in the ozone decomposition (which are most reactive at pH close to the pH_{PZC}).

The ZSM-5 zeolites catalyse the removal of pollutants, however they do not operate through radical mechanism as it is clear from the results presented in chapter 4. The activity of the zeolites arises through their ability to adsorb ozone and pollutants and promote surface reactions between the adsorbed molecules. It has been observed that the activity of the zeolites is independent of the nature of counter ions. The catalytic activity of zeolites was the highest at acidic pH values and it decreases with the increase of pH.

The adsorption of the pollutants plays a significant role in the catalytic ozonation process on zeolites and alumina, supporting this view the alumina was not found to be effective for VOCs removal, however it effectively catalyses the removal of ibuprofen. Therefore, it is concluded that surface reactions play a significant role in the catalytic ozonation process.

The presence of phosphates, TBA and humic acid did not have a significant effect on the catalytic ozonation process in the presence of ZSM-5 zeolites. However, the activity of alumina was greatly reduced. The zeolites show excellent reuse performance in the presence of deionised and drinking water, however the activity of alumina was gradually reduced in the presence of drinking water.

Despite the increasing research efforts in the field of catalytic ozonation that is mainly focused on the introduction of new catalysts the mechanisms are still largely known. It is very important to have an understanding of the mechanisms of catalytic ozonation in order to apply this technique in water treatment at an industrial scale. The encouraging results obtained from current research work will help to understand the catalytic ozonation process in two different types of catalysts (zeolites and alumina). It has been confirmed that alumina operates through an advanced oxidation process. Furthermore, the formation of reactive oxygen species such as superoxide ion radical and hydrogen peroxide has been confirmed for the first time in ozonation in the presence of alumina. Additionally, a direct proof of the formation of hydroxyl radicals has been obtained by using coumarin as probe molecule. In this research work a detailed investigation has been done in order to understand the processes occurring in the presence of ZSM-5 zeolites, it has been found that zeolites do not promote the formation of hydroxyl radicals.

The work on different kind of pollutants at varying conditions further helps to understand that why catalysts are effective for some pollutants and under certain conditions.

The advanced oxidation catalysts may not be very effective in the water containing high concentrations of inorganic ions and natural organic matter; therefore ZSM-5 zeolites can be good catalysts in such environmental conditions as indicated by the results presented in the current study. However, zeolites do not promote the hydroxyl radicals therefore they are not effective for the removal of highly ozone resistant pollutants (organic acids). It is recommended that by using a combination of ZSM-5 zeolites and alumina better results can be obtained. In future more work is required for feasible implementation to industrial scale. In this regard following recommendations for further work are suggested.

- Since adsorption of pollutants plays important role in the catalytic ozonation process, therefore, a combination of both zeolites and alumina can be tested to remove pollutants from drinking water.
- Since the mechanisms of other catalysts are largely unknow as indicated in literature review, therefore the mechanisms of other catalysts can be assessed by using spectroscopic probes (coumarin, amplex red and NBD-Cl).
- Since the reaction by-products may decompose aqueous ozone, leading to the formation of ROS, therefore identification and evaluation of reaction intermediates are important to further understanding of the process.
- For realistic applications of catalytic ozonation, in addition to a single target pollutant, mixtures of micropollutants can be tested.
- The catalyst effectiveness must be assessed by using TOC analyser in order to investigate the total mineralization of pollutants.

- To investigate the mass transfer limitations it is proposed to run a continuous catalytic ozonation system.

REFERENCES

References

[1] B. Kasprzyk-Hordern, M. Ziolek, J. Nawrocki, Applied Catalysis B: Environmental, 46 (2003) 639-669.

[2] P. Pocostales, P. Alvarez, F.J. Beltran, Chemical Engineering Journal, 168 (2011) 1289-1295.

[3] B. Kasprzyk-Hordern, Raczyk-Stanisa, U. Awiak, J. Aswietlik, J. Nawrocki, Applied Catalysis B: Environmental, 62 (2006) 345-358.

[4] B. Kasprzyk-Hordern, P. Andrzejewski, A. Dalbrowska, K. Czaczyk, J. Nawrocki, Applied Catalysis B: Environmental, 51 (2004) 51-66.

[5] Y. Yang, J. Ma, Q. Qin, X. Zhai, Journal of Molecular Catalysis A: Chemical, 267 (2007) 41-48.

[6] F.J. Beltran, F.J. Rivas, R. Montero-de-Espinosa, Applied Catalysis B: Environmental, 39 (2002) 221-231.

[7] T. Zhang, C. Li, J. Ma, H. Tian, Z. Qiang, Applied Catalysis B: Environmental, 82 (2008) 131-137.

[8] Y. Dong, H. Yang, K. He, X. Wu, A. Zhang, Applied Catalysis B: Environmental, 82 (2008) 163-168.

[9] P.C.C. Faria, J.J.M. Orfao, M.F.R. Pereira, Applied Catalysis B: Environmental, 79 (2008) 237-243.

[10] P.C.C. Faria, J.J.M. Orfao, M.F.R. Pereira, Applied Catalysis B: Environmental, 83 (2008) 150-159.

[11] H. Fujita, J. Izumi, M. Sagehashi, T. Fujii, A. Sakoda, Water Research, 38 (2004) 166-172.

[12] J. Nawrocki, B. Kasprzyk-Hordern, Applied Catalysis B: Environmental, 99 (2010) 27-42.

[13] C. Cooper, R. Burch, Water Research, 33 (1999) 3695-3700.

[14] F. Qi, B. Xu, Z. Chen, J. Ma, Water Environment Research, 81 (2009) 592-597.

[15] B. Kasprzyk, J. Nawrocki, Ozone: Science & Engineering, 24 (2002) 63-68.

[16] C.A. Guzman-Perez, J. Soltan, J. Robertson, Journal of Environmental Science and Health, Part B, 47 (2012) 544-552.

[17] M. Ernst, F. Lurot, J.-C. Schrotter, Applied Catalysis B: Environmental, 47 (2004) 15-25.

[18] L.Chen, F.Qi, B.Xu, Z.Xu, J.shen, K.Li, Water Science and Technology, 6 (2006) 43-51.
[19] F. Qi, B. Xu, Z. Chen, J. Ma, D. Sun, L. Zhang, Separation and Purification Technology, 66 (2009) 405-410.
[20] F. Qi, Z. Chen, B. Xu, J. Shen, J. Ma, C. Joll, A. Heitz, Applied Catalysis B: Environmental, 84 (2008) 684-690.
[21] J. Lin, A. Kawai, T. Nakajima, Applied Catalysis B: Environmental, 39 (2002) 157-165.
[22] H. Fujita, J. Izumi, M. Sagehashi, T. Fujii, A. Sakoda, Water Research, 38 (2004) 159-165.
[23] N.A.S. Amin, J. Akhtar, H.K. Rai, l, Chemical Engineering Journal, 158 (2010) 520-527.
[24] V.S.R.R. Pullabhotla, C. Southway, S.B. Jonnalagadda, Catalysis Communications, 9 (2008) 1902-1912.
[25] Y. Takeuchi, H. lwamoto, N. Miyata, S. Asano, M. Harada, Separations Technology, 5 (1995) 23-34.
[26] H. Valdes, V.J. Farfan, J.A. Manoli, C.A. Zaror, Journal of Hazardous Materials, 165 (2009) 915-922.
[27] H. Valdes, R.F. Tardon, C.A. Zaror, Environmental Technology, (2012) 1-9.
[28] M.B.Rubin, The history of ozone: the schonbein period, 1839-1869, Bull. Hist. Chem, (2001).
[29] B. Brunekreef, S.T. Holgate, Air pollution and health, The Lancet, 360 (2002) 1233-1242.
[30] B.J. Finlayson-Pitts, J.N. Pitts, Science, 276 (1997) 1045-1051.
[31] G. Tegge, Ullmann's Encylopedia of industrial chemistry 5th edition, Starch - Stärke, 43 (1991) 79-79.
[32] T.A. Ternes, J. Stüber, N. Herrmann, D. McDowell, A. Ried, M. Kampmann, B. Teiser, Water Research, 37 (2003) 1976-1982.
[33] D.C. McDowell, M.M. Huber, M. Wagner, U. von Gunten, T.A. Ternes, Environmental Science & Technology, 39 (2005) 8014-8022.
[34] K. Urashima, C. Jen-Shih, Dielectrics and Electrical Insulation, IEEE Transactions on, 7 (2000) 602-614.

[35] B. Langlais, D.A. Reckhow, D.R. Brink, Ozone in water treatment applications and engineering, in, Lewis Publishers, (1991).
[36] J. Staehelin, J. Hoigne, Environmental Science & Technology, 16 (1982) 676-681.
[37] J. Hoigne, H. Bader, Water Research, 10 (1976) 377-386.
[38] J. Hoigne, H. Bader, Water Research, 17 (1983) 173-183.
[39] F.J. Beltran, Ozone Reaction Kinetics for Water and Waste water systems, Lewis Publishers, 2004.
[40] R.G. Rice, Ozone Science and Engineering, 18 (1996) 477-515.
[41] W.H. Glaze, Environmental Health Perspectives, 69 (1986) 151-157.
[42] Alberto D, A.G. Zaikov, Reactions and properties of Monomers and Polymers, Nova Science Publishers, New York, 2006.
[43] M.B. Rubin, Helvetica Chimica Acta, 86 (2003) 930-940.
[44] C. Gottschalk, J.A. Libra, A. Saupe, Ozonation of water and waste water, Wiley-VCH, Weinheim, (2000).
[45] J. Staehelin, J. Hoigne, Environmental Science & Technology, 19 (1985) 1206-1213.
[46] V. Camel, A. Bermond, Water Research, 32 (1998) 3208-3222.
[47] V.G. Urs, Water Research, 37 (2003) 1469-1487.
[48] S. Echigo, H. Yamada, S. Matsui, S. Kawanishi, K. Shishida, Water Science and Technology, 34 (1996) 81-88.
[49] A. Rathi, H.K. sharma, Journal of Hazardous Materials, 102 (2003) 231-241.
[50] T.K. lau, W. Chu, N. Graham, Water Research, (2007) 765-774.
[51] E.J. Rosenfeldt, K.G. Linden, S. Canonica, U. von Gunten, Water Research, 40 (2006) 3695-3704.
[52] R. Sauleda, E. Brillas, Applied Catalysis B: Environmental, 29 (2001) 135-143.
[53] E. Piera, J.C. Calpe, E. Brillas, X. Domenech, J. Peral, Applied Catalysis B: Environmental, 27 (2000) 169-177.
[54] R. Gracia, J.L. Aragues, J.L. Ovellerio, Ozone: Science & Engineering, 18 (1996) 195-208.
[55] F.J. Beltrain, F.J. Rivas, R.Montero-de-Espinosa, 39 (2005) 3553-3564.
[56] D.S. Pines, D.A. Reckhow, Environmental Science & Technology, 36 (2002) 4046-4051.
[57] R. Gracia, J.L. Aragues, J.L.O. S. Cortes, 12th World Congress of the Internatiuonal Ozone Association, (1995) 75.

[58] S. Cortes, J. Sarasa, P. Ormad, R. Gracia, J.L. Ovelleiro, Ozone: Science and Engineering, 22 (2000) 415-426.
[59] Y. Pli, M. Ernst, J.-C.H. Schrotter, Ozone: Science & Engineering, 25 (2003) 393-397.
[60] J. Rivas, E. Rodriguez, F.J. Beltran, J.F. Garcia-Araya, P. Alvarez, Journal of Envirinmental Science and Health B, 36 (2001) 317-330.
[61] M.M. Ksenofontova, A.N. Mitrofanova, N.A. Mamleeva, A.N. Pryakhin, V.V. Lunin, Ozone: Science & Engineering, 25 (2003) 505-512.
[62] C.H.H. Wu, C.H.-Y. Kuo, C.H.L. Chang, Journal of Hazardous Materials, 153 (2008) 1052-1058.
[63] M. Matheswaran, S. Balaji, S.J. Chung, I.S. Moon, 8 (2007) 1497-1501.
[64] R. Munter, M. Tirapido, Y.V. Veressinina, proceedings of Estonian Academy of Science Chemistry, 54 (2005) 16-23.
[65] R. Andreozzi, M.S. Lo casale, R. Marotta, G. Pinto, A. Pollio, Water Research, 34 (2000) 4419-4429.
[66] Z. Yunrui, Z. Wanpeng, L. Fudong, W. Jianbing, Y. Shaoxia, Chemosphere, 66 (2007) 145-150.
[67] C.H. Ni, J.N. Chen, Water Science and Technology, 43 (2001) 213-220.
[68] F.J. Beltran, F.J. Rivas, R. Montero-de-Espinosa, Industrial & Engineering Chemistry Research, 42 (2003) 3210-3217.
[69] J. Ma, N.J.D. Grahm, Water Research, 33 (1999) 785-793.
[70] M. Sanchez-Polo, J. Rivera-Utrilla, Journal of Chemical Technology & Biotechnology, 79 (2004) 902-909.
[71] P.M. Alvarez, F.J. Beltrain, J.P. Pocostales, F.J. Masa, Applied Catalysis B: Environmental, 72 (2007) 322-330.
[72] R. Rosal, A. Rodríguez, M.S. Gonzalo, E. García-Calvo, Applied Catalysis B: Environmental, 84 (2008) 48-57.
[73] R. Rosal, M.S. Gonzalo, A. rodriguez, E. Garcia-Calvo, Journal of Hazardous Materials, 169 (2009) 411-418.
[74] R. Rosal, M.S. Gonzalo, P.L. K. Boltes, J.J. vaquero, E. Garcia-Calvo, Journal of Hazardous Materials, 172 (2009) 1061-1068.
[75] F.J. Beltrain, F.J. Rivas, R. Montero-de-Espinosa, Applied Catalysis B: Environmental, 47 (2004) 101-109.

[76] J. Zhang, K. H. Lee, L. Cui, T.S. Jeong, Journal of Industrial and Engineering Chemistry, 15 (2009) 185-189.
[77] G. Moussavi, M. Mahmoudi, Chemical Engineering Journal, 152 (2009) 1-7.
[78] W. Qin, X. Li, J. qi, Langmuir, 25 (2009) 8001-8011.
[79] S.M. Avramescu, C. Bradu, I. Udrea, N. Mihalache, F. Ruta, Catalysis Communications, 9 (2008) 2386-2391.
[80] M. Muruganandham, J.J. Wu, Applied Catalysis B: Environmental, 80 (2008) 32-41.
[81] J. Qu, H. Li, H. He, Catalysis Today, 90 (2004) 291-296.
[82] I. Udrea, C. Bradu, Ozone Science and Engineering, 25 (2003) 335-343.
[83] S.T. Oyama, Catalysis Reviews : Science and Engineering, 42 (2000) 279-322.
[84] F.J. Beltran, F.J. Rivas, R. Montero-de-Espinosa, Applied Catalysis B: Environmental, 47 (2004) 101-109.
[85] R. Andreozzi, V. Caprio, A. Insola, R. Marotta, V. Tufano, Water Research, 32 (1998) 1492-1496.
[86] S. P. Tong, W. P. Lie, W. H. Leng, Q.Q. Zhang, Chemosphere, 50 (2003) 1359-1364.
[87] Y. Dong, H. Yang, K. He, S. Song, A. Zhang, Applied Catalysis B: Environmental, 85 (2009) 155-161.
[88] M. Jekel, R. Seith, Water Supply, 18 (2000) 628-631.
[89] J. S. Park, H. Choi, K.H. Ahn, Water Science and Technology, 47 (2003) 179-184.
[90] J. S. Park, H. Choi, K. H. Ahn, J.W. Kang, Ozone: Science & Engineering, 26 (2004) 141-151.
[91] P. Jong-Sup, C. Heechul, C. Jaewon, Water Research, 38 (2004) 2285-2292.
[92] F.J. Beltran, F.J. Rivas, R. Montero-de-Espinosa, Water Research, 39 (2005) 3553-3564.
[93] T. Zhang, J. Ma, Journal of Molecular Catalysis A: Chemical, 279 (2008) 82-89.
[94] M. Sui, L. Sheng, K. Lu, F. Tian, Applied Catalysis B: Environmental, 96 (2010) 94-100.
[95] F. Han, V.S.R. Kambala, M. Srinivasan, D. Rajarathnam, R. Naidu, Applied Catalysis A: General, 359 (2009) 25-40.
[96] M. Ye, Z. Chen, X. Liu, Y. Ben, J. Sken, Journal of Hazardous Materilas, 167 (2009) 1021-1027.
[97] A. Colombo, G. Cappelletti, S. Ardizzone, I. Biraghi, C. Bianchi, D. Meroni, C. Pirola, F. Spadavecchia, Environmental Chemistry Letters, 10 (2012) 55-60.

[98] M. Carbajo, F.J. Rivas, F.J. Beltran, P. Alvares, F. Median, Ozone: Science & Engineering, 28 (2006) 229-235.
[99] N. Karpel Vel Leither, H. Fu, Topics in Catalysis, (2005) 249-256.
[100] F. Delanoe, B. Acedo, N. Karpel Vel Leither, B. Legube, Applied Catalysis B: Environmental, 29 (2001) 315-325.
[101] H. Fu, N. Karpel Vel Leither, B. Legube, New Journal of Chemistry, 26 (2002) 1662-1666.
[102] T. Zhang, W. Li, J.-P. Croué, Environmental Science & Technology, 45 (2011) 9339-9346.
[103] E.C. Chetty, V.B. Dasireddy, S. Maddila, S.B. Jonnalagadda, Applied Catalysis B: Environmental, 117-118 (2012) 18-28.
[104] C.A. Zaror, Journal of Chemical Technology & Biotechnology, 70 (1997) 21-28.
[105] C.A. Guzman-Perez, J. Soltan, J. Robertson, Separation and Purification Technology, 79 (2011) 8-14.
[106] F.J. Beltran, J.P. Pocostales, P.M. Alvarez, J. Jaramillo, Journal of Hazardous Materials, 169 (2009) 532-538.
[107] J. Ma, M. Sui, T. Zhang, C. Guan, Water Research, 39 (2005) 779-786.
[108] L. Zhao, J. Ma, Z. Sun, Z. Liu, Y. Yang, Frontiers of Environmental Science & Engineering in China, 2 (2008) 44-50.
[109] L. Zhao, J. Ma, Z.Z. Sun, Applied Catalysis B: Environmental, 79 (2008) 244-253.
[110] N. Sano, T. Yamamoto, D. Yamamoto, S. I. Kim, A. Eiad Ua, H. Sinomiya, M. Nakaiwa, Chemical Engineering and Processing, 46 (2007) 513-519.
[111] K. He, Y.M. Dong, Z. Li, L. Yin, A.M. Zhang, Y.C. Zheng, Journal of Hazardous Materials, 159 (2008) 587-592.
[112] F. Qi, B. Xu, L. Zhao, Z. Chen, L. Zhang, D. Sun, J. Ma, Applied Catalysis B: Environmental, 121–122 (2012) 171-181.
[113] F. Qi, B. Xu, Z. Chen, J. Ma, D. Sun, L. Zhang, F. Wu, Journal of Hazardous Materials, 168 (2009) 246-252.
[114] B.S. Kim, H. Fujita, Y. Sakai, A. Sakoda, M. Suzuki, Water Science and Technology, 46 (2002) 35-41.
[115] B. Kasprzyk-Hordern, J. Nawrocki, Ozone: Science & Engineering, 25 (2003) 185-194.

[116] I. Nowak, B. Kasprzyk-Hordern, M. Ziolek, J. Nawrocki, Studies in Surface Science and Catalysis, 141 (2002) 591-598.
[117] B. Kasprzyk-Hordern, K. Gromadzka, P. Andrzejewski, J. Nawrocki, Ochrona Srodowiska, 25 (2003) 65-69.
[118] B. Kasprzyk-Hordern, A. Dabrowska, J. s Wietlik, J. Nawrocki, Ozone: Science & Engineering, 26 (2004) 367-380.
[119] B. Kasprzyk-Hordern, J. Andrzejewski, J. Nawrocki, Ozone: Science & Engineering, 27 (2005) 301-310.
[120] D.B. Ward, C. Tizaoui, M.j. Slater, Ozone: Science & Engineering, 26 (2004) 475-486.
[121] D.B. Ward, C. Tizaoui, M.j. Slater, Ozone: Science & Engineering, 25 (2003) 485-495.
[122] G. McKay, G. Mcaleavey, Chemical Engineering Research & Design, 66 (1988) 531-536.
[123] G. Mezohegyi, F.P. van der Zee, J. Font, A. Fortuny, A. Fabregat, Journal of Environmental Management, 102 (2012) 148-164.
[124] Z.-Q. Liu, J. Ma, Y.-H. Cui, B.-P. Zhang, Applied Catalysis B: Environmental, 92 (2009) 301-306.
[125] F.J. Beltrain, J. Rivas, P.M. Alvarez, R. Montero-de-Espinoza, Ozone: Science & Engineering, 24 (2002) 227-237.
[126] A.k. Bin, Ozone: Science & Engineering, 28 (2006) 67-75.
[127] D. Bhattacharyya, T.F. Van Dierdock, S.D. West, A.R. Freshour, Journal of Hazardous Materilas, 41 (1995) 73-93.
[128] A.R. Freshour, S. Mawhinney, D. Bhattacharyya, Water Research, 30 (1996) 1949-1958.
[129] K. Gromadzka, J. Nawrocki, Ozone: Science & Engineering, 28 (2006) 85-94.
[130] C. Tizaoui, M.J. Slater, Ozone: Science & Engineering, 25 (2003) 315-332.
[131] V.S.R. Rajaskhar Pullabhotla, S.B. Jonnalagadda, Industrial & Engineering Chemistry Research, 48 (2009) 9097-9105.
[132] B. Kasprzyk-Hordern, Advances in Colloid and Interface Science, 110 (2004) 19-48.
[133] T. Shirai, H. watanabe, M. Fuji, M. Takahashi, Journal of Gifu Japan, 9 (2009) 23-31.

[134] C.N. Satterfield, Heterogeneous catalysis in industrial practice, McGraw Hill, U.S.A, (1991).
[135] M.E. Davis, R.F. Lobo, Chemistry of Materials, 4 (1992) 756-768.
[136] A. Jentys, G. Warecka, M. Derewinski, J.A. Lercher, The Journal of Physical Chemistry, 93 (1989) 4837-4843.
[137] D.H. Olson, W.O. Haag, W.S. Borghard, Microporous and Mesoporous Materials, 35-36 (2000) 435-446.
[138] J. W. Ward, Applied Industrial Catalysis, 3 (1984) 272-392.
[139] N. L. Dias Filho, D.R.d. Carmo, Adsorption at Silica, Alumina and Related Surfaces, in: Encyclopedia of Surface and Colloid Science, Marcel Dekker, New York, 2004, pp. 191.
[140] M.E. Davis, Accounts of Chemical Research, 26 (1993) 111-115.
[141] A. Corma, Chemical Reviews, 95 (1995) 559-614.
[142] K. Fisher, K. Huddersman, New Journal of Chemistry, 26 (2002).
[143] A.V. Ivanov, G.W. Graham, M. shelef, Applied Catalysis B: Environmental, 21 (1999) 243-258.
[144] J. Datka, E. Tuznik, Zeolites, 5 (1985) 230-232.
[145] H. Ichihashi, H. Sato, Applied Catalysis A: General, 221 (2001) 359-366.
[146] M.C. Campa, V. Indovina, G. Minelli, G. Moretti, I. Pettiti, P. Porta, A. Riccio, Catalysis Letters, 23 (1994) 141-149.
[147] J.D. Sherman, Proceedings of the National Academy of Science of U.S.A, 96 (1999) 3471-3478.
[148] M.E. Karaman, D.A. Antelmi, R.M. Pashley, Colloids and Surfaces A: Physicochemical and Engineering Aspects, 182 (2001) 285-298.
[149] A.V. Ivanov, G.W. Graham, M. Shelef, Applied Catalysis B: Environmental, 21 (1999) 243-258.
[150] S. Tanada, M. Kabayama, N. Kawasaki, T. Sakiyama, T. Nakamura, M. Araki, T. Tamura, Journal of Colloid and Interface Science, 257 (2003) 135-140.
[151] J. Nawrocki, C. Dunlap, A. McCormick, P.W. Carr, Journal of Chromatography A, 1028 (2004) 1-30.
[152] G.V. Buxton, journal of Physical and Chemical Refrence Data 17 (1988) 513.
[153] J. Hoigne, H. Bader, Water Research, 17 (1983) 173-183.

[154] R. Flyunt, A. Leitzke, G. Mark, E. Mvula, E. Reisz, R. Schick, C. von Sonntag, , The Journal of Physical Chemistry B, 107 (2003) 7242-7253.
[155] I.B. Afanas' ev, Superoxide ion: Chemistry and Biological Implications, in, CRC Press, Florida, 1989.
[156] D.T. Sawyer, Oxygen Chemistry, Oxford University Press, New York, 1991.
[157] Aryeh A. Frimer, I. Rosenthal, in: F. CRC Press (Ed.), 1982.
[158] R. Poupko, I. Rosenthal, The Journal of Physical Chemistry, 77 (1973) 1722-1724.
[159] R. Atkinson, Chemical Reviews, 86 (1986) 69-201.
[160] G.N.R. Tripathi, Journal of the American Chemical Society, 120 (1998) 4161-4166.
[161] C.W. Jones, in: J.H. Clark (Ed.), The Royal Society of Chemistry, Cambridge, UK, 1999.
[162] J. March, Advanced Organic Chemistry; Reactions, Mechanisms and Structure, in, McGraw-Hill Book Company, New York, 1977.
[163] J.K. Kim, I.S. Metcalfe, Chemosphere, 69 (2007) 689-696.
[164] S.-K. Han, K. Ichikawa, H. Utsumi, Water Research, 32 (1998) 3261-3266.
[165] H. Bader, V. Sturzenegger, J. Hoigné, Water Research, 22 (1988) 1109-1115.
[166] G. Bartosz, Clinica Chimica Acta, 368 (2006) 53-76.
[167] Dikalov S, Grigor ev IA, Voinov M, B. E, Biochemistry Biophysics Research Communication, 248 (1998) 211-215.
[168] Dikalov S, Skatchkov M, Fink B, B. E, Nitric Oxide: Biology and Chemistry, 1 (1997) 423-431.
[169] Roubaud V, Sankarapandi S, Kuppusamy P, Tordo P, Z. JL, Analytical Biochemistry, 247 (1997) 404-411.
[170] Bielski BHJ, Cabelli DE, A. RL<, Ross AB, journal of Physics and Chemistry, 14 (1985) 1041-1100.
[171] M.W. Sutherland, B.A. Learmonth, Free Radical Research, 27 (1997) 283-289.
[172] M.I. Heller, P.L. Croot, Analytica Chimica Acta, 667 (2010) 1-13.
[173] R.O. Olojo, R.H. Xia, J.J. Abramson, Analytical Biochemistry, 339 (2005) 338-344.
[174] H. Bader, V. Sturzenegger, J. Hoigne, Water Research, 22 (1988) 1109-1115.
[175] K.-i. Ishibashi, A. Fujishima, T. Watanabe, K. Hashimoto, Electrochemistry Communications, 2 (2000) 207-210.
[176] Q. Xiang, J. Yu, P.K. Wong, Journal of Colloid and Interface Science, 357 (2011) 163-167.

[177] M. Zhou, Z. Diwu, N. Panchuk-Voloshina, R.P. Haugland, Analytical Biochemistry, 253 (2002) 162-168.
[178] J. Yu, W. Wang, B. Cheng, B.-L. Su, Enhancement of Photocatalytic Activity of Mesporous TiO2 Powders by Hydrothermal Surface Fluorination Treatment, The Journal of Physical Chemistry C, 113 (2009) 6743-6750.
[179] H. Kobayashi, E. Gil-Guzman, A.M. Mahran, R.K. Sharma, D.R. Nelson, A.J.Thomas, A. Agarwal, Journal of Andrology, 22 (2001) 568-574.
[180] Y. Kambayashi, K. Ogino, Journal of Toxicological Science, 28 (2003) 139-148.
[181] T. Preocanin, N. Kally, Croatica Chemical Acta, 79 (2006) 95-106.
[182] A.D. Eaton, L.S. Clesceri, E.W. Rice, A.E. Greenberg, Standard methods for the examination of water & waste water, 21 ed., (2005).
[183] O. Hamdaoui, Batch study of liquid-phase adsorption of methylene blue using cedar sawdust and crushed brick, Journal of Hazardous Materials, 135 (2006) 264-273.
[184] H. Czili, A. Horváth, Applied Catalysis B: Environmental, 81 (2008) 295-302.
[185] G.T. Chi, K.D. Huddersman, Journal of Chromatography A, 1139 (2007) 95-103.
[186] P.A. Jacobs, R. Von Ballmoos, The Journal of Physical Chemistry, 86 (1982) 3050-3052.
[187] D.W. Breck, Zeolites Molecular Sieves, in, Willey, New York, 1974.
[188] G. Jones, L. Indig, New Journal of Chemistry, 20 (1996) 231-232.
[189] D. Clark, J. jimenez-Morais, G. Jones, E. Zanardi-Lamardo, C.A. Moore, R.G. Zika, Marine Chemistry, 78 (2002) 121-135.
[190] J.P.C. J.A. Leenheer, Enivronmental Science & Technology, 37 (2003) 18-26.
[191] J. Oldenburg, E. M. Quenzel, U. Harbrecht, A. Fregin, W. Kress, C.R. Muller, H. J. Hertfelder, R. Schwaab, H. H. Brackmann, P. Hanfland, British journal of Haematology, 98 (1997) 240-244.
[192] C.H. Tasai, A. Stern, J.F. Chiou, C.L. Chern, T.Z. Liu, Journal of Argricultural and Food Chemistry, 49 (2001) 2137--2132-2141.
[193] A. I. Okezie, P. Lester, Methods in Enzymology 2003 (1994) 57-66.
[194] G.L. Newton, J.R. Milligan, Radiation Physics and Chemistry, 75 (2006) 473-478.
[195] T. Hirakawa, Y. Nosaka, Langmuir, 18 (2002) 3247-3254.
[196] K. Ishibashi, A. Fujishima, T. Watanabe, K. Hashimoto, Electrochem. Commun., 2 (2000) 207.

[197] G. Louit, S. Foley, J. Cabillic, H. Coffigny, F. Taran, A. Valleix, J.P. Renault, S. Pin, Radiation Physics and Chemistry, 72 (2005) 119-124.
[198] H. Czili, A. Horvath, Applied Catalysis B: Environmental, 81 (2008) 295-302.
[199] J. Yu, L. Qi, M. Jaroniec, The Journal of Physical Chemistry C, 114 (2010) 13118-13125.
[200] W.H. Glaze, J.-W. Kang, D.H. Chapin, Ozone: Science & Engineering, 9 (1987) 335-352.
[201] J. Staehelin, R.E. Buehler, J. Hoigne, The Journal of Physical Chemistry, 88 (1984) 5999-6004.
[202] P.M. Alvarez, J.F. Garcia-Araya, F.J. Beltran, I. Giraldez, J. Jaramillo, V. Gómez-Serrano, Carbon, 44 (2006) 3102-3112.
[203] L. Zhao, J. Ma, Z. Sun, H. Liu, Applied Catalysis B: Environmental, 89 (2009) 326-334.
[204] T. Zhang, P. Hou, Z. Qiang, X. Lu, Q. Wang, Chemosphere, 82 (2011) 608-612.
[205] K. Kosaka, H. Yamada, S. Matsui, S. Echigo, K. Shishida, Environmental Science & Technology, 32 (1998) 3821-3824.
[206] R. Schick, I. Strasser, H.-H. Stabel, Water Research, 31 (1997) 1371-1378.
[207] N. Soh, Analytical and Bioanalytical Chemistry, 386 (2006) 532-543.
[208] V. Brezovaj, S.A. Gabovaj, D. Dvoranovaj, A. Stajko, Journal of Photochemistry and Photobiology B: Biology, 79 (2005) 121-134.
[209] T. Oritani, N. Fukuhara, T. Okajima, F. Kitamura, T. Ohsaka, Inorganica Chimica Acta, 357 (2004) 436-442.
[210] L. Zhao, Z. Sun, J. Ma, H. Liu, Environmental Science & Technology, 43 (2009) 2047-2053.
[211] M. Suh, P.S. Bagus, S. Park, M.P. Rosynek, J.H. Lunsford, The Journal of Physical chemistry B, 104 (2000) 2736-2742.
[212] D. Carlone, Zeolites catalysed Ozonolysis, in: Chemical engineering, Worcester Polytechnic institute, 2010, pp. 47.
[213] B. Halling-Sorenson, S. Nors Nielsen, P.F. Lanzky, F. Ingerslev, H.C. Holten Lutzhoft, S.E. Jorgensen, Chemosphere, 36 (1998) 357-393.
[214] M.M. Huber, S. Canonica, G.-Y. Park, U. von Gunten, Oxidation of Pharmaceuticals during Ozonation and Advanced Oxidation Processes, Environmental Science & Technology, 37 (2003) 1016-1024.

[215] M. Klavarioti, D. Mantzavinos, D. Kassinos, Environment International, 35 (2009) 402-417.
[216] H.S. Brown, D.R. Bishop, C.A. Rowan, Am J Public Health, 74 (1984) 479-484.
[217] Y. Pi, L. Zhang, J. Wang, Journal of Hazardous Materials, 141 (2007) 707-712.
[218] B. Legube, N. Karpel Vel Leitner, Catalysis Today, 53 (1999) 61-72.
[219] H. Einaga, A. Ogata, Journal of Hazardous Materials, 164 (2009) 1236-1241.
[220] H. Einaga, A. Ogata, Environmental Science & Technology, 44 (2010) 2612-2617.
[221] M.N. Jones, N.D. Bryan, Advances in Colloid and Interface Science, 78 (1998) 1-48.
[222] in, yorkshire waters, huddersfield , west yorkshire.
[223] L. Zhao, B. Shen, J. Gao, C. Xu, Journal of Catalysis, 258 (2008) 228-234.

APPENDIX

Appendix A (Loss of VOCs due to volatization)

Before the ozonation and catalytic ozonation of VOCs (chapter 5) in the reaction column, the of VOCs loss due to volatization has been calculated and the results are presented in the following tables

Table A.1: Loss of cumene inside the column without ozonation

Concentrations	Concentrations (mg/L)			Average concentration (mg/L)	% Loss
Initial Conc.	20.16	16.03	17.0	17.7 ± 2.3	
Final Conc.	18.4	15.4	16.89	16.9 ± 1.5	4.7 ± 4

Table A.2: Loss of 1,2-dichlorobenzene inside the column without ozonation

Concentrations	Concentrations (mg/L)			Average concentration (mg/L)	% Loss
Initial Conc.	2	2.3	1.8	2.03 ± 0.3	
Final Conc.	1.95	2.1	1.7	1.92 ± 0.2	4.2 ± 3

Table A.3: Loss of trilorobenzene inside the column without ozonation

Concentrations	Concentrations (mg/L)			Average concentration (mg/L)	% Loss
Initial Conc.	0.32	0.267	0.251	0.281 ± 0.04	
Final Conc.	0.31	0.267	0.239	0.274 ± 0.04	2.5 ± 2

From the above tables it has been seen that average % loss in the case of cumene is 4.7 ± 4% while it is 4.2 ± 3%, 2.5 ± 2% for dichlorobenzene and trichlorobenzene. This may be due to the vapour pressure of VOCs. Since vapour pressure is in order of cumene > dichlorobenzene > trichlorobenzene. As the % loss is not significant hence the analytes can be used for further experiments inside the column.

Appendix B (pH changes during the ozonation and catalytic ozonation)

The appendix B show the results of change in pH during the ozonation and catalytic ozonation process

Table A.4: Change in pH during the ozonation and catalytic ozonation of coumarin (initial pH= 3)

Time(min)	Change in pH ± SD					
	O_3	Z1000H/O_3	Z900Na/O_3	Z25H/O_3	Z25Na/O_3	Alumina/O_3
0	3.01 ± 0.01	3.02 ± 0.01	3.01 ± 0.01	3.02 ± 0.01	3.01 ± 0.01	3.01 ± 0.01
5	3.01 ± 0.01	3.01 ± 0.01	3.02 ± 0.01	3.01 ± 0.03	3.03 ± 0.01	3.03 ± 0.02
10	3.02 ± 0.02	3.02 ± 0.01	3.02 ± 0.01	3.01 ± 0.01	3.05 ± 0.02	3.05 ± 0.02
15	3.01 ± 0.02	3.01 ± 0.03	3.02 ± 0.02	3.02 ± 0.02	3.06 ± 0.01	3.04 ± 0.01
20	3.02 ± 0.02	3.02 ± 0.02	3.01 ± 0.02	3.02 ± 0.02	3.06 ± 0.01	3.06 ± 0.01
25	3.03 ± 0.02	3.01 ± 0.01	3.02 ± 0.02	3.01 ± 0.01	3.07 ± 0.02	3.06 ± 0.02
30	3.01 ± 0.02	3.01 ± 0.02	3.01 ± 0.02	3.02 ± 0.01	3.06 ± 0.02	3.09 ± 0.02

Table A.5: Change in pH during the ozonation and catalytic ozonation of coumarin (initial pH= 6.2)

Time(min)	Change in pH ± SD					
	O_3	Z1000H/O_3	Z900Na/O_3	Z25H/O_3	Z25Na/O_3	Alumina/O_3
0	6.21± 0.01	6.21 ± 0.01	6.23 ± 0.01	6.21 ± 0.01	6.22 ± 0.01	6.21 ± 0.01
5	6.22 ± 0.02	6.22 ± 0.02	6.24 ± 0.01	6.20 ± 0.01	6.23 ± 0.02	6.24 ± 0.01
10	6.21 ± 0.02	6.23 ± 0.02	6.28 ± 0.02	6.18 ± 0.02	6.28 ± 0.02	6.25 ± 0.01
15	6.18 ± 0.02	6.25 ± 0.01	6.26 ± 0.02	6.19 ± 0.02	6.26 ± 0.02	6.29 ± 0.02
20	6.19 ± 0.01	6.21 ± 0.02	6.27 ± 0.02	6.18 ± 0.01	6.27 ± 0.03	6.32 ± 0.02
25	6.18 ± 0.01	6.23 ± 0.03	6.28 ± 0.03	6.18 ± 0.01	6.28 ± 0.02	6.34 ± 0.02
30	6.18 ± 0.01	6.24 ± 0.01	6.28 ± 0.02	6.18 ± 0.01	6.28 ± 0.01	6.31 ± 0.02

Table A.6: Change in pH during the ozonation and catalytic ozonation of coumarin (initial pH= 8.8)

Time(min)	Change in pH ± SD					
	O_3	Z1000H/O_3	Z900Na/O_3	Z25H/O_3	Z25Na/O_3	Alumina/O_3
0	8.82± 0.01	8.82 ± 0.01	8.81 ± 0.01	8.83 ± 0.01	8.82 ± 0.01	8.82 ± 0.01
5	8.80 ± 0.01	8.81 ± 0.02	8.86 ± 0.01	8.81 ± 0.03	8.86 ± 0.02	8.86 ± 0.02
10	8.81 ± 0.01	8.80 ± 0.01	8.89 ± 0.02	8.80 ± 0.02	8.85 ± 0.02	8.89 ± 0.02
15	8.78 ± 0.01	8.81 ± 0.02	8.85 ± 0.01	8.79 ± 0.01	8.89 ± 0.01	8.89 ± 0.01
20	8.79 ± 0.01	8.79 ± 0.01	8.88 ± 0.02	8.78 ± 0.02	8.92 ± 0.02	8.91 ± 0.01
25	8.80 ± 0.02	8.79 ± 0.01	8.87 ± 0.01	8.78 ± 0.01	8.93± 0.03	8.92 ± 0.01
30	8.79 ± 0.02	8.79 ± 0.02	8.88 ± 0.01	8.77 ± 0.01	8.94 ± 0.02	8.93 ± 0.03

Table A.7: Change in pH during the ozonation and catalytic ozonation of coumarin (initial pH= 13)

Time(min)	Change in pH ± SD					
	O_3	Z1000H/O_3	Z900Na/O_3	Z25H/O_3	Z25Na/O_3	Alumina/O_3
0	13.03 ± 0.01	13.03 ± 0.02	13.03 ± 0.02	13.02 ± 0.01	13.01 ± 0.01	13.02 ± 0.01
5	13.01 ± 0.03	13.03 ± 0.01	13.03 ± 0.02	13.02 ± 0.01	13.02 ± 0.01	13.03 ± 0.02
10	13.02 ± 0.03	13.01 ± 0.01	13.04 ± 0.02	13.01 ± 0.01	13.04 ± 0.01	13.01 ± 0.02
15	12.99 ± 0.03	13.04 ± 0.01	13.01 ± 0.02	13.01 ± 0.01	13.02 ± 0.01	13.02 ± 0.03
20	13.01± 0.02	13.01 ± 0.01	13.02 ± 0.01	13.02 ± 0.02	13.02 ± 0.02	13.01 ± 0.03
25	12.99 ± 0.01	13.04 ± 0.01	13.03 ± 0.01	13.02 ± 0.02	13.01 ± 0.02	13.03 ± 0.03
30	13.01 ± 0.02	13.04 ± 0.01	13.03 ± 0.02	13.01 ± 0.02	13.03 ± 0.01	13.01 ± 0.03

The above tables show the results of pH changes during the ozonation and catalytic ozonation of coumarin (chapter 4). It is clear from the results that there is no significant change in pH during the process has been observed. Similar results have been obtained for all other experiments conducted in this research work.

Appendix C (Colour changes in the catalytic process of amplex red and NBD-Cl)

The Figure A.1 shows the change in the colour in an ozonation sample of NBD-Cl in the presence of alumina. As described in the chapter 4 that the reaction of superoxide with NBD-Cl results in the formation of a yellow fluorescent product. The Figure A.1 clearly indicates the formation of yellow colour product.

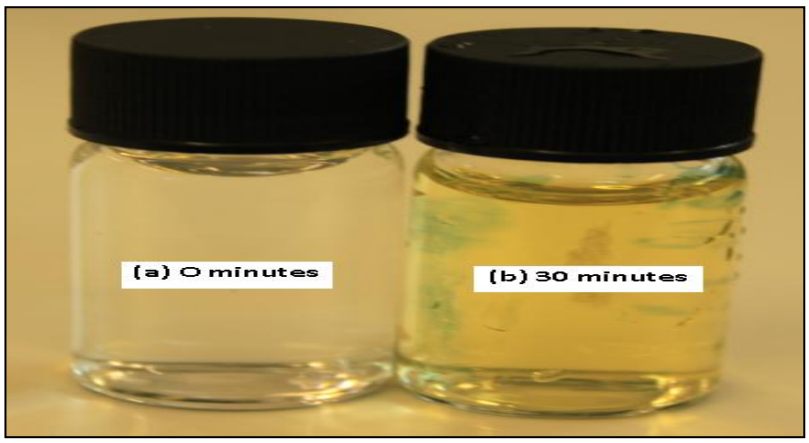

Figure A.1: Change in the colour of solution in the ozonation of NBD-Cl in the presence of alumina at pH 8.8.

The Figure A.2 shows the colour changes during the ozonation process in the presence of alumina during hydrogen peroxide studies. This indicates the formation of pink colour resorufin (the product of the reaction of amplex red and hydrogen peroxide)

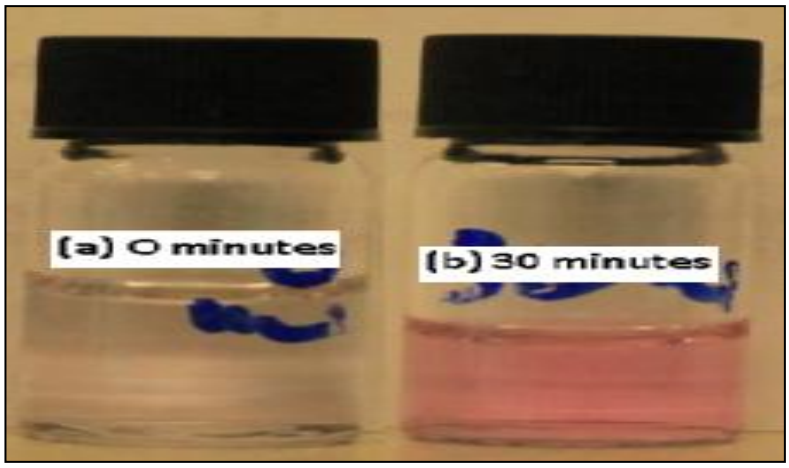

Figure A.2: Change in the colour of solution in the ozonation of amplex red in the presence of alumina at pH 6.2.

Appendix D (Adsorption optimum time of VOCs and ibuprofen)

The results presented in Figure A.4 show that optimum time (1 hour) of adsorption of VOCs on zeolites and alumina. The Figure A.3 shows the results of ibuprofen adsorption on alumina and ZSM-5 zeolites is 4 hrs. After this time no significant change in the concentration of adsorbed ibuprofen has been observed. Therefore, this time was selected for the determination of adsorption capacities as described in chapter 2.

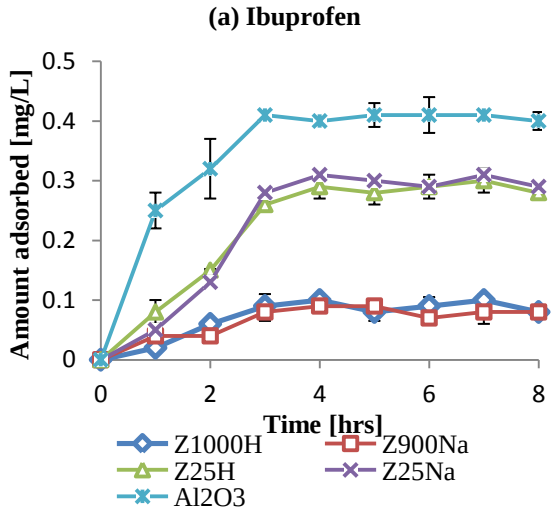

Figure A.3: Adsorption optimum time of adsorption for the removal of ibuprofen by ZSM-5 zeolites and alumina ($C_{o\ (ibu)}$ = 20.0 mg/L, T = 20^{o}C; pH = 7.2; pH_{30min} = pH_{o} + 0.1; catalyst amount = 1.0 g; V = 25 mL).

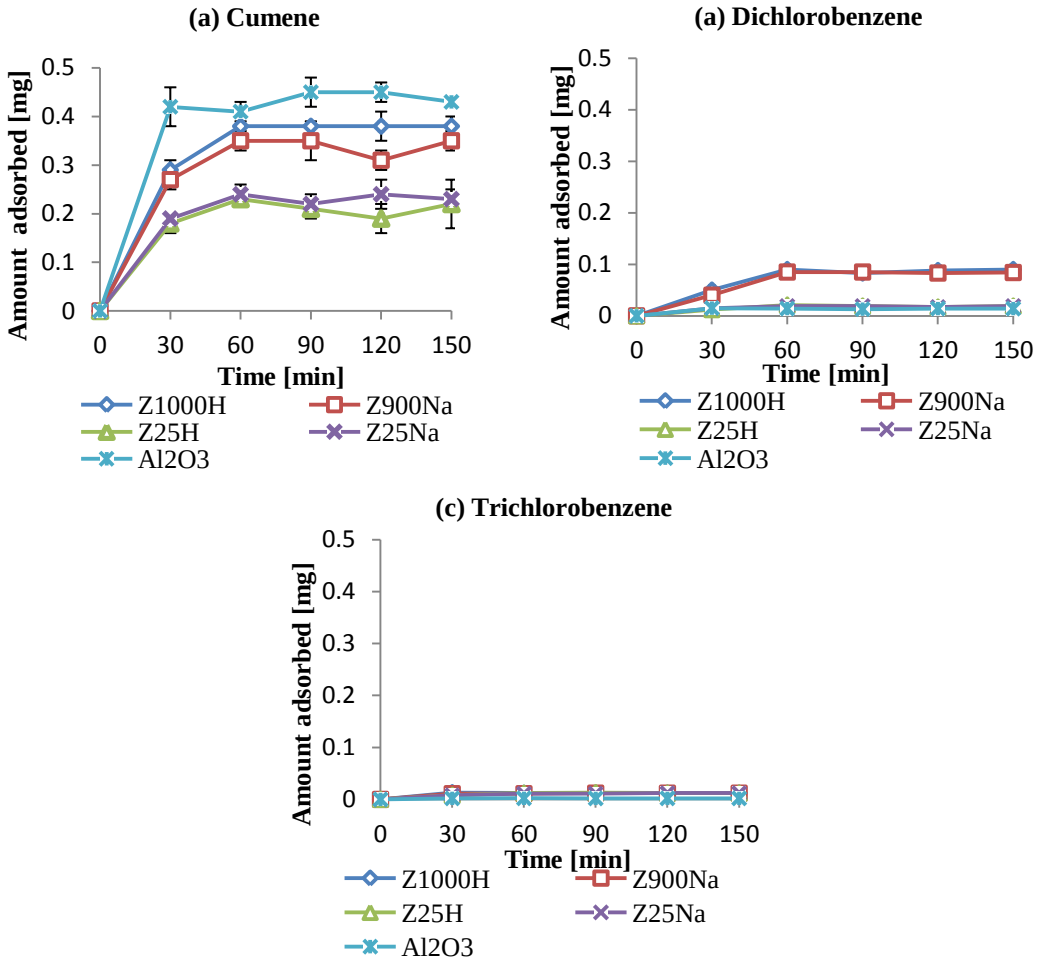

Figure A.4: Adsorption optimum time of adsorption for the removal of VOCs by ZSM-5 zeolites and alumina ($C_{o\,(cum)}$ = 19.2 mg/L, C_{0DCB} = 3.5 mg/L and C_{0TCB} = 0.5; T = 20^{o}C; pH = 6; pH_{30min} = pH_{o} + 0.2; catalyst amount = 1.0 g; V = 25 mL).

Appendix E (Off-gas ozone during the ozonation and catalytic ozonation)

The results of ozone gas come out of the reactor during the ozonation and catalytic ozonation have been presented in appendix e. The results show that slightly higher amount of ozone come out during the ozonation alone when compared with ozonation in the presence of catalysts (30 minutes). This may be due to the adsorption and decomposition of ozone on catalysts. Additionally, the results at different pH indicate that less gaseous ozone come out at higher pH values , this may be due to the low stability of ozone at higher pH values in the water therefore

more ozone may be consumed and less come out. The results at pH 13.0 show that ozonation and catalytic ozonation have similar ozone concentrations this may indicate that catalysts are not active at this pH as described in the chapter 4. It is important to note that in the case of VOCs study gaseous ozone has not been found. This may be due to low initial dose of ozone. Therefore, most of the ozone reacted with water and gaseous ozone come out may be less than that of the limit of detections of the method.

Table A.8: Gaseous ozone concentrations during the ozonation and catalytic ozonation of coumarin

pH	**Gaseous ozone concentrations (mg/L) ± SD**					
	O_3	**Z1000H/O_3**	**Z900Na/O_3**	**Z25H/O_3**	**Z25Na/O_3**	**Alumina/O_3**
pH 3.0	2.3 ± 0.1	1.8 ± 0.1	1.7 ± 0.2	1.8 ± 0.1	1.7 ± 0.2	1.4 ± 0.2
pH 6.2	1.3 ± 0.1	0.8 ± 0.1	0.6 ± 0.3	0.8 ± 0.1	0.8 ± 0.2	0.5 ± 0.1
pH 8.8	0.8 ± 0.2	0.6 ± 0.1	0.3 ± 0.1	0.3 ± 0.1	0.2 ± 0.1	0.1 ± 0.1
pH 13.0	0.2 ± 0.1	0.2 ± 0.1	0.3 ± 0.1	0.3 ± 0.2	0.2 ± 0.1	0.2 ± 0.1

Table A.9: Gaseous ozone concentrations during the ozonation and catalytic ozonation of NBD-Cl

pH	**Gaseous ozone concentrations (mg/L) ± SD**					
	O_3	**Z1000H/O_3**	**Z900Na/O_3**	**Z25H/O_3**	**Z25Na/O_3**	**Alumina/O_3**
pH 3.0	2.1 ± 0.2	1.8 ± 0.1	1.8 ± 0.1	1.8 ± 0.1	1.7 ± 0.2	1.4 ± 0.2
pH 6.2	1.1 ± 0.3	0.5 ± 0.3	0.8 ± 0.1	0.7 ± 0.1	0.8 ± 0.1	0.3 ± 0.1
pH 8.8	1.0 ± 0.1	0.7 ± 0.1	0.7 ± 0.1	0.6 ± 0.1	0.6 ± 0.1	0.1 ± 0.1
pH 13.0	0.1 ± 0.1	0.3 ± 0.1	0.2 ± 0.1	0.1 ± 0.2	0.2 ± 0.1	0.2 ± 0.1

Table A.10: Gaseous ozone concentrations during the ozonation and catalytic ozonation of amplex red

pH	Gaseous ozone concentrations (mg/L) ± SD					
	O_3	Z1000H/O_3	Z900Na/O_3	Z25H/O_3	Z25Na/O_3	Alumina/O_3
pH 3.0	2.0 ± 0.2	1.6 ± 0.2	1.6 ± 0.1	1.7 ± 0.1	1.5 ± 0.3	1.3 ± 0.1
pH 6.2	1.3 ± 0.2	0.6 ± 0.1	0.5 ± 0.3	0.6 ± 0.2	0.7 ± 0.1	0.5 ± 0.1
pH 8.8	1.1 ± 0.2	0.3 ± 0.2	0.5 ± 0.1	0.5 ± 0.2	0.4 ± 0.2	0.2 ± 0.1
pH 13.0	0.2 ± 0.1	0.3 ± 0.1	0.2 ± 0.1	0.3 ± 0.1	0.3 ± 0.1	0.3 ± 0.1

Table A.11: Gaseous ozone concentrations during the ozonation and catalytic ozonation of ibuprofen

pH	Gaseous ozone concentrations (mg/L) ± SD					
	O_3	Z1000H/O_3	Z900Na/O_3	Z25H/O_3	Z25Na/O_3	Alumina/O_3
pH 3.0	1.5 ± 0.2	0.8 ± 0.2	0.9 ± 0.2	0.7 ± 0.2	0.7 ± 0.2	0.4 ± 0.1
pH 7.2	0.8 ± 0.1	0.4 ± 0.1	0.5 ± 0.3	0.4 ± 0.1	0.4 ± 0.2	0.1 ± 0.1
pH 13.0	0.2 ± 0.1	0.1 ± 0.1	0.2 ± 0.1	0.3 ± 0.2	0.3 ± 0.1	0.3 ± 0.1

Appendix F (Absorbance spectrum of resrufin in ozonation in the presence of alumina)

The figure A.5 clearly indicates that the formation of resrufin increases in ozonation in the presence of alumina. This clearly suggested that ozone decomposition in the presence of alumina leads to the formation of H_2O_2.

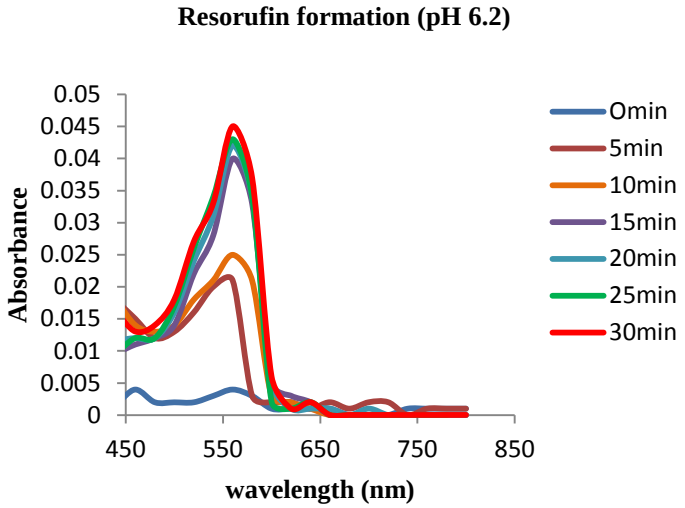

Figure A.5: Resorufin formation during the ozonation in the presence of alumina (C_{oAmp}= 20 mg/L; catalyst = 2.0 mg/L; T = 25^{o}C; pH = 6.2; pH_{t30min} = 6.2 ± 0.2; V = 190 mL).

Appendix G (First order plots of ozone decay in ozonation alone and ozonation in the presence of catalysts at pH 3.0, 6.0 and 13.0)

The figure A.6, A.7, A.8, A.9, A.10 ans A.11 clearly indicates that ozone decay at pH 3.0, 6.0 and 13.0 in the case of ozonation alone and ozonation in the presence of catalysts follows first order kinetics.

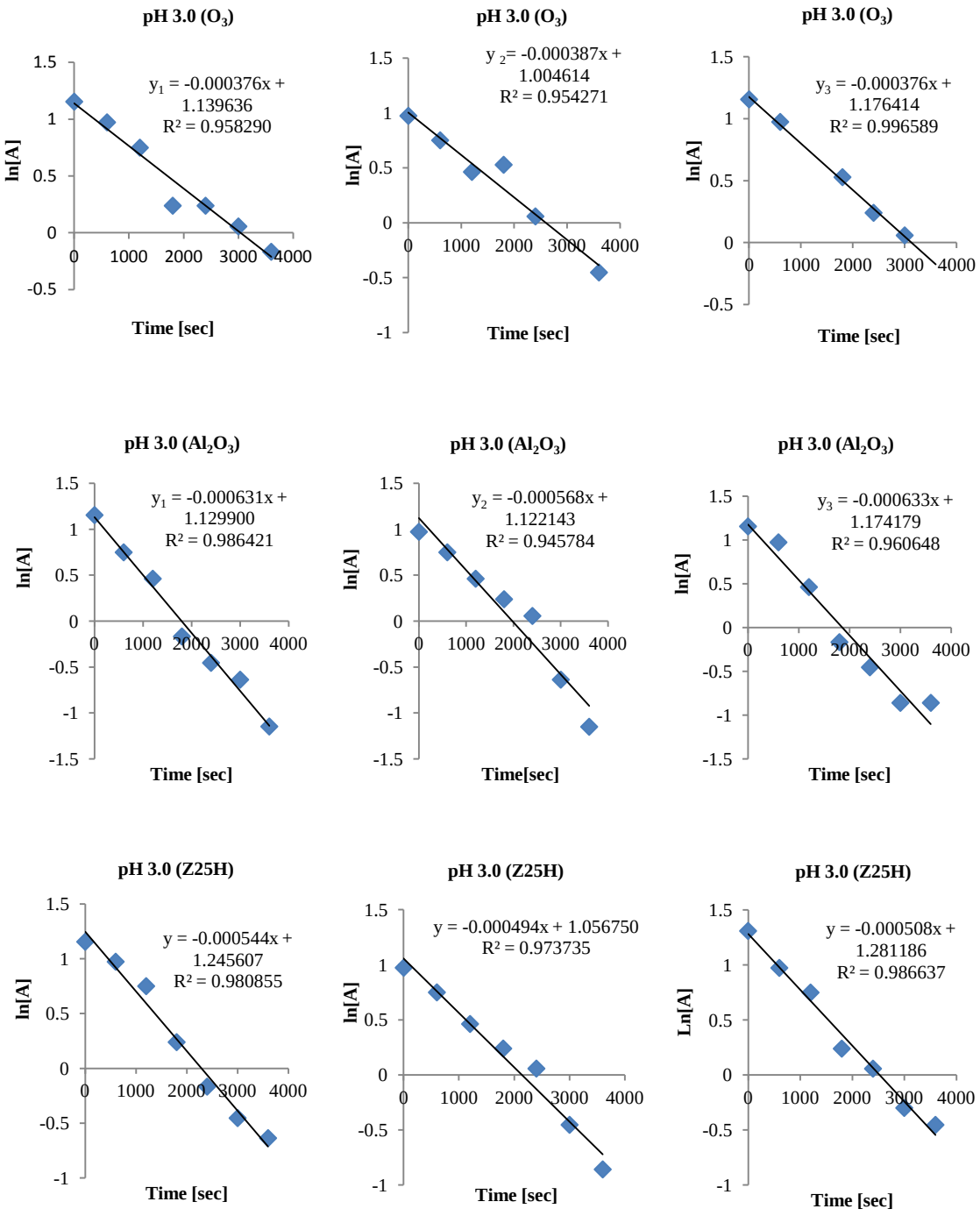

Figure A.6: First order kinetic plots of ozonation alone, Al_2O_3/O_3 and Z25H/O_3 ($O_{3\ initial}$ = 3.0 mg/L; catalyst = 0.95 mg/L; T = 25°C; pH = 3.0; V = 190 mL).

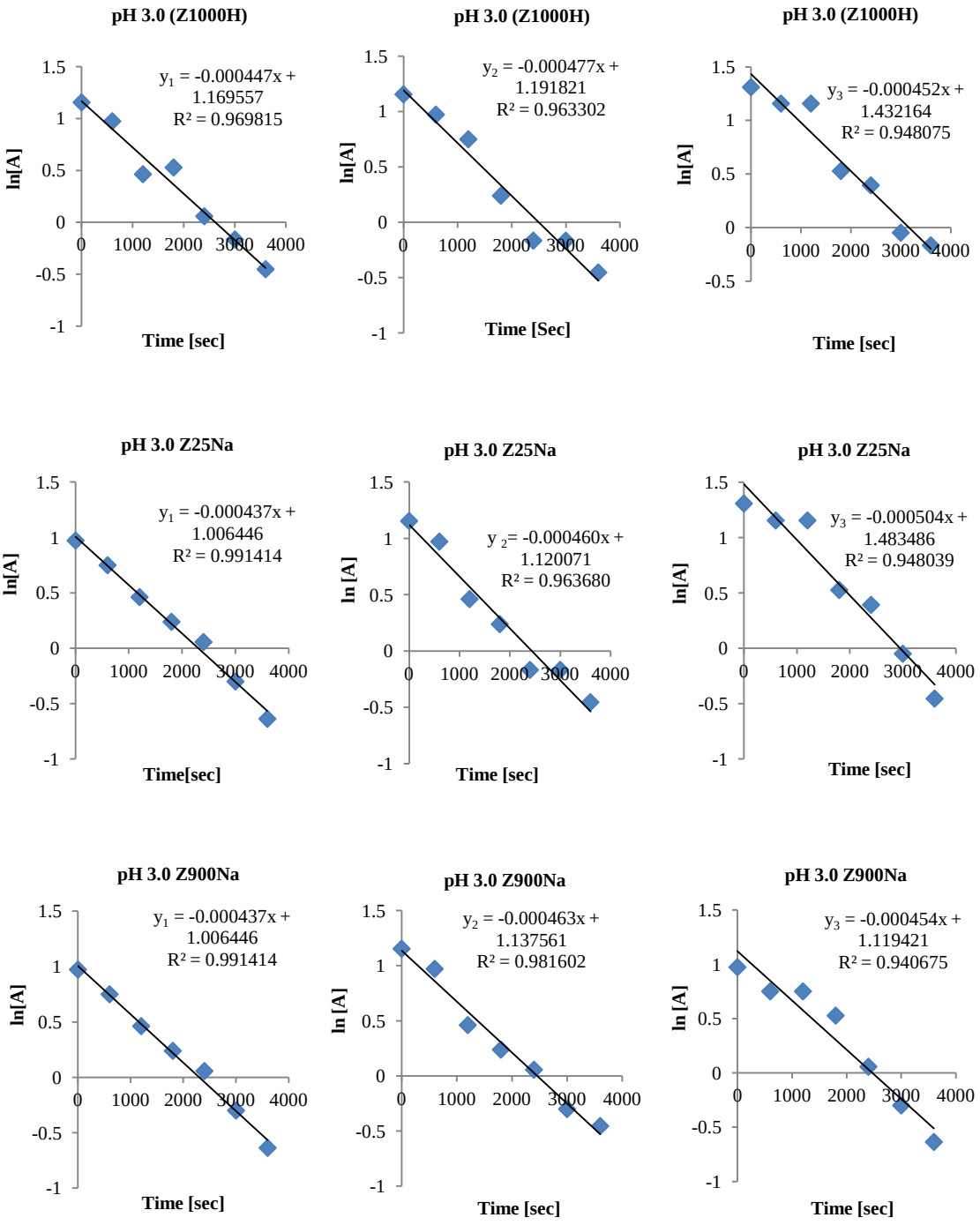

Figure A.7: First order kinetic plots of Z900Na, Z1000H/O_3 and Z25H/O_3 ($O_{3\ initial}$ = 3.0 mg/L; catalyst = 0.95 mg/L; T = 25°C; pH = 3.0; V = 190 mL).

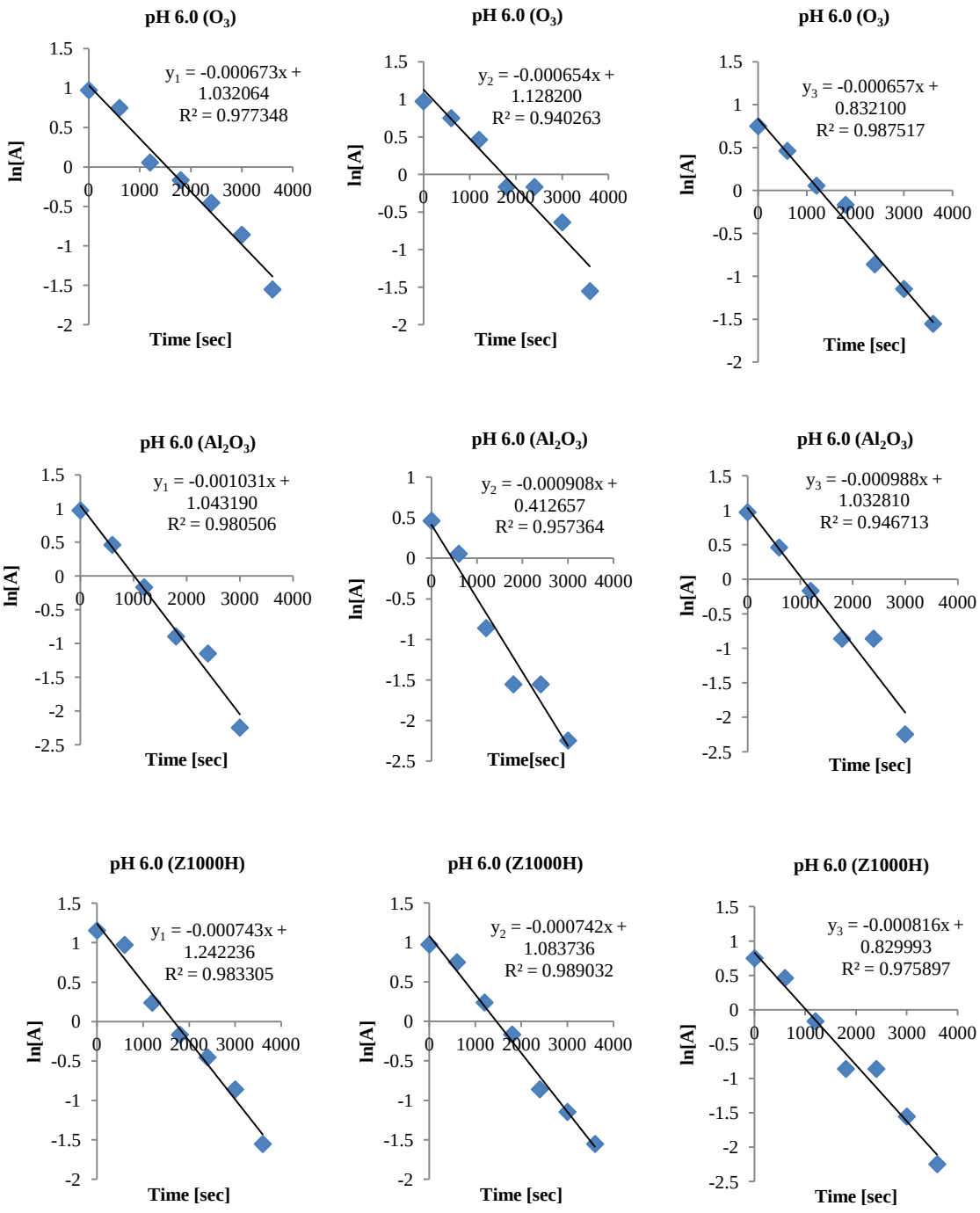

Figure A.8: First order kinetic plots of ozonation alone, Z1000H/O_3 and Al_2O_3/O_3 ($O_{3\ initial}$ = 2.1 mg/L; catalyst = 0.95 mg/L; T = 25°C; pH = 6.0; V = 190 mL).

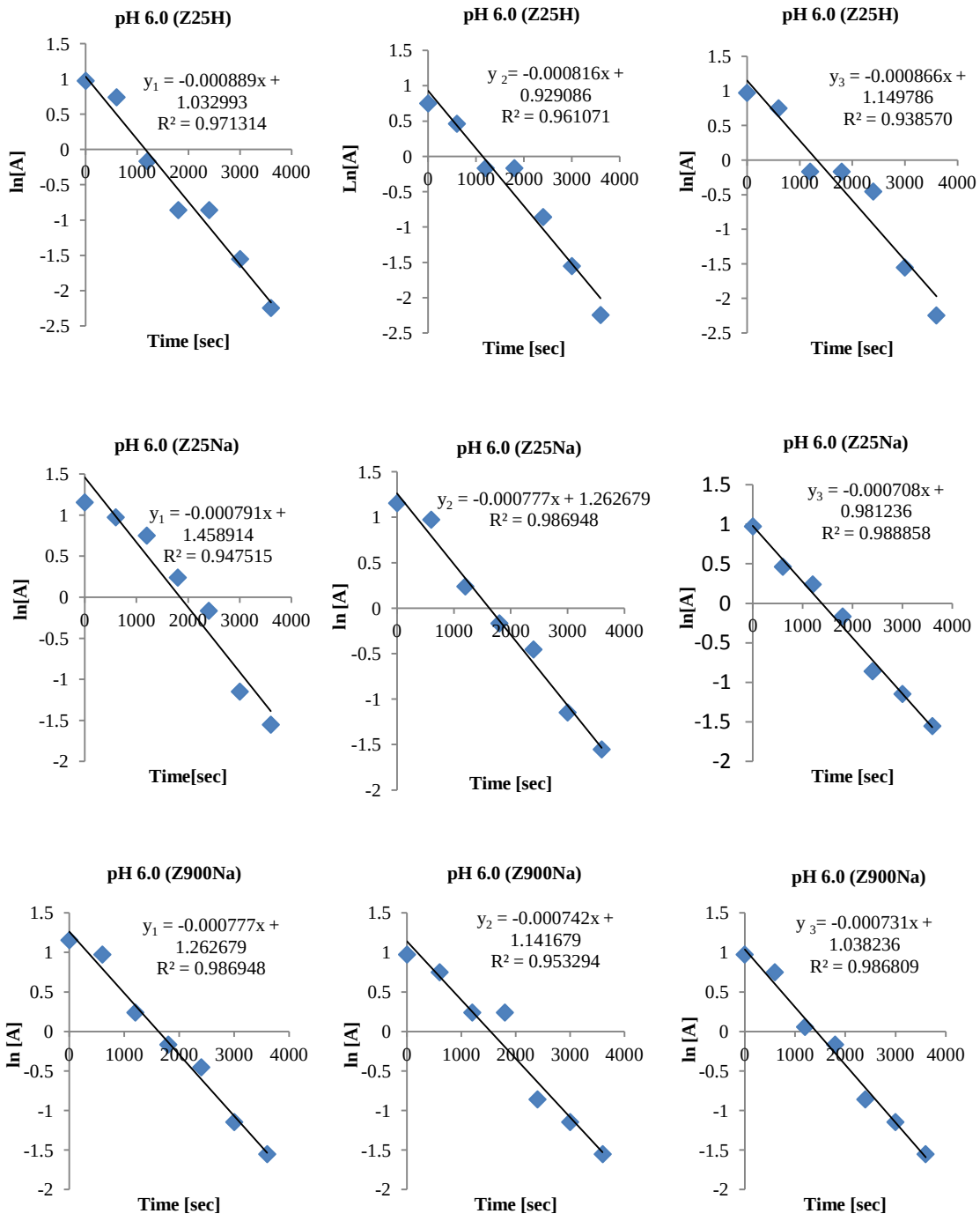

Figure A.9: First order kinetic plots of Z25H/O_3, Z25Na/O_3 and Z900Na/O_3 ($O_{3\ initial}$ = 2.1 mg/L; catalyst = 0.95 mg/L; T = 25^{o}C; pH = 6.0; V = 190 mL).

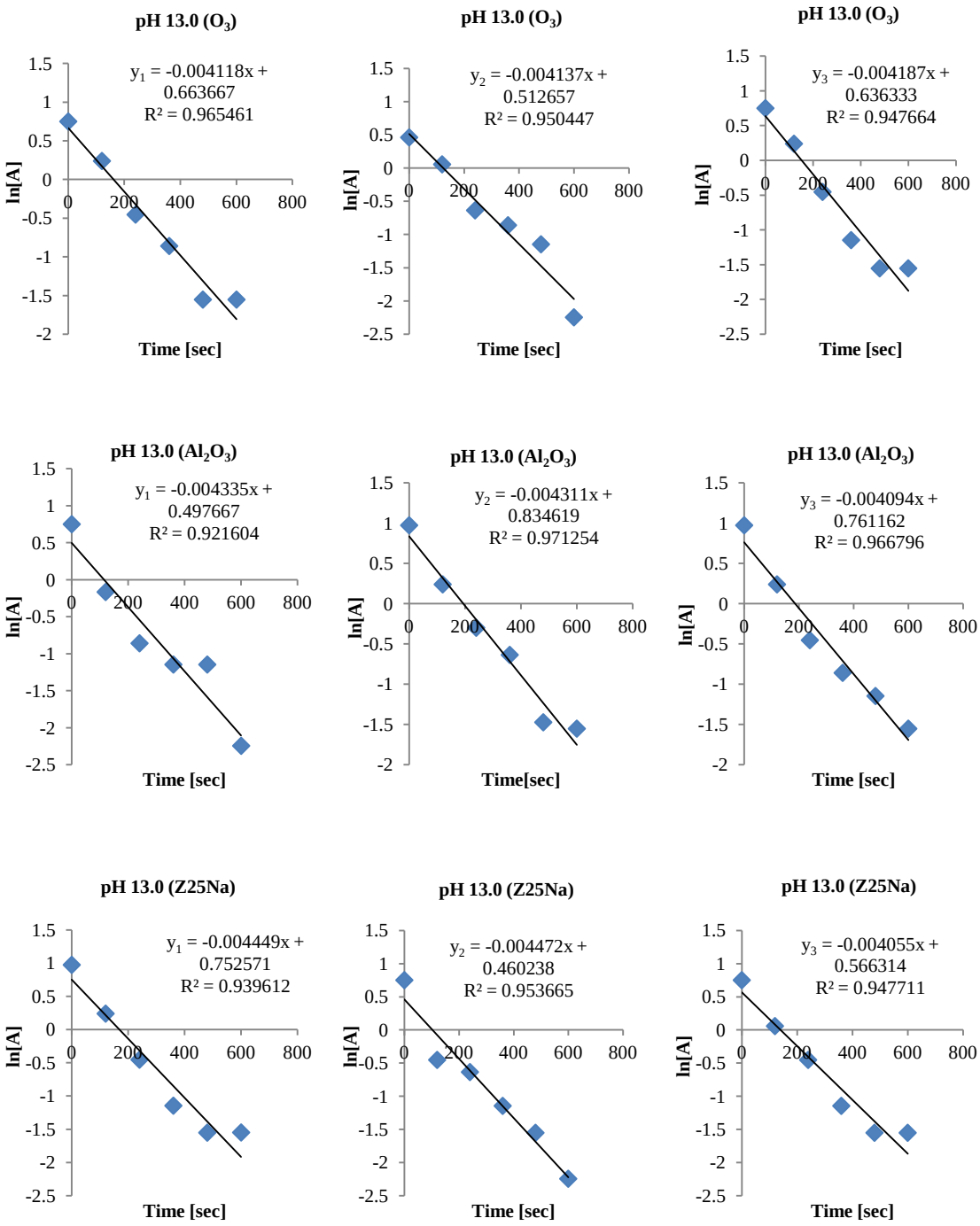

Figure A.10: First order kinetic plots of O_3, Z25Na/O_3 and Al_2O_3/O_3 ($O_{3\ initial}$ = 1.5 mg/L; catalyst = 0.95 mg/L; T = 25°C; pH = 13.0; V = 190 mL).

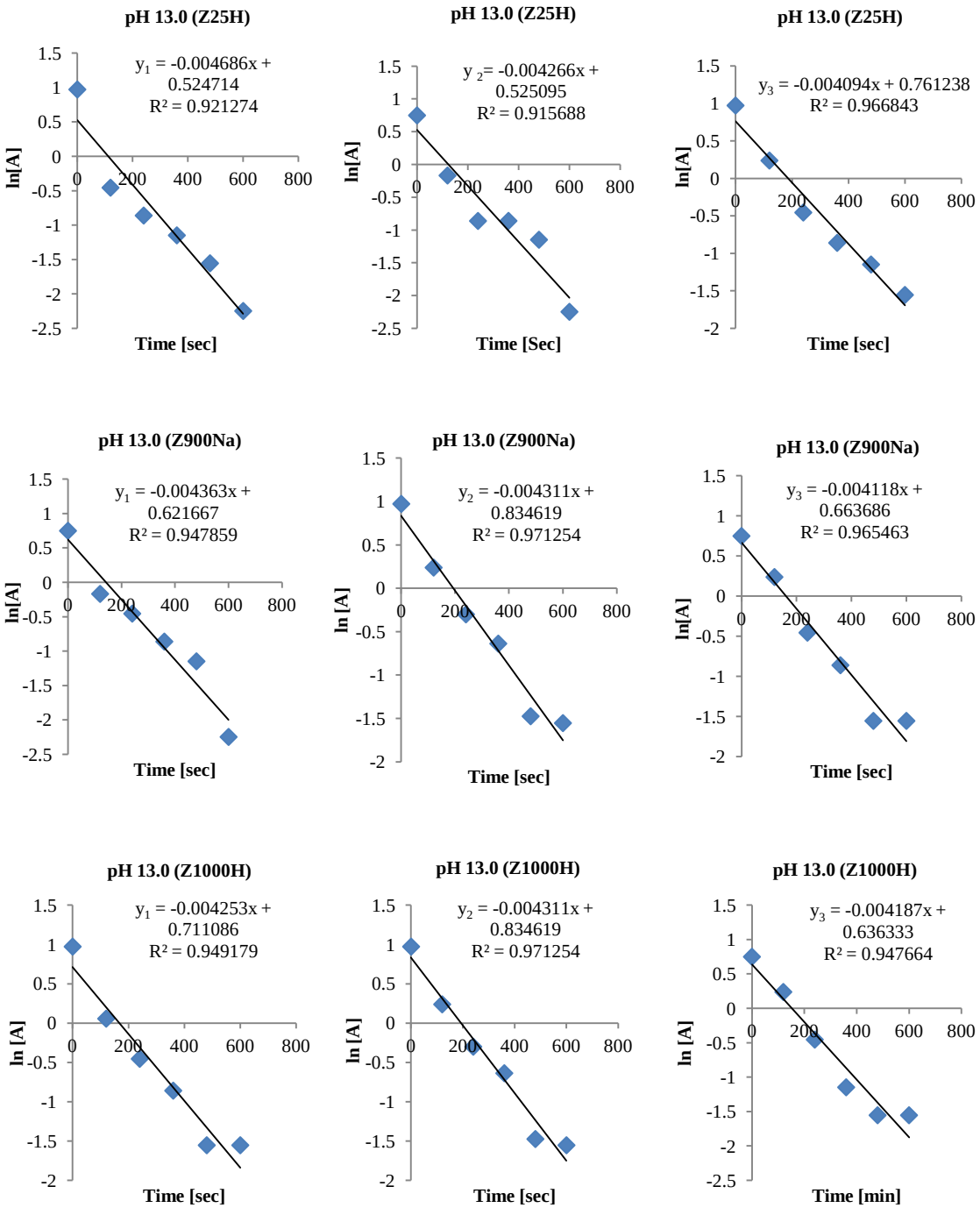

Figure A.11: First order kinetic plots of Z25H /O_3, Z900Na/O_3 and Z1000H/O_3 ($O_{3\ initial}$ = 1.5 mg/L; catalyst = 0.95 mg/L; T = 25^{o}C; pH = 13.0; V = 190 mL).